

**Structural and functional characterization of novel
mitochondrial acyl-CoA thioesterase Them5/CTMP2**

Inauguraldissertation

zur

Erlangung der Würde eines Doktors der Philosophie

vorgelegt der

Philosophisch-Naturwissenschaftlichen Fakultät

der Universität Basel

von

Elena Yurievna Zhuravleva

aus Moskau, Russland

Basel, 2013

Genehmigt von der Philosophisch-Naturwissenschaftlichen Fakultät der Universität

Basel auf Antrag von Dr. Brian A. Hemmings, Prof. Dr. Jean Pieters,
und Prof. Dr. Matthias Wymann

Basel, den 24.05.2011

Prof. Dr. Martin Spiess

(Dekan)

TABLE OF CONTENTS

i Abbreviations	6
ii Summary	8
1 General introduction	11
1.1 Mitochondria: connection of morphology and signaling	11
1.1.1 <i>Fusion and fission proteins</i>	13
1.1.2 <i>Phospholipids of mitochondria</i>	14
1.1.3 <i>Synthesis and remodeling of cardiolipin</i>	15
1.1.4 <i>Role of cardiolipin in diseases</i>	17
1.2 Energy metabolism in the cell	19
1.2.1 <i>Fatty acid synthesis</i>	19
1.2.2 <i>Fatty acid degradation/β-oxidation</i>	21
1.2.3 <i>Oxidative phosphorylation and the electron transfer chain</i>	24
1.3 Thioesterases and their role in the cell	27
1.3.1 <i>α/β thioesterases</i>	29
1.3.2 <i>Hotdog fold thioesterases</i>	30
1.3.3 <i>Functions of mammalian hotdog-fold thioesterases</i>	32
1.3.4 <i>CTMP/Them4: mitochondrial acyl-CoA thioesterase and negative regulator of PKB signaling</i>	35
1.4 PKB signaling pathway and its regulation	37
1.4.1 <i>Activating stimuli and upstream kinases</i>	38
1.4.2 <i>Negative regulation of PKB by phosphatases</i>	41
1.4.3 <i>Role of PKB in insulin resistance, non-alcoholic fatty liver disease and hepatosteatosis</i>	44
2 Aim of the thesis	48

3 Results	49
3.1 Analysis of the novel acyl-CoA thioesterase Them5 reveals a role in mitochondrial morphology and fatty liver disease development	49
<i>Elena Zhuravleva, Heinz Gut, Debby Hynx, David Marcellin, Christopher K. E. Bleck, Christel Genoud, Peter Cron, Jeremy J. Keusch, Bettina Dummler, Mauro Degli Esposti, Brian A. Hemmings</i>	
<i>Manuscript submitted</i>	
3.2 The role of the CTMP2/Them5 protein in PKB signaling: further characterization of <i>Them5</i> ^{-/-} mice	107
3.2.1 <i>Interconnected mitochondria in Them5</i> ^{-/-} <i>primary hepatocytes and β-</i> <i>cells</i>	107
3.2.2 <i>Enhanced insulin sensitivity in Them5</i> ^{-/-} <i>mice</i>	110
3.2.3 <i>PI3K/PKB signaling is enhanced in Them5</i> ^{-/-} <i>mice</i>	111
3.2.3 <i>OXPHOS complexes are affected upon loss of Them5</i>	114
3.2.5 <i>Mouse embryonic fibroblasts as a model for studying Them5</i> <i>function</i>	115
4 Experimental procedures	119
5 General discussion	123
6 References	130
7 Appendix	142
7.1 Role of PKB/Akt in liver diseases	142
<i>Zhuravleva E., Tschopp O., Hemmings B.A. (2010). In “Signaling Pathways in Liver Diseases”, 2nd edition. Ed. Dufour J.F. and Clavien P.A. Springer- Verlag.</i>	
7.2 The Carboxyl Terminal Modulator Protein (CTMP) regulates mitochondrial dynamics	160

*Parcellier A., Tintignac L.A., Zhuravleva E., Duemmler B., Brazil D.P.,
Olivieri V., Schenk S., Cron P., Hynx D. Hemmings B.A. PLoS ONE, 2009;
4(5):e5471*

7.3 Carboxy-Terminal Modulator Protein (CTMP) is a mitochondrial protein that sensitizes cells to apoptosis	171
<i>Parcellier A., Tintignac L.A., <u>Zhuravleva E.</u>, et al. Cell Signal, 2009; 21(4):639-50</i>	
7.4 PKB and the mitochondria: AKTing on apoptosis	184
<i>Parcellier A., Tintignac L.A., <u>Zhuravleva E.</u>, Hemmings B.A. Cell Signal, 2008; 20:21-30</i>	
8 Acknowledgements	195
9 Curriculum vitae	196

i ABBREVIATIONS

4HBT	4-hydroxybenzoyl-CoA thioesterase
Å	Angstrom
Acot	acyl-CoA thioesterase
acyl-CoA	acyl-CoenzymeA
Asp/D	aspartic acid
ATP	adenosine triphosphate
CL	cardiolipin
CoA	coenzyme A
CTMP	carboxyl terminal modulator protein
FAS	fatty acid synthase
Glu/E	glutamic acid
KO	knock-out
MCL	monolysocardiolipin
mtDNA	mitochondrial DNA
MTS	mitochondrial targeting sequence
OXPHOS	oxidative phosphorylation
PBS	phosphate-buffer saline
PI3K	phosphoinositide 3-kinase
PKB	protein kinase B
ROS	reactive oxygen species
RT	room temperature
SBFSEM	serial block-face scanning electron microscopy
Ser/S	serine
TCA cycle	tricarboxylic acid cycle (Krebs cycle)
Them4	thioesterase superfamily member 4

Them5	thioesterase superfamily member 5
Thr/T	threonine
WT	wildtype

ii SUMMARY

Thioesterases hydrolyze thioester bonds in a variety of substrates, including fatty acid CoA esters, and palmitoylated or myristoylated proteins, and participate in lipid metabolism, α - and β -oxidation, cholesterol metabolism, and other processes. According to their folding and the catalytic reaction mechanism, thioesterases are subdivided into two groups: α/β -hydrolases and hotdog-fold thioesterases. Whereas α/β hydrolases have been well characterized in mammals, the second group of enzymes, mammalian hotdog thioesterases have been studied to a much lesser extent (Hunt and Alexson, 2002).

CTMP/Them4 protein has been identified in a yeast two-hybrid screening as an interactor and negative regulator of PKB (Maira et al., 2001). We have recently shown that CTMP/Them4 is a mitochondrial protein which is released from mitochondria after apoptosis induction and promotes cell death (Parcellier et al., 2009a). Other reports have implicated CTMP/Them4 in glioblastoma development and in ischemia-induced neuronal cell death (Knobbe et al., 2004; Miyawaki et al., 2009). CTMP is located in the intramembrane space and is associated with the inner mitochondrial membrane. Proper processing of CTMP is important for maintaining mitochondrial morphology. In a knock-out mouse model we have shown that mitochondria from *CTMP1^{-/-}* mice are more elongated and interconnected; these results were confirmed in a cell culture system by using siRNA against CTMP (Parcellier et al., 2009b).

Human CTMP2/Them5 protein shares 38% similarity with Them4, which has previously been shown to be an acyl-CoA thioesterase with a broad substrate range (Zhao et al., 2009). Interestingly, while Them4 orthologs have been found in yeast and lower eukaryotes, Them5 orthologs have only been found in higher eukaryotes.

Therefore, we were keen to investigate CTMP2/Them5. We have determined structures of both human Them4 and Them5 and confirmed that these proteins belong to the hotdog class of thioesterases. Previous reports have shown that mammalian hotdog proteins are organized in tetrameric or higher-order structures. However, both CTMP/Them4 and CTMP2/Them5 form homodimers, and thus seem to be more closely related to bacterial hotdog thioesterases. We also identified residues which participate in the formation of active centers and are important for the acyl-CoA hydrolysis. Although Them4 and Them5 have very similar folding, they exhibit structural differences and different substrate specificity. For example, Them4 reacts with acetyl-CoA, whereas Them5 does not hydrolyze it.

Hotdog-fold thioesterases play very diverse biological roles, and their function in mammals has not been fully studied. We could show that Them5-deficient mice are viable and fertile, and show no gross developmental abnormalities. Similarly to Them4, which has been reported to localize in mitochondria, Them5 is also a mitochondrial protein. Them5 is located in the mitochondrial matrix and the inner mitochondrial membrane, facing the matrix side. We therefore analyzed the morphology of mitochondria in Them5 knock-out mice. We demonstrate that *Them5*^{-/-} mice are characterized by a highly interconnected and elongated mitochondrial network compared to wildtype control mice. However, loss of Them5 does not affect the biogenesis of mitochondria. More importantly, we show that overexpression of a thioesterase-dead version of Them5 in a cell culture system leads to the appearance of a more elongated and interconnected mitochondrial network, similar to the phenotype observed in *Them5*^{-/-} tissues, indicating that the enzymatic activity of Them5 is important for maintaining normal mitochondrial morphology.

In order to assess the lipid profile after Them5 ablation, we performed a detailed mass spectrometry analysis of lipid extracts from *Them5*^{-/-} and control mitochondria.

We found that loss of Them5 leads to a two-fold increase in major species of monolysocardiolipin (MCL), which act as upstream metabolites in the remodeling cycle of cardiolipin (CL). CL is a phospholipid localized predominantly within the inner mitochondrial membrane (Esposti et al., 2003). On the basis of these results, we propose that Them5 has a rather specific action *in vivo*, namely that of regulating the initial metabolism of mitochondrial CL by maintaining, in particular, the pool of acyl groups used to re-acetylate one metabolic intermediate of cardiolipin, SP2-MCL (stearoyl-di-palmitoyl-monolysocardiolipin). More importantly, Them5 knock-out mice develop fatty livers and show deregulation of enzymes participating in lipid metabolism. Interestingly, young *Them5*^{-/-} males are insulin-hypersensitive, which we have shown in both *in vivo* and *in vitro* settings. We were able to demonstrate that insulin-induced PKB phosphorylation is stronger and more sustained in knock-out tissues, and this led us to suggest that Them5/CTMP2, in addition to CTMP/Them4, also participates in regulation of PKB signaling.

This work presents a structural and functional analysis of two members of a previously uncharacterized class of mammalian hotdog-fold enzymes. In addition, our data indicate for the first time a connection between the loss of thioesterase activity, mitochondrial morphology and function, and development of fatty liver disease. Considering that very limited information is available about the biological role of mitochondrial hotdog-fold thioesterases in mammals, our work provides a framework for future research in this area.

1. GENERAL INTRODUCTION

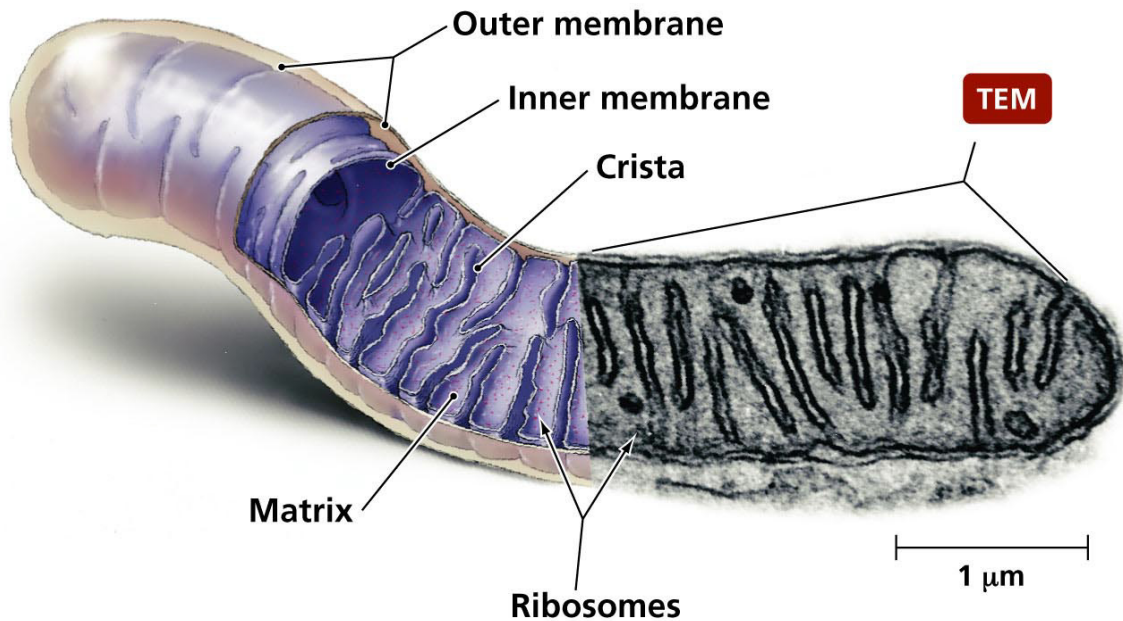
1.1 MITOCHONDRIA: CONNECTION OF MORPHOLOGY AND SIGNALING

Mitochondria are cellular organelles that are believed to be a result of a symbiotic relationship between eubacteria and the eukaryotic cell. This allowed cells to survive in a new environment, utilizing aerobic metabolism (Green and Reed, 1998). Following endosymbiosis, genes were rapidly lost or transferred to the nuclear genome, which was important for the survival of the endosymbiont. This had to be compensated either by the transfer of some of these gene products from the nucleus, or by the transport of other proteins to replace them. As a consequence of some genes' integration into the nuclear genome, proteins had to acquire mitochondrial targeting sequences. This also led to the development of protein import machinery into the mitochondria.

Without oxidative phosphorylation, animal cells would have depended on anaerobic glycolysis for all their ATP production; aerobic mitochondria produce up to 95% of the cells' ATP via oxidative phosphorylation (da Fonseca et al., 2008).

The role of mitochondria as “powerhouses” in the cell is crucial. They are the location of three of the most important energy-generating pathways in humans: oxidative phosphorylation (OXPHOS), fatty-acid β -oxidation, and the tricarboxylic acid (TCA) cycle. However, they are also important components of signaling cascades. In addition to their role as amplifiers in apoptotic events, they also produce reactive oxygen species (ROS) that act as second messengers. The localization of mitochondria in the cell is also not random: they accumulate mainly in the places where high amounts of ATP are needed, or where regulation of Ca^{2+} signaling is required. To ensure the good performance of all these functions, mitochondrial populations should be very dynamic. They constantly undergo processes of fusion

and fission, maintaining a balance between tubular highly interconnected and fragmented morphology.



Copyright © 2006 Pearson Education, Inc., publishing as Benjamin Cummings.

Figure 1.1

Schematic view of mitochondria. Mitochondria are composed of an outer membrane surrounding an inner membrane folded into cristae that increase the surface area available to membrane-bound molecules involved in energy transfer. The mitochondrial matrix contains enzymes, circular DNA, and ribosomes.

Mitochondria have two membranes, the outer mitochondrial membrane (OMM) and the inner mitochondrial membrane (IMM), which have different functions and composition. These two membranes, in turn, define the intramembrane space (IMS) and the mitochondrial matrix. The organelle plasticity is achieved by the ability of the IMM and OMM membranes to fuse in a coordinated manner. By regulating the relative rates of fusion and fission, the morphology of the mitochondrial population can be significantly altered, which has important consequences for mitochondrial functions.

1.1.1 Fusion and fission proteins

A number of fusion/fission machinery components have been identified, first in yeast and then later in mammalian cells (see Figure 1.5). Two dynamin-like GTPases, mitofusins 1 and 2 (Mfn1/2), are located at the outer mitochondrial membrane and are principal regulators of the fusion process (Chen et al., 2003). Another protein involved in fusion is the GTPase OPA1, which also belongs to the dynamin family. It is located in the intramembrane space and is associated with the inner mitochondrial membrane (Spinazzi et al., 2008). Both Mfn2 and OPA1 are known to be involved in neurodegenerative diseases (Alexander et al., 2000; Engelfried et al., 2006; Verhoeven et al., 2006),

Mitochondrial fission depends on the dynamin-related protein 1 (Drp1). It is located in the cytoplasm and translocates to mitochondria in response to cellular and mitochondrial cues. Fis1 is an outer membrane protein that faces the intramembrane space, and its overexpression leads to mitochondrial fragmentation. Additionally, Fis1 and Drp1 interact with each other (Yoon et al., 2003). This is rather a transient event, and dissociation of the complex is required for efficient fission. However, the above interaction process has been described more complete in yeast, which have another adaptor protein of the interaction process, Mdv1 (Naylor et al., 2006). Mammalian are lacking its ortholog (or it has not been identified yet), and the fission process mechanics is still to be fully described.

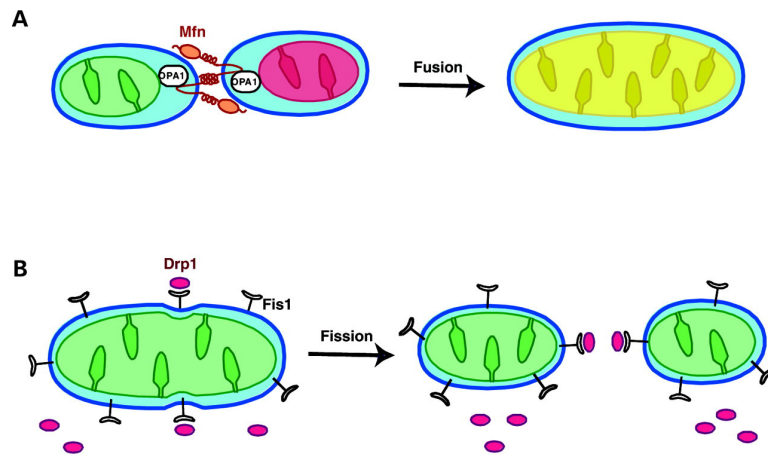


Figure 1.2

Mitochondrial fusion and fission molecules. (A) Fusion molecules. Mfn is a mitochondrial outer membrane protein with a cytosolic GTPase domain (orange oval) and two coiled coil regions (coils). The C-terminal coiled coil mediates oligomerization between Mfn molecules on adjacent mitochondria. OPA1 (white oval) is a GTPase in the intermembrane space. Mfns and OPA1 coordinate mitochondrial fusion, as shown by the mixing of green and red matrix markers to produce yellow. (B) Fission molecules. Fis1 is localized uniformly to the mitochondrial outer membrane, whereas Drp1 is localized to the cytosol and punctate spots on mitochondria[or Fis1?]. Some of these spots are constriction sites that lead to mitochondrial fission. Taken from (Chen and Chan, 2005)

1.1.2 Phospholipids of mitochondria

Phospholipids (PL) are important components of mitochondrial membranes. The relative abundance of different PLs varies little among different cell types, indicating that major changes cannot be tolerated. Indeed, changes in the PL spectrum have been associated with altered mitochondrial structure and function. The most abundant proteins in mitochondria are cardiolipin (CL) and phosphatidylinositol, which comprise ca. 40% and 30% of total mitochondrial PLs, respectively (see Figure 1.6). In mammalian cells, mutations in phosphatidylglycerol phosphate synthase eliminate phosphatidylglycerol and CL pools, leading to alterations in mitochondrial structure and functions (Ohtsuka et al., 1993).

CLs are particularly interesting phospholipids, located in the inner mitochondrial membrane. CL is a dimeric phospholipid, composed of a glycerol backbone and four acyl chains. CL is an important regulator of the biophysical properties of cellular membranes; it is known to favor membrane fold creation. Also, CL forms clusters

and non-bilayer structures. Additionally, it strongly interacts with many different proteins, including mitochondrial membrane transport complexes, the fusion protein OPA1, cytochrome *c*, and components of respiratory complexes, which leads to specific features of CL-associated disorders.

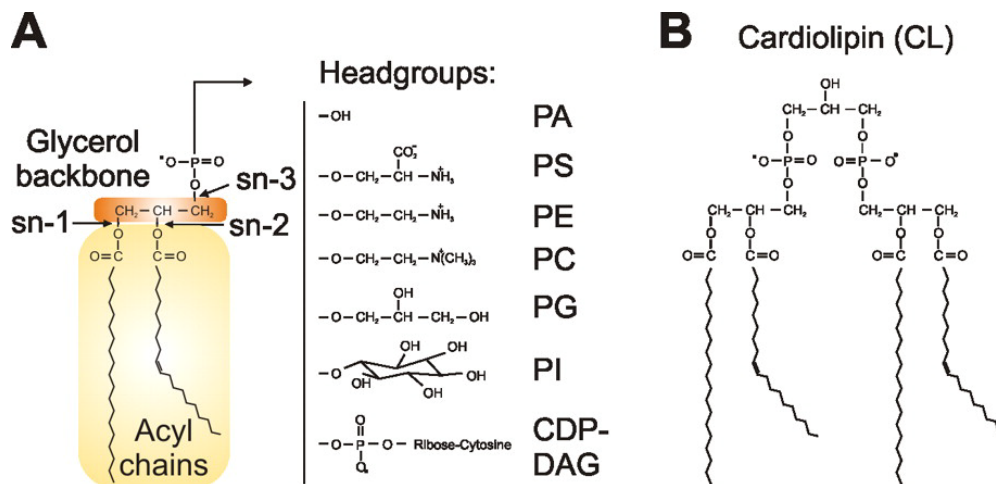


Figure 1.3

Phospholipids in mitochondrial membranes. (A) The central structural element of phospholipids is a glycerol backbone. Acyl chains that can vary in length and saturation are attached to the sn-1 and sn-2 hydroxyl groups. Distinct hydrophilic head groups can be attached at the sn-3 position of the glycerol backbone via a phosphodiester bond and confer unique biophysical properties that distinguish the different phospholipid classes: phosphatidic acid (PA), phosphatidylserine (PS), phosphatidylethanolamine (PE), phosphatidylcholine (PC), phosphatidylglycerol (PG), phosphatidylinositol (PI), and CDP-DAG. CDP-DAG is an intermediate that does not accumulate in significant amounts in mitochondrial membranes under normal conditions. (B) CL is a lipid unique to mitochondria, which consists of two PA moieties covalently linked to each other by a glycerol bridge, with phosphodiester bonds at the sn-1 and sn-3 positions of the bridging glycerol. Taken from (Osman et al., 2011).

1.1.3 Synthesis and remodeling of cardiolipin

Cardiolipin is synthesized from its precursors PG and CDP-DAG, and after primary synthesis CL chains are remodeled and CL achieves its final maturation. The enzymes responsible for CL synthesis and remodeling are outlined in Figure 1.4

The mature acyl chain composition of CL cannot be explained by the substrate-specificity of CL synthase. This implies that additional mechanisms are involved in achieving the final composition by acyl chain remodeling. Remodeling can occur either by the deacylation-reacylation cycle, or by transacylation. Deacylation is

mediated by phospholipase A, where the formation of monolyso-CL (MCL) is followed by CoA-dependent reacylation (Figure 1.4A) (Ma et al., 1999; Taylor and Hatch, 2003).

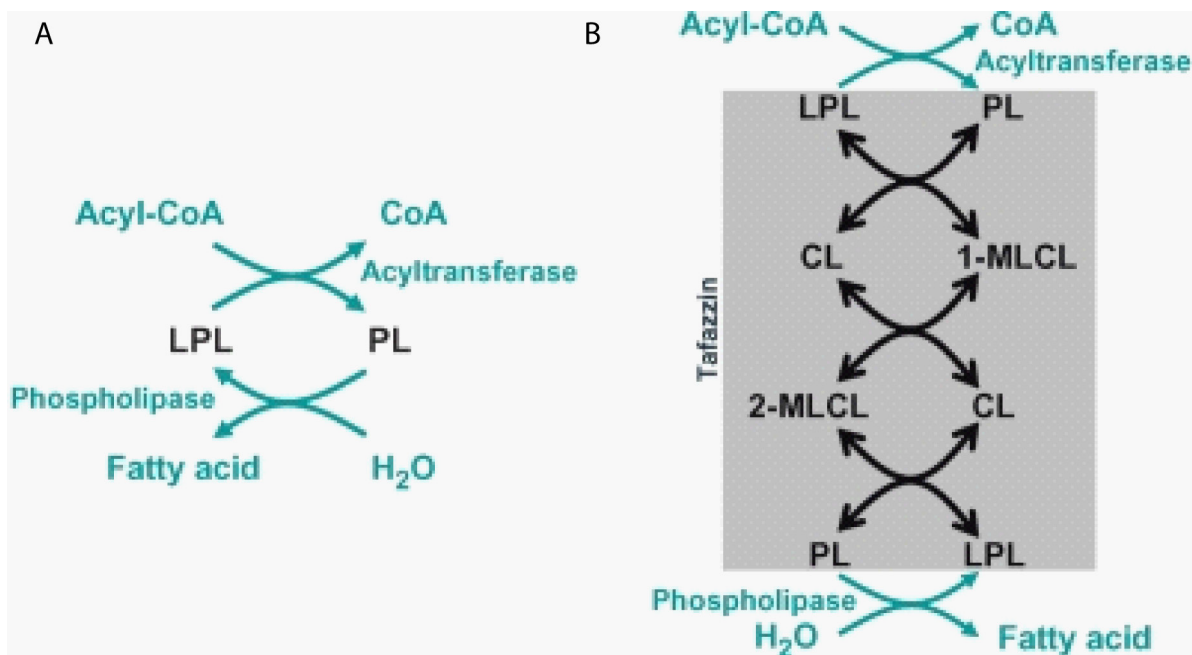


Figure 1.4

Phospholipid remodeling pathways (Schlame, 2008). (A) Phospholipid remodeling by the deacylation-reacylation cycle (Lands cycle). This pathway is used for remodeling of other PLs (not CL). However, it may still be indirectly involved in CL remodeling, providing necessary turnover of fatty acids. (B) CL remodeling by phospholipid transacylation. CL remodeling is catalyzed by a single enzyme tafazzin, which mediates several transacylation reactions (highlighted in the grey box). Tafazzin is equally active with the substrates 1-monolysocardiolipin (1-MLCL) and 2-monolysocardiolipin (2-MLCL). Because it can also transfer acyl groups from CL to MLCL, it can function as a positional isomerase. The acyl groups are directly transferred from the phospholipid (PL) to the lysophospholipid (LPL), and no acyl-enzyme intermediate is present, since free fatty acids are not released in the absence of an acyl acceptor.

The enzymes involved in this process are acyltransferases, which have been shown to exert specificity toward linoleic and oleic acyls, which are predominantly found in mature species of CL (Taylor and Hatch, 2009) (Cao et al., 2004). However, ALCAT1, the first identified CL-remodeling acyltransferase, lacks preference towards linoleic acid as a substrate. These enzymes are sensitive to the thyroid status and oxidative stress; ALCAT1 has been shown to be upregulated in diet-induced obesity, leading to pathological remodeling of CL due to its lack of preference towards linoleic

acid as a substrate (Cao et al., 2009a), (Li et al., 2010). The second way of CL remodeling, transacylation, involves the transfer of an acyl chain from PC to MCL, forming lyso-PC and CL. This is mediated by the enzyme tafazzin. The acyl groups are transferred directly from the phospholipid to the lysophospholipid, with no acyl intermediate, because free fatty acids are not released in the absence of an acyl acceptor (Figure 1.4B).

1.1.4 Role of cardiolipin in diseases

Mutations in the tafazzin gene (chromosome Xq28) are associated with Barth syndrome, an X-linked recessive disorder, clinically characterized by cardiomyopathy, growth delay, and neutropenia (Vreken et al., 2000). As a result of the tafazzin mutations, CL remodeling is impaired, and abnormal profiles of CL can be detected. CL levels are lower, MCL levels are increased, and the acyl chain composition is shifted towards unsaturated species (Xu et al., 2006). As a consequence of CL/MCL imbalance, mitochondria of taz-deficient cells show abnormalities in the cristae and compromised bioenergetic mitochondrial coupling (van Gestel et al., 2010). Loss of the acyl-CoA binding protein Acb1p leads to a similar phenotype, resulting in the accumulation of short acyl chains (fewer than 16 carbon atoms) in CL (Rijken et al., 2009). It has been proposed that CL is required for Bid/Bax activation and oligomerization during apoptosis (Kuwana et al., 2002). Bax oligomerization requires tBid and occurs after it has translocated to mitochondria. However, the data from Iverson et al. question the role of CL in this process (Iverson et al., 2004). In contrast, the authors suggest that CL is required for cytochrome *c* retention within the cristae, supporting the two-step mechanism of cytochrome *c* release, which states that CL is required for binding cytochrome *c* to the inner mitochondrial membrane (Ott et al., 2002) (See Figures 1.5 and 1.6).

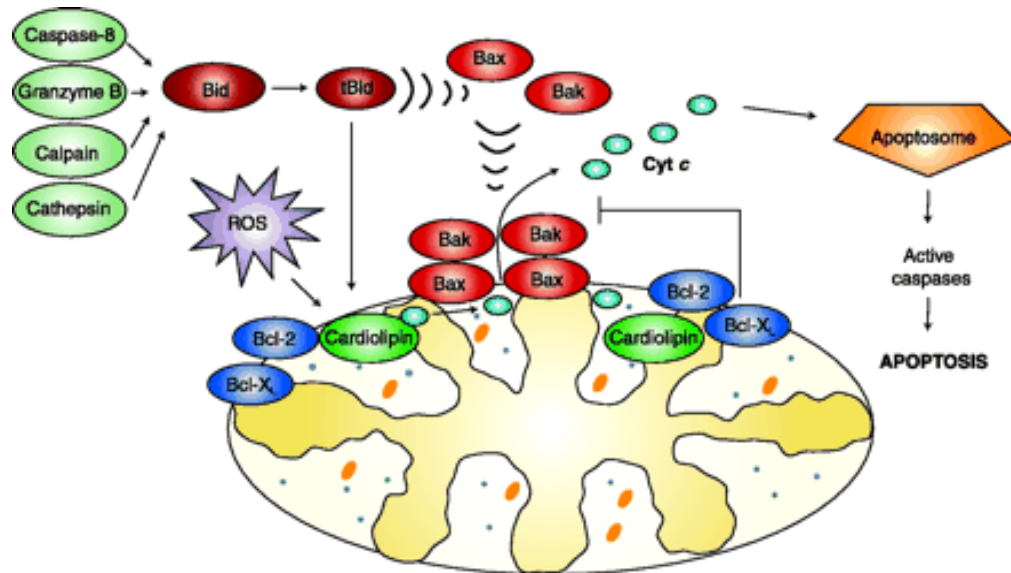


Figure 1.5

Regulation of cytochrome *c* release from mitochondria. The mitochondrial outer membrane is permeabilized by tBid, which promotes the oligomerization and insertion of Bax and Bak. Cytochrome *c* release is initiated by the dissociation of the hemoprotein from its binding to cardiolipin in the inner mitochondrial membrane, which is stimulated by cardiolipin peroxidation (mediated by ROS). Once released into the cytosol, cytochrome *c* triggers pro-caspase-activation via the apoptosome mechanism. Taken from (Fariss et al., 2005).

Additionally, CLs are very prone to peroxidation by ROS due to the high content of unsaturated fatty acids and their location near the site of ROS production (Paradies et al., 2001). Reduction of mitochondrial phosphatidylethanolamine or CL leads to abnormal mitochondrial morphology and the appearance of more mitochondria with respiratory defects (Claypool et al., 2008a). CL stimulates OPA1 oligomerization and its GTPase activity (Ban et al., 2010). Lipid binding by the yeast OPA1 ortholog, Mgm-1, is required for mitochondrial membrane fusion (DeVay et al., 2009). Impaired processing of OPA1 leads to aberrant morphology, which emphasizes the importance of membrane composition for maintaining mitochondrial morphology.

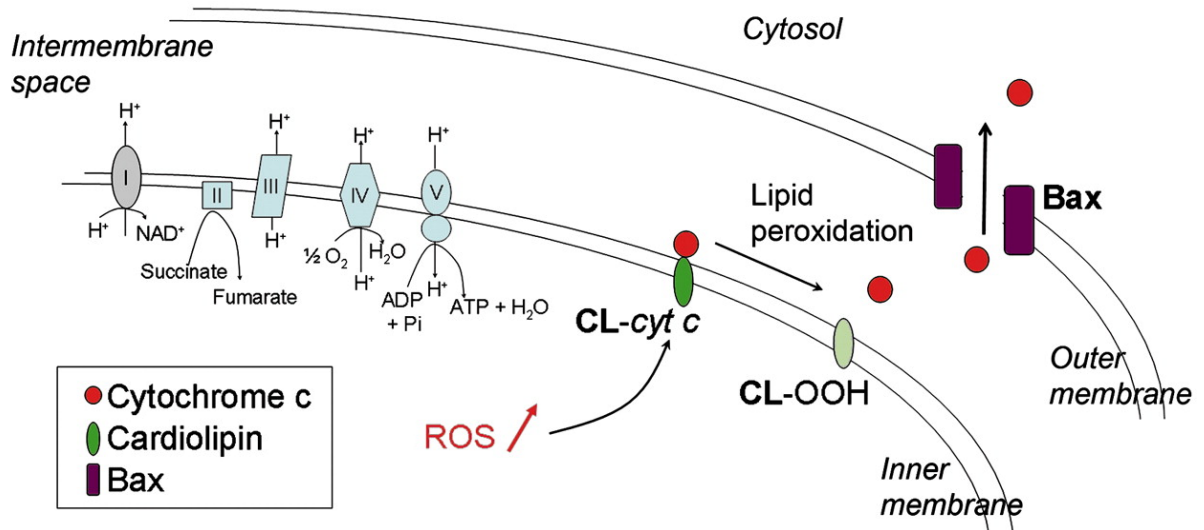


Figure 1.6. Cardiophilin peroxidation in mitochondria

Increased production of ROS in mitochondria leads to oxidation of cardiophilin. Cardiophilin peroxidation, in turn, affects the binding of cytochrome *c* to the mitochondrial inner membrane, leading to an increased soluble pool of cytochrome *c* in the IMS. Consequently, upon permeabilization of the OMM by activated Bax, a larger amount of mitochondrial cytochrome *c* can be released, making it more likely for a cell to undergo apoptosis (adapted from (Perier et al., 2005)).

1.2 ENERGY METABOLISM IN THE CELL

1.2.1 Fatty acid synthesis

Once fatty acids (FAs) enter a cell, they either diffuse or are transported to the mitochondria, peroxisomes, or endoplasmic reticulum. Fatty Acid Binding Proteins (FASBPs), which regulate FA uptake and intracellular transport, may function as carriers of FAs in the cytoplasm. In animal cells, β -oxidation takes place in mitochondria and peroxisomes: this pathway is similar to a reversal of fatty acid synthesis. Similarly, FA synthesis takes place in at least two subcellular compartments in eukaryotic cells: cytoplasm and mitochondria. Cytosolic FAS in eukaryotes relies on the activity of a multifunctional, multidomain enzyme (FAS-I) to

catalyze the repetitive FA synthesis steps, whereas the mitochondrial system (FAS-II) depends on individual, monofunctional enzymes that catalyze individual reactions. Regulation of fatty acid synthesis, or lipogenesis, occurs via the action of lipogenic enzymes, namely fatty acid synthase (FAS), acetyl-CoA carboxylase (ACC), and ATP citrate lyase (ACL).

ACC is the rate-limiting enzyme in fatty acid synthesis. Two major isoforms of ACC exist: ACC1 and ACC2. ACC1 is cytosolic and is present in liver, adipose, and lactating mammary glands. ACC2 is expressed in heart, liver, and skeletal muscle. ACC2 associates with CPT1, thereby participating in CPT1 downregulation by malonyl-CoA, produced by ACC. ACC1 is activated upon polymerization, which is not the case for ACC2. However, both ACC1 and ACC2 are allosterically activated by citrate and inhibited by long- and short-chain fatty acids, products of fatty acid synthesis. Additionally, ACC activity can be affected by phosphorylation. Thus, ACC1 phosphorylation by AMPK leads to its inhibition. Also, increased levels of cAMP, mediated by glucagon, and the subsequent increase in PKA activity lead to ACC phosphorylation. As a result, insulin (re-feeding) stimulates ACC and FA synthesis, whereas starvation leads to a decrease in FA synthesis.

At the transcriptional level, regulation of these lipogenic genes in response to glucose and insulin occurs via SREBP-1/2, liver X receptors, and ChREBP.

Fatty acid synthesis plays an important role in animal development, as shown by knock-out studies: ACC1 and FAS full body deletion causes embryonic lethality (Abu-Elheiga et al., 2003) (Chirala et al., 2003).

1.2.2 Fatty acid degradation/ β -oxidation

β -oxidation provides a lot of energy for essential cellular functions, and each cellular compartment metabolizes a specific set of FAs, e.g. very-long chain, long chain,

saturated, non-saturated, short- or medium-chain fatty acids, eicosanoids, and bile acid intermediates. Mitochondria receive shortened products from peroxisomes, which are either further oxidized, or utilized in the production of ketone bodies to provide energy for extrahepatic tissues (Hunt and Alexson, 2002) (see Figure 1.3).

For degradation via the mitochondrial β -oxidation pathway, the acyl group of cytosolic acyl-CoA passes the mitochondrial membrane bound to carnitine via a carnitine shuttle operated by carnitine-acylcarnitine translocase. Then acyl groups are transferred to CoA. Mammalian carnitine acyltransferases are characterized by different chain-length specificity: carnitine O-palmitoyltransferase I and II (CPT-I/II), present on both sides of the mitochondrial inner membrane, react specifically with long-chain acyl-CoA compounds; carnitine O-acyl transferases, found in peroxisomes and mitochondria, react on C_2 --- C_{10} from acyl-CoA.

The process of fatty-acid oxidation occurs through the sequential removal of 2-carbon units by oxidation at the β -carbon position of the fatty acyl-CoA molecule.

There are multiple enzymes, which vary in their chain-length specificity, for each of the β -oxidation steps. Schematically, the β -oxidation pathway is presented in Figure 1.7.

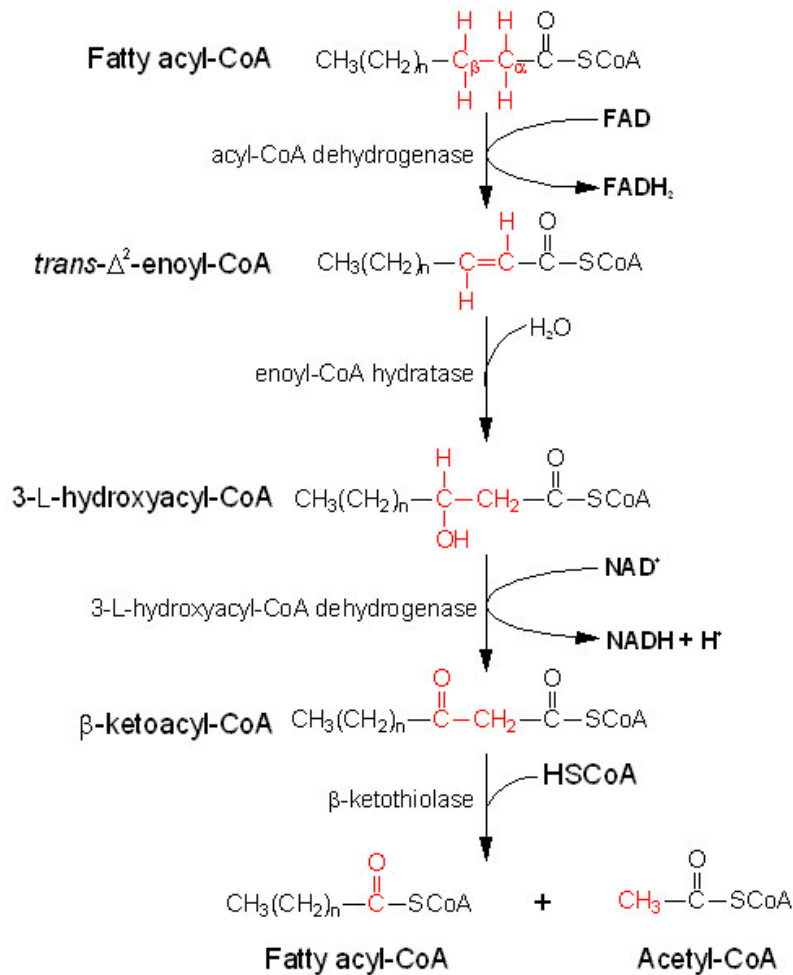


Figure 1.7

Mitochondrial β -oxidation. The mitochondrial fatty acid β -oxidation pathway contains four reaction steps including acyl-CoA dehydrogenases, enoyl-CoA hydratase, β -hydroacyl CoA dehydrogenase, and β -ketoacyl CoA thiolase. The last three steps of β -oxidation are performed by a highly organized single enzymatic complex, known as mitochondrial trifunctional protein, associated with the inner mitochondrial membrane. Completely independent enzymes responsible for β -oxidation of medium- and short-chain fatty acids are located in the mitochondrial matrix.

Each round of β -oxidation produces one mole of NADH, one mole of FADH₂, and one mole of acetyl-CoA. Acetyl-CoA then enters the TCA cycle, resulting in the production of an additional three moles of NADH, one mole of FADH₂, and one mole of ATP. The resultant NADH and FADH₂ enter then the respiratory chain to produce ATP.

β -oxidation regulation is very much dependent on the organ of interest. Thus, liver is capable of high rates of β -oxidation and ketogenesis. Under fed conditions, when glucose levels are high, free fatty acids levels are low and CPT1 is inhibited by high levels of malonyl-CoA. Thus, the carbon flux is from glucose to *de novo* lipogenesis

via citrate and malonyl-CoA (see Figure 1.8). During starvation, FFA levels in blood rise in response to a higher glucagon/insulin ratio, and activate adipose tissue triacylglycerol lipase. Hepatic malonyl-CoA levels are lowered due to both a slower efflux of citrate from mitochondria and to phosphorylation (i.e. inactivation) of ACC by AMPK, again in response to a higher glucagon/insulin ratio. Hence, β -oxidation and ketogenesis are activated and an increase in ketone bodies is observed.

In extrahepatic tissues, where there is no active lipogenesis (heart and skeletal muscle), β -oxidation provides contractile energy. The rate of β -oxidation increases upon demand, e.g. an increased work rate and ATP demand lead to faster oxidative phosphorylation and TCA cycle activity. NADH and acetyl-CoA levels decrease and thus β -oxidation flux increases.

Control of mitochondrial β -oxidation occurs at several levels. One of them is the entry of acyl groups into the mitochondria. This is achieved via regulation (inhibition) of CPTI by malonyl-CoA. Another is intramitochondrial, since β -oxidation consists of several enzymes with overlapping chain-specificities.

Product inhibition is a potent way to regulate the activity of β -oxidation enzymes. Thus, acyl-CoA dehydrogenases are inhibited via their enoyl-CoA products, as well as via 3-oxoacyl-CoA esters (which are formed two steps down the pathway). Crotonase (enoyl-CoA hydratase) is similarly inhibited by acetoacetyl-CoA. 3-oxoacyl-CoA thiolase is inhibited by acetyl-CoA, leading to feedback inhibition of β -oxidation due to inhibition of acetyl-CoA disposal to ketogenesis, the TCA cycle, or acetyl-carnitine. However, 3-oxoacyl-CoA thiolase is not inhibited by its acyl-CoA product. Regulation also happens at the level of acetyl-CoA disposal to ketogenesis. Depletion of free CoA, which is limited in mitochondria, inhibits both CPTII and 3-oxoacyl-CoA thiolase, as well as other mitochondrial enzymes which are dependent on free CoA.

The respiratory chain is also quite tightly linked to β -oxidation. β -oxidation supplies substrates used by complexes I and III, which are then used to generate energy in the form of ATP. Consequently, inhibition of either of the electron transfer chain stages results in β -oxidation inhibition. There are also data supporting not only the functional, but also the physical, association of ETC with fatty acid oxidation enzymes (Wang et al., 2010). This is not surprising, given the localization of both components of β -oxidation and OXPHOS in the IMM.

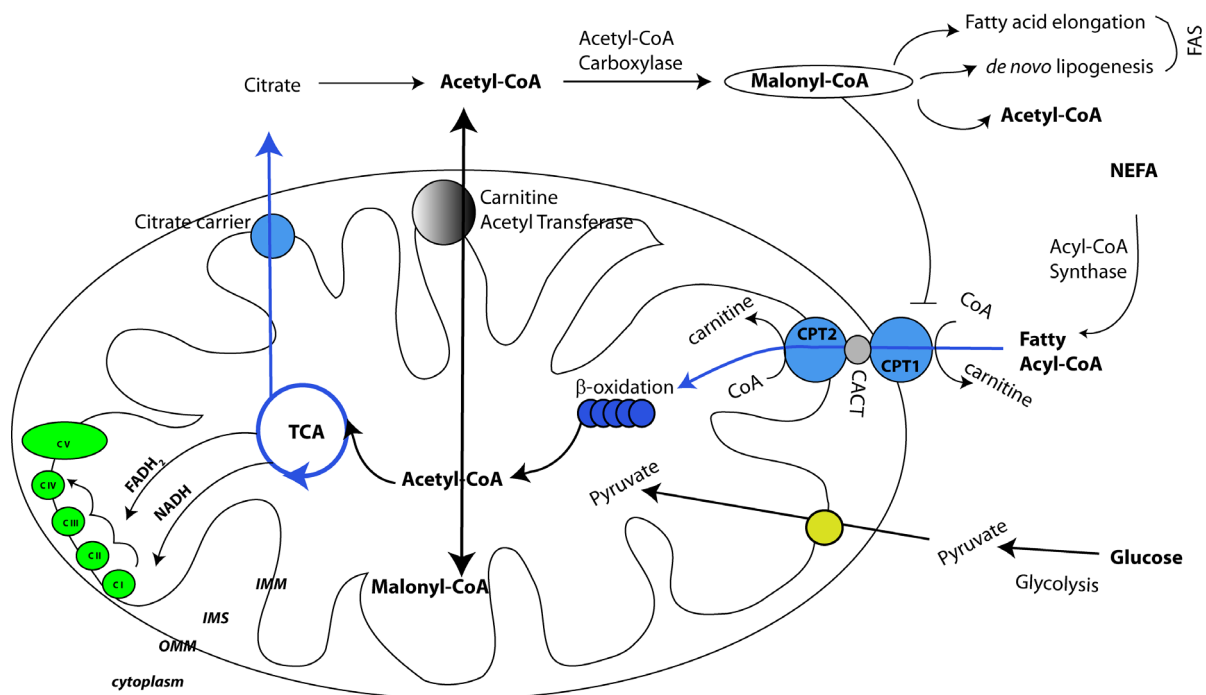


Figure 1.8. Fatty acid synthesis and degradation: modulation of CPTI activity

See the text of the section 1.2.2 for explanations (modified from (Eaton et al., 1996))

1.2.3. Oxidative phosphorylation and the electron transfer chain

Four major protein complexes that facilitate electron and proton flow are located in the inner mitochondrial membrane. Complexes I and II transfer electrons from the TCA cycle-generated NADH and FADH₂ to CoQ, then to complex III (CoQ reductase), then to cytochrome c, then to complex IV (cytochrome c oxidase), and

then to molecular oxygen, finally producing water (Figure 1.9). At the same time, protons cross the IMM at complexes I, III, and IV, generating an electrochemical gradient, which will be used by ATP synthase (complex V, but technically not a member of the respiratory chain).

Two alternative models have been proposed for the organization of the OXPHOS system. The first is the random collision model, where all the components are independent of each other and the electron transfer is possible due to transient meeting by the complexes (Hackenbrock et al., 1986). The second, the “solid-state” model proposed more than 55 years ago, postulates that enzyme components are assembled into a huge supramolecular energy-converting machine (Chance and Williams, 1955). Recently it has been demonstrated that supercomplexes do indeed exist and can function as respirasomes (Acin-Perez et al., 2008). Thus, the solid-state model should be reconsidered when developing a new model of the respiratory chain: coexistence of both individual complexes and various supercomplexes should be taken into account. This model also proposes that supercomplex composition may vary according to tissue type or energy demand.

The proper assembly of respiratory complexes is mediated via the biophysical properties of the inner mitochondrial membrane. Cardiolipin (CL), the major phospholipid of the IMM, is associated with complexes I, III, IV, and V, and the major carrier proteins for adenine nucleotides and phosphates (Osman et al., 2011). Also, reconstruction of complex IV and the ADT/ATP carrier (ACC) activity *in vitro* demonstrated a strong need for CL (Hoffmann et al., 1994). Overall, it is accepted that CL, although not mandatory for OXPHOS, significantly improves the efficiency of this process (Claypool et al., 2008a; Claypool et al., 2008b).

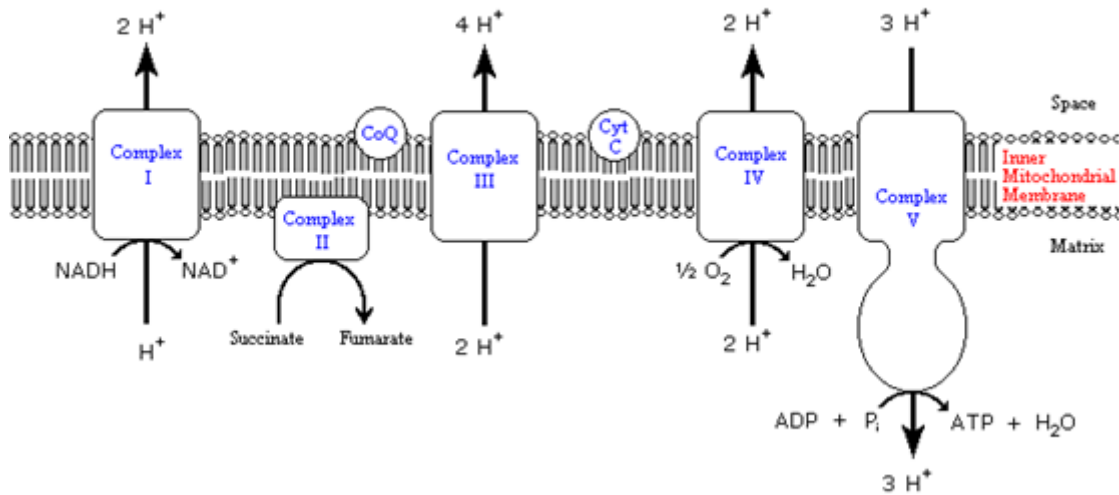


Figure 1.9

Schematic view of the electron transfer chain. Reduced substrates (NADH and FADH₂) are oxidized, with electrons passing to the enzyme complexes of the electron transfer chain (ETC) and the protons being pumped into the IMS of the mitochondria, forming a large proton motive force (PMF). The PMF consists of an electrical ($\Delta\psi$) and a chemical (ΔP) component and is maintained by the ETC. Functionally, the ETC consists of four multiprotein complexes (CI-CIV) and the electron carrier coenzyme Q10 (CoQ) and cytochrome *c* (Cyt C). Electrons are extracted from NADH at complex I and FADH at complex II, and are transported by CoQ to complex III. Subsequently, electrons are transferred to complex IV by cytochrome *c*, where they are donated to molecular oxygen to form water. The energy released from electron transfer is used to drive trans-IMM proton efflux, establishing the PMF. By allowing backflow of protons, ATP is then produced by complex V (F₀F₁-ATP synthase). The ETC complexes, together with complex V, constitute the OXPHOS (oxidative phosphorylation) system.

In yeast, structural changes in the organization of the respiratory complexes when CL is absent are directly associated with functional consequences, such as cooperation between the complexes or their stability (Zhang et al., 2002). Patients with Barth syndrome, a cardiomyopathy which involves mutation of tafazzin, are characterized by unstable OXPHOS complex association, and, as a consequence, by defects in respiratory chain activities (McKenzie et al., 2006).

Mitochondrial morphology depends very much on the energetic state of the cell. For example, a decrease in mitochondrial membrane potential leads to organelle fragmentation. It has been suggested that compromised membrane potential blocks fusion by Opa1 degradation, which leads, in turn, to the activation of fission machinery (Cereghetti et al., 2008). Grown on glucose yeasts are characterized by low levels of respiration; however, when glucose is depleted cells increase their

respiratory capacity and mitochondria are forming interconnected network. Later, when culture reaches saturation, mitochondrial network tends to fragment (Sauvanet et al., 2010). On the other hand, changes in mitochondria-shaping proteins can affect the bioenergetic state of the cell. Impaired fusion and activated fission processes can cause mitochondrial dysfunction. Blockage of fission by downregulation of Drp1 may lead to a loss of mtDNA, a decrease of mitochondrial respiration, and an increase in ROS (Parone et al., 2008). In β -cells, for example, it has been shown that inhibition of the fission machinery may lead to decreased mitochondrial autophagy, accumulation of oxidized proteins and, in turn, impaired insulin secretion (Twig et al., 2008).

Phospholipids, in addition to the already known proteins such as Opa1, Mfn1/2, etc., have become new players in the field of mitochondrial dynamics. However, a recent publication from our group introduced another interesting molecule, CTMP/Them4, to the area of mitochondrial morphology (Parcellier et al., 2009b).

1.3 THIOESTERASES AND THEIR ROLE IN THE CELL

Thioesterases are ubiquitous and diverse enzymes; they are present in bacteria, archaea, and up to eukaryotes. They hydrolyze thioester bonds in a variety of substrates, including fatty acid CoA esters, and palmitoylated or myristoylated proteins; they participate in lipid metabolism; they regulate levels of fatty acids and CoA, cell membrane composition, α - and β -oxidation, cholesterol metabolism (Hunt and Alexson, 2002).

According to their folding and the catalytic reaction mechanism, thioesterases are subdivided into two groups: α/β -hydrolases and hotdog-fold thioesterases. There is no apparent sequence similarity between these two groups of enzymes; however, within the α/β -hydrolase group there is quite a high degree of sequence

conservation. Interestingly, hotdog-fold enzymes show no strong amino acid similarity. On the other hand, these enzymes have very conserved folding: β -sheets wrapped around a central α -helix, from where they received their name. However, both groups of enzymes hydrolyse a thioester bonds and release free fatty acids and CoASH (or any other moiety) (see Figure 1.10).

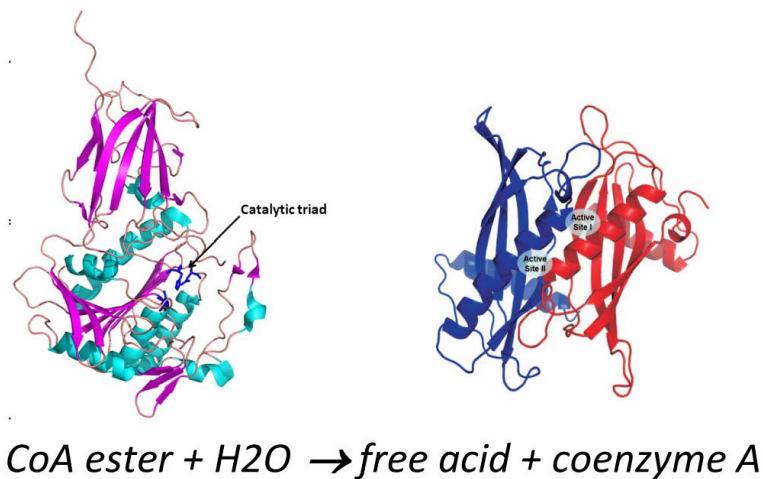


Figure 1.10

Examples of two major classes of thioesterases. (A) α/β hydrolase Acot2 with a classical Ser-Asp-His catalytic triad. From (Pidugu et al., 2009). (B) Hotdog-fold thioesterase Acot7 (in stylized representation with monomers in red and blue). Two putative active sites are present within each dual hotdog fold, site I and site II. From (Forwood et al., 2007).

Although the majority of mammalian thioesterases are α/β -hydrolases and have been relatively well studied, mammalian hotdog-fold enzymes have been less well described. Recent publications concerning hotdog-fold hydrolases in mammals include: Acot13/Them2, a thioesterase with dual (mitochondrial and cytoplasmic) localization; and Acot7, which has been implicated in eicosanoid synthesis in the cytoplasm and inflammatory processes (Cao et al., 2009b; Forwood et al., 2007). As well as there being only seven known hotdog-fold enzymes in mammals (Acot7-9, Acot11, Acot13, Them4 and Them5), published data describe mainly their cytoplasmic or peroxisomal forms. In contrast, α/β thioesterases have been studied considerably better. This group of enzymes includes Acot1 (known previously as

CTE-1, cytoplasmic thioesterase 1), Acot2 (mitochondrial thioesterase 1, MTE1), the lysosomal protein palmitoyl thioesterase 1 (see Figure 1.11).

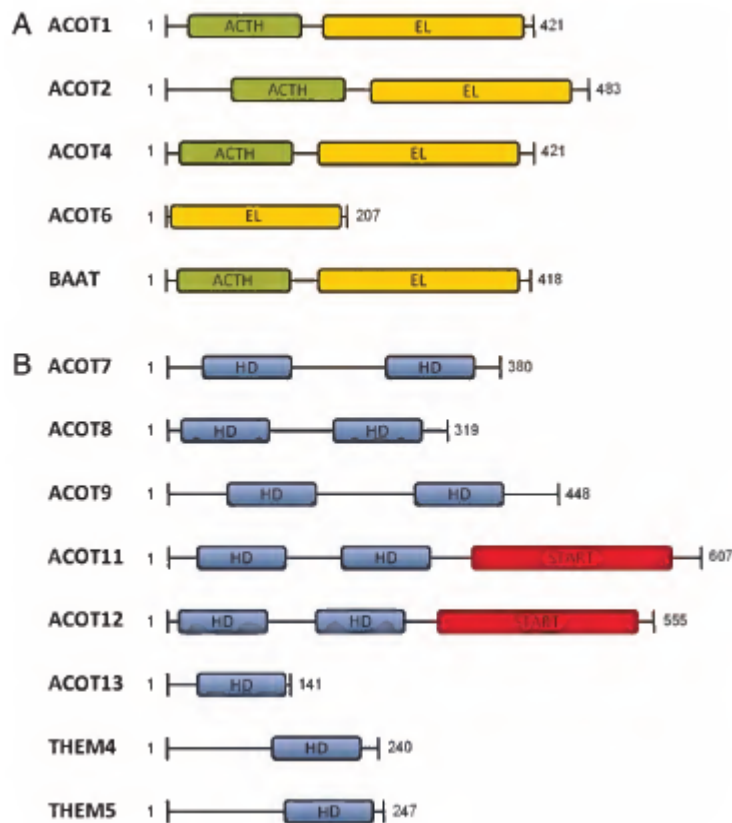


Figure 1.11
Domain organisation of (A) human type I (α/β) and (B) type II (hotdog fold) acyl-CoA thioesterases (ACOTs).

Closest homologues (THEM4 and THEM5) are included for comparison. Abbreviations: ACTH, acyl-CoA thioester hydrolase domain; BAAT, bile acid CoA:amino acid N-acyltransferase; EL, esterases lipase domain; HD, “hotdog” fold domain; START, steroidogenic acute regulatory protein (StAR)-related lipid transfer domain; THEM, thioesterase superfamily member. Taken from (Brocker et al., 2010)

1.3.1 α/β thioesterases

α/β -thioesterases can act towards different types of substrates. Based on that, they can be subdivided into protein thioesterases and acyl-CoA thioesterases.

Protein thioesterases

Protein thioesterases act on palmitoylated or myristoylated proteins. This is particularly important for regulation of protein trafficking, protein-protein interactions, and signaling. One well characterized protein, palmitoylthioesterase 1 (PPT1), has been implicated in the development of infantile neuronal ceroid lipofuscinosis, a severe neurodegenerative disease in children (Ahtiainen et al., 2006; Waliyany et al.,

2000). Ppt1, a lysosomal enzyme, cleaves thioester linkages in S-acylated proteins and removes palmitate residues, facilitating the degradation of these proteins. Ppt1 deficiency leads to the activation of an unfolded protein response, ER and oxidative stress, and neuronal apoptosis (Zhang et al., 2006) (Wei et al., 2008).

α/β fold acyl-CoA thioesterases and their functions

Acyl-CoA thioesterases are important participants in metabolic pathways in the cell. They are substrates for the majority of pathways that use fatty acids for energy production or for synthesis of complex lipids; they are substrates for β -oxidation in mitochondria and peroxisomes and ω -oxidation in the endoplasmic reticulum.

Termination of fatty acid synthesis is one of the established functions of α/β -fold acyl-CoA thioesterases. For example, thioesterase I is part of the multifunctioning enzyme fatty acid synthase (FAS), where it functions as an acyl-releasing domain. Induction of some of the thioesterases by peroxisome proliferators suggests that they are involved in lipid metabolism (Di Nunzio et al., 2009; Dongol et al., 2007; Westin et al., 2004).

1.3.2 Hotdog-fold thioesterases

Hotdog-fold proteins include a variety of enzymes, mainly thioesterases, which are involved in a number of metabolic processes, including cholesterol biosynthesis and plasma membrane composition. The hotdog fold, which is formed of several anti-parallel β -sheets wrapped around an α -helix, is found in all branches of life. However, up to now few mammalian proteins of this group have been described.

The key feature of such thioesterases is that the hotdog domain does not exist as a single entity: it must form at least dimeric structures. The proteins contain either one copy of the domain and form homodimers and/or more complex structures, or have two copies of the domain, which dimerize with each other. The tertiary structures

vary and can include either dimers, tetramers, or hexamers (Dillon and Bateman, 2004) (Figure 1.12).

Recently, Pidugu et al. presented an analysis of hotdog-fold proteins of known structures that allows classification of these proteins with regard to the nature of their substrate and oligomeric state (Pidugu et al., 2009). In this analysis, normal members of the PAAI family, like *E. coli* PAAI or human Them2, form tetramers in a back-to-back arrangement of the β -sheets, while other PAAI family members, like the hypothetical proteins with PDB codes 1IXI (*P. horikoshii*), 2HBO (*C. crescentus*), and 2OV9 (*Rhodococcus* sp.), are present as homodimers only, with altered tetramerization sequence motifs. The catalytic machinery of this class of proteins is well conserved, and is composed of an HGG motif and Asp/Thr residues. The carboxylate moiety is thought to deprotonate a water molecule prior to its nucleophilic attack on the thioester bond of the CoA-coupled fatty acid substrate, while the HGG motif at the N-terminal end of the central hotdog helix places the substrate thioester carbonyl group in the right position (Zhao et al., 2009).

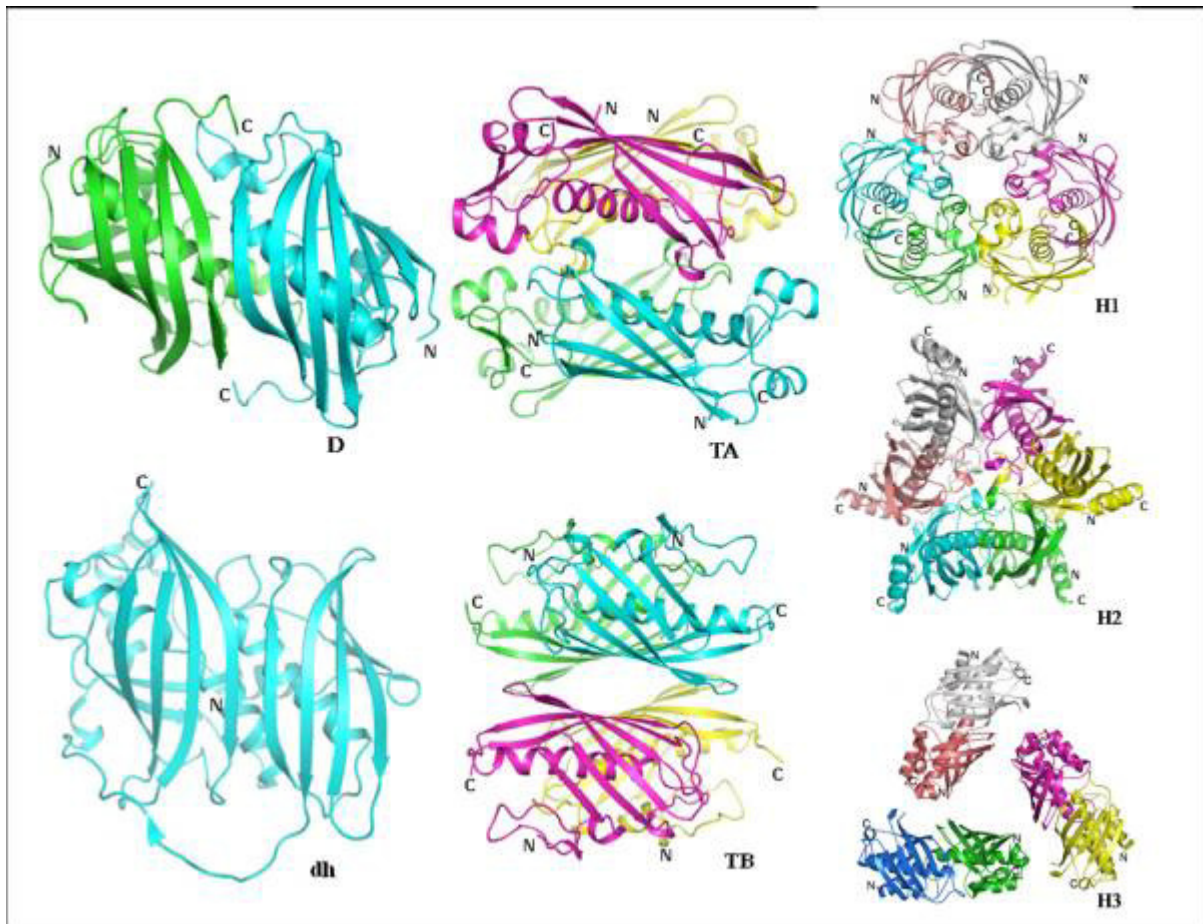


Figure 1.12

Various quaternary associations of hot dog fold proteins. D, dimer; dh, double hotdog; H1, hexamer with active site loops at interface; H2, hexamer with N-terminal helices at interface; H3, hexamer with head-to-tail arrangement of dimers; TA, tetramer with central helix interactions; TB, tetramer with back-to-back stacking of the β -sheets. $D_{dh}A$ (dimer of double hotdog with central helix interactions) is similar to TA while $D_{dh}B$ (dimer of double hotdog with back-to-back interaction of the β -sheets) is similar to TB. Tr_{dh} (trimer of double hotdog) is similar to H2. Taken from (Pidugu et al., 2009).

1.3.3 Functions of mammalian hotdog-fold thioesterases

The biological role of hotdog-fold thioesterases has not been fully addressed. A sequence and structure analysis of the hotdog fold-containing proteins carried out recently showed that consensus motifs in proteins may define the function and give a hint of the biological relevance of the proteins (Pidugu et al., 2009). These results suggest the substrate type that may be used by enzymes; however, they cannot provide information about any potential physiological role.

It has been suggested that Acot7 participates in the mediation of inflammatory reactions via involvement in eicosanoid metabolism (Forwood et al., 2007; Serek et

al., 2006). It has multiple splice variants, resulting in proteins with different subcellular localization; however, the biological role has only been addressed for its cytoplasmic isoform (Forwood et al., 2007). Them2, another mammalian hotdog thioesterase, also displays dual localization, cytosolic and mitochondrial (Cheng et al., 2006; Wei et al., 2009). It has been identified among proteins regulated by HNF4 α , raising the possibility that Them2 may be involved in renal cell carcinoma pathogenesis (Lucas et al., 2005). Another study has shown its interaction with the StarD2 protein (phosphatidylcholine transfer protein (PC-TP, a.k.a. StarD2)), suggesting that it has a role in fatty acid metabolism (Kanno et al., 2007).

Physiological roles of acyl-CoA and acyl-CoA thioesterases, and their deficiencies

In mitochondria, acyl-CoA thioesterases (Acots) lower increased levels of acyl-CoA (which have been imported through CPTI/II across the mitochondrial membrane from the cytosol). As a consequence, they counteract enhanced β -oxidation and reduce mitochondrial stress caused by any imbalance between fatty acid oxidation and TCA cycle/electron transfer chain activity during fatty acid overload. During these periods, when levels of acyl-CoA are high, excessive amounts of esters are preferentially hydrolyzed by Acots. It has been shown that the major site of H₂O₂ production during FA overload are the peroxisomes, and not the mitochondria (Elsner et al., 2011). In addition, mitochondrial β -oxidation may not be able to cope with the elevated levels of long-chain fatty acids which are associated with obesity and type 2 diabetes. This overload results in a larger proportion of fatty acids being metabolized via the peroxisomal β -oxidation system, leading to increased levels of toxic H₂O₂. Some inborn human disorders of mitochondrial fatty acid β -oxidation are known, and are characterized by fasting-induced episodes of hypoketotic-hypoglycemia, metabolic acidosis, hyperammonemia, and fatty livers (Roe, 2001).

During metabolic stress which induces hypoglycemia (fasting, thermal stress, viral infection), a “normal” infant should produce ketone bodies as a combined result of mitochondrial FAO and ketogenesis. This provides an alternate fuel to help spare glucose as metabolic requirements increase. In addition, β -oxidation is required to energize gluconeogenesis. Thus, in an infant with an inborn error in this pathway the glycogen stores are quickly depleted during metabolic stress. Due to an inadequate ketogenic response and other mechanisms, this infant would be unable to maintain blood glucose levels. These characteristic clinical symptoms are termed Reye-like syndrome (Gosalakkal and Kamoji, 2008). Patients have a varying phenotype ranging from no clinical signs to sudden death.

Several mouse models have been generated to study different steps during mitochondrial β -oxidation of fatty acids (Spiekerkoetter and Wood, 2010); they include mainly different types of dehydrogenases, and CPT-1a/b deficiencies (Spiekerkoetter and Wood, 2010).

In general, when sufficient nutrients are available, fatty acids are stored as triacylglycerol (TAG), mainly in adipocytes, and are released during starvation or metabolic stress. However, other non-adipose tissues are also able to deposit TAG, e.g. liver, β -cells, muscle, heart, and this leads to lipotoxicity.

Intracellular levels of acyl-CoA are known to correlate with insulin resistance and may lead to lipotoxicity in non-adipose tissues (Li et al., 2008a). The usual concentration of long-chain acyl-CoAs in the cytoplasm is between 1 and 20 μ M, although local concentrations can also be higher. Furthermore, the concentration of acyl-CoA and ACBP are similar, which suggests that most acyl-CoA is bound to its carrier.

The involvement of acyl-CoA in insulin sensitivity/resistance might be tissue-specific. In the pancreas, levels of acyl-CoA have been shown to regulate insulin secretion,

because in β -cells an increase in acyl-CoA levels enhances K_{ATP} channel activity and reduces β -cell excitability (Herrero et al., 2005).

Although there are a lot of indications of the importance of acyl-CoA levels in metabolic regulation, no direct mechanism has been proposed. In addition, the role of other fatty acid metabolites has not yet been completely resolved.

CTMP/Them4 is part of the PKB signaling regulation network and, when released from mitochondria upon induction of apoptosis, sensitizes cells to death by negatively affecting PKB phosphorylation and, in turn, activation (Maira et al., 2001; Parcellier et al., 2009a). A recent publication has shown that Them4 is a mitochondrial acyl-CoA thioesterase, with its activity directed mainly towards long-chain fatty acids (Zhao et al., 2009). Mitochondrial localization and the importance of correct CTMP/Them4 processing indicate the role this protein may play in the regulation of mitochondrial morphology (Parcellier et al., 2009b).

1.3.4 CTMP/Them4: mitochondrial acyl-CoA thioesterase and negative regulator of PKB signaling

The CTMP/Them4 protein has been identified in a yeast two-hybrid screening as interacting with and negatively regulating PKB (Maira et al., 2001). Additionally, there is information regarding hypermethylation of the CTMP promoter region in glioblastoma patients (Knobbe et al., 2004). Later, we showed that CTMP is a nuclear-encoded protein and is translocated to the mitochondria via its mitochondrial targeting sequence (MTS), which is cleaved off later on by mitochondrial peptidases (Parcellier et al., 2009a). The protein is located in the intramembrane space and is associated with the inner mitochondrial membrane. Cleavage of MTS, or, in other words, proper processing of CTMP, is important for maintaining mitochondrial morphology. In a knock-out mouse model we have shown that mitochondria from

CTMP1^{-/-} mice are more elongated and interconnected; these results were confirmed in a cell culture system using siRNA against CTMP (Parcellier et al., 2009b). CTMP interacts with Letm1, an inner mitochondrial membrane protein whose gene is located on chromosome 4 (4p16.3), in a region not present in patients suffering from Wolf-Hirschhorn syndrome (Endele et al., 1999; Piao et al., 2009) (see Figure 1.13). This syndrome is characterized by a neurological phenotype (seizures, mental retardation, etc.). Certain controversy exists concerning the Letm1 protein: it has been suggested as either a mitochondrial Ca²⁺/H⁺ antiporter, or K⁺/H⁺ exchanger (Jiang et al., 2009; Nowikovsky et al., 2004). Nevertheless, Letm1 protein and its yeast homolog, products of the YOL027 gene, have also been implicated in the regulation of mitochondrial morphology.

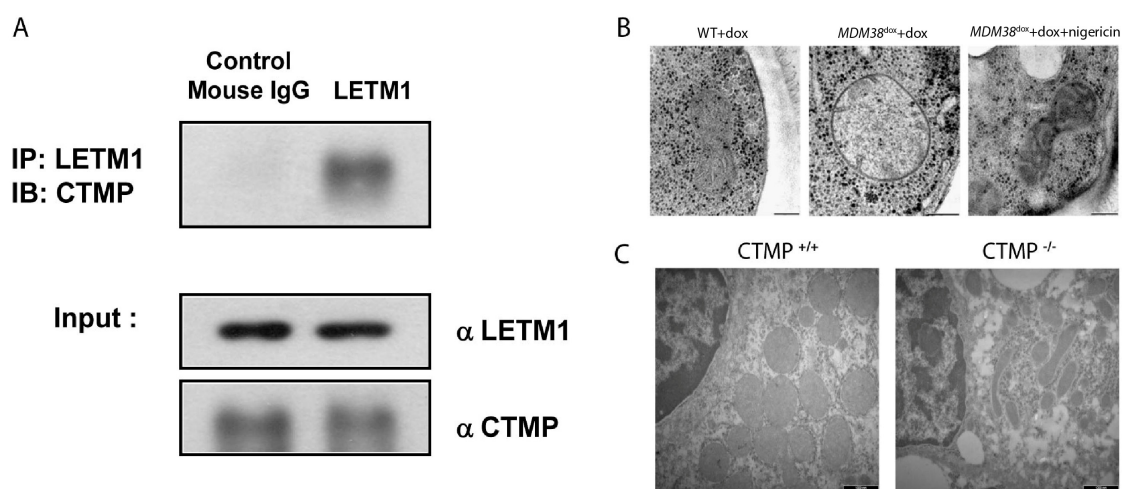


Figure 1.13

Interaction of CTMP protein with Letm1. (A) The interaction between the CTMP protein and Letm1 was assessed by co-immunoprecipitation. HEK 293 cell extracts were incubated with anti-LETM1 antibody and bound CTMP was assessed by immunoblotting with anti-CTMP antibody. From (Piao et al., 2009). (B) The yeast homolog of the Letm1 protein, Mdm38, has been shown to have K⁺/H⁺ exchange activity. Its loss is shown to associate with a number of phenotypes, such as reduced content of respiratory chain complexes, altered mitochondrial morphology, and loss of mitochondrial K⁺/H⁺ exchange activity resulting in osmotic swelling. The addition of nigericin, a polyether ionophore, can rescue the observed mitochondrial phenotype. From (Nowikovsky et al., 2004). (C) The loss of the CTMP protein leads to changes in mitochondrial morphology, resulting in the appearance of more elongated and interconnected organelles. Taken from (Parcellier et al., 2009b).

CTMP is also known as Them4, which stands for thioesterase superfamily member 4 (gene ID 117145 in Entrez/NCBI). The Pfam database shows the presence of a 4HBT domain in the CTMP protein, which is named after the founding member of the hotdog thioesterase family, 4-hydroxybenzoyl-CoA thioesterase (PF03061 accession in Pfam). Recently, CTMP has been experimentally shown to have thioesterase activity directed mainly towards fatty acid CoA esters (Zhao et al., 2009). Based on a 3D homology search, the authors proposed threading model of CTMP crystal structure which, together with the bioinformatics prediction, places CTMP into the thioesterase family, specifically hotdog-fold thioesterases.

The role of the CTMP protein as a negative regulator of PKB has been corroborated in the settings of apoptosis. We have shown that CTMP processing is important for its subsequent release from mitochondria upon induction of apoptosis (Parcellier et al., 2009a). Once released, it negatively regulates PKB phosphorylation, thereby promoting cell survival. In addition to *in vitro* apoptosis stimulation, CTMP inhibits PKB in response to ischemia-induced cell death, and prevents hippocampal neuronal injury in mouse models (Miyawaki et al., 2009). Thus, we have shown that mitochondrial acyl-CoA thioesterase CTMP/Them4 is an important regulatory component of PI3K/PKB signaling.

1.4 PKB SIGNALING PATHWAY AND ITS REGULATION

PKB/Akt is a ubiquitous and evolutionarily conserved serine/threonine kinase that is recognized as a major coordinator of various intracellular signals. It controls cell responses to extrinsic stimuli and regulates cell metabolism, proliferation, and survival. Proper tuning of PKB activity via direct or indirect mechanisms is of the utmost importance for stringent regulation of PKB-dependent cellular activities. Many

diseases, such as cancer or metabolic disorders, are the result of, or are associated with, aberrant activity of the PI3K/PTEN/PKB pathway. PKB has been implicated in the development of type 2 diabetes mellitus, non-alcoholic fatty liver disease, insulin resistance, liver tumors.

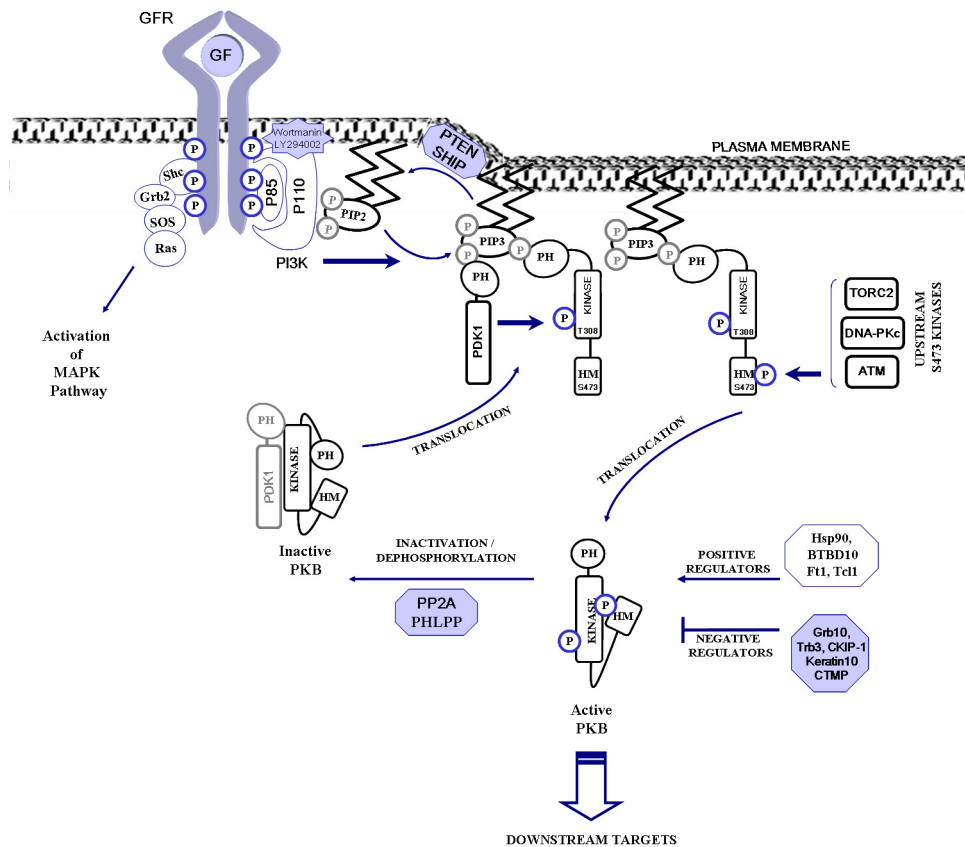
Serine/threonine kinase PKB/Akt is one of the major targets of phosphatidylinositol 3-kinase (PI3K)-generated signals and is involved in the regulation of cell growth, proliferation, apoptosis, glucose metabolism, angiogenesis, and migration.

The mammalian genome encodes three isoforms of Akt/PKB: Akt1/PKB α , Akt2/PKB β , and Akt3/PKB γ , which are highly conserved despite being the products of three different genes located on different chromosomes. When PKB is fully activated and is exerting its biological functions, it is phosphorylated at two sites, one located within the activation loop of the kinase domain (Thr308 in PKB α) and the other within the HM (Ser473).

1.4.1 Activating stimuli and upstream kinases

Growth factor binding promotes the recruitment and activation of class I PI3K after autophosphorylation of the receptor on tyrosine residues. At the membrane, PI3K phosphorylates PtdIns(4,5)P₂ to form PtdIns(3,4,5)P₃, which then serves as the docking site for a subgroup of proteins with PH domains. PI3K is involved in the regulation of a wide range of cellular processes, such as cell growth, proliferation, differentiation, motility, survival, and intracellular trafficking: many of these PI3K effects are mediated by downstream PKB. The constitutive activation of class I PI3K due to a gain-of-function mutation (in the p110 α catalytic subunit, for example) or the downregulation of its negative regulator PTEN (lipid phosphatase and tensin homolog deleted on chromosome 10) are striking features of many human cancers (Samuels et al., 2005).

Thus, inactive PKB/Akt is translocated to the plasma membrane (PM), undergoes a conformational change, attaches to a phospholipid through a PH domain and becomes phosphorylated (schematic representation of PKB activation is shown in Figure 1.14). Once recruited to the PM, PKB is activated in a two-step process that requires phosphorylation on both Thr308 in the activation loop of the kinase domain and Ser473 within the hydrophobic motif of the regulatory domain. Thr308 is phosphorylated by PDK1 kinase, which is recruited to the PM through its PH domain; there is also evidence that PKB may be pre-complexed with PDK1 in cytoplasm (Alessi et al., 1997; Calleja et al., 2007).



PKB monophosphorylated on Thr308 has ca. 10% of the activity of the fully phosphorylated enzyme. Additional Ser473 phosphorylation stabilizes the active conformation, allowing most PKB molecules to become fully active (Yang et al., 2002). The PI3K-related protein kinase family TORC2 complex, DNA-PK, and ATM are responsible for PKB-S473 phosphorylation. The fact that mTORC2 is a Ser473 kinase for PKB is widely recognized (Bhaskar and Hay, 2007; Sarbassov et al., 2005).

Work done on knock-out mice and *Drosophila* cells has provided genetic evidence favoring the hypothesis that components of the rapamycin-insensitive Rictor-mTOR complex have a shared positive role in the phosphorylation of the hydrophobic motif site of PKB (Sarbassov et al., 2005). DNA-PK has also been identified as an upstream Ser473 kinase of PKB (Bozulic et al., 2008; Feng et al., 2004); it phosphorylates PKB on Ser473 after DNA damage, thus promoting survival in response to genotoxic stress *in vivo* (Bozulic et al., 2008).

Figure 1.14

Schematic representation of PKB activation and regulation. Activation of growth factor receptors (GFR) by a ligand (insulin, growth factors (GF)) induces their autophosphorylation and recruits the p85 regulatory subunit of phosphatidylinositol 3-kinase (PI3K). Subsequent activation of the p110 catalytic subunit leads to phosphorylation of phosphoinositol-(4,5)-bis phosphate (PIP2) and formation of the phosphoinositol-(3,4,5)-tris phosphate (PIP3). PIP3 is a substrate for lipid phosphatase, the tensin homolog PTEN, and the SH2-domain-containing inositol polyphosphate 5-phosphatase SHIP, which act as endogenous inhibitors of the PI3K-dependent pathway, indirectly inhibiting PKB activity. Wortmannin and LY294002 also inhibit PI3K. Once formed, PIP3s serve as docking sites for the PH domains of PDK1 and PKB, which translocate to the plasma membrane from the cytoplasm. As a result of this translocation, inactive PKB is phosphorylated by PDK1 on Thr308 in a regulatory kinase domain. There are data to suggest that PKB is already pre-complexed with PDK1 in the cytoplasm. The second phosphorylation event on Ser473 in the hydrophobic motif (HM) by upstream kinases such as TORC2, DNA-PKc, and ATM is cell-type and stimulus specific. It leads to conformational changes in the PKB molecule and full activation of the kinase. Activated PKB then translocates to different subcellular compartments, such as the nucleus, ER, Golgi, and mitochondria, where it exerts its biological activity. Protein phosphatase 2A (PP2A) and a PH domain leucine-rich repeat protein phosphatase (PHLPP) dephosphorylate and inactivate PKB. Other negative regulators of PKB are Grb10, carboxyl-terminal modulator protein (CTMP), tribbles homolog 3 (Trb3), casein kinase 2-interacting protein-1 (CKIP-1), and keratin 10. Positive regulation of PKB activity may be achieved through interaction with BTBD10 and the heat shock proteins Hsp90 and Hsp27, which protect the PKB molecule from dephosphorylation. T-cell leukemia antigen-1 (Tcl-1) and fused toes protein-1 (Ft1) may also function as positive PKB regulators.

1.4.2 Negative regulation of PKB by phosphatases

Certain cellular mechanisms counteract PKB activation. Negative regulation of PKB could be mediated either by a direct mechanism, such as intra-molecular interactions, or indirectly by modulation of factors important for PKB activation.

The best-studied negative regulator of the PI3K/PKB pathway is PTEN, a tumor suppressor protein that is often inactivated in many disorders characterized by PKB hyperactivation, such as cancers and some metabolic diseases (described in detail below). This molecule acts as a lipid phosphatase by dephosphorylating PIP3 at the D3 position, converting it to PIP2. This leads to inhibition of the PI3K pathway and reduces recruitment of PDK1 and PKB to the PM, and thus subsequently decreases PKB activity. At the transcriptional level, PTEN is positively regulated by p53, Myc, Egr-1, and PPAR γ , whereas Ras, JNK, Notch, and miR-21 are negative regulators of PTEN transcription (reviewed in (Salmena et al., 2008)). Downregulation due to the loss of promoter activity or loss-of-function mutations of PTEN are distinct characteristics of many neoplastic diseases, including hepatocellular carcinoma (Horie et al., 2004; Hu et al., 2007).

Given that PKB is activated by increased phosphorylation, protein phosphatases are direct negative regulators acting on phosphorylated PKB. Protein phosphatase 2A (PP2A) acts as a negative regulator by dephosphorylating PKB at both sites (Andjelkovic et al., 1996; Ugi et al., 2004), but particularly at Thr308 (Gao et al., 2005). Heat shock protein 90 (Hsp90), a general chaperone to numerous targets, may inhibit PP2A-mediated dephosphorylation, offering PKB protection from inactivation. BTB (POZ) domain-containing protein 10 (BTBD10) has also been reported to interact with PKB and protect it from PP2A-mediated dephosphorylation (Nawa et al., 2008).

A further phosphatase directly dephosphorylating Ser473 is the PH domain leucine-rich repeat protein phosphatase PHLPP, which has a PP2C-like catalytic core, is not sensitive to okadaic acid, and binds directly to PKB via a C-terminal PDZ motif (Gao et al., 2005). This phosphatase is markedly reduced in several colon cancer and glioblastoma cell lines with elevated PKB phosphorylation. Recently, a second PHLPP isoform, PHLPP2, has been cloned (Brognard et al., 2007). In parallel to the different tissue expression patterns and substrate specificities of the different PKB isoforms, the PHLPP isoforms have been reported to show specificity for distinct PKB isoforms. PHLPP1 was shown to affect PKB β/γ , while PHLPP2 influences the activity of PKB α/γ , with marked differences in the affected PKB substrates. These data led to speculation that PHLPP1 may regulate PKB β and affect glucose metabolism, whilst PHLPP2 may be involved mostly in the regulation of PKB α and cell survival (Brognard et al., 2007).

Regulation of the PI3K/PKB pathway by reactive oxygen species

Reactive oxygen species (ROS), which are now recognized as second messengers, play an important role in regulating the PI3K/PKB/PTEN pathway. At lower concentrations, they are required for normal cell functioning and intracellular signaling; “physiological” ROS are produced at the plasma membrane by NADP(H) oxidases in a response to stimulation of many growth factors (Rhee, 2006; Tonks, 2006) (See Figure 1.15). Oxidative stress, which is prevalent in malignant, as well as diabetic, conditions, and impaired mitochondrial function lead to increased levels of intracellular ROS.

The primary source of ROS is the superoxide O_2^- , which is generated by complex I and complex III of the electron transfer chain in the mitochondria; superoxide is then converted to hydrogen peroxide H_2O_2 by superoxide dismutase, and then to oxygen

and water by a number of enzymes that include catalase, glutathione peroxidases (Gpx), and thioredoxin. The highly reactive $\text{OH}\cdot$ radical is a product of H_2O_2 transformation via Fenton's reaction; it reacts instantaneously with the nearest molecules. H_2O_2 activity is directed towards redox-sensitive cysteine residues within proteins. It is a weak oxidizing agent, and its effects depend on the concentration. PTEN and PTP1B have been shown to be direct targets of ROS: oxidation of active Cys residues in their molecules leads to the formation of inactive configurations, which cannot function normally (Tonks, 2006).

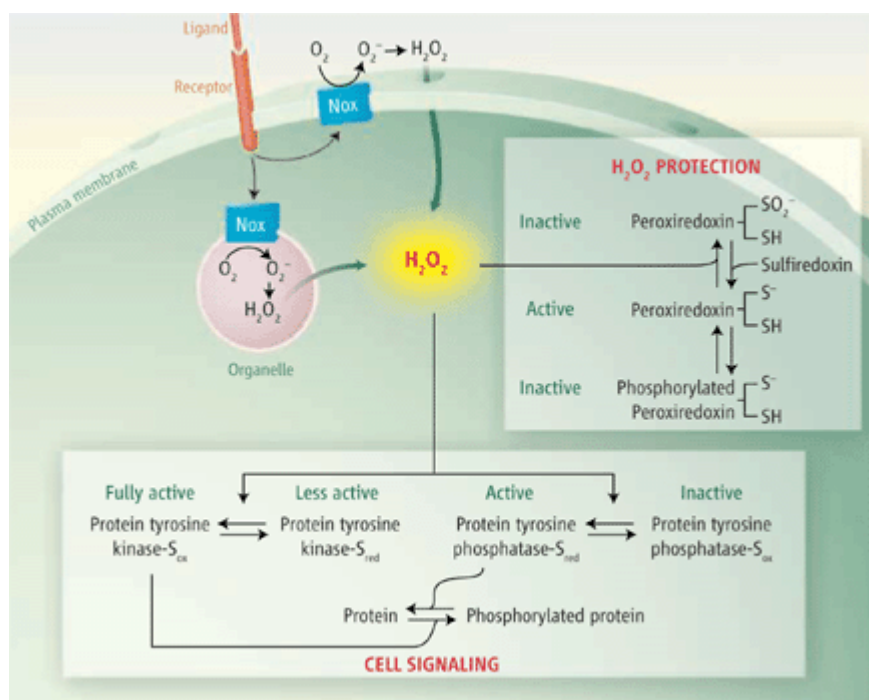


Figure 1.15

H_2O_2 production, protection, and signaling actions. The activation of various cell surface receptors activates Nox, situated either in the plasma membrane or in the membrane of organelles such as endosomes, to produce H_2O_2 . To function as an intracellular signaling molecule, H_2O_2 must be imported into the cytosol. Cytosolic H_2O_2 enhances protein tyrosine phosphorylation by inactivating protein tyrosine phosphatases while activating protein tyrosine kinases. Transient protection of the H_2O_2 signal from abundant cytosolic peroxiredoxin appears to be caused by reversible inactivation of these enzymes through either hyperoxidation or phosphorylation. Taken from (Rhee, 2006).

In addition to PTEN and PTP1B actively participating in PI3K/PKB signaling and promoting insulin sensitivity, it has been shown that ROS are important contributors to maintaining insulin sensitivity (Loh et al., 2009). Thus, Gpx1 activity has been

shown to interfere with insulin function by substantially decreasing the amount of intracellular ROS required for insulin sensitizing. Mice overexpressing Gpx1 develop insulin resistance and obesity, whereas Gpx1 knock-out mice display insulin hypersensitivity as a result of enhanced PI3K/PKB signaling (McClung et al., 2004), (Loh et al., 2009).

1.4.3 Role of PKB in insulin resistance, non-alcoholic fatty liver disease and hepatosteatosis

Among liver diseases, non-alcoholic fatty liver disease (NAFLD) is becoming increasingly common; every third adult and tenth child/adolescent in the USA is affected by this condition (Angulo, 2007). NAFLD is considered to be a hepatic manifestation of a metabolic syndrome. The prerequisite feature of NAFLD is increased accumulation in hepatocytes of lipids, which can originate either from increased levels of non-esterified fatty acids (NEFA) circulating in the blood or from enhanced *de novo* synthesis of lipids in the cells. Although simple steatosis seems to have a relatively benign clinical course, a subgroup of patients develops inflammatory changes, known as non-alcoholic steatohepatitis (NASH) and, potentially, liver cirrhosis which carries an increased risk of hepatocellular carcinoma (Rector et al., 2008). An increase in intracellular lipid metabolites may lead to activation of the PI3K/PKB pathway. Initial overactivation of the signaling cascade then results in IRS-1 inhibition, which mediates a negative feedback effect on PI3K activation, leading finally to the inhibition of insulin signaling. Patients with NAFLD display lower levels of phosphorylated PKB and an increase in Bax/Bcl-2 ratio (Piro et al., 2008). A similar situation has been described for activated PKC ϵ , which led to decrease in insulin-stimulated IRS-2 phosphorylation and hepatic insulin resistance (Samuel et al., 2004). Later, insulin resistance involves other peripheral organs, such

as skeletal muscle and adipose tissue, eventually becoming systemic. Under physiological conditions, insulin released from the pancreas decreases glucose output from the liver but stimulates glucose uptake by muscle and adipose tissue. In patients with insulin resistance, a syndrome associated with impaired metabolic clearance of glucose, the concentration of NEFA in the bloodstream increases due to the high lipogenic effect of insulin. NEFA act by reducing adipocyte and muscle glucose uptake and promoting hepatic glucose output, which leads to increased blood glucose concentration. Obesity worsens that situation and leads to increased levels of NEFA released directly into the portal vein from visceral adipose. This adds to the vicious cycle, leading to even higher insulin resistance.

The current view of NAFLD development may be presented as a “two-hit theory”: Liver degeneration due to lipid accumulation occurs first and this condition is later boosted by inflammatory cytokines, endotoxins, iron accumulation, and oxidative stress (Mendez-Sanchez et al., 2007). To a large extent, the latter is caused by increased intracellular lipids. The effects of lipotoxicity on β cells (Joseph et al., 2004; Lupi et al., 2002) and cardiomyocytes (Dyntar et al., 2001) have been studied most, but hepatocytes are also significantly affected, via a direct or an indirect mechanism, often displaying mitochondrial dysfunction (Li et al., 2008b). Key characteristics of mitochondrial dysfunction are respiratory chain defects that lead to an increase in ROS production. This, in turn, has damaging effects on cellular organelles and molecules. In addition to damaging mtDNA and respiratory chain enzymes, an increase in ROS leads to the oxidation of many cytoplasmic enzymes, including PTEN. Thus it is now clear that ROS are not only deleterious for the cell but are very important with respect to signaling molecules (Rhee, 1999). Their presence at low concentrations helps maintain certain basal levels of kinase activity, namely PI3K/PKB, in cells not supplemented with growth factors. However, when

cells are overloaded with ROS, this may lead to hyperactivation of the PI3K/PTEN/PKB pathway, inhibition of FoxO1 and PGC-1 α , and transcription of adipogenic-, lipogenic-, and β -oxidation-related genes. This leads to liver steatosis and, potentially, to hepatic tumorigenesis.

The role of cell types other than hepatocytes in insulin resistance should not be neglected. Sinusoidal liver cells are often ignored, but they are an important factor in the maintenance of the pathological situation of insulin resistance, exacerbating the oxidative damage of hepatocytes, as well as secreting the pro-inflammatory cytokines TNF- α and IL6 (Leclercq et al., 2007). It has been suggested that the degree of insulin sensitivity depends on the state of activation of stellate cells, which have phosphorylated IR and IRS1 when activated and do not respond further to insulin, thus failing in glucose uptake. Their activation brings hepatic tissue one step closer to the development of fibrosis and, ultimately, cirrhosis (Delibegovic et al., 2007; Leclercq et al., 2007).

Involvement of phosphatases in insulin sensitivity

Targeting the PI3K/PKB pathway via a decrease in phosphatase activity, and negative regulation of PKB activity, is beneficial for the restoration of insulin sensitivity. This is shown by the protein tyrosine phosphatase 1 B (PTP1B), which negatively regulates insulin receptor and IRS-1 signaling knock-out mice. Disruption of the PTP1B gene in mice leads to enhanced insulin sensitivity and a decrease in adipose mass. In mice with polygenic insulin resistance, PTP1B deficiency results in improved glucose tolerance and a decrease in the occurrence of diabetes (Xue et al., 2007). Similarly, muscle-specific KO of PTP1B also has a beneficial effect on insulin sensitivity (Delibegovic et al., 2007).

Another clear example of increased insulin sensitivity due to loss of lipid

phosphatase activity is PTEN knock-out mice. Quite unexpectedly, in addition to the insulin-hypersensitive phenotype, liver-specific PTEN knock-outs suffer from hepatomegaly and fatty livers, being at the same time leaner than their wildtype littermates (Stiles et al., 2004). These mice have low levels of NEFA in the plasma and relative hypoinsulinemia, concomitant with the higher PKB activity. They display an increased liver glycogen content and enhanced FA synthesis and secretion. PTEN null mice are, in principle, a further model of NAFLD that does not involve overnutrition, and is not polygenic in nature. These mice are valuable because of the absence of obesity/type 2 diabetes, which is not thought to be mandatory for insulin resistance but only an associated complication. PTEN null mice provide a new insight into the *in vivo* role of PTEN, underlying the importance of negative PKB regulators in the liver insulin-signaling pathway. Hepatocellular carcinoma (HCC), recognized as a complication of NAFLD, is often accompanied by PTEN downregulation, leading to a poor prognosis for HCC patients (Sato et al., 2000). Deregulation of PTEN activity may be due to hypermethylation of its promoter (Ping et al., 2006) or loss-of-function mutations (Wang et al., 2007). Alternatively, PTEN may be the target of increased ROS in cells, leading to its oxidation and the blockage of the catalytic cysteine residues important for proper function (Lee et al., 2002). In this context, PTEN heterozygous and liver-specific KOs are invaluable models for studying the pathogenesis of NAFLD, which later develops into steatohepatitis and progresses to liver carcinoma without any additional exogenous treatment.

2. AIM OF THE THESIS

The aim of my thesis was to functionally characterize the novel protein CTMP2/Them5. This protein has been identified in the laboratory of Brian Hemmings as a paralog of the CTMP1/Them4 protein. CTMP1 was previously described as an interactor and negative regulator of protein kinase B (PKB)/Akt. We have shown that CTMP1 is a mitochondrial protein and exerts its function once released from mitochondria upon apoptosis induction. In addition, it has been shown to regulate mitochondrial morphology. The role of CTMP2/Them5 is currently largely unknown; in the databases both CTMP1/Them4 and CTMP2/Them5 are classified as hotdog-fold thioesterase family members. Thus, the work focused on the functional and structural characterization of CTMP2/Them5 protein by using *Them5*^{-/-} mouse models and *in vitro* approaches.

3. RESULTS

3.1

Analysis of the novel acyl-CoA thioesterase Them5 reveals a role in mitochondrial morphology and fatty liver disease development.

Elena Zhuravleva¹, Heinz Gut¹, Debby Hynx¹, Christopher K. E. Bleck^{1,2}, David Marcellin³, Christel Genoud¹, Peter Cron¹, Jeremy J. Keusch¹, Bettina Dummier¹, Mauro Degli Esposti⁴, Brian A. Hemmings^{1*}

¹ Friedrich Miescher Institute for Biomedical Research, Maulbeerstrasse 66, 4058 Basel, Switzerland

² Center for Cellular Imaging and Nano Analytics C-CINA, Focal Area Structural Biology and Biophysics, Biozentrum University Basel, WRO-1058 Mattenstrasse 26, 4058 Basel, Switzerland

³ Novartis Pharma AG, Forum 1, Novartis Campus, 4056 Basel, Switzerland

⁴ Faculty of Life Sciences, The University of Manchester, Michael Smith building, Oxford Road, M13 9PT Manchester, UK

Analysis of the novel acyl-CoA thioesterase Them5 reveals a role in mitochondrial morphology and fatty liver disease development

Elena Zhuravleva¹, Heinz Gut¹, Debby Hynx¹, David Marcellin², Christopher K. E. Bleck^{1,3}, Christel Genoud¹, Peter Cron¹, Jeremy J. Keusch¹, Bettina Dummmler¹, Mauro Degli Esposti⁴, Brian A. Hemmings¹

¹ Friedrich Miescher Institute for Biomedical Research, Maulbeerstrasse 66, 4058 Basel, Switzerland

² Novartis Pharma AG, Forum 1, Novartis Campus, 4056 Basel, Switzerland

³ Center for Cellular Imaging and Nano Analytics C-CINA, Focal Area Structural Biology and Biophysics, Biozentrum University Basel, WRO-1058 Mattenstrasse 26, 4058 Basel, Switzerland

⁴ Faculty of Life Sciences, The University of Manchester, Michael Smith Building, Oxford Road, M13 9PT Manchester, UK

SUMMARY

Acyl-CoA thioesterases hydrolyze thioester bonds in acyl-CoA metabolites. The majority of mammalian thioesterases are α/β -hydrolases and have been well studied, but Hotdog-fold enzymes have been less well described. Here, we present a structural and functional analysis of a new mammalian mitochondrial thioesterase, Them5. Them5 and its paralog Them4 adopt the classical Hotdog-fold structure and form homodimers in crystals, representing a new group of these enzymes. *In vitro* Them5 shows strong thioesterase activity with long-chain acyl-CoAs. *Them5*^{-/-} mice have highly interconnected mitochondria; this effect depends on the enzymatic activity of Them5. Loss of Them5 specifically alters the remodeling process of the mitochondrial phospholipid cardiolipin. *Them5*^{-/-} mice develop fatty livers, lipid metabolism is deregulated, and mitochondrial respiration and β -oxidation are impaired.

This paper presents this novel mitochondrial thioesterase Them5 and its specific role in the cardiolipin remodeling process, connecting it to the development of fatty liver and related conditions.

Highlights

- Them5 is a novel mitochondrial acyl-CoA thioesterase of the Hotdog-fold family
- Them5 enzymatic activity is important for mitochondrial morphology and function
- Loss of Them5 specifically alters re-acylation of cardiolipin with long acyl-CoAs
- *Them5*^{-/-} mice develop fatty livers due to the accumulation of acyl-CoAs

INTRODUCTION

Thioesterases hydrolyze thioester bonds in a variety of substrates, including fatty acid CoA esters and palmitoylated or myristoylated proteins; and participate in lipid metabolism (Hunt and Alexson, 2002). According to their protein fold and the catalytic reaction mechanism, thioesterases are subdivided into two groups: α/β -hydrolases and Hotdog-fold thioesterases. Subcellular localization of thioesterases varies: they are found in the cytoplasm, peroxisomes, and mitochondria. Whereas the majority of mammalian thioesterases are α/β -hydrolases and have been well studied, mammalian Hotdog-fold enzymes have only been described to a lesser extent. Here, we present a new mammalian mitochondrial thioesterase, Them5, that belongs to the Hotdog-fold enzyme family. It is encoded by the nuclear genome and is imported into mitochondria, where it resides in the matrix and is also found to associate with the inner mitochondrial membrane facing the matrix side. We show that Them5 is a thioesterase which directs its activities towards fatty acid-CoA esters. We have determined the crystal structure of Them4 and Them5 at resolutions of 1.6 Å and 1.45 Å respectively, and have shown that they adopt the classical Hotdog-fold, with six β -sheets wrapped around a central α -helix. Recent studies have shown that mammalian Hotdog proteins are organized in tetrameric or higher-order structures but both Them4 and Them5 form independent homodimers in crystals, thus representing a new group of these enzymes. We have also identified residues which participate in the formation of the active center, and describe general structural features of these enzymes.

The physiological role of mammalian Hotdog-fold thioesterases has not been well described, except in recent studies concerning Acot13/Them2, which have shown both mitochondrial and cytoplasmic localization, and Acot7, which has been implicated in inflammatory processes (Cao et al., 2009; Forwood et al., 2007). To study the physiological role of Them5, we generated knock-out mice which show a highly interconnected, elongated mitochondrial network compared to wildtype mice. Overexpression of a thioesterase-dead version of Them5 in cell culture leads to the appearance of an interconnected mitochondrial network as

in *Them5*^{-/-} tissues, indicating that the enzymatic activity of Them5 is important for maintaining normal mitochondrial morphology. *Them5*^{-/-} mice show increased levels of a specific metabolite of cardiolipin (CL) among their mitochondrial lipids, indicating that Them5 activity is implicated in the remodeling of CL within mitochondria. Knock-out mice develop fatty liver disease and β -oxidation is impaired, accompanied by an overall deregulation of lipid metabolism. These phenotypic effects can be explained by the loss of thioesterase activity of Them5 in mitochondria, where long-chain acyl-CoAs cannot be hydrolyzed any more and are then exported into the cytosol, contributing to intracellular lipid accumulation. Hence, our study identifies Them5 as a novel enzyme participating in CL metabolism, whose removal progressively reverberates from mitochondria to the metabolism of fatty acids in the whole body.

RESULTS

Them4/5 are dimers of a Hotdog-fold

Them4 and Them5 genes are located on chromosome 1 in humans, 20kb apart (chromosome 3 in mice, and 10kb apart) and share exon-intron structure (Figure S1A). A search of databases shows that Them4 orthologs are present in lower eukaryotes, including yeasts (FMP10, NC_001137.2), whereas Them5 orthologs have only been found in mammals (Figure S1B). Bioinformatics analysis of the Them5 protein suggests that it belongs to the Hotdog-fold thioesterase family of proteins.

We used the molecular replacement method to determine the crystal structures of human Δ 34Them5 and Δ 36Them4 to a resolution of 1.45Å and 1.6 Å, respectively (data collection and refinement statistics are given in Table S1). Δ 34Them5 crystallized in space group C222₁, with one molecule per asymmetric unit (a.u.) representing half of the biologically active homodimer, while Δ 36Them4 crystallized in space group P1 with two independent homodimers per a.u. Clear electron density allowed model building of residues 52-247 (Δ 34Them5) and 42-234 (Δ 36Them4), with a disordered stretch of residues that could not be

built in both structures due to lack of electron density (102-111 and 81-105 for $\Delta 36\text{Them4}$ and $\Delta 34\text{Them5}$, respectively). Crystal structures of $\Delta 36\text{Them4}$ and $\Delta 34\text{Them5}$ show that both proteins do indeed belong to the Hotdog-fold superfamily typical of thioesterases (Figure 1A). The core structure of the thioesterase Hotdog fold encompasses residues 119-231 and 125-237 for $\Delta 36\text{Them4}$ and $\Delta 34\text{Them5}$, respectively, and consists of a long central α -helix surrounded by a six-stranded curved antiparallel β -sheet. In both proteins, two of these core domains form a stable homodimer related by a two-fold symmetry axis, and the extension of the β -sheets to a continuous anti-parallel 12-stranded β -sheet contributes the most to dimer stabilization. In both molecules, ~120 N-terminal residues are mostly in a coiled conformation, with the exception of extended α -helices formed by residues 55-68 ($\Delta 36\text{Them4}$) and 64-79 ($\Delta 34\text{Them5}$) that is tightly attached to the convex side of the curved β -sheet via hydrophobic interactions with the first and second strand. The two proteins have a very similar structure and have an r.m.s. deviation of only 0.8 Å (0.8 Å r.m.s. deviation over 165 residues) at a sequence identity of 38%. A search of the Protein Data Bank (PDB) using DALI identified the structures of a hypothetical *P. aeruginosa* protein PA5202 (1ZKI, 1.6Å, 115), the *T. thermophilus* protein PAAI (1J1Y, 1.4Å, 110), and the human Them2 protein (3F5O, 2.1Å, 124) as being most similar to $\Delta 36\text{Them4}$ (PDB codes, r.m.s. deviations, and length of the structural alignments given in parentheses) (Holm and Sander, 1993). The same analysis for $\Delta 34\text{Them5}$ showed that the structures of a putative thioesterase YHDA from *L. lactis* (3GEK, 1.7Å, 120), human Them2 (3F5O, 2.0Å, 122), and the PAAI protein from *T. thermophilus* (1WLV, 1.9Å, 116) were structurally most related.

Figure 1. Them4 and Them5 are Hotdog-fold dimers

(A) Crystal structures of $\Delta 34$ Them5 (blue and orange) and $\Delta 36$ Them4 (gray, transparent) are superimposed and displayed in a stylized representation. N- and C-terminal residues in the $\Delta 34$ Them5 structure are labeled, and disordered stretches that are not included in the model are shown as dotted lines.

(B) Surface representations of the $\Delta 34$ Them5 crystal structure rotated through $\sim 120^\circ$ along a vertical axis. Surface-exposed residues conserved in both Them4 and Them5 (for the ClustalW multiple sequence alignment see Figure S2) are highlighted in red and orange (computed using ConSurf, <http://consurf.tau.ac.il/>, ConSurf color code 9, 8, respectively). A black circle indicates the putative binding site of the CoA-linked acyl chain, an asterisk marks the catalytic center, and an arrow points to Them5 residues Glu168 and Lys172 which interrupt the long open channel present in the Them4 structure. A blue circle shows conserved residues on the surface of the central β -sheet that are likely to be involved in binding the CoA phospho-ADP module. Them5 residues 89-101 and 238-247 are not displayed to make the image clearer.

(C) Stylized representation of the putative $\Delta 36$ Them4 active site. Homodimer subunits are shown in cyan and gray, with those residues expected to be involved in catalysis and substrate recognition displayed as sticks (atom colors).

(D) Stylized representation of the putative $\Delta 34$ Them5 active site. Similar representation as in (C), but with homodimer subunits and active site residues in blue and orange.

(E) ClustalW multiple sequence alignment of selected Them5 (human, mouse, giant panda, bovine) and Them4 (bovine, rat, mouse, human) sequences (without predicted MTS). Conserved residues are boxed in red, and secondary structure elements present in the $\Delta 34$ Them5 and $\Delta 36$ Them4 crystal structures are indicated at the top and bottom of the alignment, respectively. The first residues present in the crystallographic models are highlighted with open arrows. Disordered stretches with no electron density, not included in the models, are shown in yellow shading; mutations used in this study are highlighted with red triangles (dimerization mutants) and a red asterisk (enzymatically inactive mutant).

Them5 is a functional acyl-CoA thioesterase

We analyzed the protein sequences of the Them4 and Them5 remote homologs in order to find conserved sequence motifs (Figure S2). By using structural information from 4HBT thioesterase from the founding family member *Arthrobacter* sp. SU, hTHEM2, Acot7 and comparing this with the Them5 protein sequence, we proposed residues that may be important for Them4/5 secondary and tertiary structure formation and enzymatic activity. Our analysis pointed to the presence of a highly conserved HGG...D motif, which has also recently been reported to be an important consensus sequence motif in many thioesterases, and which is present in all aligned sequences (Pidugu et al., 2009). As expected from our sequence analysis, both $\Delta 36$ Them4 and $\Delta 34$ Them5 crystal structures have two active sites per homodimer, located at the end of each Hotdog helix, with residues from both subunits contributing to catalysis. The main catalytic residues are indeed the HGG motif 152-154 and 158-160 (for $\Delta 36$ Them4 and $\Delta 34$ Them5, respectively) on one subunit and Asp161/Thr177 ($\Delta 36$ Them4) and Asp167/Thr183 ($\Delta 34$ Them5) located on the other subunit (Figure 1C,D). These residues are supposed to bind and hydrolyze the thioester moiety of the acyl-CoA

substrate. They are located in the middle of a long L-shaped channel which is limited in length by a stretch of residues from the N-terminal part (74-79 in $\Delta 36$ Them4 and 83-88 in $\Delta 34$ Them5) that likely defines the length of the CoA-coupled fatty acids accepted for turnover. This channel is less deep and less open in Them5, where the Them4 residues Ala162 and Met166 are positionally exchanged with Glu168 and Lys172 which, together with Asn91, form an extended and elevated hydrogen bond network.

In order to characterize the Them4/5 molecules more closely, a ConSurf analysis was carried out and the functionally relevant residues were mapped onto the surface of the Them5 crystal structure (Figures 1B, S2). As expected, the catalytic machinery is fully conserved, and comparison with related structures reveals Asp161 (Them4) and Asp167 (Them5) to be critically important.

We next confirmed that Them5 is an active thioesterase *in vitro*. Full-length Them5 purified after expression in bacteria does hydrolyze acyl-CoAs (Figures 2A, S3A). Interestingly, Them5 showed high activity toward long-chain acyl-CoA esters, which was comparable to published data about Them4 (Figure 2C) (Zhao et al., 2009). However, in contrast to Them4 (Zhao et al., 2009), Them5 showed very low activity with acetyl-CoA as a substrate (Figures 2A,C, S3A,B). Thus, Them5 does indeed have a different substrate specificity, as suggested by our structural analysis of substrate binding channels (Figure 1B,C,D). The ConSurf analysis identified a conserved region at the end of the L-shaped acyl-CoA binding channel that consists of Ser78, Thr112, Arg113, and Tyr123 (Them4). In Them4, these residues define the end of the hydrophobic flat-shaped channel which is thought to bind the acyl group. The substrate binding channel of Them5 is strikingly different: side chains of Glu168 and Lys172 form a polar, barrier-like elevation in the middle of this channel, restricting binding to the conserved residues (Ser87, Thr117, Arg118, Tyr129) that form a cavity (Figure 1B). These differences in acyl binding sites likely result in different affinities for substrates, thereby determining specificity.

According to our crystallographic model of the active centers of Them4 and Them5 (Figure 1 C,D), we propose that D167 in Them5 is the key catalytic residue. Indeed, when alanine was

substituted, the D167A Them5 mutant did not display any catalytic activity, which is consistent with our hypothesis (Figures 2B,C, S3B).

We carried out size exclusion chromatography experiments to study the oligomeric states of Them4/5 in solution using highly purified recombinant proteins. Similarly to studies published previously, we found that $\Delta 36$ Them4 elutes as a dimer of around 46 kDa, with a minor fraction present as a homotetramer (~105 kDa) (Zhao et al., 2009). $\Delta 34$ Them5, on the other hand, elutes as a homodimer with an apparent molecular mass of ~45 kDa (Figure S4B). A strong argument for the dimeric state of Them4/5 in their native form is also the fact that they always appear as independent homodimers, irrespective of the crystal packing and number of molecules in the a.u. (Figure S4A). In all of these cases, neither molecules in the a.u. nor molecules related by crystallographic symmetry have any higher oligomeric state than independent homodimers. This finding was confirmed in an analysis of the quaternary structure of molecules in the crystals using the PISA software (Krissinel and Henrick, 2007). We transfected Them5 mutants cDNA lacking the mitochondrial targeting sequence (MTS) and having mutations in either the α -helix or the β -sheet needed for dimerization in HEK293 cells, and found that they expressed at low levels only, probably due to their intrinsic instability (Figure S4C,D). Those results confirm that Them5 does indeed form dimers, and cannot exist as a monomer in solution.

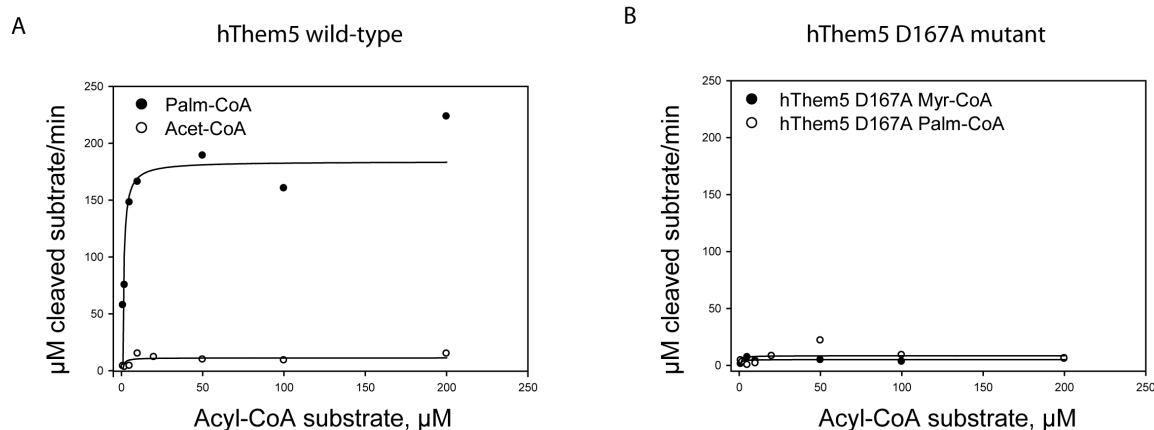


Figure 2. Them5 is an acyl-CoA thioesterase

(A) Saturation curves of reaction rate for acyl-CoA substrates obtained for wildtype hThem5 and (B) D167A hThem5 mutant at 37°C. Lines indicate fitting of the experimental data to the Michaelis-Menten equation.

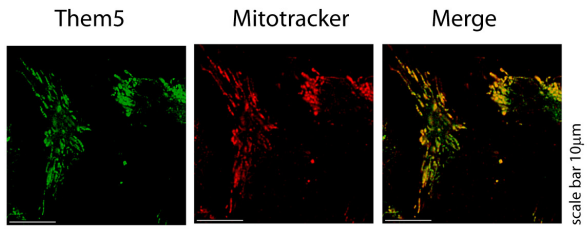
(C) Them5 hydrolyses long-chain acyl-CoA esters. Steady-state kinetic constants for hThem5-catalyzed hydrolysis of selected acyl-CoAs obtained at pH7.5 and 22°C or 37°C. The reaction was carried out in the presence of 0.5 mM DTNB and followed at 412nm wavelength.

Them5 is a mitochondrial protein

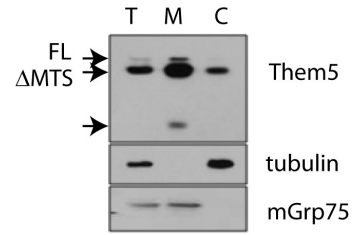
Bioinformatical analysis of Them5 [MitoProt, TargetP, iPSORT] showed the presence of the mitochondrial targeting sequence in the N-terminal part of the human Them5 protein, and its orthologs in other species (Figure S2). Immunofluorescence analysis shows an overlap of the staining pattern of the protein with the mitochondria-specific marker MitoTracker Red (Figure 3A). Confocal image analysis showed 85.5% co-localization of endogenous protein with MitoTracker Red. According to the bioinformatical analysis using MitoProt II, the cleavage site is located after Ser32 (Claros and Vincens, 1996). Like the majority of nuclear-encoded mitochondrial proteins, Them5 possesses a mitochondrial targeting signal which is

cleaved off by mitochondrial proteases once the protein has been imported into the mitochondria. This explains the appearance of the double band in western blot experiments. The Them5 sequence lacks a conserved consensus motif for MPP cleavage (RXX(X)SX), and we could not identify any residues important for that cleavage (data not shown). Besides, the MTS of Them4 and Them5 are different, which may be reflected in different intramitochondrial localization of the proteins (see below). Anti-Them5 antibodies detected two bands of protein on immunoblots, corresponding to the processed (faster migrating band) and non-processed forms of the Them5 protein (Figure 3B). Additionally, we were able to detect a band at around 17 kDa, which appears in the mitochondrial fraction samples (Figure 3B). It is most likely to be a product of further protein processing in mitochondria. However, the biological relevance of this cleaved form is not yet clear. By overexpressing a C-terminally HA-tagged version of Them5 we were able to confirm that the full-length protein resides specifically in the mitochondria (Figures 3C, S5A), whereas a mutant lacking the first 37 N-terminally located amino acids (Δ MTS) is excluded from mitochondria (Figure 3D). We chose to delete the first 37 amino acids because of the secondary structure prediction of a positively charged random coil from this region (Combet et al., 2000). To assess mitochondrial localization of Them5 in more detail, we performed immunogold electron microscopy. The 2D-EM analysis of cells overexpressing HA-tagged Them5 and endogenous Them5 in U2OS cells (Figure 3E) showed that Them5 is located mainly in the matrix of mitochondria and on the internal face of the inner mitochondrial membrane (IMM). The intramitochondrial localization of Them5 is different from that of Them4, which has been previously shown to reside in the intermembrane space of mitochondria (Parcellier et al., 2009a).

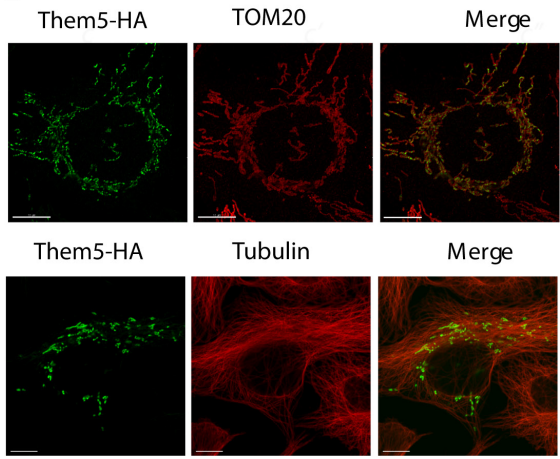
A



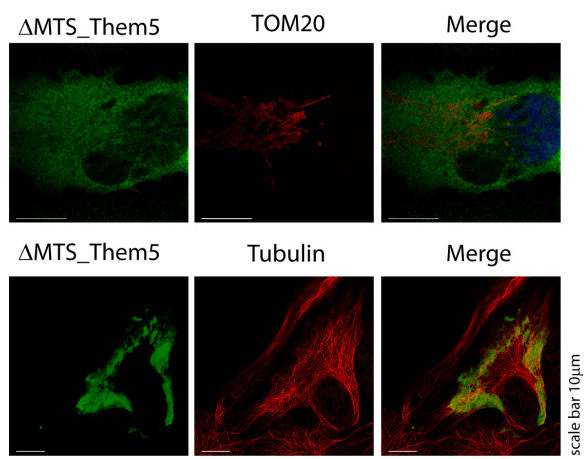
B



C



D



E

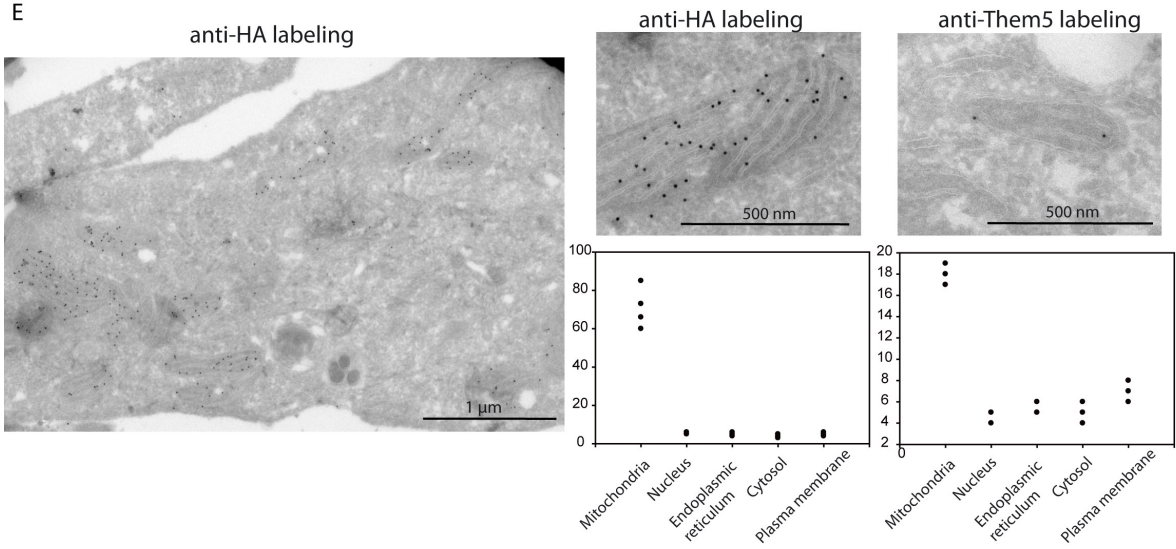


Figure 3. Them5 is a mitochondrial protein localized in the mitochondrial matrix, and is associated with the matrix side of the inner mitochondrial membrane

(A) Immunofluorescence analysis of mitochondrial localization of hThem5. U2OS cells were fixed and stained with antibodies against hThem5. Mitotracker Red was used for mitochondria visualization. Co-localization of Them5 with Mitotracker Red is 85.5%, as assessed by Imaris analysis of the confocal images.

(B) HEK293 cells were transfected with hThem5 and 30 micrograms of total lysate or mitochondrial/cytoplasmic fractions were separated by SDS-PAGE and immunoblotted for hThem5, tubulin and mitochondrial Grp75. Note the presence of an upper double band, indicating full length Them5 (FL) and Them5 without mitochondrial targeting sequence (Δ MTS). The presence of an additional lower band in the mitochondrial fraction suggests further Them5 processing in mitochondria. T - total, M - mitochondrial, C - cytoplasmic fraction.

(C) U2OS cells expressing full-length hThem5-HA and (D) Δ MTS Them5-HA were fixed and stained with antibodies against HA-tag, hThem5, TOM20, and tubulin. Full-length Them5 is localized in mitochondria (C), whereas the mutant lacking MTS is excluded from the mitochondria (D, Figure S5C). Images were taken using the confocal microscope LSM700. Scale bar is 10 μ m. At least four independent experiments were performed, with a minimum of 10 transfected cells analyzed.

(E) Immunogold-electronmicroscopy staining of U2OS cells transfected with HA-tagged hThem5. Sections were probed with anti-HA antibodies, and images were taken at high resolution (left and middle panels). To detect endogenous protein, sections of non-transfected cells were probed with anti-hThem5 antibodies (right panel). Staining was mainly detected in mitochondria. Positive signals of anti-Them5 labeling were quantified in different cellular compartments. Two independent preparations of grids were quantified according to the procedure described elsewhere (Lucocq et al., 2004; Mayhew and Lucocq, 2008). Quantification shows prevalence of the signal in mitochondria, with some background in other cellular compartments for both endogenous and transfected proteins (bottom left and middle panels, correspondingly).

Loss of thioesterase activity of Them5 leads to changes in mitochondrial morphology

To investigate the physiological role of Them5, we generated mice deficient in the Them5 protein (Figure S6). Considering the mitochondrial localization of Them5, we looked at whether its absence affected mitochondrial morphology by performing a serial block-face scanning electron microscopy analysis of hepatocytes. 2D electron microscopy images showed elongated, predominantly filamentous mitochondria in Them5-mutant mice (Figure 4A). Subsequent 3D reconstruction of the mitochondria showed a 2-fold increase in the volume of mitochondria from Them5^{-/-}, and the formation of a highly interconnected network, which was dramatically different from the wildtype mitochondria (Figure 4B). Starvation affected both wildtype and Them5^{-/-} mitochondria, resulting in an increased volume of organelles and the formation of a more interconnected network. Additionally, starvation increased the morphological differences between WT and KO cells, leading to a nearly 3-fold difference (Figure 4B,C).

Given that mitochondria from Them5 knock-out mice are more interconnected than wildtype organelles, we checked whether the mtDNA copy number was affected in *Them5*^{-/-} mice. To analyze this, we assessed mRNA levels of ND1 and COX1, single-copy mitochondrial genes, and TFAM, a mitochondrial transcription factor, in mice at 6 and 12 months of age (Figures 4, S7A). Quantification of mitochondrial number in the EM stacks also showed a similar trend toward reduced numbers of mitochondria. However, the difference was not statistically significant (data not shown). This suggests that the loss of Them5 affects mitochondrial morphology, but not biogenesis.

We next asked whether changes in mitochondrial morphology are caused by the loss of Them5 thioesterase activity. To answer this question, we analyzed mitochondrial morphology in cells transfected with wildtype or thioesterase-dead hThem5, or a vector control (Figure 4E). Analysis of reconstructed mitochondria in cells overexpressing a thioesterase-dead D167A mutant of Them5 showed an increase in volume (by 45%), and an elongated and more interconnected mitochondrial network compared to the cells transfected with wildtype protein (Figure 4F,G). The length of mitochondria increased by almost 35% upon D167A mutant overexpression, while overexpression of wildtype protein did not lead to any significant change, indicating the importance of Them5 enzymatic activity in maintaining mitochondrial morphology.

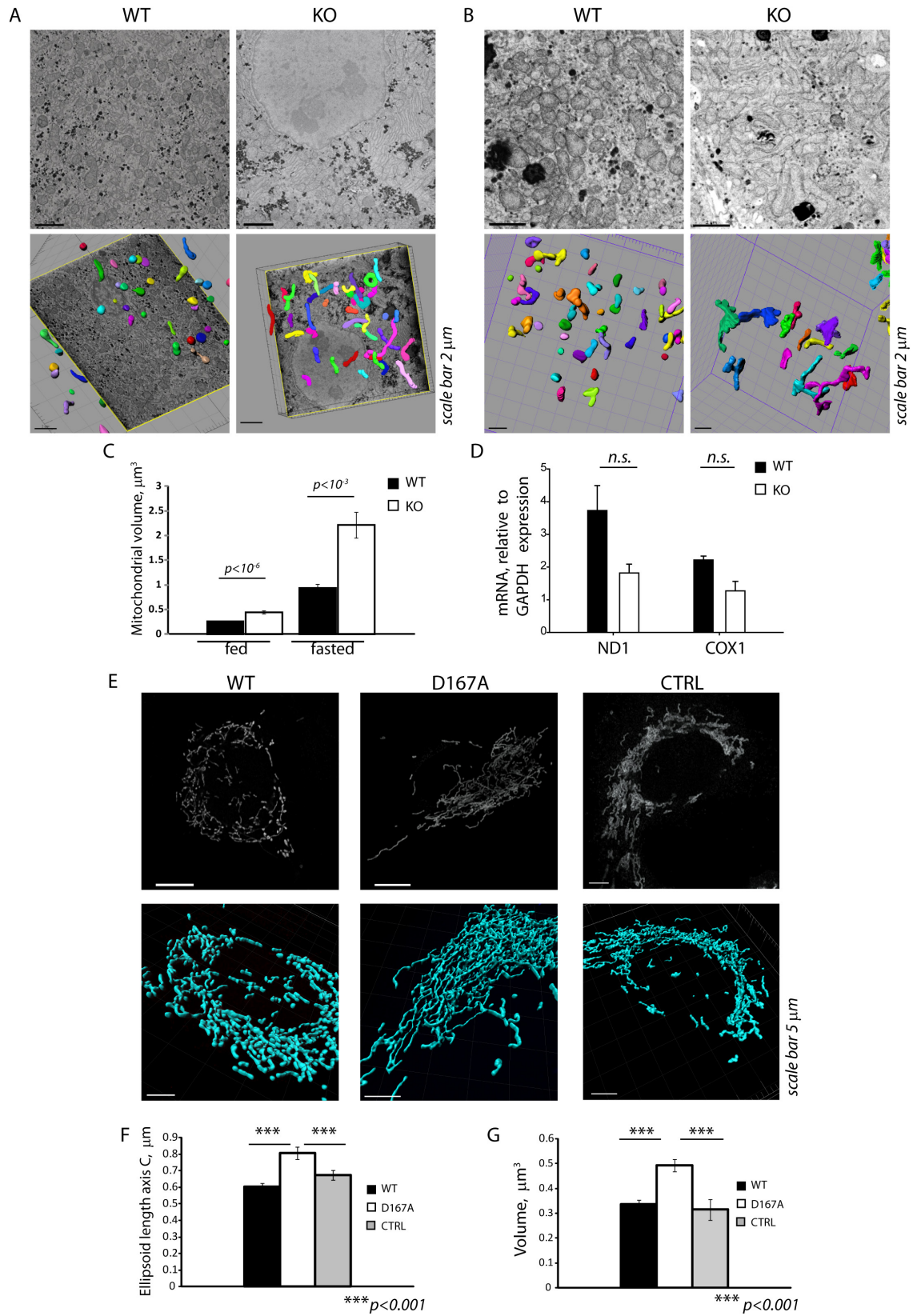


Figure 4. Loss of the enzymatic activity of Them5 protein results in more interconnected and elongated mitochondria

(A-B) Electron micrographs of Them5 wildtype and mutant hepatocytes (8000× magnification) obtained by serial block-face scanning EM, and 3D reconstruction of mitochondria showing elongated and interconnected mitochondria in Them5KO mice (A right panels and B right panels) compared to wildtype littermates (A left panels and B left panels) in fasted (A) and fed (B) state (males, 3 months old).

(C) Quantification of the mitochondria volume in Them5 wildtype and knock-out hepatocytes. A minimum of 15 mitochondria per cell were reconstructed in a minimum of three cells per mouse per genotype. Data is presented as mean and S.E.M. $p < 10^{-6}$.

(D) Mitochondrial DNA copy number in Them5 wildtype and knock-out hepatocytes, as assessed by real-time PCR of single-copy mitochondrial genes (NADH dehydrogenase subunit 1 (ND1) and cytochrome c oxidase subunit 1 (COX1)) and normalized to GAPDH levels (n=3).

(E) U2OS cells were transfected with wildtype Them5, D167A-Them5 mutant, or vector control coupled with IRES-GFP expression; mitochondria were visualized with anti-TOM20 staining. Confocal images were taken with $0.5 \times 0.5 \times 0.2 \mu\text{m}$ pixel size. 3D reconstruction and object splitting (bottom panels) were performed with Imaris software. Scale bar 10 μm .

(F-G) Length (F) and volume (G) of 3D reconstructed mitochondria in cells transfected with wildtype, D167A-Them5, or vector control were quantified. Data from three independent experiments are presented as mean and S.E.M. (minimum 10 cells per experiment were analyzed). *** $p < 0.001$.

Them5 knock-out mice develop non-alcoholic fatty liver disease

Mice lacking the Them5 protein are born in an expected Mendelian ratio and have no gross developmental abnormalities. However, Them5 knock-out mice have increased liver weight with no changes in total body weight (Figure 5A). Analysis of liver sections and primary hepatocytes from knock-out mice revealed lipid accumulation, which explains the increased liver weights (Figure 5B). Lipid accumulation develops with age: young mice have no signs of it even though they already show changes in mitochondrial morphology (Figures 5B, 4A). In contrast to the chow diet, a high fat diet leads to an increase in body weight (with no changes in food intake) of *Them5*^{-/-} mice, indicating reduced ability to cope with increased fatty acid load, compared to *Them5*^{+/+} mice (Figure S8A). The loss of Them5 exacerbates fatty liver development, leading to pronounced lipid accumulation, inflammatory infiltration, and further increases in UCP2 expression, compared to the wildtype control (Figure S8C,D). By the age of 6-9 months, *Them5*^{-/-} mice develop fatty livers. The accumulation of lipids in the liver is accompanied by hypoketonia and impaired β -oxidation (Figure 5C,D). Plasma levels of free fatty acids also increase significantly in *Them5*^{-/-} upon fasting (Figure 5E). Additionally, fatty acid synthase (FAS) mRNA levels are similar between mutant and control mice in the fasted state, but are not induced in *Them5*^{-/-} upon re-feeding (Figure 5F). Upregulation of FAS normally occurs in response to elevated levels of acetyl-CoA, a product

of β -oxidation, and is negatively regulated by fatty acids. Hence, impaired β -oxidation and lipid steatosis may explain the failure of FAS induction. In line with hypoketosis and reduced oxidation of ^{14}C -palmitic acid, the levels of carnitine palmitoyl transferase 1 (CPT1) are not increased after fasting (Figure 5G). However, CPT1 mRNA is upregulated in *Them5*^{-/-} when mice are normally fed, probably as a consequence of higher intracellular levels of fatty acids. Also as a result of lipid accumulation, expression of the UCP2 protein is considerably increased in *Them5*^{-/-} (Figure 5H).

Analysis of respiration of *Them5*^{-/-} mitochondria revealed no major changes in basal respiration, but significant decreases in state 3, state 4o, and state 3u (Figure 5I). The respiratory control ratio, RCR, is lower in both *Them5*^{-/-} liver mitochondria and MEFs (35% and 20%, respectively) (Figures 5J, S8), indicating an increased uncoupling of knock-out mitochondria, which could be explained by elevated UCP2 expression (Figures 5I, S9D). An electron flow assay revealed reduced coupling of OXPHOS both in sites I (pyruvate+malate) and II (succinate) in *Them5*^{-/-} mice (Figure 5K). Also, the impaired β -oxidation and TCA cycle resulting from *Them5* loss can be accounted for by the observed decrease (almost 50%) in maximal respiratory rates attained by the oxidation of endogenous substrates (Figure 5I).

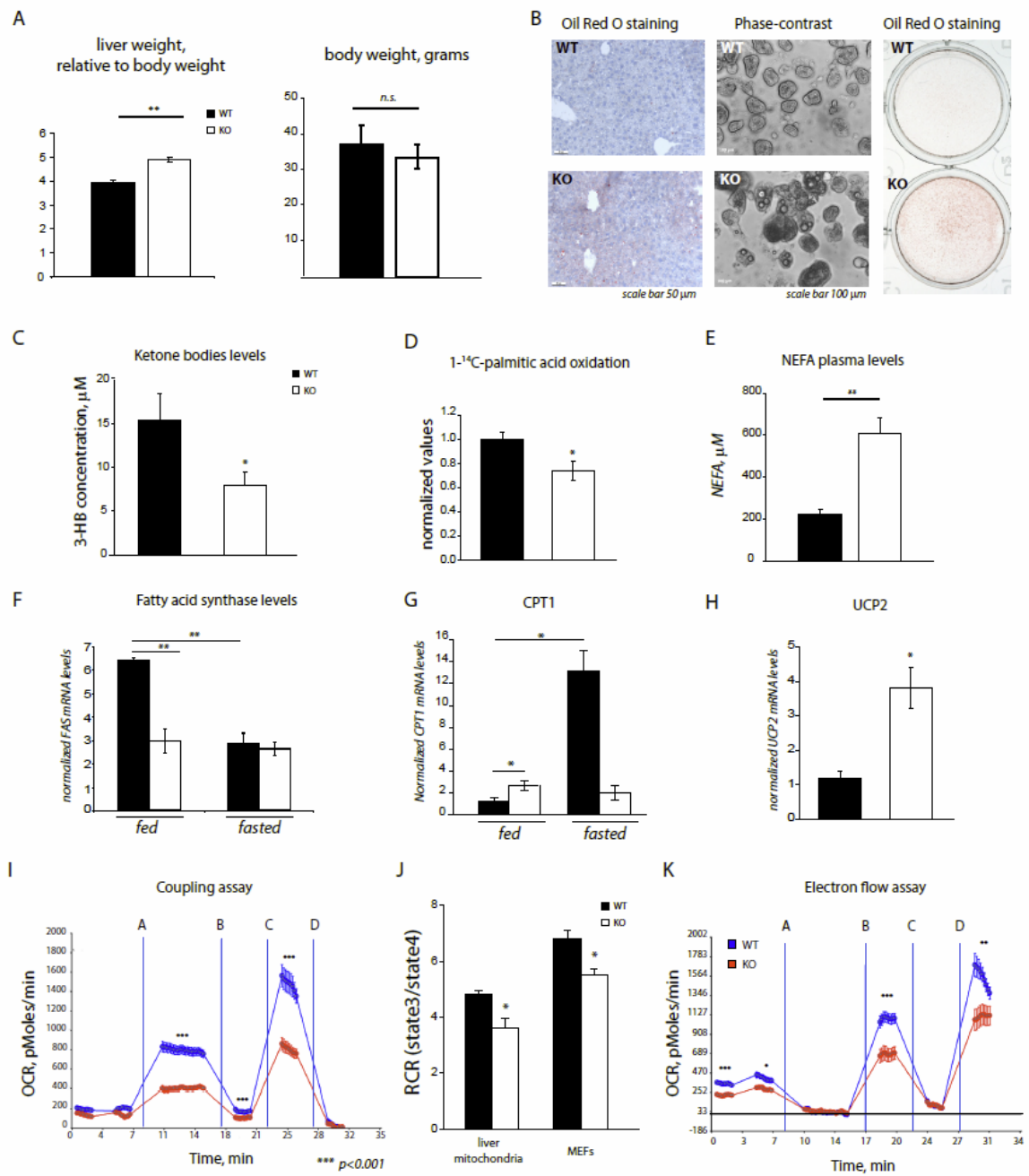


Figure 5. Loss of Them5 leads to the development of fatty liver

(A) Increased liver weight/body weight ratio (left panel), but no changes in total body weight (right panel) are detected between *Them5^{+/+}* and *Them5^{-/-}* (n=8-11).

(B) Age-dependent accumulation of lipids in liver. Oil Red O (ORO) staining of liver sections from wildtype or *Them5^{-/-}* mice at the age of 6 months (right panel). Phase-contrast images (middle panel) and ORO staining (left panel) of primary hepatocytes from wildtype and *Them5^{-/-}* mice at the age of 9 months.

(C) Decreased levels of serum 3-hydroxybutyrate (3-HB) in *Them5^{-/-}* upon fasting (males, 12 months old, n=5-6) and (D) lower rates of 1-¹⁴C-palmitic acid oxidation by primary hepatocytes indicate impaired β -oxidation.

(E) Increased plasma levels of non-esterified fatty acids in *Them5^{-/-}* mice compared to wildtype (6-7 months old) were detected after 8 hours of starvation (n=5).

(F) Fatty acid synthase and (G) CPT1 mRNA in liver of fasted and fed *Them5^{-/-}* and wildtype mice (6-7 months of age) was determined by qRT-PCR and normalized to GAPDH mRNA (n=3-4 per group).

(H) Increased levels of UCP2 mRNA were measured by qRT-PCR in liver samples from *Them5^{-/-}* mice, as compared to controls (males, 6-7 months of age, n=4 per group).

(I) Oxygen consumption rates were measured for *Them5^{-/-}* and wildtype liver mitochondria using a Seahorse XF24 analyzer in the presence of rotenone and succinate in the initial mix. A – ADP, B – Oligomycin, C – FCCP, D – Antimycin D (n=10).

(J) Respiratory Control Ratio (RCR, state3/state4) is significantly reduced in Them5KO liver mitochondria and MEFs compare to wildtype controls (35% and 20% decrease, respectively, n=8-10). For respirometry analysis of MEFs see Figure S9.

(K) Impaired electron transport and reduced coupling of OXPHOS in *Them5^{-/-}* liver mitochondria, as assessed by electron flow assay, measured with a Seahorse XF24 analyzer. Pyruvate+malate+FCCP were present in the mix from the start. A – rotenone, B – succinate, C – antimycin A, D – ascorbate/TMPD.

* p<0.05, ** p<0.01, *** p<0.001.

Them5 ablation modifies the metabolism of mitochondrial cardiolipin

In order to ascertain the specific metabolic defect which results in FFA accumulation, we carried out a detailed mass spectrometry (MS) analysis of mitochondrial lipids extracted from *Them5^{-/-}* and control mice. The MS results showed very specific changes in the lipid profile of cardiolipin (CL) and its metabolites (Figure 6A). Loss of Them5 leads to a two-fold increase in major species of monolyso-cardiolipin (MCL) (Figure 6B), which act as upstream metabolites in the remodeling cycle of CL. CL is a phospholipid localized predominantly within the inner mitochondrial membrane (Esposti et al., 2003). On the basis of these results, we propose that Them5 has a rather specific role *in vivo*, namely that of regulating the initial metabolism of mitochondrial CL by maintaining, in particular, the pool of acyl groups used to re-acetylate one metabolic intermediate of cardiolipin, SP2-MCL (stearoyl-di-palmitoyl-monolysocardiolipin) (Figure 6A,B). It is likely that the accumulation of this and other palmitoyl-containing MCL species reflects an early impairment in the remodeling cycle of CL, which progressively adds long unsaturated fatty acids to the saturated precursors, producing the mature forms enriched in linoleyl (Schlame, 2008). Reduction of thioesterase activity as a consequence of Them5 loss results in an almost two-fold decrease in free fatty acids

detected in mitochondria. The free fatty acids are trapped in long acyl-CoA molecules that are not normally required for CL remodeling (Figure 6C,D).

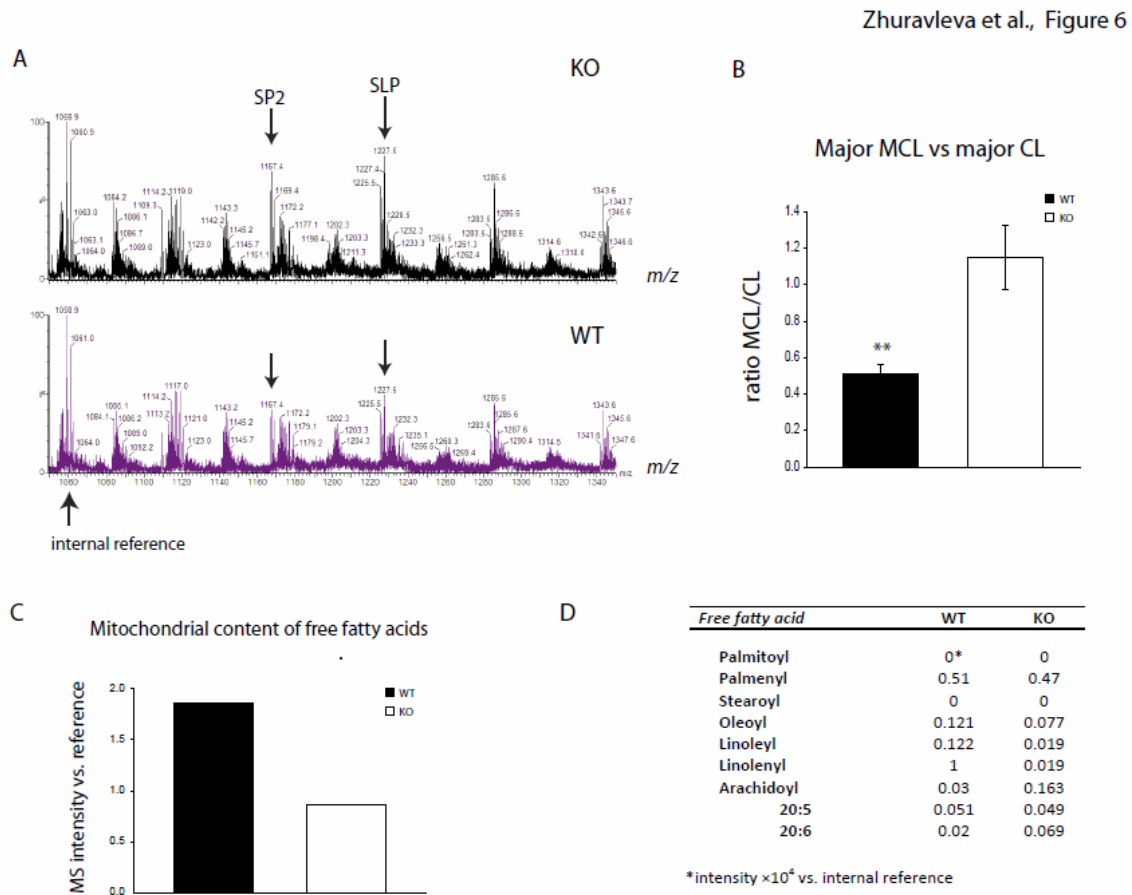


Figure 6. Them5 is a new player in cardiolipin remodeling

(A) Mass spectrometry (MS) profiles of Them5KO (top) and wildtype (bottom) mitochondrial lipids. SP2 – Stearoyl-di-Palmitoyl-Monolysocardiolipin/ Na_2H .

(B) Quantification of an increase in major monolysocardiolipin (MCL) over cardiolipin (CL) levels upon Them5 ablation.

(C) Quantification of a total mitochondrial content of free fatty acids and (D) detailed composition of FFA from Them5 wildtype and KO liver mitochondria, as assayed by MS. Note the strong decrease in linolenic acid in *Them5*^{-/-} samples compared to wildtype.

DISCUSSION

We have shown that Them5 is a novel protein that belongs to the mitochondrial proteome. Our results show that Them5 is involved in the metabolism of cardiolipin, a mitochondrial phospholipid, specifically in its early remodeling with long acyl-CoA species. This new evidence provides a chemical and metabolic explanation for the observed mitochondrial phenotype associated with the genetic ablation of Them 5, also throwing new light on the biological function of its paralog Them 4.

Indeed, we became interested in Them5 due to its similarity to CTMP/Them4, whose gene is located just 20kb away from that of Them5. Analysis of the phylogenetic tree shows that the Them5 gene appeared only in mammals, whereas Them4 orthologs can be found as far back as yeasts. Them5 seems to have appeared as a result of gene duplication, and thus Them4/5 may be paralogs. Them5 has a mitochondrial targeting sequence at the N-terminal and is imported into the mitochondria, where further processing occurs. It is localized only inside the mitochondrial organelle (both matrix and IMM), in contrast to Them 4 (Parcellier et al., 2009a). Indeed, the N-terminal pre-sequences are not conserved between the Them4 and Them5 proteins.

We determined the structures of $\Delta 36$ Them4 and $\Delta 34$ Them5 at high resolution, and showed that both Them4 and Them5 belong to the Hotdog-fold class of proteins. Those proteins include a variety of enzymes, mainly thioesterases, which participate in the metabolism of fatty acids and cholesterol (Hunt and Alexson, 2002). The Hotdog fold, which is formed by several anti-parallel β -sheets wrapped around an α -helix, is found in all branches of life. However, up to now few mammalian proteins have been described in this group.

In our experiments, we found that Them4 is mainly present as a homodimer, with a small fraction forming tetramers, while Them5 forms homodimers only. Them4/5 would be the only characterized mammalian 4HBT thioesterases which have a dimeric quaternary structure, but it is still possible that Them4/5 can form higher order oligomers in their specific environment in the mitochondria, either upon interaction with membranes or proteins, or

upon substrate binding. It has been shown that members of the PAAI family, like *E. coli* PAAI or human Them2, form tetramers in a back-to-back arrangement of the β -sheets, while other PAAI family members, like the hypothetical proteins with PDB codes 1IXI (*P. horikoshii*), 2HBO (*C. crescentus*), or 2OV9 (*Rhodococcus* sp.), are present as homodimers only, with altered tetramerization sequence motifs. Given that the predominant oligomeric species of both human Them4 and Them5 is homodimeric, they seem to be most related to the homodimer subclass of the PAAI family. Thus, taken together, our results suggest that Them4 and Them5 form a separate group of mammalian thioesterases.

Analysis of functionally relevant residues revealed the catalytic machinery, composed of the HGG motif and the Asp/Thr residues, to be conserved. The carboxylate moiety is thought to deprotonate a water molecule prior to its nucleophilic attack on the thioester bond of the CoA-coupled fatty acid substrate, while the HGG motif at the N-terminal end of the central Hotdog helix places the substrate thioester carbonyl group in the right position (Zhao et al., 2009).

Them4 and Them5 proteins contain a highly variable sequence stretch (~83-109 and ~91-114 for Them4 and Them5, respectively) that is partially disordered in both crystal structures. Residues 81-105 could not be built in the Them4 structure due to low electron density, whereas the corresponding region in Them5 extends much further. In the Them5 structure, 12 additional residues could be modeled (Ser90-Pro101), but the conformation is likely to be influenced by the crystal packing. In the C222₁ crystal layers of Them5 molecules are stabilized by a β -sheet-like crystal contact formed by neighboring C-termini, as well as stretches of the variable sequence region between symmetry related molecules. Despite the fact that these residues partially close the active site cavity, it is unlikely that the conformation represents a snapshot of a lid-like closure of the acyl binding site, thereby controlling substrate access. The function of this highly variable sequence stretch remains unclear, but we suggest that it adopts a stable conformation upon substrate binding or interaction with another protein. Interestingly, a study carried out with a Them4 peptide (residues 95-119) that contains parts of this variable sequence, including the highly

conserved FTR motif, showed that it induced apoptosis in pancreatic adenocarcinoma cell lines by interfering with the PKB/Akt pathway (Simon et al., 2009). Although parts of the peptide map to surface-exposed and disordered Them4 residues, we found Phe111, the residue to which the effect was attributed, to be buried in the protein core at the dimerization interface.

The biological role of thioesterases has not been fully addressed. Consensus motifs and structural analysis can propose substrate types, but cannot provide information about the potential physiological roles of the Hotdog-fold proteins (Pidugu et al., 2009). Cytoplasmic Acot7 is thought to be involved in eicosanoid metabolism (Forwood et al., 2007; Serek et al., 2006). Them2 is thought to participate in the pathogenesis of renal cell carcinoma (Lucas et al., 2005), and in fatty acid metabolism (Kanno et al., 2007).

CTMP/Them4 has been reported to be a part of the PKB signaling regulation network (Maira et al., 2001; Parcellier et al., 2009a). Recently, it has been shown that Them4 is a mitochondrial acyl-CoA thioesterase with a preference for long-chain fatty acids (Zhao et al., 2009). Data obtained from Them5 knock-out mice suggest that it has a role in the regulation of mitochondrial morphology. Our analysis showed a 2-fold increase in mitochondrial volume, most likely as a result of the formation of a highly interconnected network. This becomes more pronounced upon starvation, which leads to an almost 3-fold difference in volume. However, mitochondrial biogenesis is not affected by the loss of the Them5 protein. Previous analysis of Them4-deficient cells has shown similar changes in mitochondrial morphology without any affect on number, suggesting that Them4 may be involved in mitochondrial fusion processes (Parcellier et al., 2009b). However, the new evidence presented here for its paralog Them5 suggests that the alteration in mitochondrial morphology may well derive from an alteration in mitochondrial lipid metabolism.

Sequence analysis shows 38% similarity between hThem4 and hThem5 proteins, which is reflected in highly similar 3D-structures. Differences between the proteins are localized primarily to the N-terminus and the MTS. Mapping these sequence differences onto the structures reveals distinct structural features, highlighting potential functional differences

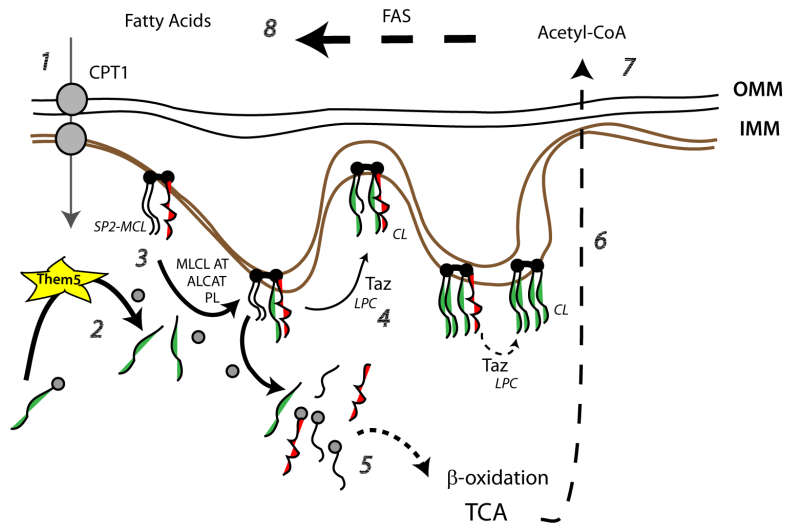
between Them4 and Them5. The main sequence differences map onto the partially disordered loop covering the active site cleft, as well as onto the bottom of this same cleft, the putative binding site for the CoA-linked fatty acid alkyl chain. This might provide a structural explanation for the differential substrate preferences exhibited by Them4 and Them5. Hence, Them5 may be a prominent thioesterase for long-chain acyl-CoA molecules in mitochondria.

Our results show that changes in mitochondrial morphology due to a lack of Them5 protein are most likely linked to its enzymatic activity. Considering the late appearance of Them4 in evolution, and the even later appearance of Them5, one can speculate that these proteins evolved to perform specific and non-overlapping functions in the mitochondria.

Analysis of Them5 knock-out mice revealed an age-dependant progression of fatty liver disease. Mutant mice displayed hypoketosis and showed decreased β -oxidation rates. They failed to upregulate FAS upon fasting, which is also indicative of impaired β -oxidation and TCA cycle, and may be a consequence of the increase in cytoplasmic fatty acids. As a consequence of decreased β -oxidation and increased levels of UCP2, the maximal respiratory capacity and respiratory control ratio are lower in *Them5*^{-/-} cells. Additionally, Them5KO mitochondria show reduced coupling of OXPHOS. Detailed MS analysis of lipid metabolites indicated that ablation of Them5 induced the accumulation of a major species of monolysocardiolipin (MCL), which acts as an upstream metabolite in the remodeling cycle of cardiolipin (CL). CL is the major phospholipid of the inner mitochondrial membrane, whose synthesis and remodeling occurs predominantly within mitochondria (Esposti et al., 2003; Schlame, 2008). We propose that Them5 thioesterase activity may regulate the initial metabolism of CL by maintaining the pool of acyl groups that re-acylate, in particular stearoyl- and palmitoyl-containing MCL species that lie upstream in the CL remodeling cycle (Figure 7A). Remodeling is essential for CL functions, which include the regulation of mitochondrial bioenergetic processes and mitochondrial dynamics (Osman et al., 2011; Schlame, 2008). The plasticity and dynamics of mitochondria are highly dependent on the content of CL and other lipids. In particular, the balance between CL and MCL is essential to

dynamically maintain cristae homeostasis (Acehan et al., 2011; Ban et al., 2010; Rujiviphat et al., 2009). Thus, our initial observation that thioesterase activity of Them5 is important for mitochondrial morphology (Figure 4) can be rationalized by the results of subsequent MS analysis showing more than a two-fold increase in major MCL species relative to CL species (Fig. 6). The membrane tubulation propensity of MCL would probably account for the elongated appearance of Them5-deficient mitochondria. Additionally, reduced thioesterase activity as a consequence of Them5 ablation (Figure 7B) will trap a portion of the mitochondrial pool of CoA into long acyl-CoA molecules. Those that are not normally used in the local CL remodeling metabolism (e.g. stearoyl-CoA) will then leave the mitochondria and subsequently be hydrolyzed to free fatty acids by cytosolic or peroxisomal thioesterases. The process will produce extra-mitochondrial accumulation of free fatty acids, which will build up in hepatocytes once their release capacity as cholesterol esters or triglycerides is saturated. In support of this interpretation, we found only minimal changes in the acyl group distribution of phospholipids synthesized outside mitochondria (Figure S10). Of note, a recent study has shown that altering the supply of acyl-CoA metabolites modifies CL remodeling (Rijken et al., 2009). The cytosolic accumulation of free fatty acids, again due to the above mechanism, would induce feedback inhibition of FAS by its product palmitate. Moreover, our finding of impaired β -oxidation in *Them5*^{-/-} implies a reduced production of acetyl-CoA, with consequent reduction in mitochondrial citrate and its export into the cytosol, where it is required for FAS initiation. Ultimately, the accumulation of fatty acids, observed in *Them5*^{-/-} animals, originates from the alteration in CL remodeling within mitochondria, due to the reduced capacity of utilizing long acyl-CoA metabolites caused by Them5 loss. We have identified a novel class of mitochondrial thioesterases, Them4 and Them5, and proposed their likely biological function. Further research on the involvement of Them5 in the regulation of mitochondrial lipid metabolism and mitochondrial dynamics will shed more light on these and related topics, such as oxidative stress.

A



B

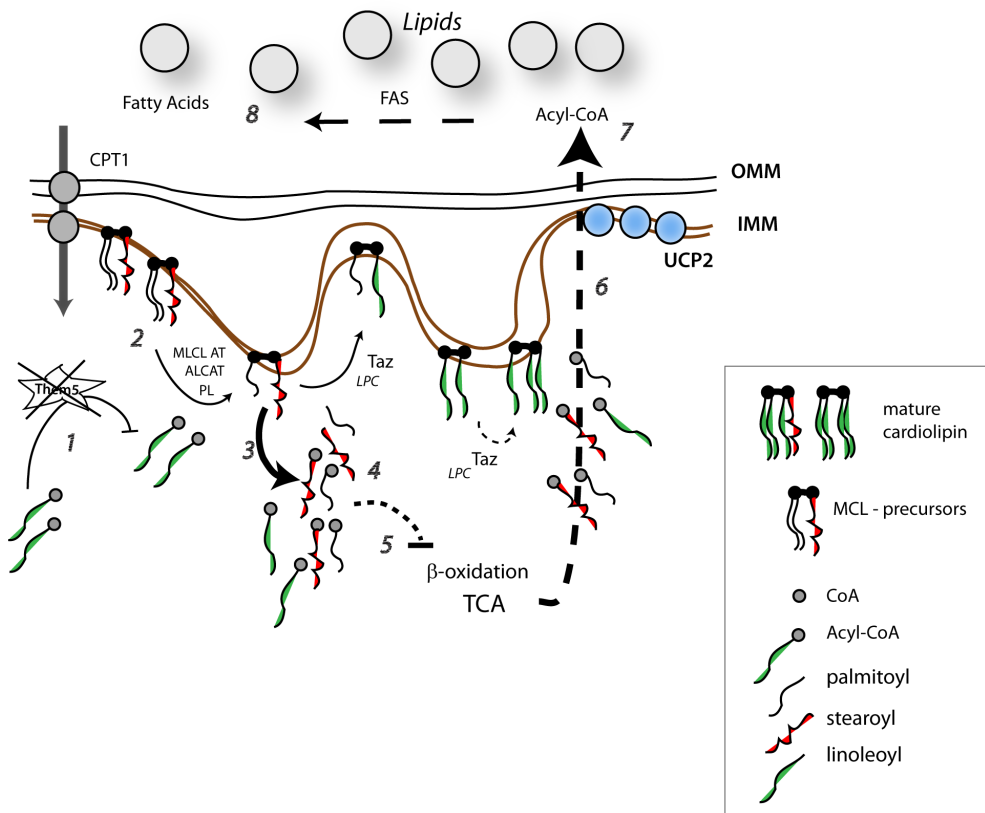


Figure 7. Proposed scheme of Them5 function in mitochondria

(A) Fatty acids are imported into mitochondria from cytosol via CPT transporters (1). Acyl-CoAs are hydrolyzed by Them5 (2), releasing acyl chains used for re-acylation of the CL precursor, SP2-MCL, by ALCAT or MCLAT (3). The other steps of CL remodeling are mediated by Taz (tafazzin), a transacylase that catalyzes transfer of one acyl from a PL donor (like PC) to an MCL precursor (4). Normally, stearoyl and palmitoyl acyls are re-esterified and can be used in β -oxidation and, subsequently, TCA (5). The final product acetyl-CoA is then transported to the cytosol (6), where it becomes a substrate for fatty acid synthesis (7,8).

(B) Them5 ablation (1) leads to accumulation of the CL precursor SP2-MCL (2). However, short and saturated acyl species of CL are still produced by CL synthase and are degraded by local phospholipases (3), leading to the accumulation of palmitic and stearic fatty acids (4) and concomitant depletion of the limited mitochondrial CoA pool. Overall, it results in β -oxidation inhibition (5), upregulation of UCP2 (6), and increased export of these acids to the cytosol and storage of them as lipid droplets (7). This will cause an increase in basal levels of CPT1 (8), and eventually release lipids into the bloodstream.

CL – cardiolipin; LPC – lysophosphatidylcholine; MCL – monolysocardiolipin; CPT – carnitine-palmitoyl transferase; UCP2 – uncoupling protein 2; CoA – coenzyme A; ALCAT – acyl-CoA:lysocardiolipin acyltransferase; MCLAT – monolysocardiolipin acyltransferase; TCA – tricarboxylic acid cycle.

EXPERIMENTAL PROCEDURES

Immunostaining

For immunostaining experiments, cells were plated on coverslips and optionally transfected with corresponding DNA the next day. 24 h later, cells were either fixed with 4% FA and permeabilized with 0.2% Triton X-100 as described elsewhere (Parcellier et al., 2009a), or were fixed and permeabilized with methanol/acetone (1:1 v/v) for 5 min at -20°C . To visualize mitochondria, cells were stained with 20 nM Mitotracker Red prior to fixation for 15 min at 37°C . Afterwards, cells were washed with PBS and incubated with primary antibodies of appropriate dilution in 1% BSA/1% goat serum overnight. This was followed by incubation with secondary anti-mouse conjugated with Alexa488 or Alexa568, together with 1 μM To-Pro-3 iodide (Molecular Probes Inc) for 30 min at room temperature. Afterwards, slides were washed, mounted with Prolong Gold mounting media (Invitrogen), and visualized using an LSM510/LSM700 laser scanning microscope.

Immuno-electronmicroscopy

This was performed according to the protocol described elsewhere with slight modifications (Slot and Geuze, 2007). Immunolabeling was carried out using anti-hThem5 at a dilution of 1/50 and anti-HA at 1/200 (Clontech, Cat. No. 631207); 10 nm protein A-gold (UMC-Utrecht University, Utrecht, The Netherlands) was used at 1:50 dilution.

Crystallization and structure determination

Crystallographic methods are described in the Supplementary material section. Data collection and refinement statistics are given in Table S1.

Thioesterase activity assay

The reaction mixture contained recombinant protein, fatty acyl-CoA substrate (Larodan Fine Chemicals, Sweden) at concentrations ranging from 1 to 200 μM , 50 mM HEPES, 50 mM KCl, and 0.5 mM DTNB (5,5-Dithiobis(2-nitrobenzoic acid)) in 1 ml total volume. Reactions

were observed spectrophotometrically at 412 nm ($\epsilon=13.6 \text{ mM}^{-1} \text{ cm}^{-1}$) at 22°C or 37°C using a UV1800 spectrophotometer controlled by UVPro2.33 software (Shimadzu Schweiz GmbH).

Lipid extraction and MS analysis

Phospholipids were extracted from purified mitochondria and analyzed by electrospray mass spectrometry as described previously (Moisoi et al., 2009), (Esposti et al., 2003).

ACKNOWLEDGEMENTS

We thank Michael Rebhan for help with the initial bioinformatics analysis, Patrick Schwarb and Aaron Ponti for their help with image analysis, Ahmad Bechara for the electron microscopy data discussion, David Knight for MS analysis and Sara Oakeley for critical reading of the manuscript. We would also like to thank the staff of beamlines X10SA and X06DA at the Swiss Light Source (Villigen, Switzerland) for their excellent support in X-ray data collection. E.Z. was supported by a Swiss Bridge fellowship. Work in Manchester was undertaken with the FLS Biomolecular Analysis Facility. The Friedrich Miescher Institute for Biomedical Research is a part of the Novartis Foundation.

REFERENCES

Acehan, D., Vaz, F., Houtkooper, R.H., James, J., Moore, V., Tokunaga, C., Kulik, W., Wansapura, J., Toth, M.J., Strauss, A., and Khuchua, Z. (2011). Cardiac and skeletal muscle defects in a mouse model of human Barth syndrome. *J Biol Chem* **286**, 899-908.

Ban, T., Heymann, J.A., Song, Z., Hinshaw, J.E., and Chan, D.C. (2010). OPA1 disease alleles causing dominant optic atrophy have defects in cardiolipin-stimulated GTP hydrolysis and membrane tubulation. *Hum Mol Genet* **19**, 2113-2122.

Cao, J., Xu, H., Zhao, H., Gong, W., and Dunaway-Mariano, D. (2009). The mechanisms of human hotdog-fold thioesterase 2 (hTHEM2) substrate recognition and catalysis illuminated by a structure and function based analysis. *Biochemistry* 48, 1293-1304.

Claros, M.G., and Vincens, P. (1996). Computational method to predict mitochondrially imported proteins and their targeting sequences. *Eur J Biochem* 241, 779-786.

Combet, C., Blanchet, C., Geourjon, C., and Deleage, G. (2000). NPS@: network protein sequence analysis. *Trends Biochem Sci* 25, 147-150.

Esposti, M.D., Cristea, I.M., Gaskell, S.J., Nakao, Y., and Dive, C. (2003). Proapoptotic Bid binds to monolysocardiolipin, a new molecular connection between mitochondrial membranes and cell death. *Cell Death Differ* 10, 1300-1309.

Forwood, J.K., Thakur, A.S., Guncar, G., Marfori, M., Mouradov, D., Meng, W., Robinson, J., Huber, T., Kellie, S., Martin, J.L., Hume, D.A., and Kobe, B. (2007). Structural basis for recruitment of tandem hotdog domains in acyl-CoA thioesterase 7 and its role in inflammation. *Proc Natl Acad Sci U S A* 104, 10382-10387.

Holm, L., and Sander, C. (1993). Protein structure comparison by alignment of distance matrices. *J Mol Biol* 233, 123-138.

Hunt, M.C., and Alexson, S.E. (2002). The role Acyl-CoA thioesterases play in mediating intracellular lipid metabolism. *Prog Lipid Res* 41, 99-130.

Kanno, K., Wu, M.K., Agate, D.S., Fanelli, B.J., Wagle, N., Scapa, E.F., Ukomadu, C., and Cohen, D.E. (2007). Interacting proteins dictate function of the minimal START domain phosphatidylcholine transfer protein/StarD2. *J Biol Chem* 282, 30728-30736.

Krissinel, E., and Henrick, K. (2007). Inference of macromolecular assemblies from crystalline state. *J Mol Biol* 372, 774-797.

Lucas, B., Grigo, K., Erdmann, S., Lausen, J., Klein-Hitpass, L., and Ryffel, G.U. (2005). HNF4alpha reduces proliferation of kidney cells and affects genes deregulated in renal cell carcinoma. *Oncogene* 24, 6418-6431.

Lucocq, J.M., Habermann, A., Watt, S., Backer, J.M., Mayhew, T.M., and Griffiths, G. (2004). A rapid method for assessing the distribution of gold labeling on thin sections. *J Histochem Cytochem* 52, 991-1000.

Maira, S.M., Galetic, I., Brazil, D.P., Kaech, S., Ingley, E., Thelen, M., and Hemmings, B.A. (2001). Carboxyl-terminal modulator protein (CTMP), a negative regulator of PKB/Akt and v-Akt at the plasma membrane. *Science* 294, 374-380.

Mayhew, T.M., and Lucocq, J.M. (2008). Quantifying immunogold labelling patterns of cellular compartments when they comprise mixtures of membranes (surface-occupying) and organelles (volume-occupying). *Histochem Cell Biol* 129, 367-378.

Moisoi, N., Klupsch, K., Fedele, V., East, P., Sharma, S., Renton, A., Plun-Favreau, H., Edwards, R.E., Teismann, P., Esposti, M.D., Morrison, A.D., Wood, N.W., Downward, J., and Martins, L.M. (2009). Mitochondrial dysfunction triggered by loss of HtrA2 results in the activation of a brain-specific transcriptional stress response. *Cell Death Differ* 16, 449-464.

Osman, C., Voelker, D.R., and Langer, T. (2011). Making heads or tails of phospholipids in mitochondria. *J Cell Biol* 192, 7-16.

Parcellier, A., Tintignac, L.A., Zhuravleva, E., Cron, P., Schenk, S., Bozusic, L., and Hemmings, B.A. (2009a). Carboxy-Terminal Modulator Protein (CTMP) is a mitochondrial protein that sensitizes cells to apoptosis. *Cell Signal* 21, 639-650.

Parcellier, A., Tintignac, L.A., Zhuravleva, E., Dummler, B., Brazil, D.P., Hynx, D., Cron, P., Schenk, S., Olivieri, V., and Hemmings, B.A. (2009b). The Carboxy-Terminal Modulator Protein (CTMP) regulates mitochondrial dynamics. *PLoS One* 4, e5471.

Pidugu, L.S., Maity, K., Ramaswamy, K., Surolia, N., and Suguna, K. (2009). Analysis of proteins with the 'hot dog' fold: prediction of function and identification of catalytic residues of hypothetical proteins. *BMC Struct Biol* 9, 37.

Rijken, P.J., Houtkooper, R.H., Akbari, H., Brouwers, J.F., Koorengel, M.C., de Kruijff, B., Frentzen, M., Vaz, F.M., and de Kroon, A.I. (2009). Cardiolipin molecular species with shorter acyl chains accumulate in *Saccharomyces cerevisiae* mutants lacking the acyl coenzyme A-binding protein Acb1p: new insights into acyl chain remodeling of cardiolipin. *J Biol Chem* 284, 27609-27619.

Rujiviphat, J., Meglei, G., Rubinstein, J.L., and McQuibban, G.A. (2009). Phospholipid association is essential for dynamin-related protein Mgm1 to function in mitochondrial membrane fusion. *J Biol Chem* 284, 28682-28686.

Schlame, M. (2008). Cardiolipin synthesis for the assembly of bacterial and mitochondrial membranes. *J Lipid Res* 49, 1607-1620.

Serek, R., Forwood, J.K., Hume, D.A., Martin, J.L., and Kobe, B. (2006). Crystallization of the C-terminal domain of the mouse brain cytosolic long-chain acyl-CoA thioesterase. *Acta Crystallogr Sect F Struct Biol Cryst Commun* 62, 133-135.

Simon, P.O., Jr., McDunn, J.E., Kashiwagi, H., Chang, K., Goedegebuure, P.S., Hotchkiss, R.S., and Hawkins, W.G. (2009). Targeting AKT with the proapoptotic peptide, TAT-CTMP: a novel strategy for the treatment of human pancreatic adenocarcinoma. *Int J Cancer* 125, 942-951.

Slot, J.W., and Geuze, H.J. (2007). Cryosectioning and immunolabeling. *Nat Protoc* 2, 2480-2491.

Zhao, H., Martin, B.M., Bisoffi, M., and Dunaway-Mariano, D. (2009). The Akt C-terminal modulator protein is an acyl-CoA thioesterase of the Hotdog-Fold family. *Biochemistry* 48, 5507-5509.

Supplemental Information

Analysis of novel Acyl-CoA thioesterase Them5 reveals a role in mitochondrial morphology and fatty liver disease development.

Elena Zhuravleva, Heinz Gut, Debby Hynx, David Marcellin, Christopher K. E. Bleck, Christel Genoud, Peter Cron, Jeremy J. Keusch, Bettina Dummler, Mauro Degli Esposti, Brian A. Hemmings

SUPPLEMENTAL EXPERIMENTAL PROCEDURES

Crystallization, X-ray data collection, and structure determination. Crystals of $\Delta 36$ Them4 were obtained *via* the vapor diffusion method by mixing 100 nl of protein solution (4.3 mg/ml $\Delta 36$ Them4, 50 mM CHES pH 9.5, 200 mM NaCl, 5 mM TCEP) with 100 nl of reservoir solution containing 100 mM Tris pH 7.0, 200 mM NaCl and 30 % Peg 3000. Crystals were cryoprotected with 20 % ethylene glycol and frozen in liquid nitrogen before data collection at the Swiss Light Source (SLS) synchrotron, Villigen, Switzerland. The structure of $\Delta 36$ Them4 was solved by the molecular replacement method using PHASER (McCoy et al., 2005). A homology model of the conserved thioesterase hot-dog fold was constructed with the MODELLER software and used as a search model (Sali and Blundell, 1993). Clear solutions for four molecules per asymmetric unit forming together two homodimers of the thioesterase fold were obtained. Phases calculated from this initial model were used for automated model building of the full molecule in PHENIX and BUCCANEER (Adams et al.). (Ref BUCCANEER)

Crystals of $\Delta 34$ Them5 were obtained by mixing 100 nl of protein solution (4.0 mg/ml $\Delta 34$ Them5, 20 mM Tris pH 7.5, 200 mM NaCl, 5 mM TCEP) with 100 nl of reservoir solution (100 mM Phosphate-citrate pH 4.2, 10 % PEG 3000, 200 mM NaCl). Crystals

were cryoprotected with 30 % ethylene glycol and frozen in liquid nitrogen before data collection at the SLS. The structure of $\Delta 34$ Them5 was solved by the molecular replacement method using PHASER with the structure of $\Delta 36$ Them4 as search model (McCoy et al., 2005). One Them5 chain per asymmetric unit was found representing half of the homodimeric thioesterase molecule. Phases from this solution were calculated and used for automatic model building with PHENIX (Adams et al.). Them4 and Them5 models were further improved by the crystallographic simulated annealing routine followed by individual B-factor refinement in PHENIX (Adams et al.). All structures were refined by several rounds of manual rebuilding in COOT (Emsley and Cowtan, 2004) followed by refinement in PHENIX (Adams et al.). Final structures were validated using the molprobtity server (<http://molprobtity.biochem.duke.edu/>) and COOT (Emsley and Cowtan, 2004). Structural images for figures were prepared with PyMOL (<http://pymol.sourceforge.net/>).

Analytical gel-filtration studies. Human THEM4 (amino acids 37-240) and THEM5 (amino acids 35-247) proteins were expressed with C-terminal His₆ tags using a pOPINE vector and *E. coli* Rosetta2 DE3 cells (Berrow et al., 2007). The target proteins were purified on nickel-nitrilotriacetic acid beads (Qiagen) followed by gel-filtration on a HiLoad 16/60 Superdex 200 column (GE Healthcare) and concentrated to 6 mg/ml in gel-filtration buffer (50 mM Tris, pH 8.5, 200 mM NaCl, 10 mM TCEP and 0.02% NaN₃). Analytical gel-filtration runs were performed in the same buffer on a Tricorn Superdex 200 10/300 GL (GE Healthcare) column, previously calibrated with molecular weight standards (ferritin 440 kDa, catalase 232 kDa, aldolase 158 kDa, albumin 67 kDa, ovalbumin 43 kDa, chymotrypsinogen A 25 kDa and ribonuclease A 13.7 kDa). A total volume of 100 μ l containing THEM proteins (at a final concentration of 0.9 mg/ ml) was

injected onto the Superdex 200 10/300 column and separated at a flow rate of 0.75 ml/min.

Sequences:

Human THEM4 37-240 (24,252.2 Da)

MSSEEVILKDCSVPNPSWNKDLRLLFDQFMKKCEDGSWKRLPSYKRTPTEWIQDFKTH
FLDPKLMKEEQMSQAQLFTRSFDDGLGFYVMFYNDIEKRMVCLFQGGPYLEGPPGFI
HGGAIATMIDATVGMCAMMAGGIVMTANLNINIKRPIPLCSVVMINSQLDKVEGRKFFV
SCNVQSVDEKTLYSEATSLFIKLNPAKSLTKHHHHHH

Human THEM5 35-247 (24,894.5 Da)

MGSSTDSMFSRFLPEKTDLDYALPNASWCSDMLSLYQEFLEKTKSSGWIKLPSFKSN
RDHIRGLKLPSGLAVSSDKGDCRIFTRCIQVEGQGFYVIFQPTQKKSVCFLFQPGSYL
EGPPGFAHGGSLAAMMDETFSKTAFLAGEGLFTLSLNIRFKNLPVDSLVMMDVEVDKIE
DQKLYMSCIAHSRDQQT VYAKSSGVFLQLQLEEEESPQKHHHHHH

Cell culture

HEK293 and U2OS were grown in DMEM in the presence of 10% serum bovine serum. For transfection experiments, cells were plated in 6-well plates or 6-or 10-cm dishes and transfected the next day using JetPEI reagent (Polyplus Transfection™) for HEK293, and Fugene 6 (Roche) for U2OS cell lines.

RNA extraction, reverse transcription reaction and qRT-PCR analysis

Total RNA was extracted from tissues or cells using TRIzol Reagent (Invitrogen, Life Technologies) according to the manufacturer's protocol. The concentration of RNA was

determined with NanoDrop Spectrophotometer (Nanodrop Technologies) and 2 µg of RNA were used for reverse transcription reaction. qRT-PCR was performed using an Applied Biosystems ABI7000 Sequence Detection system. A 25 µl of reaction mixture included 12.5 µl of 2x SYBR Green Master mix (Applied Biosystems), oligos and cDNA in appropriate concentrations.

Subcellular fractionation of cells was performed according to procedure described elsewhere (Parcellier et al., 2009a).

Western blotting

For Western blot analysis, protein lysates were prepared using a lysis buffer (50 mM Tris-HCl pH 8.0, 150 mM NaCl, 1% NP-40, 40 mM β-glycerophosphate, 10% glycerol, 4 µM leupeptin, 0.05 mM phenylmethylsulfonyl fluoride, 1 mM benzamidine, 50 mM NaF, 1 mM Na₃VO₄, 5 mM EDTA, 1 µM Microcystin LR). Homogenates were centrifuged (14,000 rpm for 20 min at 4°C) to remove cell debris. Protein concentrations were determined using the Bradford assay, and proteins separated with 15%, 12.5%, or 10% sodium dodecyl sulfate-polyacrylamide gel electrophoresis and then transferred to Immobilon-P PVDF membranes (Millipore).

Antibodies

hThem5 monoclonal antibodies were generated by repeated immunization of BALB/c mice with 50–100 µg of purified full-length GST-hThem5 protein (produced in *E. coli*), using Stimune (Prionics AG, Schlieren, Switzerland) as an adjuvant. Two months after the priming injection, splenic lymphocyte cells were fused with the P3AG8.653 myeloma cell line (ATCC) and cultured according to standard procedures. Monoclonal anti-Them5 antibodies are IgG1.

Anti-Myc (9E10), anti-HA (12CA5), α -tubulin (YL 1/2) were used as hybridoma supernatants. The commercial mouse anti-mHsp70 was from Affinity BioReagents, rabbit anti-cytochrome c was from Cell Signaling Technology, rabbit anti-Tom20 and rabbit anti-HA (Y11) were purchased from Santa Cruz Biotechnology.

Imaging

For the analysis of mitochondrial morphology, the images were $0.5\mu\text{m} \times 0.5\mu\text{m} \times 0.2\mu\text{m}$, and were deconvolved afterwards with the Huygens Software (Scientific Volume Imaging B.V.) via Hygens Remote Manager. Image analysis was performed with the Imaris software (Bitplane, Zurich).

Electron microscopy

Samples we prepared according to standard procedures. Briefly, tissues or cells were fixed in 2.0% PFA/2.5% glutaraldehyde in 0.1 M sodium cacodylate buffer, washed in 0.1 M cacodylate buffer (pH 7.4), subsequently postfixated in 1% OsO₄/1.5% KFeCN and then 1% OsO₄ in cacodylate buffer, rinsed in ddH₂O, stained with 1% uranyl acetate in water for 20 min, then rinsed in water, gradually dehydrated in ethanol (50%-100%), and embedded in Durcupan resin. Serial block-face scanning electron microscopy was performed using the 3View™ SBFSEM system (Gatan, Inc.) under low-vacuum conditions. Images were taken at a resolution of 4096×4096 pixels with 50 nm slices, all controlled by DigitalMicrograph software (Gatan, Inc.) and then processed using Imaris software.

Generation of Them5 knock-out mouse

A targeting vector was generated that contains a 3.7 kb 5' homology region, an IRES/lacZ/neo cassette, and a 5 kb 3' homology region. A genomic DNA fragment of

about 1.3 kb, including the ATG start codon in exon 1 and the full sequence of exon2, is deleted in the targeting vector. The targeting vector was linearized with NotI and electroporated into 129/Ola ES cells. Screening of ES cell clones was performed by Southern Blotting. DNA was digested with EcoRV and probed with an external probe (green box spanning sequence 16980-17663, Figure S6C). An internal probe was then used on NdeI digested DNA (green box spanning sequence 9652-10154, Figure S6D) for further characterization of ES cell clones positive for homologous recombination. Correctly targeted ES cells were used to generate chimeras. Male chimeras were mated with wild type C57BL/6 females to obtain *Them5*^{-/-} mice, which were intercrossed to produce Them5 homozygous mutants.

Free fatty acids measurement

Levels of free fatty acids in plasma of *Them5*^{-/-} and wildtype mice were measured using ZenBio serum/plasma Fatty Acid detection kit (ZenBio, Inc.).

Ketone bodies measurement

Levels of 3-Hydroxybutyrate (3-HB) were determined with Autokit 3-HB test for quantitative determination of 3-hydroxybutyrate (3-HB) in serum or plasma (WAKO).

Cellular fatty acid oxidation

Isolated hepatocytes were incubated for 1 h in scintillation vials in Krebs Ringer buffer with 3% fatty acid free BSA, with 1 mM 1-¹⁴C-palmitic acid with specific activity 1 mCi/mmol (Hartmann Analytic GmbH). Radiolabeled CO₂ was collected in center wells with Whatman #1 filter paper and 200 µl of 1 M methylbenzethonium hydroxide in methanol. At the end of the incubation, 300 µl of 5M H₂SO₄ was added to volatilize the remaining CO₂, and the solution was incubated for another 30 min. The center wells

were then placed in other scintillation vials and 8 ml of scintillation liquid were added and counted on a β -counter.

Preparation and culture of primary mouse embryonic fibroblasts (MEFs)

Mouse embryonic fibroblasts (MEFs) were derived from E13.5 embryos. Cells were cultured in DMEM containing 10% fetal calf serum under low oxygen conditions (3%) at 37°C (vom Brocke et al., 2006). All experiments were performed with primary MEFs (passages 3-15).

Respirometry analysis was performed with Seahorse XF24 analyzer (Seahorse Bioscience, Billerica, MA, USA). Mitochondria were isolated from liver of Them5 WT and KO mice, protein was quantified using BCA (Pierce), and 5 μ g of protein per well were plated on polyethyleneimine-treated plates (1:15000 dilution from a 50% solution from Sigma-Aldrich). For coupling assay an initial mix contained succinate and rotenone (10mM and 2 μ M, correspondingly). After an Oxygen Consumption Rate (OCR) baseline measurement, ADP, oligomycin, carbonyl cyanide 4-(trifluoromethoxy)-phenylhydrazone (FCCP), and antimycin A were sequentially added to each well to the final concentrations of 4mM, 2.5 μ g/ml, 4 μ M and 4 μ M respectively, and changes in the OCR were analyzed. For electron flow assay the initial mix contained malate, pyruvate, and FCCP (2mM, 10mM, 4 μ M final concentrations, correspondingly). After the initial OCR measurement, subsequent injections of rotenone, succinate, antimycin A and ascorbate/ N_1,N_1,N_1,N_1 -tetramethyl-1,4-phenylene diamine (TMPD) (2 μ M, 10mM, 4 μ M, 10mM/100 μ M final concentrations, respectively) were performed, and changes in OCR were analyzed. The measurement was performed accordingly to the protocol provided by manufacturer.

Mice

Mice were housed in groups of 3 with 12 hour-dark/light cycles and free access to food and water, in accordance to the Swiss Animal Protection Ordinance. All procedures were performed with approval of the appropriate authorities.

For the high fat diet experiments mice were housed according to their genotypes, but not more than in groups of 3. After weaning mice were kept on high fat diet for 13-15 weeks. High fat diet was from KLIBA NAFAG #2126 (Kaiseraugst, Switzerland) and contained 45 % kcal % fat.

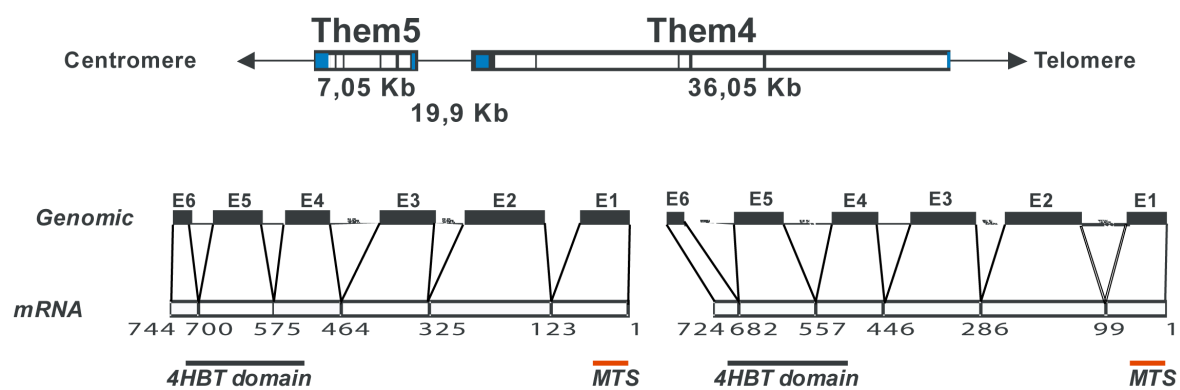
Statistical analysis

Data are provided as means \pm standard errors of the means (SEM), where n is the number of independent experiments. All data were subjected to the one-way analysis of variance (ANOVA), Student t-test, or Mann-Whitney test, as applicable. The significance is indicated as *** for $p < 0.001$, ** for $p < 0.01$ and * for $p < 0.05$

SUPPLEMENTAL FIGURES

Zhuravleva et al., Figure S1

A



B

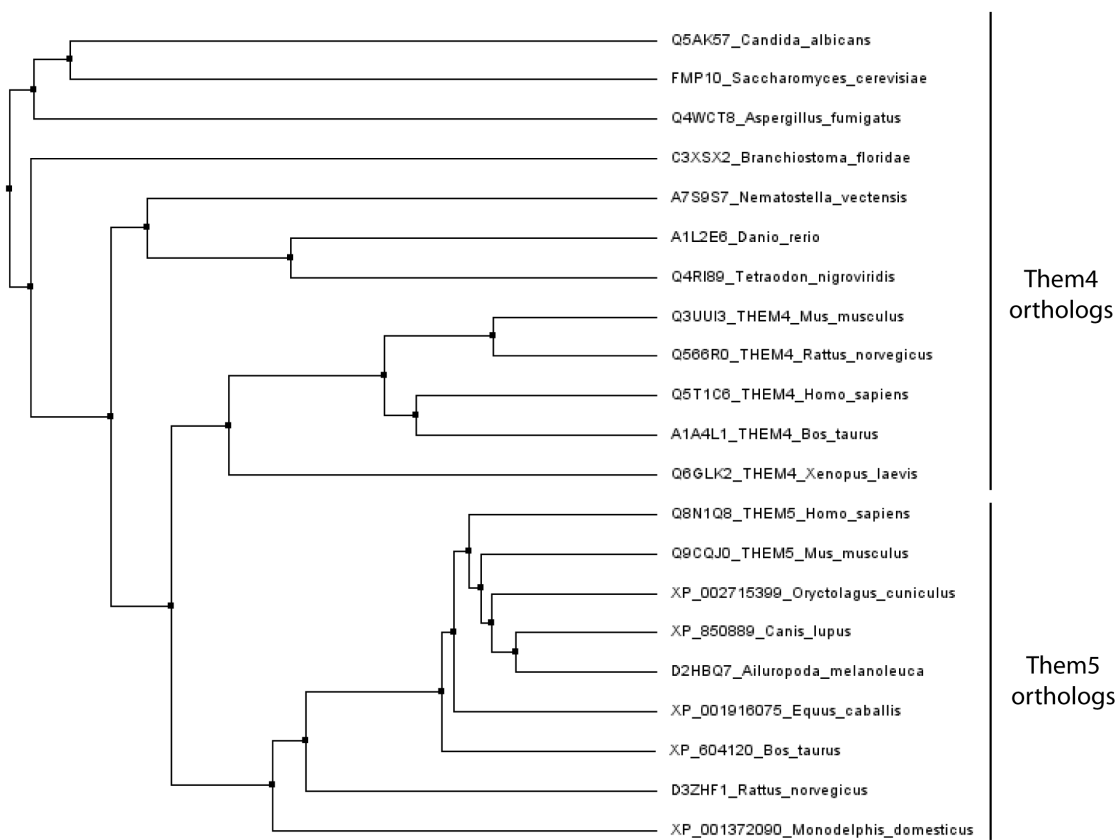


Figure S1. Them5 gene appears later in evolution but shares similar structure with Them4

(A) Cartoon representation of hThem4 and hThem5 genes.

Genomic (upper panel) and exon-intron structure and mRNA cartoon representation (lower panel) of hThem4 and hThem5 genes (4HBT - 4-hydroxybenzoyl-CoA thioesterase domain, MTS - mitochondrial targeting sequence).

(B) Phylogenetic tree of Them4 and Them5 orthologs in different species.

Them4 orthologs are found in lower eukaryotes, such as yeasts and chordata (Them4 orthologues upper group); Them5 orthologs, however, are present only in mammals (lower group).

Data collection and refinement statistics

	Them4	Them5
<i>Data collection</i>		
Space group	P1	C222 ₁
Cell constants		
a, b, c [Å]	50.5, 58.2, 69.7	45.5, 88.8, 105.4
α, β, γ [°]	90.0, 71.1, 64.6	90.0, 90.0, 90.0
λ [Å]	0.96	1.00
Resolution range [Å]	30.0-1.6 (1.66-1.60)	30.0-1.45 (1.49-1.45)
Unique reflections	83501	70847
Completeness [%]	93.4 (84.0)	96.8 (96.7)
Multiplicity	1.9	2.1
R_{sym} [%]^a	4.8 (21.6)	2.8 (37.3)
I/σ(I)	22.7 (3.2)	17.1 (2.1)
<i>Refinement</i>		
Resolution range [Å]	30.0-1.6	25.0-1.45
Reflections used	83486	70480
R-factor [%]	19.3	17.7
R_{free} [%]	22.6	19.4
r.m.s bond lengths [Å]	0.007	0.006
r.m.s bond angles [°]	1.07	1.06
Wilson B-factor [Å²]	24.8	24.4
Mean B-factor [Å²]	20.2	25.0
Ramachandran plot		
regions (favored, allowed) [%]	99.1, 0.9	97.8, 2.2

^a $R_{\text{sym}} = \frac{\sum_{hkl} \sum_j |I_{j,hkl} - \langle I_{hkl} \rangle|}{\sum_{hkl} \sum_j I_{j,hkl}}$ where $\langle I_{hkl} \rangle$ is the average of the intensity $I_{j,hkl}$ over $j = 1, \dots, N$ observations of symmetry equivalent reflections hkl . Numbers in parentheses refer to values in the highest resolution shell.

Table S1. Data collection and refinement statistics

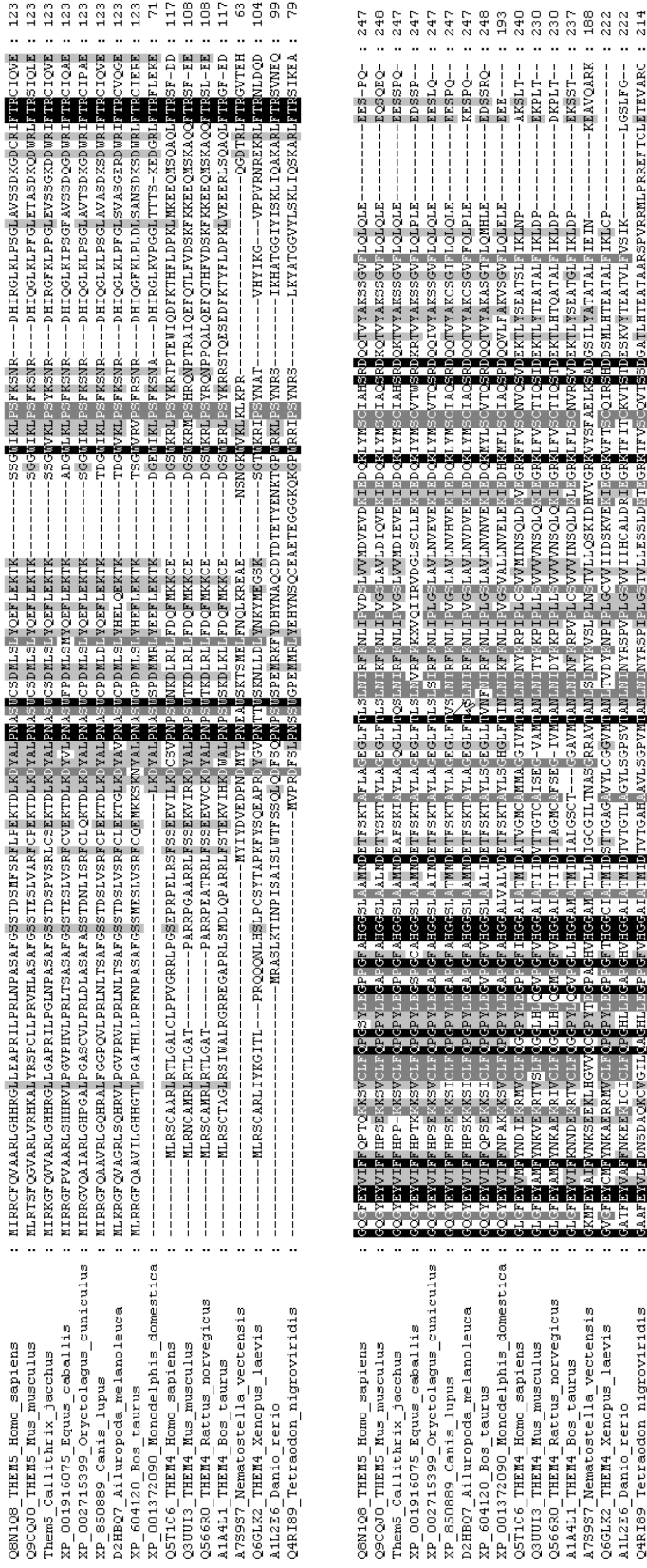


Figure S2. ClustalW multiple sequence alignment of Them4/5 and their orthologs in other species used for ConSurf computational analysis. ClustalW multiple sequence alignment of Them4/5 and their orthologs in other species used for ConSurf computational analysis (<http://consurf.tau.ac.il/>). The alignment shows conserved residues (highlighted in dark-grey and grey). Also note the lack of conservation in mitochondrial targeting sequences (N-terminal part of the sequences) between Them4 and Them5 orthologous groups.

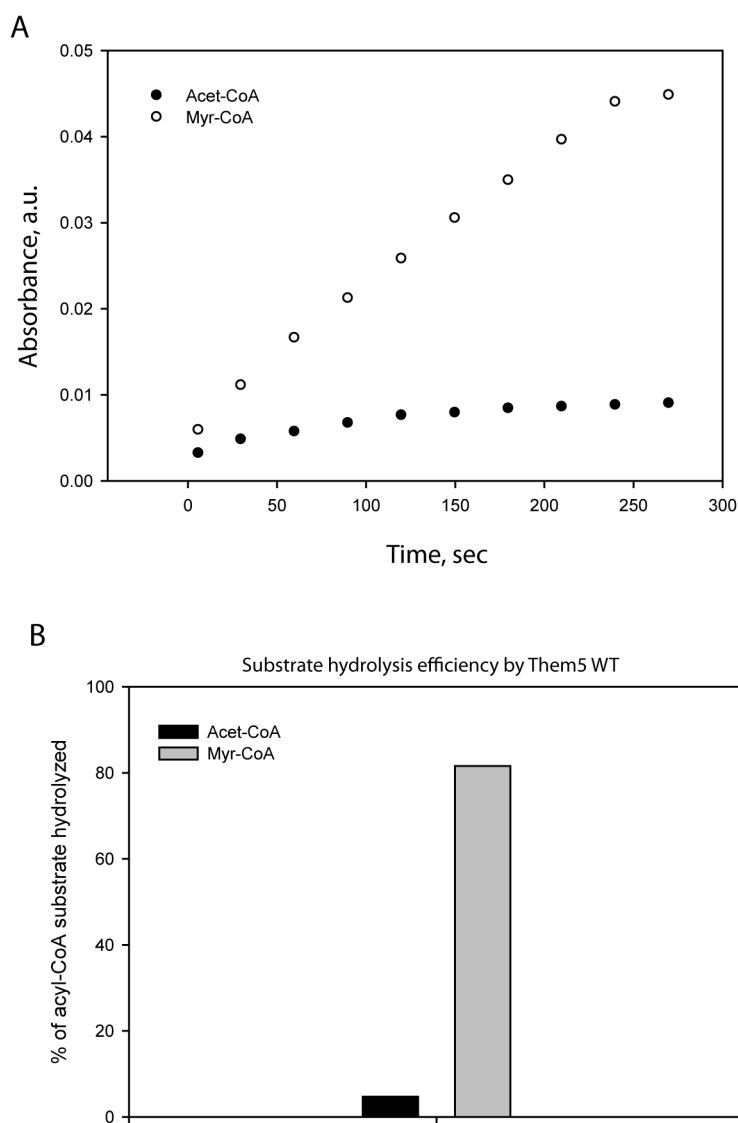
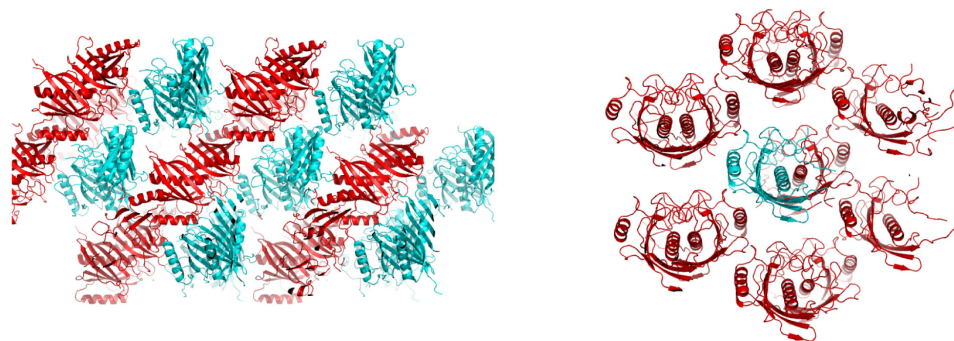


Figure S3. Wild-type hThem5 has a hydrolase activity directed towards myristoyl-CoA, but not acetyl-CoA

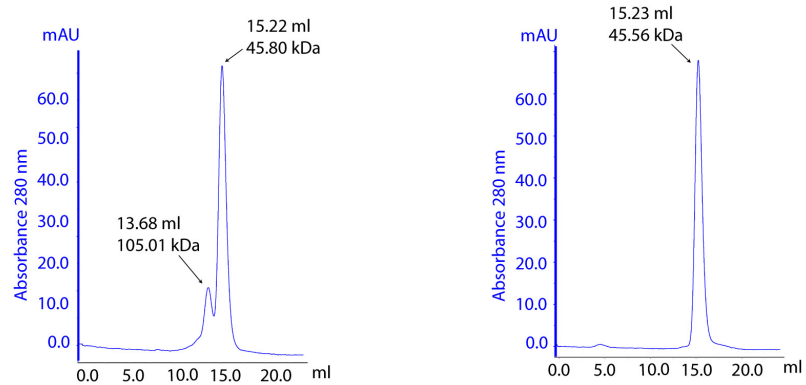
(A) Time-dependent change of absorbance (selected time points) reflecting hydrolysis of 20 μ M myristoyl- and acetyl-CoA by wild-type hThem5. Reaction was monitored at 412nm at 37 $^{\circ}$ C in the presence of 5 μ g of enzyme.

(B) Efficiency of substrate hydrolysis (acetyl- and myristoyl-CoA) by wild type hThem5 after 20min of reaction.

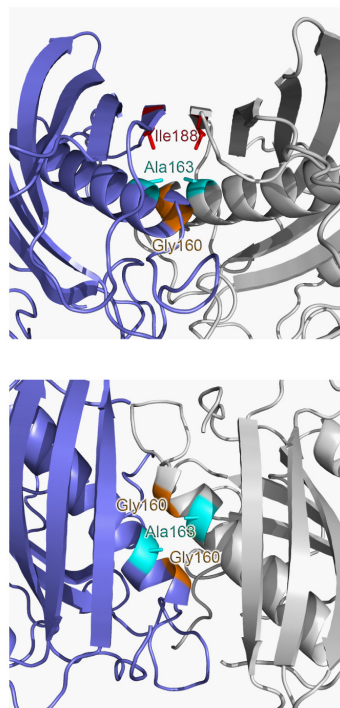
A



B



C



D

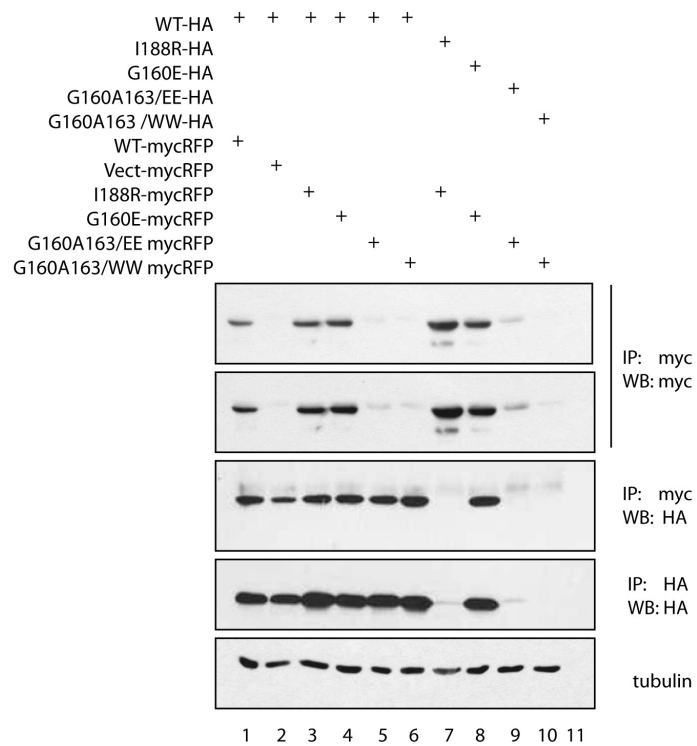


Figure S4. Them4 and Them5 are forming homodimers

(A) Crystal packing of $\Delta 36$ Them4 (left panel) and $\Delta 34$ Them5 (right panel) molecules in the P1 and in the C222₁ crystal lattice, respectively. Adjacent layers of symmetry-related molecules forming the crystal are displayed in cyan and red in cartoon representation. $\Delta 34$ Them5 molecules are shown in cartoon representation with the content of the asymmetric unit colored in cyan (1/2 of the $\Delta 34$ Them5 homodimer) and the symmetry-related molecules displayed in red.

The structure of $\Delta 36$ Them4 was solved in space group P1 (two homodimers in the a.u.) and C222₁ (one homodimer in the a.u., data not shown), while the structure of $\Delta 34$ Them5 was solved in space group C222₁ (1/2 homodimer in the a.u.), C2 (three homodimers in the a.u., data not shown), and P2₁ (one homodimer in the a.u., data not shown). In all of these cases $\Delta 36$ Them4 and $\Delta 34$ Them5 are independent homodimers.

(B) Analytical size-exclusion chromatography experiments displaying the oligomeric states of $\Delta 36$ Them4 (left panel) and $\Delta 34$ Them5 (right panel) in solution. $\Delta 36$ Them4 shows an equilibrium between a homodimeric species (15.22 ml, 45.80 kDa, 48.50 kDa) and a tetrameric species (dimer of homodimers, 13.68 ml, 105.01 kDa, 97.01 kDa) whereas $\Delta 34$ Them5 elutes as a homodimer only (15.23 ml, 45.56 kDa, 49.79 kDa). Elution volumes, approximate molecular weight and expected molecular weight are given in parentheses, respectively.

(C) Detailed view of Them5 mutation sites created to disrupt the homodimer. Sites are located at the homodimer interface and mapped onto the $\Delta 34$ Them5 crystal structure (side view, left upper panel; top view, left bottom). The Them5 subunits are shown as cartoon models (blue and gray) while mutated residues are shown as sticks and colored in red (Ile188), orange (Gly160), and cyan (Ala163). The most C-terminal α -strand of both subunits is not shown in the bottom view for clarity reasons.

(D) Co-immunoprecipitation experiments with Δ MTS-Them5 wild-type and mutants with HA and myc-RFP tags. HEK293cells were transfected with the corresponding cDNAs, 24hours after lyzed and proteins were precipitated with anti-myc antibodies and then probed with indicated antibodies. Mutations were introduced in the central helix, leading to instability of a dimer due to the electrostatic repulsion or steric hindrance (G160W/E, A163W/E); another mutation was made in order to disturb anti-parallel β -sheet formation (I188R). Double 160E163E and 160W163W mutants have very low levels of expression, but still can be co-precipitated with wildtype Them5 (lanes 5 and 6). However, co-transfection of two differently tagged mutants greatly diminishes their expression levels and abolishes interaction/co-precipitation (lanes 9 and 10).

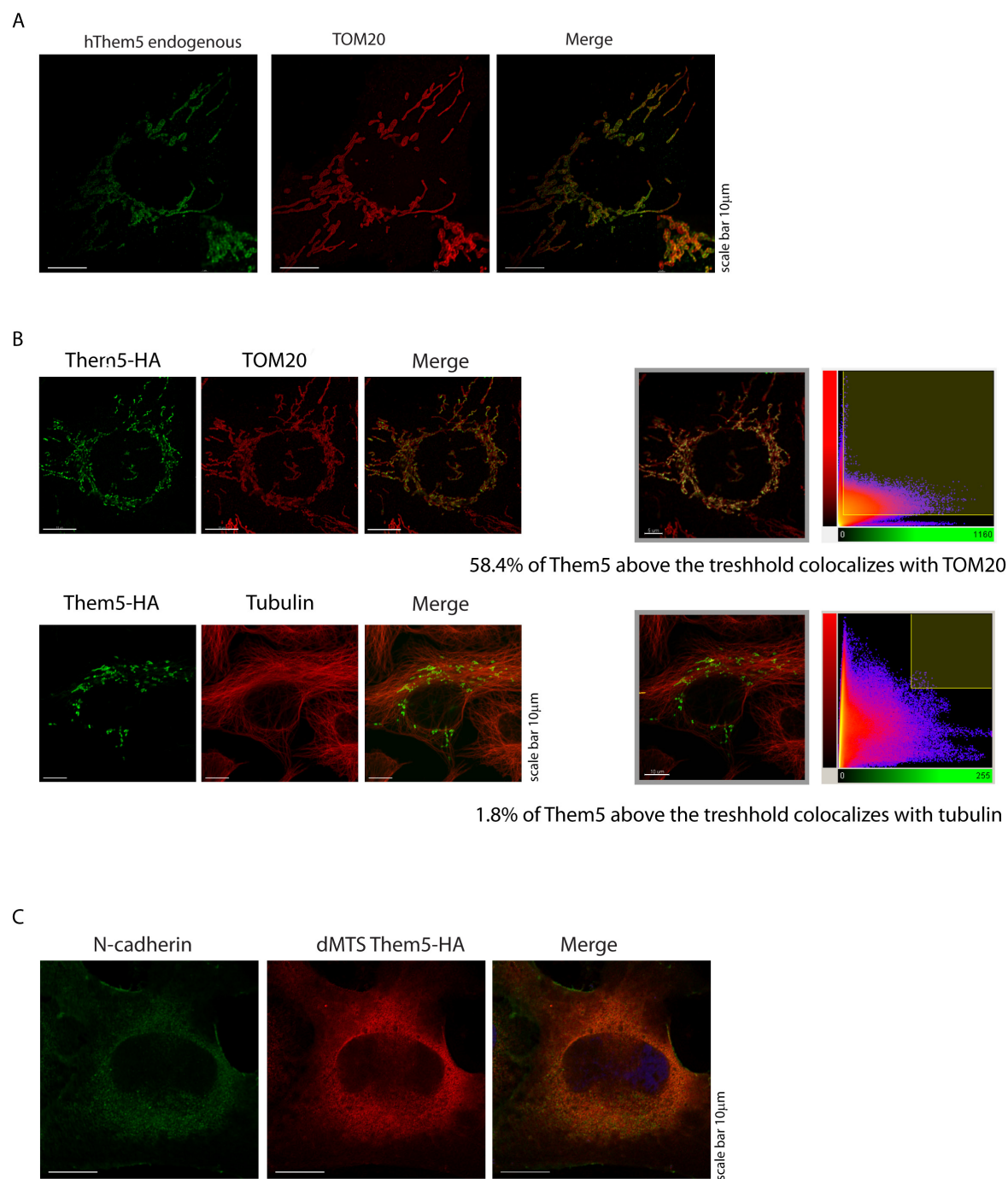


Figure S5. Mitochondrial localization of Them5 protein

(A) Immunofluorescence analysis of endogenous Them5. U2OS cells were fixed and stained with antibodies against hThem5 protein. Mitochondria were visualized with TOM20 protein.

(B) Examples of quantifications, carried out for Them5 and TOM20 (upper panel) and Them5 and tubulin (lower panel). Images were taken with the confocal microscope and analyzed with the Imaris Coloc software. The threshold of each channel was determined and percentage of colocalized pixels was quantified. Quantification showed 58.4% of colocalization of FL_Them5 with TOM20, 1.89% with tubulin (for Figure 3C); 12.5% colocalization of Δ MTS_Them5 with TOM20, 88.2% with tubulin (for Figure 3D).

(C) Immunofluorescence analysis of overexpressed Δ MTS_Them5 and N-cadherin.

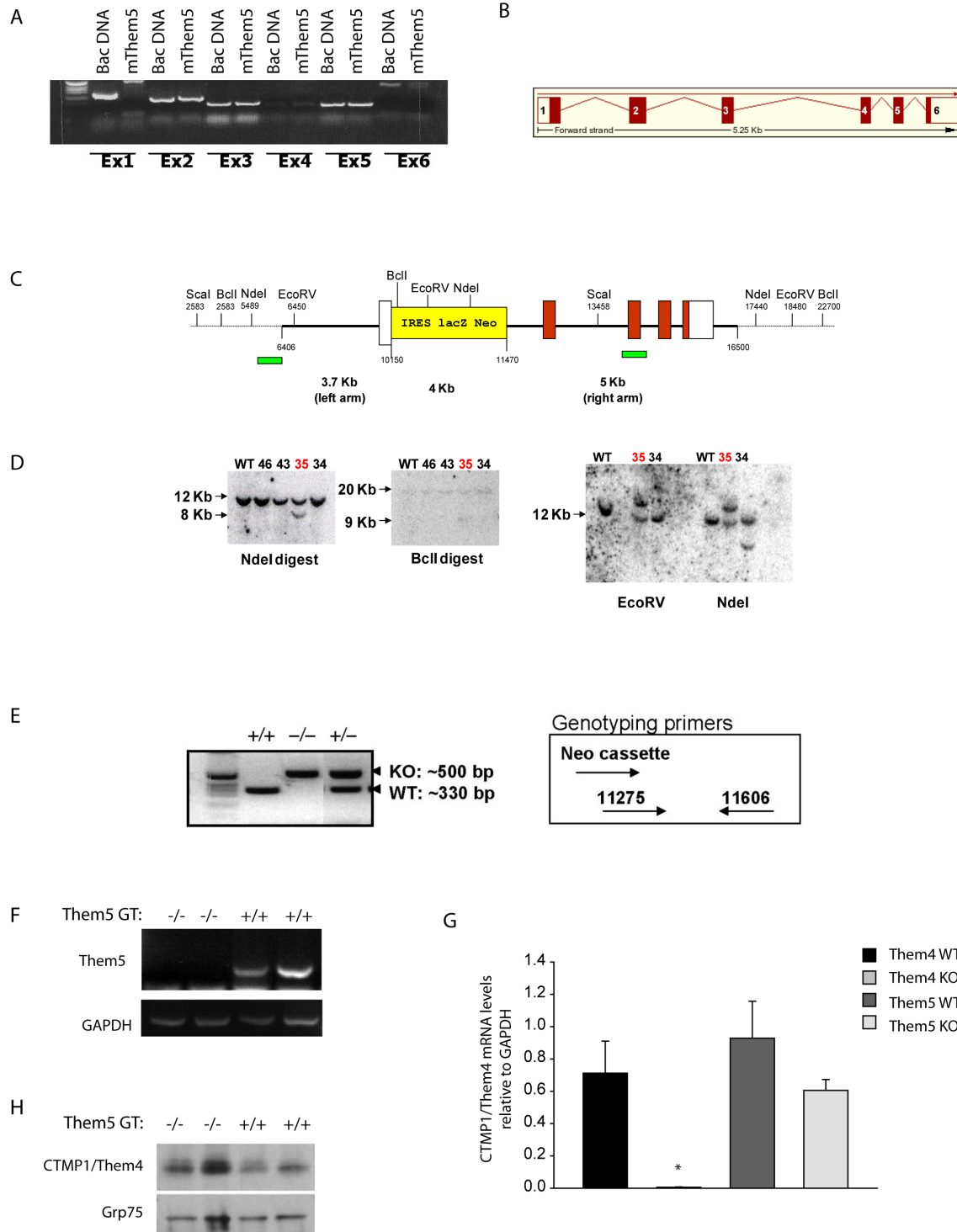


Figure S6. Generation of Them5 knock-out mouse

(A) Presence of mThem5 genomic DNA in BAC clone was verified by PCR of individual exons (cloned mThem5 cDNA is positive control). BAC clone was used as PCR template for generating left and right homology region of targeting vector.

(B) Transcript structure of mTHEM5 gene in mice. White areas represent untranslated regions (Ensembl database).

(C) Targeted *mThem5* allele. A targeting vector was generated that contains a 3.7 kb 5' homology region, an IRES/lacZ/neo cassette, and a 5 kb 3' homology region. A genomic DNA fragment of about 1.3 kb, including the ATG start codon in exon 1 and the full sequence of exon2, is deleted in the targeting vector. The targeting vector was linearized with NotI and electroporated into 129/Ola ES cells.

(D) Screening of ES cell clones was performed by Southern Blotting. DNA was digested with EcoRV and probed with an external probe (green box spanning sequence 16980-17663). An internal probe was then used on NdeI digested DNA (green box spanning sequence 9652-10154) for further characterization of ES cell clones positive for homologous recombination. Correctly targeted ES cells (highlighted in red) were used to generate chimeras. Male chimeras were mated with wildtype C57BL/6 females to obtain *Them5*^{+/-} mice, which were intercrossed to produce Them5 homozygous mutants.

(E) Progeny were genotyped for the presence of a targeted allele by multiplex PCR. The following primers were used for genotyping: P1-as 5'-GCA GCA GGC TGA ACT GAC TGA GG-3'; P2/KO-s 5'- GCT GCC TCG TCC TGC AGT TCA TTC-3''; P3/WT-s 5'-CAG GCG GCT GGA TTA AAC TAC C-3'. One reaction amplifies a 500 bp fragment from the targeted allele and the second reaction amplifies a 330 bp fragment from the wildtype allele.

(F) Total RNA was extracted from *Them5*^{-/-} and *Them*^{+/+} liver, and Them5 was amplified with specific primers. Each lane represents separate animal.

(G) mRNA levels of CTMP/Them4 were assessed by real-time PCR in Them5 WT and KO mice (n=4-5). No significant changes in Them4 mRNA level were detected upon Them5 knock-out.

(H) Western blot analysis of mitochondrial fractions from Them5 WT and KO liver (each lane represents separate animal). 30 µg of protein lysate were loaded on the gel and probed with anti-CTMP1/Them4 antibodies and Grp75 as a loading control.

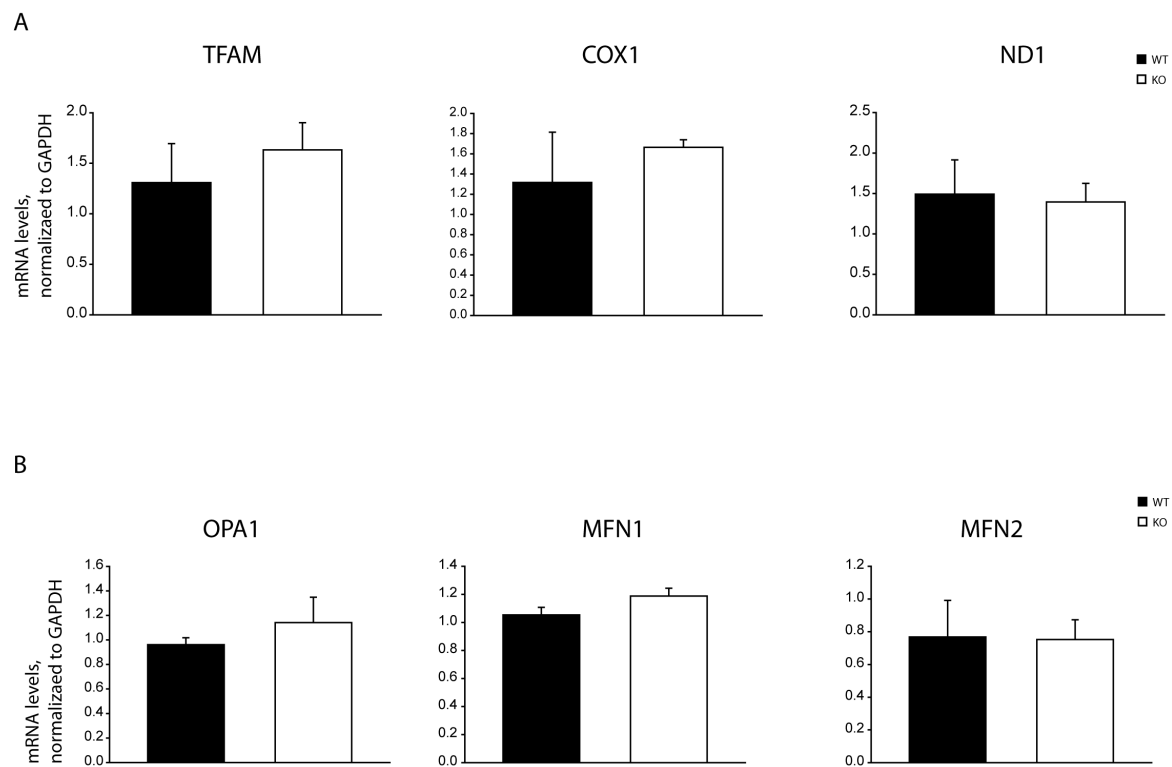


Figure S7. *Them5*^{-/-} mice show no changes in mtDNA copy number and mitochondrial fusion genes expression

Them5^{+/+} and *Them5*^{-/-} mice (males, 12 months old, random fed) were sacrificed and gene expression was measured by real-time PCR. No changes in mRNA expression between samples from *Them5*^{+/+} and *Them5*^{-/-} were detected in neither (A) nuclear encoded mitochondrial transcription factor TFAM and single copy mitochondrial genes COX1 and ND1, nor in (B) expression of mitochondrial fusion genes (OPA1, MFN1, MFN2).

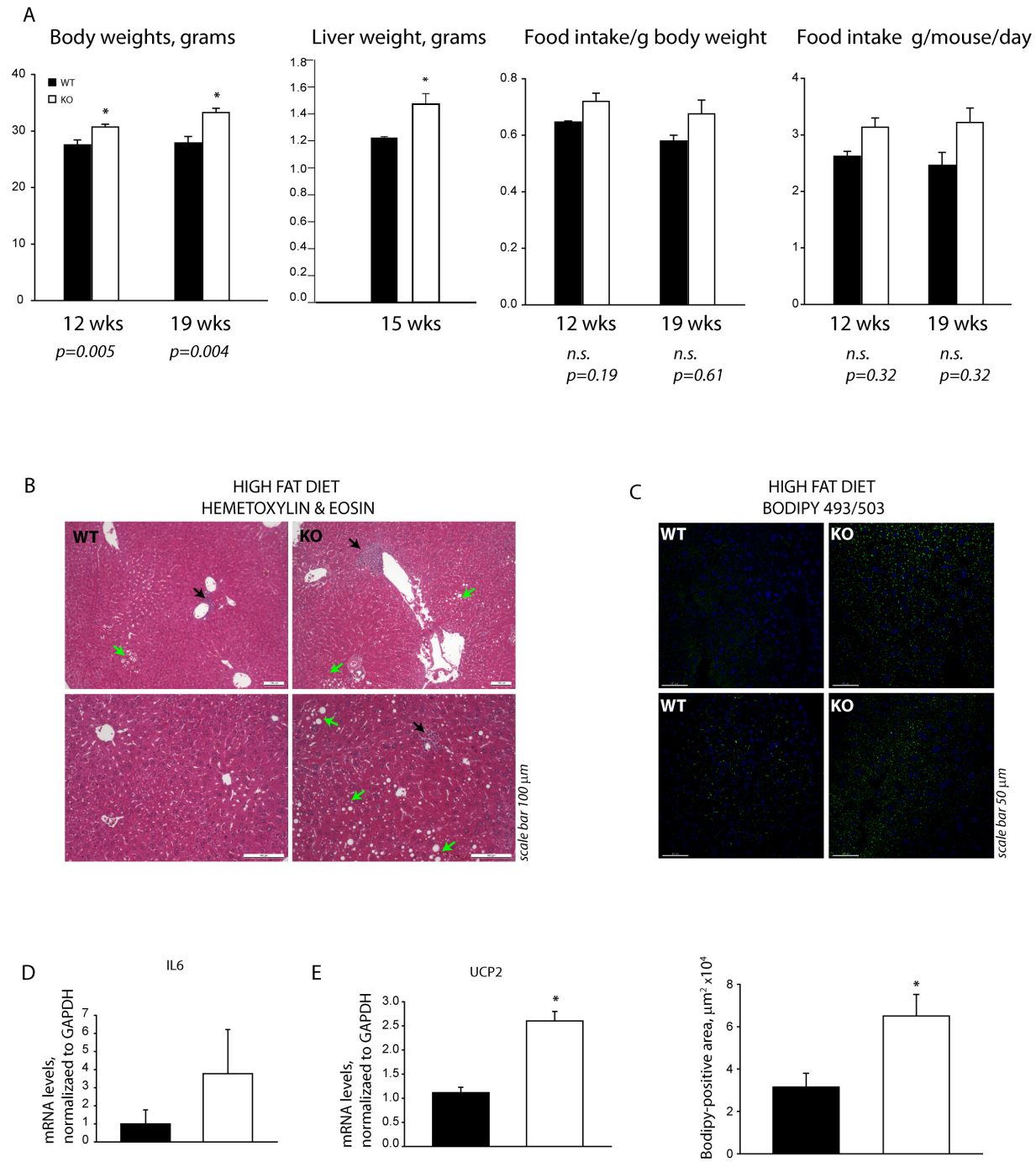


Figure S8. Loss of Them5 exacerbates fatty liver development upon high fat diet (HFD) treatment

Mice (males, n=6-8) were kept on HFD for 15 weeks and analyzed afterwards.

(A) Increase in body weights and liver weights of *Them5*^{-/-} mice (left panels), but no significant changes in food intake (measured as per gram per body weight and gram/mouse/day – right panels) were detected.

(B) Hematoxylin-eosin staining of liver sections from *Them5*^{+/+} (left panels) and *Them5*^{-/-} mice (right panels) kept on high fat diet for 15 weeks. Lipid accumulation is indicated with green arrows, lymphocytic infiltration - with black arrows. Note more pronounced inflammatory changes in *Them5*^{-/-} samples.

(C) Lipid accumulation was assessed by staining with BODIPY 493/503 of liver sections (10µm thickness). Nuclei were stained with TO-PRO 3 (both from Molecular Probes, Invitrogen). Images were taken with LSM700 and analyzed with Imaris software (Bitplane, Zurich). Quantification (bottom panel) shows almost 2-fold increase in BODIPY-positive area in *Them5*^{-/-} samples.

(D-E) RNA was extracted from livers of random fed *Them5*^{-/-} and *Them5*^{+/+} mice after 15 weeks of HFD and mRNA of (D) interleukin 6 and (E) UCP2 expression levels were measured by real-time PCR.

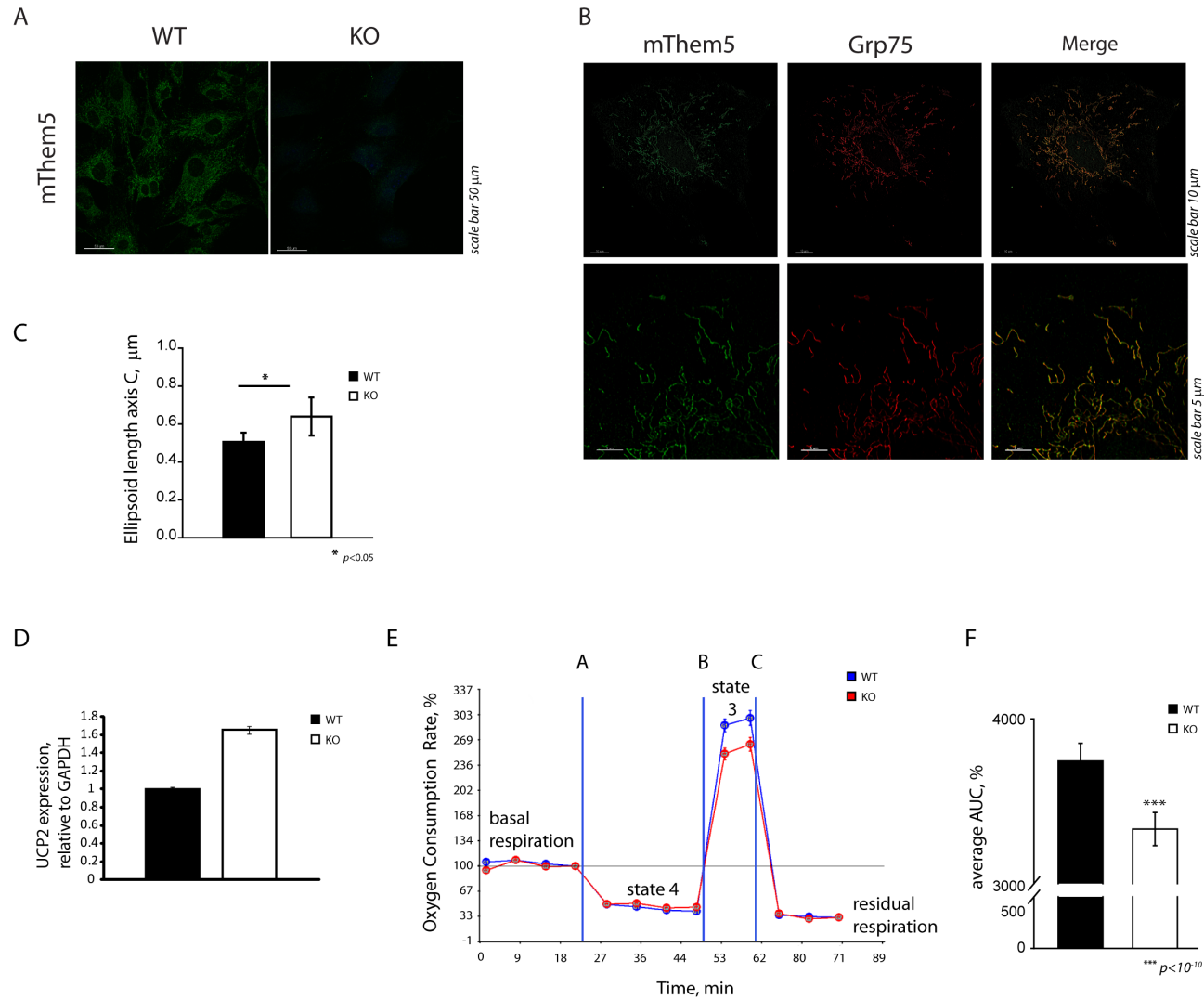


Figure S9. *Them5*^{-/-} mouse embryonic fibroblasts (MEFs) show elongated mitochondrial morphology and decreased respiratory capacity

(A) Primary MEFs from *Them5*^{-/-} and wild-type controls (gender matched siblings) were stained with anti-mouse Them5 antibodies and visualized with LSM700 microscope.

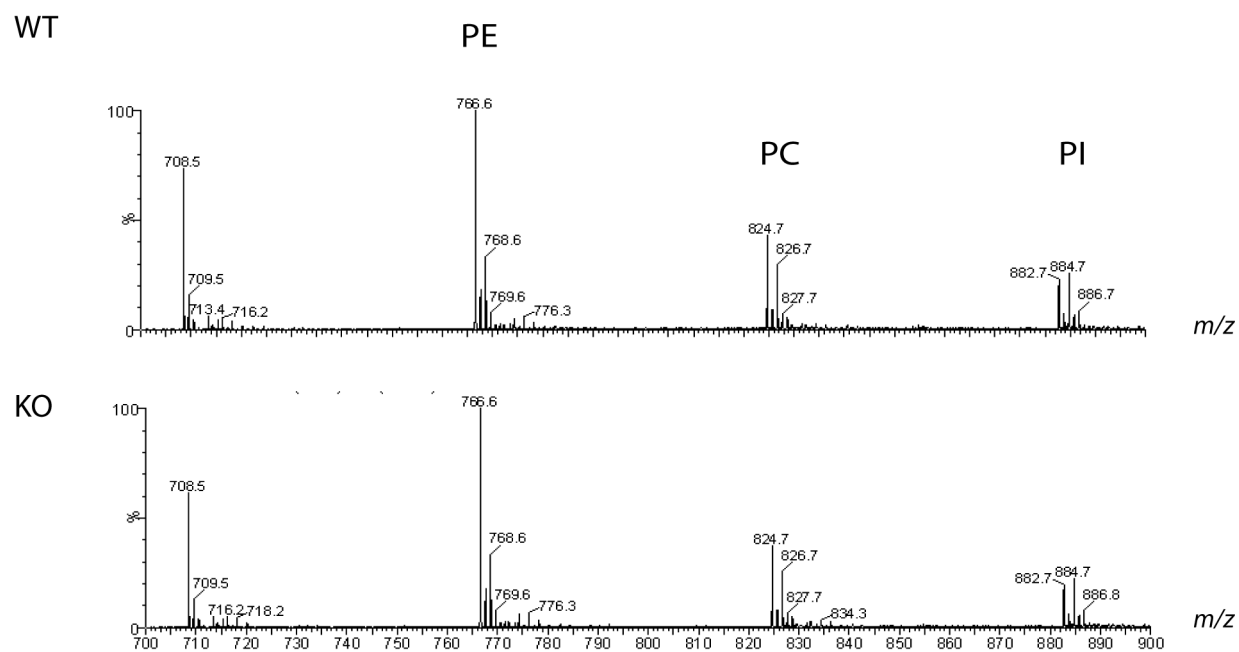
(B) Primary MEFs were co-stained with anti-mouse Them5 and anti-Grp75 (mortallin) antibodies. Images were taken with LSM700 microscope. The staining pattern shows colocalization of Them5 and Grp75.

(C) Primary MEFs from *Them5*^{-/-} and wild-type control were fixed and stained with anti-TOM20 antibodies. Confocal images were taken with the LSM700 microscope and mitochondria were reconstructed and their length was quantified with Imaris software (Bitplane, Zurich). Minimum 3 experiments were performed with at least 10 cells in each analyzed.

(D) UCP2 expression was measured by real-time PCR in primary MEFs from *Them5*^{-/-} and WT controls (from gender-matched siblings).

(E) Oxygen consumption rates were measured for *Them5*^{-/-} and WT primary MEFs using a Seahorse XF24 analyzer. A – Oligomycin, B – FCCP, C – Rotenone+Antimycin D (n=10 for each genotype).

(F) Quantification of the integral maximum respiration rate presented as area under curve (AUC) shows 20% decrease in *Them5*^{-/-}.

**Figure S10. MS profiling of mitochondrial phospholipids**

Lipid extracts were prepared from Them5 WT (upper panel) and KO mouse mitochondria (lower panel) and analyzed by mass spectrometry in a positive mode (Moiso et al., 2009). Species composition in the phospholipid region does not show major differences between WT and KO samples. Representative MS profiles are shown. PE – phosphatidylethanolamine, PC – phosphatidylcholine, PI – phosphatidylinositol

SUPPLEMENTAL REFERENCES

Adams, P.D., Afonine, P.V., Bunkoczi, G., Chen, V.B., Davis, I.W., Echols, N., Headd, J.J., Hung, L.W., Kapral, G.J., Grosse-Kunstleve, R.W., McCoy, A.J., Moriarty, N.W., Oeffner, R., Read, R.J., Richardson, D.C., Richardson, J.S., Terwilliger, T.C., and Zwart, P.H. PHENIX: a comprehensive Python-based system for macromolecular structure solution. *Acta Crystallogr D Biol Crystallogr* 66, 213-221.

Berrow, N.S., Alderton, D., Sainsbury, S., Nettleship, J., Assenberg, R., Rahman, N., Stuart, D.I., and Owens, R.J. (2007). A versatile ligation-independent cloning method suitable for high-throughput expression screening applications. *Nucleic Acids Res* 35, e45.

Emsley, P., and Cowtan, K. (2004). Coot: model-building tools for molecular graphics. *Acta Crystallogr D Biol Crystallogr* 60, 2126-2132.

McCoy, A.J., Grosse-Kunstleve, R.W., Storoni, L.C., and Read, R.J. (2005). Likelihood-enhanced fast translation functions. *Acta Crystallogr D Biol Crystallogr* 61, 458-464.

Moisoi, N., Klupsch, K., Fedele, V., East, P., Sharma, S., Renton, A., Plun-Favreau, H., Edwards, R.E., Teismann, P., Esposti, M.D., Morrison, A.D., Wood, N.W., Downward, J., and Martins, L.M. (2009). Mitochondrial dysfunction triggered by loss of HtrA2 results in the activation of a brain-specific transcriptional stress response. *Cell Death Differ* 16, 449-464.

Sali, A., and Blundell, T.L. (1993). Comparative protein modelling by satisfaction of spatial restraints. *J Mol Biol* 234, 779-815.

vom Brocke, J., Schmeiser, H.H., Reinbold, M., and Hollstein, M. (2006). MEF immortalization to investigate the ins and outs of mutagenesis. *Carcinogenesis* 27, 2141-2147.

3.2 THE ROLE OF THE CTMP2/THEM5 PROTEIN IN PKB SIGNALING: FURTHER CHARACTERIZATION OF *THEM5*^{-/-} MICE

This part of the results includes work with Them5 KO mouse that was not included in the manuscript presented in section 3.1.

3.2.1 Interconnected mitochondria in *Them5*^{-/-} primary hepatocytes and β -cells

We performed serial block-face scanning electron microscopy of primary hepatocytes from Them5 wildtype and knock-out mice, and observed more interconnected, elongated mitochondria in Them5^{-/-} tissues. Them5^{-/-} mitochondria had almost twice the volume of Them5^{+/+} mitochondria, reflecting their more interconnected phenotype. We analyzed samples from 2- and 6-month-old mice and found that the phenotype was more pronounced in the older mice. At 2 months the difference was statistically significant, although visually mitochondrial morphology had not changed considerably. However, at 6 months the difference in mitochondrial shape was striking. We also analyzed whether mitochondrial morphology changed upon fasting in Them5^{-/-} and Them5^{+/+} mice. The mitochondrial volume was increased after fasting in both wildtype and knock-out samples, and there was almost a 3-fold difference in volume.

The increased volume/interconnectivity may also be partially explained by an increase in the number of mitochondria. To analyze this, we performed real-time PCR analysis of single-copy mitochondrial genes COX2 and ND1, but did not observe any differences. Also, the quantification of mitochondria from *Them5*^{+/+} and *Them5*^{-/-} hepatocytes in the EM stacks did not show statistically significant differences between mutants and wildtype mice (Figure 3.1).

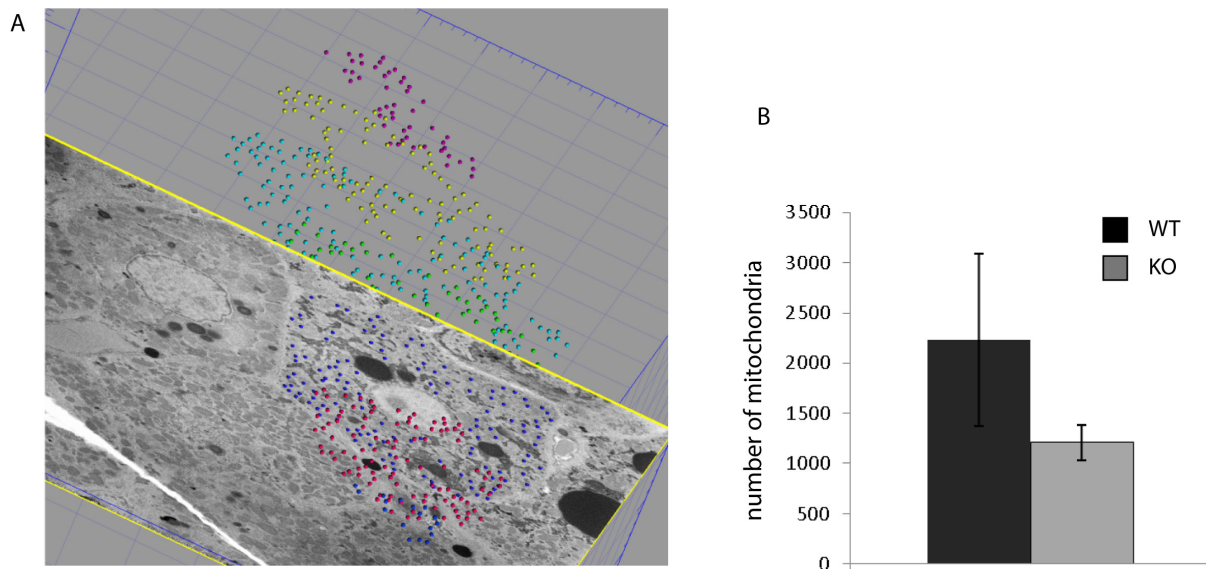


Figure 3.1

Quantification of mitochondria number in the electron microscope images. (A) Example of mitochondria number quantification in the EM stack obtained from SBFSEM of liver tissue. Mitochondria number was quantified in the slices through the whole stack of images, which was a complete cell. (B) Quantification of mitochondria in the EM stack did not show and statistically significant differences between *Them5* WT and KO hepatocytes.

We also observed that in *Them5*^{-/-} hepatocytes there may be an increased association between mitochondria and the endoplasmic reticulum (Figure 3.2), but this needs further investigation.

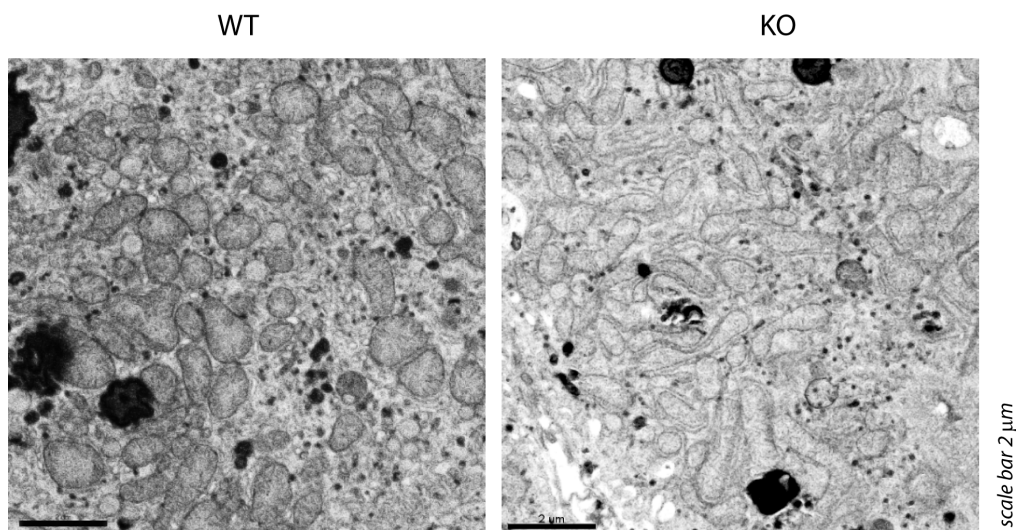


Figure 3.2

Electron micrographs of hepatocytes from *Them5* WT (left) and KO (right), showing that there may be an increased association between mitochondria and the endoplasmic reticulum.

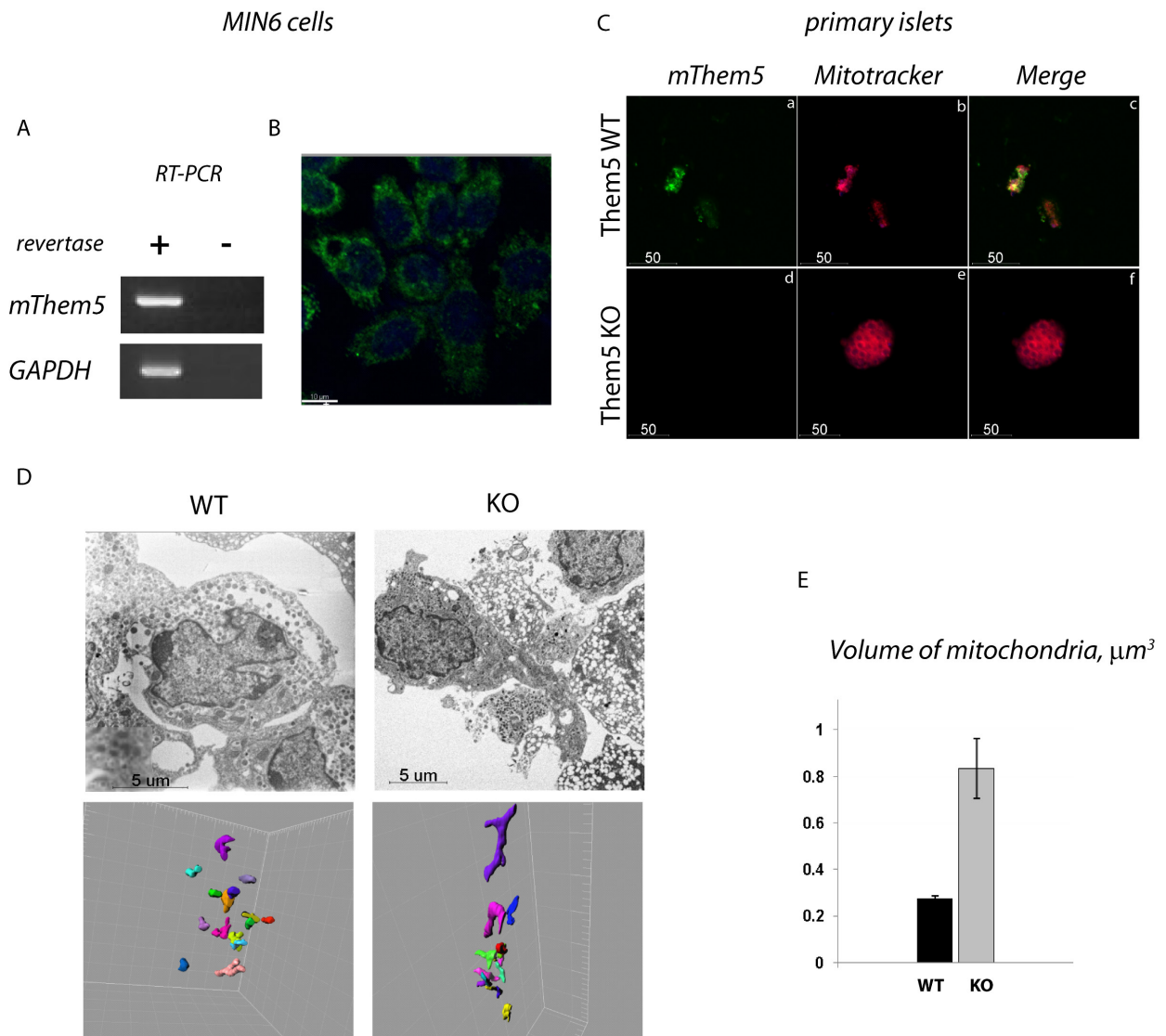


Figure 3.3

(A) Presence of Them5/CTMP2 mRNA in mouse β -cells (MIN6 cell line). Total RNA was extracted, cDNA was synthesized and PCR with corresponding primers was performed using 30ng of template. (B) Immunofluorescent staining of endogenous Them5/CTMP2 protein in MIN6 cells. (C) Endogenous Them5/CTMP2 protein is present in primary β -cells and co-localizes with the mitochondrial marker Mitotracker Red. (D) Electron micrographs of pancreatic islets isolated from Them5 WT and KO mice, obtained by serial-block face scanning EM (upper panel), and 3D reconstruction of mitochondria showing greater volume of mitochondria from Them5 KO mice (lower panel). (E) Quantification of the mitochondrial volume in Them5 KO and WT β -cells. A minimum of 15 mitochondria per cell were reconstructed in at least three cells per mouse per genotype. Data are presented as mean \pm S.E.M. $p < 0.05$.

Analysis of pancreatic β -cells showed a similar phenotype. The increase in mitochondrial volume was almost 4-fold (Figure 3.3D,E). We have not observed any other abnormalities at the EM level in β -cells. In addition, the histological analysis of the pancreas from *Them5*^{-/-} mice confirmed a typical organization of pancreatic islets, with insulin-producing β -cells concentrated in the middle, and glucagon-

secreting α -cells on the periphery of the islet structure (Figure 3.4A). We performed morphometrical analysis of pancreas from *Them5*^{-/-} female mice (and littermate controls), and found a trend to an increase in islet area in knock-out mice (Figure 3.4C). Samples from males have been collected and being processed. However, hematoxylin-eosin staining of pancreas sections revealed infiltration of the endocrine area with lymphocytes, which is usually sign of type I diabetes (Figure 3.4B). This is an unexpected observation, which needs further analysis and study.

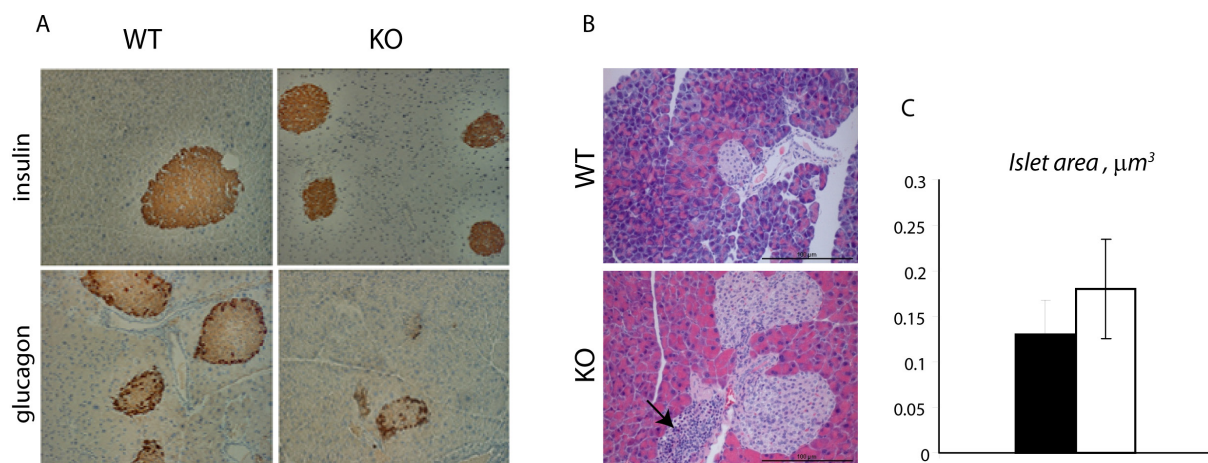


Figure 3.4

Preserved organization of pancreatic islets in *Them5*^{-/-} mice, but signs of lymphocytes infiltration and increased area of islets. (A) Immunohistochemistry (IHC) analysis of pancreas endocrine area from *Them5* KO and WT mice (males, 6 months old). *Them5* WT and KO pancreas was embedded in paraffin and cut into serial sections 5 μm thick. Slices were stained with antibodies against insulin (upper panel) and glucagon (lower panel). IHC analysis shows typical organization of endocrine pancreas. (B) H&E staining of pancreas from *Them5* WT and KO mice (males, 6 months old). *Them5*^{-/-} have larger islets and the endocrine part of the pancreas has been infiltrated with lymphocytes (indicated with an arrow). (C) Quantification of the islet area in *Them5* WT and KO pancreas (females, 6 months old). Preliminary quantification shows trend to increased area of β -cells.

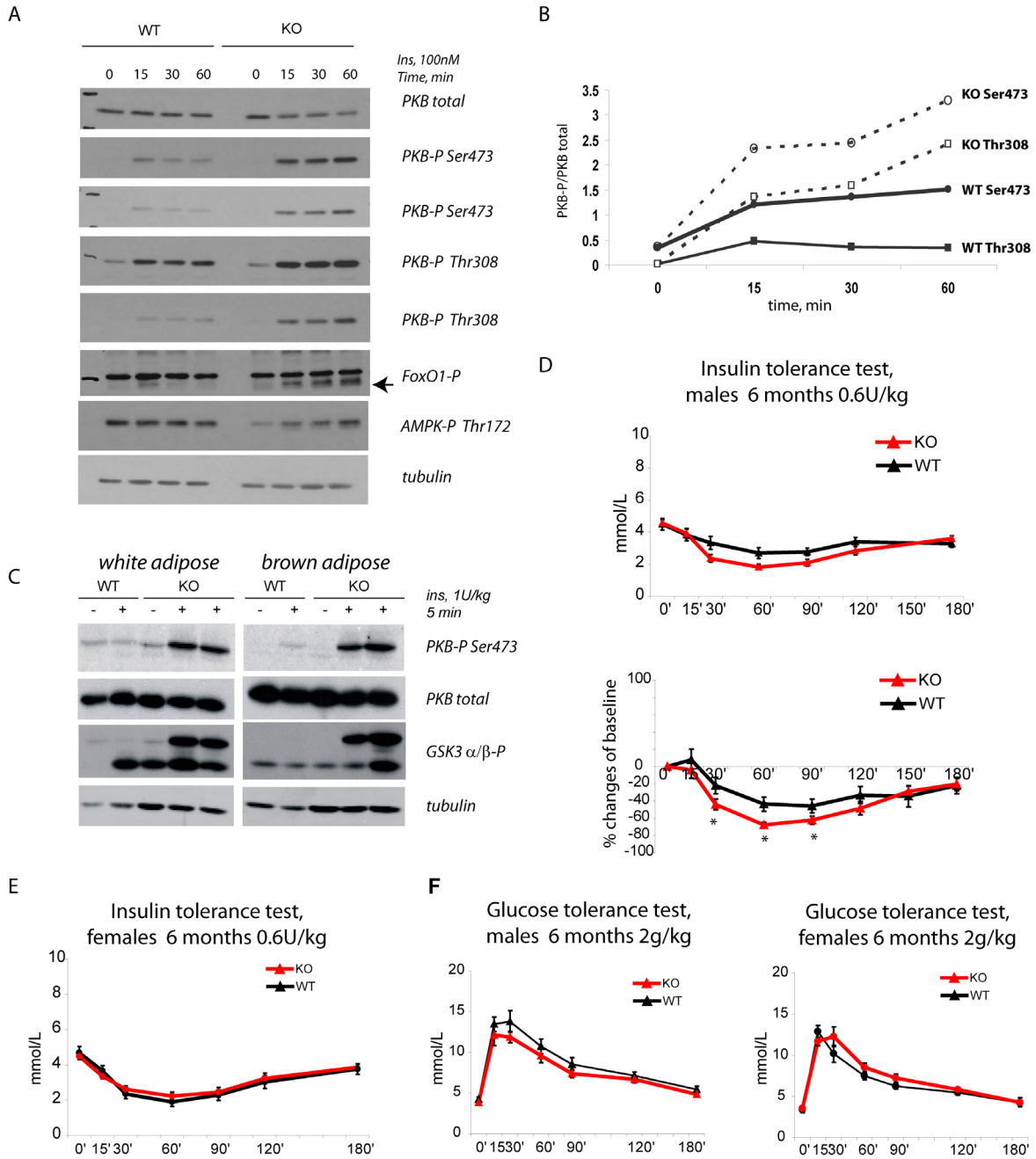
3.2.2 Enhanced insulin sensitivity in *Them5*^{-/-} mice

We examined the effect of *Them5* loss on glucose homeostasis and insulin sensitivity. *Them5*^{-/-} males and females were fed with a standard chow diet and subjected to insulin and glucose tolerance tests. Glucose tolerance test results showed no difference between WT and KO mice (Figure 3.5F). However, we observed enhanced insulin sensitivity in *Them5* KO male mice compared to WT

littermates (Figure 3.5D). The window of insulin dose given to mice was very narrow, since *Them5*^{-/-} mice suffered hypoglycemic shock and subsequently died as a result of having received too high a dose of insulin. Interestingly, only knock-out males, not females, showed differences in insulin sensitivity (Figure 3.5E). We also performed tests on 3-month-old mice, but insulin sensitivity was still unaltered in *Them5* KO females.

3.2.3 PI3K/PKB signaling is enhanced in *Them5*^{-/-} mice

Our studies indicate that increased insulin sensitivity in *Them5* knock-out mice is mainly caused by increased responsiveness of adipose tissue (both white and brown) and liver (Figure 3.5A-C). To study this, we starved mice for 8 hours and injected insulin or saline intra-venously. Increased PKB phosphorylation was observed in white and brown adipose tissue and liver. Muscle, heart, and brain did not show any difference in phosphorylated PKB levels. However, PKB was not the only kinase affected by loss of *Them5*. We also observed decreased phosphorylation of AMPK at Thr172, a major activation site, which is consistent with increased insulin sensitivity upon *Them5* deficiency (Figure 3.5A).

**Figure 3.5**

Enhanced PKB signaling in *Them5*^{-/-} mice. (A) Overactivation of PKB signaling in *Them5*^{-/-} hepatocytes. Primary hepatocytes of *Them5*^{-/-} and control mice were treated with insulin for the indicated time. Protein lysates were prepared and analyzed by western blotting with indicated antibodies. (B) Quantification of PKB-S473 and Thr-308 phosphorylation relative to total PKB levels (from the experiment described in A). (C) Overactivation of PKB signaling in *Them5*^{-/-} white and brown adipose tissue after insulin stimulation. Mice were starved overnight and injected with insulin (1U/kg) or saline, and sacrificed 5min after injection. Tissues were collected and snap-frozen in liquid nitrogen. Protein lysates were prepared and analyzed by western blotting using the antibodies indicated. (D) Enhanced insulin sensitivity in *Them5*^{-/-} males. Mice were starved overnight and injected with 0.6U/kg of insulin i.p. Blood glucose levels were measured at the time indicated. Both representations, absolute values of glucose concentration in the blood (upper panel) and percent change from the baseline values (lower panel), show statistically significant differences between *Them5*^{-/-} and control mice (n=8-11). (E) Insulin sensitivity test of *Them5*^{-/-} females and littermate controls (6 months old) showed indistinguishable blood glucose levels after insulin injection (n=8-10). (F) Glucose tolerance test, performed on *Them5*^{-/-} and control littermates (males and females, 6 months old) showed no difference in glucose clearance after i.p. injection of glucose (2g/kg of body weight). (n=8-11).

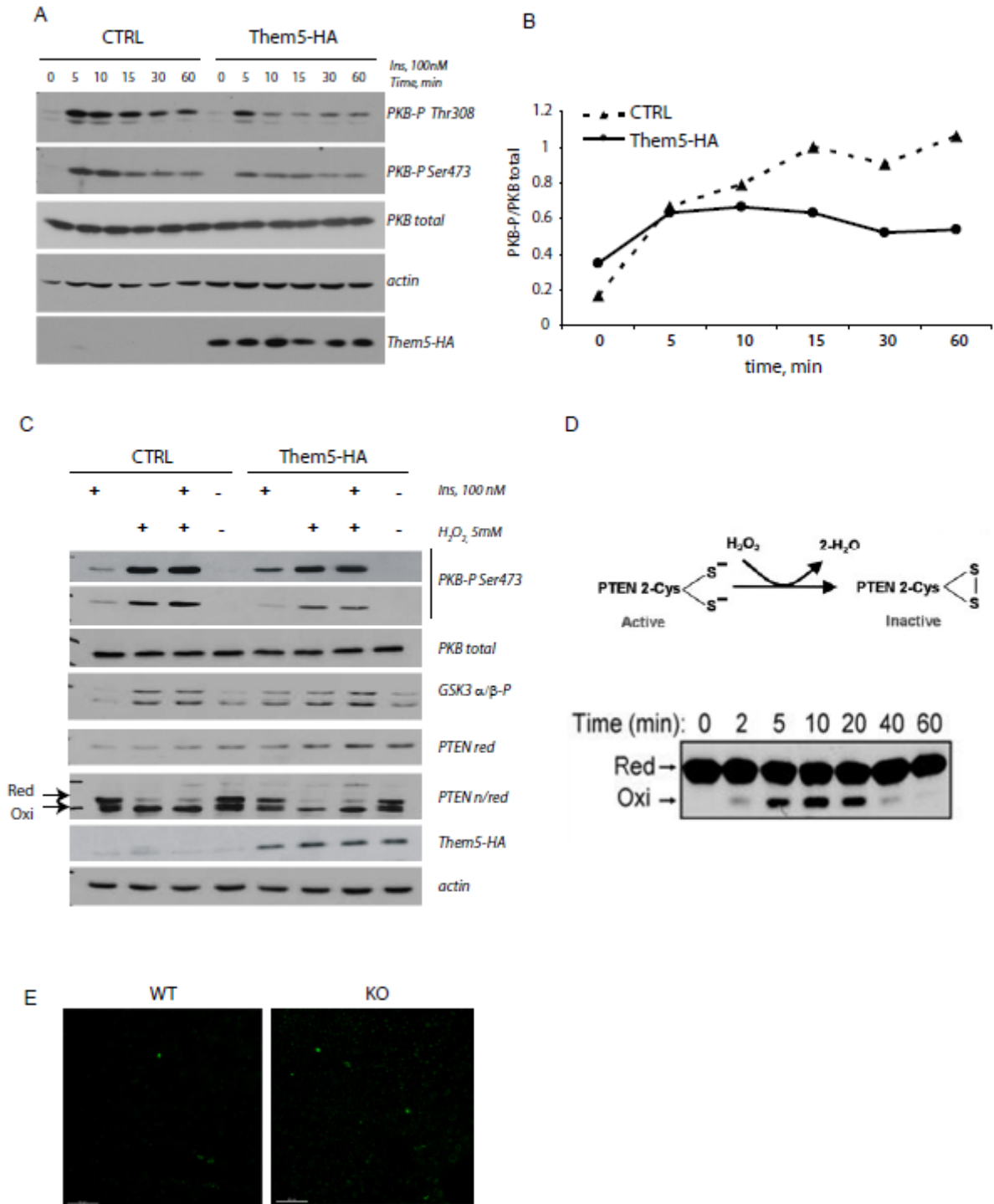


Figure 3.6

Overexpression of Them5 in HepG2 cells decreases activation of PKB signaling after insulin stimulation. (A) HepG2 cells were transfected with Them5-HA (or vector control), starved overnight, and treated with insulin (100nM) for the time indicated. Later, cells were collected and lysed, and protein extracts were analyzed by western blotting with the antibodies indicated. (B) Quantification of PKB-S473 phosphorylation relative to total PKB levels (from the experiment described in A). (C) Overexpression of Them5 lowers levels of oxidized PTEN after insulin/ H_2O_2 stimulation. HepG2 cells were transfected with Them5-HA (or vector control), starved overnight, and treated with insulin (100nM, 15min) and/or H_2O_2 (5 mM, 15min). After treatment, cells were lysed in non-reducing buffer, lysates were purged with argon, and 50 μ g of protein extract were loaded onto the gel (reducing and non-reducing conditions) and analyzed with the antibodies indicated. (D) Schematic representation of changes in PTEN redox status (taken from (Kwon et al., 2004)). (E) ROS staining of primary hepatocytes from Them5 WT and KO males (6 months old), showing increased accumulation of ROS-sensitive dye.

When overexpressed, Them5 leads to a decrease in PKB phosphorylation (Figure 3.6A). Due to the mitochondrial localization of CTMP2/Them5, we were interested in seeing if the PTEN redox status was affected by the loss of Them5. To assess this, we transfected HepG2 cells with hCTMP2-HA, starved the cells overnight, and stimulated them with H₂O₂, or with insulin. Preliminary analysis showed that overexpression of Them5/CTMP2 led to lower levels of oxidized PTEN. This indicates that an absence of Them5 promotes oxidation, i.e. inactivation of PTEN, thus positively regulating PI3K/PKB signaling (Figure 3.5C).

In line with this observation, we stained primary hepatocytes with ROS-sensitive dye. There was increased positive staining in the KO hepatocytes, indicating higher ROS levels (Figure 3.6E). However, more samples should be analyzed and quantified.

3.2.4 OXPHOS complexes are affected upon loss of Them5

We assessed levels of OXPHOS complexes after loss of Them5. We observed a decrease in complexes I, IV, and V in Them5 KO at the protein level, but not at the mRNA level (see Figure 4 and Figure S7; ND1 is part of complex I, COX1 is part of complex IV), which may be explained by changes in protein stability due to an increased MCL/CL ratio (Zhang et al., 2003). CL molecules are known to associate specifically with complexes I and IV of the respiratory chain, and are required for their functional activity (Zhang et al., 2005). Changes in CL content, upon peroxidation for example, affect activity of complexes I and III (Paradies et al., 2001, 2002). Also, in patients with Barth syndrome, aberrant respiratory complexes are detected along with the increase in MCL/CL ratio (McKenzie et al., 2006). Thus, a

decrease in protein levels of the OXPHOS complexes can be a consequence of increased levels of immature cardiolipin. More in-depth analysis of respiratory complexes is required to assess ETC functionality upon Them5 ablation.

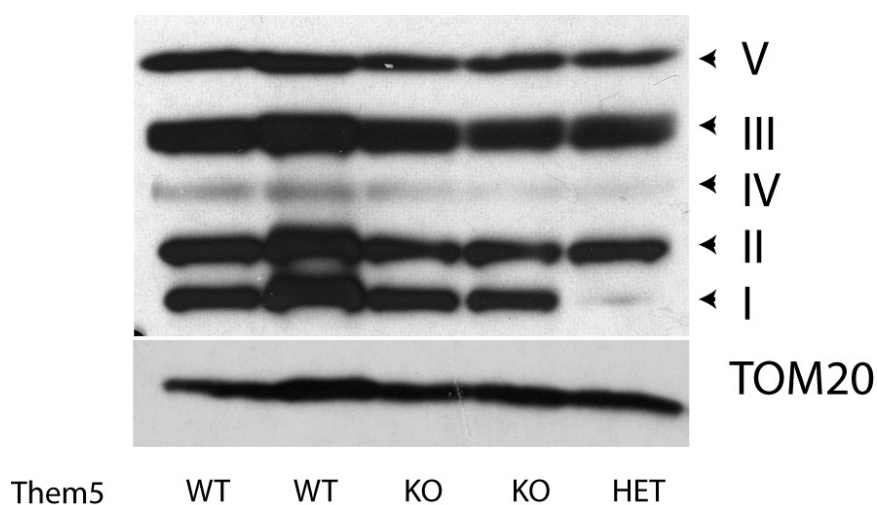


Figure 3.7

Decreased respiratory complexes in Them5 KO and HET mice. Mitochondria were isolated from Them5 KO, WT and HET mice (males, 9 months of age), and 20 μ g of mitochondria were separated by 4-20% SDS-PAGE and immunoblotted for respiratory complexes I-V components with MitoProfile® Total OXPHOS Rodent WB Antibody Cocktail (MitoSciences, Oregon, USA).

3.2.5 Mouse embryonic fibroblasts as a model for studying Them5 function

We generated mouse embryonic fibroblasts from timed matings (E13.5) of Them5 mice. Embryos were gender- and genotyped, and paired MEFs were used in the experiments (cells derived from male embryos of 2-20 passages were used).

Similarly to the WB analysis of other tissues, Them5 antibodies do not recognize endogenous levels of Them5 in MEFs. However, when we use generated antibodies in the immunofluorescence analysis, endogenous Them5 protein could be detected and was found to co-localize with mitochondrial marker Grp75 (see section 3.1) in the manuscript).

In order to analyze mitochondrial morphology, we stained primary MEFs with anti-TOM20 antibodies, and performed the analysis using the confocal microscope, with

subsequent reconstruction of mitochondria. The analysis showed a significant increase in the length of mitochondria in *Them5*^{-/-} MEFs (see section 3.1).

To analyze the response of cells to fatty-acid exposure, we treated MEFs with palmitic acid and oleic acid, for 4 and 10 hours. We did not see any significant differences in mitochondrial morphology between KO and control cells upon vehicle treatment (type of mitochondria was analyzed: fragmented, intermediate, or interconnected) (Figure 3.8A, B). After fatty-acid exposure, however, the percentage of fragmented mitochondria in *Them5* WT cells increased, with no significant changes in *Them5*^{-/-} cells. Changes in mitochondrial morphology were observed in both palmitic and oleic acid treatments (Figures 3.8, 3.9). More pronounced mitochondrial fragmentation occurred after oleic acid treatment, which is not surprising given the pro-apoptotic effects of oleic acid (Ricchi et al., 2009). In line with this, strong upregulation of fission protein Fis1 mRNA was observed in *Them5* WT cells, with no changes in *Them5*^{-/-}. We considered whether fatty acid accumulation differs between *Them5* WT and KO cells, which could potentially lead to the differences observed. However, lipid-specific BODIPY staining showed similar lipid accumulation in both WT and KO MEFs.

Our results suggest that *Them5*^{-/-} mitochondria may be more resistant to lipoapoptosis, but more experiments are required for complete characterization. To analyze whether the observed effects are dependent on the thioesterase activity of *Them5*, we generated MEF lines which overexpress the wild-type and enzyme-dead versions of the proteins. The analysis of mitochondrial morphology and functions in these cell lines is ongoing.

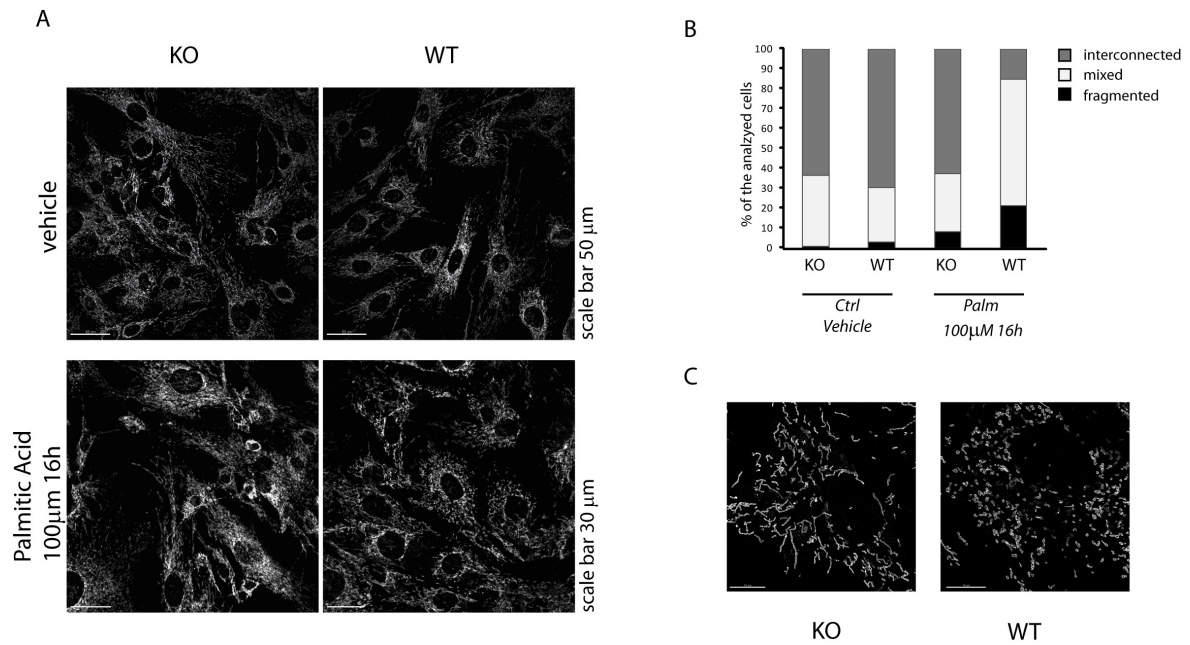


Figure 3.8

(A) MEFs were treated with palmitic acid (100 μM for 16 hours) or vehicle control (ethanol) and subsequently stained with anti-TOM20 antibodies to visualize mitochondria. (B) Different types of mitochondria (interconnected, fragmented or mixed) were quantified after treatment as described in A. Quantification shows reduced appearance of fragmented type of mitochondria in *Them5*^{-/-} MEFs upon palmitic acid treatment. (C) Representative pictures of mitochondria from form *Them5*^{-/-} (left) or *Them5*^{+/+} (right) cell, treated with palmitic acid, and visualized with anti-TOM20 antibodies (cells were treated as in A).

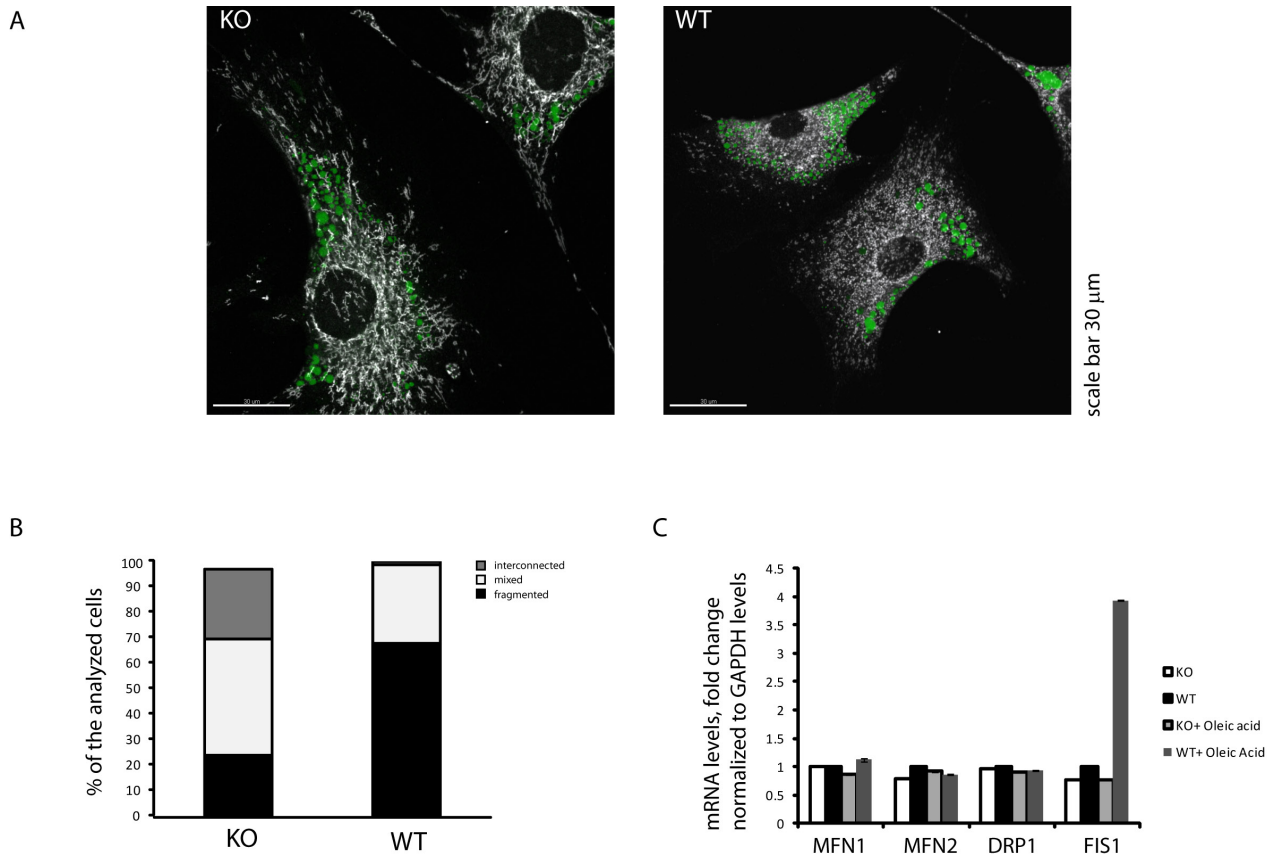
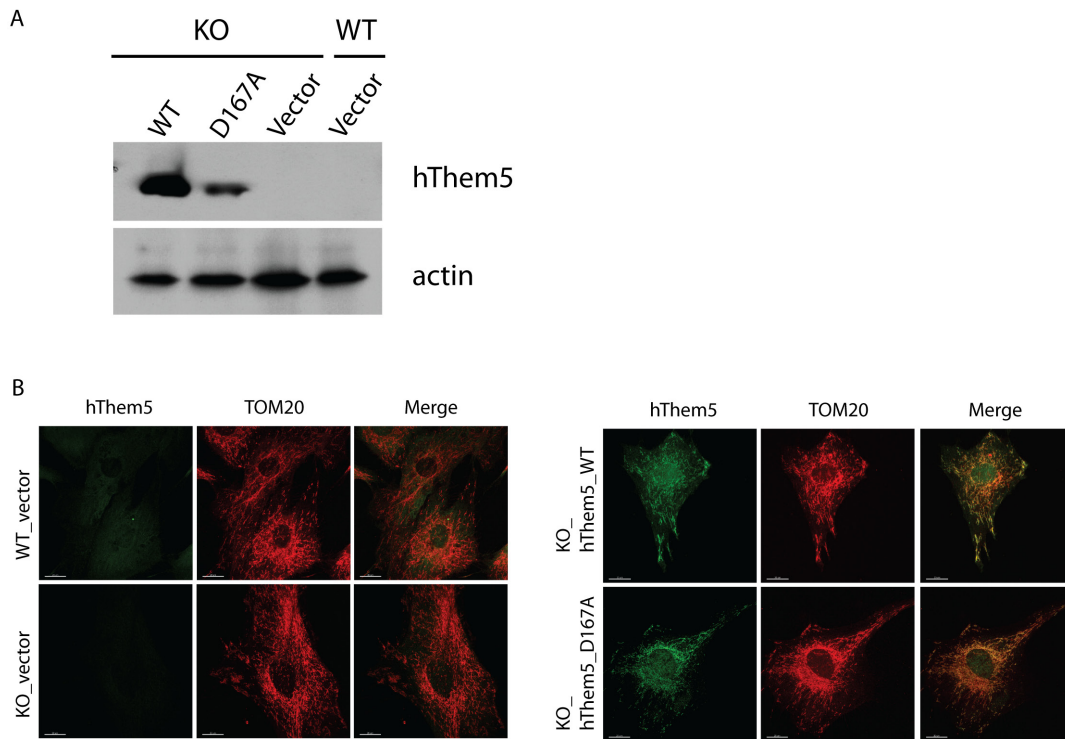


Figure 3.9

Mitochondria from Them5 KO MEFs are do not undergo fragmentation upon fatty acid exposure

(A) *Them5*^{-/-} (left) and WT (right) MEFs were treated with oleic acid (10 hours, 200μM), fixed and stained with anti-TOM20 antibodies and lipid-sensitive dye BODIPY. Lipid staining showed that both types of cell accumulate lipids upon free fatty acid exposure. (B) Mitochondria morphology was analyzed in cells treated as in A. Upon oleic acid treatment up to 60% of Them5_WT analyzed cells have predominantly fragmented mitochondria morphology, whereas *Them5*^{-/-} have only 20%. 3 independent experiments were performed with minimum 200 cells per experiment analyzed. Images were taken with Zeiss Z1 microscope and 40x magnification objective, and analyzed with AxioVision software. (C) *Them5*^{+/+} expressing MEFs upregulate Fis1 mRNA levels in response to the oleic acid treatment, whereas *Them5*^{-/-} cells show no changes in genes expression. Total RNA was extracted from the cell treated as in A (100 μM oleic acid for 16 hours or vehicle control), reversely transcribed and levels of mitochondria fusion/fission genes were assessed by real-time PCR. Data from 4 independent experiments were analyzed.

**Figure 3.10****Generation of stable MEFs expressing WT or enzyme-dead Them5**

(A) Western-blot analysis of Them5^{-/-} MEFs, stably expressing hThem5_WT, D167A, or an empty vector control, and Them5^{+/+} MEFs with a vector control (pBabe vector with puromycin resistance cassette was used for generation above constructs). Protein lysates were prepared and analyzed with SDS-PAGE, transferred to the PVDF membrane and subsequently probed with anti-hThem5 antibodies. Actin was used as a loading control. **(B)** Immunofluorescence analysis of MEFs cells lines (as described in A). Cells were grown on cover slips, fixed and probed with anti-hThem5 (anti-mouse Alexa-488 as secondary antibodies), and TOM20 (anti-rabbit Alexa-568 as secondary antibodies).

4. EXPERIMENTAL PROCEDURES**Isolation of primary hepatocytes**

Briefly, the mouse was anesthetized and a needle (30G) connected to the pump system was inserted into the portal vein. The flow of buffers was maintained at a constant speed of 3.5 ml/min. The vena cava was cut to permit the outflow of perfusion solutions. The mouse was perfused with Hanks solution I for 5 min, then with Hanks solution II for 4 min. After perfusion, the liver was cut out, transferred to a Petri dish with sterile non-supplemented Williams E medium (WEM), and

disintegrated. The cell suspension was filtered through a 70µm sterile nylon filter and washed twice with 30ml of non-supplemented 4°C WEM (centrifuged for 2min at 80g). Cells were resuspended in WEM (Williams' E medium) supplemented with 10% FCS, 100nM dexamethasone, 2mM L-glutamine, and 1% Pen/Strep, and plated on collagen pre-coated dishes (750,000 cells per well in 6-well plate format). 4 hours later the medium was changed and cells were incubated overnight and until further treatment.

Stimulation of primary hepatocytes with insulin

Cells were starved overnight and stimulated with insulin or H₂O₂. After treatment, cells were lysed in non-reducing buffer (100mM Tris-HCl, pH 6.8; 150mM NaCl; 1mM EDTA; 1% Triton X-100; 50mM N-ethylmaleimide, added freshly, stock solution prepared in ethanol), lysates were purged with argon, and 50µg of protein extract was loaded onto the gel (reducing and non-reducing conditions).

Immunofluorescence staining

Primary hepatocytes and pancreatic islets were fixed with methanol/acetone (1:1) for 5min at -20°C. The cover slips were left to air dry and afterwards were transferred to -20°C. The next day, cells were rehydrated with PBS and stained overnight with rabbit polyclonal antibodies against mouse Them5 at 4°C (1/100 dilution in PBS/1%BSA). Afterwards slides were washed three times with PBS and incubated with secondary antibodies of appropriate dilution for 1 hour at room temperature. After that, slides were washed and mounted with Prolong Gold Antifade Reagent (Invitrogen).

Primary MEFs were fixed with PFA (3.7%, pH 7.4) for 30min at room temperature, washed twice with PBS, and permeabilized with NP-40 0.01% in PBS pH 7.4 for

20min at room temperature. Slides were washed with PBS and blocked with 0.5% BSA in PBS for 30min at room temperature. Primary antibodies of appropriate dilution were applied to the slides and incubated for 1 hour at room temperature (rabbit polyclonal anti-mouse Them5 at 1/50 dilution, anti-TOM20 from Santa Cruz Biotechnologies at 1/100 dilution). Secondary antibodies of 1/200 dilution were incubated for 1 hour at room temperature. Slides were washed in PBS and mounted with Prolong Gold Antifade Reagent (Invitrogen).

***In vivo* insulin stimulation**

Insulin stimulation was performed on 2- and 24-month-old *Them5*^{-/-} mice and wildtype controls. Mice were fasted for 8 hours, terminally anesthetized with Ketamine/Xylazine and 1U/kg of insulin was injected into the *vena cava*. 5min (or 15min) later tissues were collected, snap-frozen in liquid nitrogen, and afterwards processed for western blot analysis.

Insulin and glucose tolerance tests

For glucose and insulin tolerance tests, mice (3 and 6 months old) were fasted for 8 hours, and insulin (0.6U/kg of body weight) or glucose (2g/kg of body weight) was injected intraperitoneally. Blood samples were collected at the indicated times from the tail vein, and glucose levels were determined using Glucometer Elite and Acsentia Elite test strips (Bayer).

ROS staining

For ROS staining, cells or tissue slices were fixed with PFA (3.7%, pH 7.4, in PBS) for 10min at room temperature, washed twice with PBS, and incubated with 200µl of 5µM solution of CM-H2DCFDA (Molecular Probes, Invitrogen) at 37°C for 30min.

Later, sections were washed with PBS and mounted with Prolong Gold Antifade Reagent with Dapi. Fluorescence was detected using 488nm laser illumination with an LSM700 confocal microscope.

5. GENERAL DISCUSSION

The aim of this thesis was to characterize the novel mitochondrial protein CTMP2/Them5. As previously mentioned, CTMP2/Them5 has been identified as a paralogue of CTMP/Them4, whose gene is located just 20kb away from that of Them5. A phylogenetic tree analysis shows that Them5 evolved relatively recently, in mammals only, whereas Them4 orthologs were already found in yeasts.

We have shown that Them5 is a novel protein that belongs to the mitochondrial proteome. Them5 has an N-terminally located mitochondrial targeting sequence and is imported into the mitochondria, where further processing occurs. It is localized in the mitochondrial matrix, and is also associated with the inner mitochondrial membrane facing the matrix side.

We determined the structures of $\Delta 36$ Them4 and $\Delta 34$ Them5 at high resolution and showed that both Them4 and Them5 belong to the hotdog-fold class of proteins. The hotdog fold, which is formed by several anti-parallel β -sheets wrapped around an α -helix, is found in all branches of life. However, up to now the mammalian proteins of this group have been widely left unstudied.

The key feature of such thioesterases is that the hotdog domain does not exist as a single entity: It must form at least dimeric structures. The tertiary structures vary and can include either dimers, tetramers, or hexamers (Dillon and Bateman, 2004). In our experiments we found that both CTMP1/Them4 and CTMP2/Them5 form dimers. These are the only characterized mammalian 4HBT thioesterases which have a dimeric quaternary structure. Analysis of functionally relevant residues showed a conserved catalytic machinery, composed of the HGG motif and Asp/Thr residues.

Results from both our group and others have shown that CTMP/Them4 plays an important role in regulating PKB signaling. Therefore, we were keen to investigate whether CTMP2/Them5 also has a similar effect on this pathway. Indeed, our results

with insulin tolerance tests and primary hepatocyte culture clearly indicate that Them5 KO mice are more insulin-sensitive, although we did not observe any difference between WT and KO mice in glucose tolerance tests. Additionally, levels of insulin and glucose in the plasma upon fasting seem to be similar in mutants and control mice. However, Them5/CTMP2 knock-out females had no signs of insulin hypersensitivity compare to males. With age, CTMP2 knock-out mice tend to develop fatty liver disease and display decreased hepatic insulin responsiveness. Fatty liver disease had a different progression rate in *Them5^{-/-}* mice depending on gender, as females develop signs of liver steatosis earlier than males. We cannot explain this observation yet, but clearly it requires further investigation. It is known from previous work that males and females have different predispositions to the development of certain disorders, such as fatty liver disease and diabetes (Perreault et al., 2008), (Li et al., 2010). It is unclear if the phenotype observed in *Them5^{-/-}* mice involves a hormonal regulatory mechanism. Histological analysis of the pancreas has shown a trend for increased islet mass in knock-out samples which, together with changes in mitochondrial morphology of β -cells, may be indicative of either (1) an independent phenotype that develops in the pancreas; or (2) being a part of a liver-pancreas metabolic loop, which requires further characterization. The interaction between pancreas and liver at the physiological level is an established fact, and interplay between the two organs in *Them5^{-/-}* mouse model cannot be excluded (Imai et al., 2008).

To assess lipid profiles upon Them5 ablation, we employed detailed mass spectrometry analysis (MS). The MS results show very specific changes in the lipid profile of cardiolipin and its metabolites, namely the accumulation of a major species of monolyso-cardiolipin (MCL), which acts as an upstream metabolite in the remodeling cycle of cardiolipin. CL is a phospholipid synthesized in the inner

mitochondrial membrane and subsequently re-modeled, predominantly within mitochondria (Esposti et al, 2003; Schlame, 2008). On the basis of these results, we propose that Them5 has a rather specific action *in vivo*, namely that of regulating the initial metabolism of mitochondrial cardiolipin. In particular, Them5 thioesterase activity would maintain the pool of acyl groups that serve to re-acetylate one metabolic intermediate of cardiolipin, SP2-MCL (stearoyl-di-palmitoyl-monolysocardiolipin). It is likely that the accumulation of this and other stearoyl- and palmitoyl-containing MCL species reflects an early impairment in the re-modeling cycle of cardiolipin, which progressively adds long unsaturated fatty acids to the saturated precursors, forming the mature forms of cardiolipin enriched in linoleyl (Schlame, 2008). Reduced thioesterase activity as a consequence of Them5 ablation will trap a portion of the mitochondrial pool of CoA into long acyl-CoA molecules (as indicated in Figure 6C,D). Those that are not normally used in the local metabolism of cardiolipin re-modeling (e.g. stearoyl-CoA) will then exit the mitochondria and subsequently be hydrolyzed to free fatty acids by cytosolic or peroxisomal thioesterases. The process will produce extra-mitochondrial accumulation of free fatty acids, which will progressively remain in hepatocytes once their release capacity as cholesterol esters or triglycerides is saturated. In support of this theory, we found minimal changes in the MS profile of mitochondrial fatty acids and in the acyl groups of phospholipids synthesized outside mitochondria, e.g. PI. Of note, a previous study has shown that altering the supply of acyl-CoA modifies cardiolipin re-modeling (Rijken et al, 2009).

We observed a lack of FAS mRNA induction in *Them5*^{-/-}, which can be explained in two ways. First, the cytosolic accumulation of free fatty acids by the above mechanism would induce feedback inhibition of fatty acid synthase by its product palmitate. Secondly, the finding of impaired β -oxidation in *Them5*^{-/-} mice implies a

reduced production of acetyl-CoA, with consequent reduction in mitochondrial citrate and its export into the cytosol, where it is required for FAS initiation.

We have shown that Them5 KO mice display hypoketosis and have decreased levels of β -oxidation (as measured by $^{14}\text{CO}_2$ generated from the oxidation of [1- ^{14}C]-palmitate). Due to the limited availability of CoA in *Them5*^{-/-} mitochondria, β -oxidation (and, finally, the TCA cycle) is impaired. This in turn reduces FAS (see above). Ultimately, cytosolic accumulation of fatty acids derives from the alteration in cardiolipin remodeling within mitochondria, due to the reduced potential for utilizing long acyl-CoA molecules caused by Them5 loss. Additionally, accumulation of fatty acids over time leads to the development of fatty liver disease, which is exacerbated with a high fat diet. Moreover, Them5 ablation leads to increased UCP2 expression, with enhanced basal uncoupling of mitochondria. Potentially, CPT1 expression could be elevated in random-fed mice, reflecting increased levels of fatty acids. However, *Them5*^{-/-} failed to upregulate CPT1 upon fasting, which additionally negatively affected β -oxidation.

Our data obtained through electron microscopy analysis of primary hepatocytes showed a 2-fold increase in mitochondrial volume, most probably resulting from the fact that mutant mitochondria are forming a highly interconnected network. However, mitochondrial biogenesis was not affected by the loss of the Them5 protein. We could show that overexpression of the thioesterase-dead version of the CTMP2/Them5 protein leads to the mitochondrial phenotype similar to that observed in *Them5*^{-/-} mice. In extended studies, we did not observe any measurable change in the transcript levels of Mfn1, Mfn2, or Opa1. However, the results of the detailed MS analysis of mitochondrial lipids indicated a plausible mechanism for the more tubular appearance of the mitochondria. The plasticity and dynamics of mitochondria are highly dependent upon the levels of cardiolipin and other lipids. In particular, the

balance between CL and MCL is essential to dynamically maintain crista homeostasis (Rujiviphat et al., 2009), (Ban et al., 2010), (Acehan et al., 2011). We have found that this balance is altered in *Them5*^{-/-} mitochondria, which show more than a two-fold increase in major MCL species relative to CL species. The membrane tubulation propensity of MCL would probably account for the more tubular appearance of Them5-deficient mitochondria. In any case, we propose that the elongated morphology of mitochondria is primarily derived from the increase in the MCL/CL ratio. Previous analysis of Them4-deficient cells had shown changes in the mitochondrial morphology without any affect on their biogenesis (Parcellier et al., 2009b). It was proposed that loss or accumulation of non-processed protein leads to the appearance of an interconnected mitochondrial network, suggesting defects in mitochondrial fusion processes (Parcellier et al., 2009b). One can speculate that the above-mentioned effects of CTMP/Them4 on mitochondrial morphology may involve thioesterase activity of Them4, but this should be experimentally confirmed. It cannot be excluded that the observed phenotype in *Them4*^{-/-} is mediated by an interaction with the Letm1 protein. However, the new evidence that its paralog, Them5, participates in cardiolipin remodeling suggests that the alteration in mitochondrial morphology upon Them4 ablation may well derive from alteration in the metabolism of mitochondrial lipids.

Sequence analysis shows 38% similarity between hThem4 and hThem5 proteins. This represents a high structural similarity, also observed in the similar 3D-structure of the proteins. However, certain differences exist: mapping these sequence differences onto the structures reveals distinct structural features, highlighting the potential functional variance between Them4 and Them5. These differences might provide a structural explanation for the differential substrate preferences exhibited. Additional structural differences are found at the C-terminus and on the solvent-

exposed side of the N-terminal α -helix, a finding that might indicate different interacting proteins for Them4 and Them5.

Recent work by Claypool et al. has identified a yeast homolog of Them4, FMP10, as an interactor of the ATP/ADP carrier ACC2 in the mitochondria (Claypool et al., 2008b). The authors studied an ACC2 interactome in the presence of cardiolipin, and provided a model where the physical interaction of ACC2 with complexes III and IV promotes OXPHOS efficiency in the presence vs. absence of cardiolipin.

Alterations in phospholipid and fatty acid composition have been previously detected in neural tumors (Campanella, 1992). These changes, in turn, can affect the pool of available FA used for CL remodeling. A study by Kiebish et al. has shown that mouse brain tumors contain CLs with different fatty acid composition, which are unique to each tumor type and are associated with deficiencies in electron transport chain activities (Kiebish et al., 2008). This is a very interesting finding, given that CTMP1/Them4 has been shown to be transcriptionally downregulated in glioblastoma (Knobbe et al., 2004). It is unclear whether alterations in CTMP1 levels are causative of CL changes in brain tumors, but this possibility cannot be excluded. Additionally, CTMP1 has been shown to have protective effects upon ischemia-induced cell death in neurons (Miyawaki et al., 2009). Thus, our *in vitro* evidence that CTMP1 sensitizes cell to apoptosis are confirmed by *in vivo* observations and, together with the above-mentioned publications, may indicate that CTMP1 has a role in cardiolipin-mediated effects on cell survival and apoptosis.

Enhanced insulin sensitivity in *Them5*^{-/-} mice may be a consequence of altered mitochondrial function due to lipid metabolism and cardiolipin remodeling dysregulation. The acyltransferase ALCAT1 promotes pathological remodeling of CL by enriching it with PUFA, and promotes oxidative stress. ALCAT KO mice are protected from diet-induced obesity. Additionally, they show increased insulin

sensitivity and enhanced energy expenditure. Loss of Them5 leads to effects somewhat similar to those observed in ALCAT1 KO, namely enhanced insulin sensitivity and lower AMPK phosphorylation. However, the phenotype of ALCAT1 KO mice only partially resembles that of Them5 KO. ALCAT1 KO mice show changes in glucose tolerance, and decreased fat content is accompanied by smaller size of lipid droplets. Them5 KO mice have no such manifestations.

Another important and exciting finding is that changes in mitochondrial morphology were not only observed in hepatocytes, but also in pancreatic β -cells. *Them5*^{-/-} β -cells are characterized by similar interconnected mitochondria to those observed in hepatocytes. Changes in the mitochondrial morphology are known to be linked to the bioenergetic state of the cell (Campello and Scorrano, 2010). This is especially important for β -cells, which are particularly sensitive to changes in ATP and Ca^{2+} levels (Krauss et al., 2003). Considering that Them5 affects cardiolipin remodeling, the question of energy status, insulin-secreting capabilities, etc. of β -cells should be further investigated. Analysis of the effect of Them5 loss on other tissues, such as the heart, given its exquisite sensitivity to cardiolipin alterations (Acehan et al., 2011; Ostrander et al., 2001), will undoubtedly result in many new discoveries.

6. REFERENCES

These references are cited in the General Introduction and General Discussion parts of the thesis.

Abu-Elheiga, L., Oh, W., Kordari, P., and Wakil, S.J. (2003). Acetyl-CoA carboxylase 2 mutant mice are protected against obesity and diabetes induced by high-fat/high-carbohydrate diets. *Proc Natl Acad Sci U S A* *100*, 10207-10212.

Acehan, D., Vaz, F., Houtkooper, R.H., James, J., Moore, V., Tokunaga, C., Kulik, W., Wansapura, J., Toth, M.J., Strauss, A., and Khuchua, Z. (2011). Cardiac and skeletal muscle defects in a mouse model of human Barth syndrome. *J Biol Chem* *286*, 899-908.

Acin-Perez, R., Fernandez-Silva, P., Peleato, M.L., Perez-Martos, A., and Enriquez, J.A. (2008). Respiratory active mitochondrial supercomplexes. *Mol Cell* *32*, 529-539.

Ahtiainen, L., Luiro, K., Kauppi, M., Tynnela, J., Kopra, O., and Jalanko, A. (2006). Palmitoyl protein thioesterase 1 (PPT1) deficiency causes endocytic defects connected to abnormal saposin processing. *Exp Cell Res* *312*, 1540-1553.

Alessi, D.R., James, S.R., Downes, C.P., Holmes, A.B., Gaffney, P.R., Reese, C.B., and Cohen, P. (1997). Characterization of a 3-phosphoinositide-dependent protein kinase which phosphorylates and activates protein kinase Balpha. *Curr Biol* *7*, 261-269.

Alexander, C., Votruba, M., Pesch, U.E., Thiselton, D.L., Mayer, S., Moore, A., Rodriguez, M., Kellner, U., Leo-Kottler, B., Auburger, G., Bhattacharya, S.S., and Wissinger, B. (2000). OPA1, encoding a dynamin-related GTPase, is mutated in autosomal dominant optic atrophy linked to chromosome 3q28. *Nat Genet* *26*, 211-215.

Andjelkovic, M., Jakubowicz, T., Cron, P., Ming, X.F., Han, J.W., and Hemmings, B.A. (1996). Activation and phosphorylation of a pleckstrin homology domain containing protein kinase (RAC-PK/PKB) promoted by serum and protein phosphatase inhibitors. *Proc Natl Acad Sci U S A* *93*, 5699-5704.

Angulo, P. (2007). GI Epidemiology: nonalcoholic fatty liver disease. *Alimentary Pharmacology & Therapeutics* *25*, 883-889.

Ban, T., Heymann, J.A., Song, Z., Hinshaw, J.E., and Chan, D.C. (2010). OPA1 disease alleles causing dominant optic atrophy have defects in cardiolipin-stimulated GTP hydrolysis and membrane tubulation. *Hum Mol Genet* *19*, 2113-2122.

Bhaskar, P.T., and Hay, N. (2007). The two TORCs and Akt. *Dev Cell* *12*, 487-502.

Bozulic, L., Surucu, B., Hynx, D., and Hemmings, B.A. (2008). PKBalpha/Akt1 acts downstream of DNA-PK in the DNA double-strand break response and promotes survival. *Mol Cell* *30*, 203-213.

- Brocker, C., Carpenter, C., Nebert, D.W., and Vasiliou, V. (2010). Evolutionary divergence and functions of the human acyl-CoA thioesterase gene (ACOT) family. *Hum Genomics* 4, 411-420.
- Brognard, J., Sierrecki, E., Gao, T., and Newton, A.C. (2007). PHLPP and a second isoform, PHLPP2, differentially attenuate the amplitude of Akt signaling by regulating distinct Akt isoforms. *Mol Cell* 25, 917-931.
- Calleja, V., Alcor, D., Laguerre, M., Park, J., Vojnovic, B., Hemmings, B.A., Downward, J., Parker, P.J., and Larijani, B. (2007). Intramolecular and intermolecular interactions of protein kinase B define its activation in vivo. *PLoS Biol* 5, e95.
- Campanella, R. (1992). Membrane lipids modifications in human gliomas of different degree of malignancy. *J Neurosurg Sci* 36, 11-25.
- Campello, S., and Scorrano, L. (2010). Mitochondrial shape changes: orchestrating cell pathophysiology. *EMBO Rep* 11, 678-684.
- Cao, J., Liu, Y., Lockwood, J., Burn, P., and Shi, Y. (2004). A novel cardiolipin-remodeling pathway revealed by a gene encoding an endoplasmic reticulum-associated acyl-CoA:lysocardiolipin acyltransferase (ALCAT1) in mouse. *J Biol Chem* 279, 31727-31734.
- Cao, J., Shen, W., Chang, Z., and Shi, Y. (2009a). ALCAT1 is a polyglycerophospholipid acyltransferase potently regulated by adenine nucleotide and thyroid status. *Am J Physiol Endocrinol Metab* 296, E647-653.
- Cao, J., Xu, H., Zhao, H., Gong, W., and Dunaway-Mariano, D. (2009b). The mechanisms of human hotdog-fold thioesterase 2 (hTHEM2) substrate recognition and catalysis illuminated by a structure and function based analysis. *Biochemistry* 48, 1293-1304.
- Cereghetti, G.M., Stangherlin, A., Martins de Brito, O., Chang, C.R., Blackstone, C., Bernardi, P., and Scorrano, L. (2008). Dephosphorylation by calcineurin regulates translocation of Drp1 to mitochondria. *Proc Natl Acad Sci U S A* 105, 15803-15808.
- Chance, B., and Williams, G.R. (1955). A method for the localization of sites for oxidative phosphorylation. *Nature* 176, 250-254.
- Chen, H., and Chan, D.C. (2005). Emerging functions of mammalian mitochondrial fusion and fission. *Hum Mol Genet* 14 Spec No. 2, R283-289.
- Chen, H., Detmer, S.A., Ewald, A.J., Griffin, E.E., Fraser, S.E., and Chan, D.C. (2003). Mitofusins Mfn1 and Mfn2 coordinately regulate mitochondrial fusion and are essential for embryonic development. *J Cell Biol* 160, 189-200.
- Cheng, Z., Bao, S., Shan, X., Xu, H., and Gong, W. (2006). Human thioesterase superfamily member 2 (hTHEM2) is co-localized with beta-tubulin onto the microtubule. *Biochem Biophys Res Commun* 350, 850-853.

Chirala, S.S., Chang, H., Matzuk, M., Abu-Elheiga, L., Mao, J., Mahon, K., Finegold, M., and Wakil, S.J. (2003). Fatty acid synthesis is essential in embryonic development: fatty acid synthase null mutants and most of the heterozygotes die in utero. *Proc Natl Acad Sci U S A* *100*, 6358-6363.

Claypool, S.M., Boontheung, P., McCaffery, J.M., Loo, J.A., and Koehler, C.M. (2008a). The cardiolipin transacylase, tafazzin, associates with two distinct respiratory components providing insight into Barth syndrome. *Mol Biol Cell* *19*, 5143-5155.

Claypool, S.M., Oktay, Y., Boontheung, P., Loo, J.A., and Koehler, C.M. (2008b). Cardiolipin defines the interactome of the major ADP/ATP carrier protein of the mitochondrial inner membrane. *J Cell Biol* *182*, 937-950.

da Fonseca, R.R., Johnson, W.E., O'Brien, S.J., Ramos, M.J., and Antunes, A. (2008). The adaptive evolution of the mammalian mitochondrial genome. *BMC Genomics* *9*, 119.

Delibegovic, M., Bence, K.K., Mody, N., Hong, E.G., Ko, H.J., Kim, J.K., Kahn, B.B., and Neel, B.G. (2007). Improved glucose homeostasis in mice with muscle-specific deletion of protein-tyrosine phosphatase 1B. *Mol Cell Biol* *27*, 7727-7734.

DeVay, R.M., Dominguez-Ramirez, L., Lackner, L.L., Hoppins, S., Stahlberg, H., and Nunnari, J. (2009). Coassembly of Mgm1 isoforms requires cardiolipin and mediates mitochondrial inner membrane fusion. *J Cell Biol* *186*, 793-803.

Di Nunzio, M., Danesi, F., and Bordoni, A. (2009). n-3 PUFA as regulators of cardiac gene transcription: a new link between PPAR activation and fatty acid composition. *Lipids* *44*, 1073-1079.

Dillon, S.C., and Bateman, A. (2004). The Hotdog fold: wrapping up a superfamily of thioesterases and dehydratases. *BMC Bioinformatics* *5*, 109.

Dongol, B., Shah, Y., Kim, I., Gonzalez, F.J., and Hunt, M.C. (2007). The acyl-CoA thioesterase I is regulated by PPARalpha and HNF4alpha via a distal response element in the promoter. *J Lipid Res* *48*, 1781-1791.

Dyntar, D., Eppenberger-Eberhardt, M., Maedler, K., Pruschy, M., Eppenberger, H.M., Spinass, G.A., and Donath, M.Y. (2001). Glucose and Palmitic Acid Induce Degeneration of Myofibrils and Modulate Apoptosis in Rat Adult Cardiomyocytes. *Diabetes* *50*, 2105-2113.

Eaton, S., Bartlett, K., and Pourfarzam, M. (1996). Mammalian mitochondrial beta-oxidation. *Biochem J* *320* (Pt 2), 345-357.

Elsner, M., Gehrman, W., and Lenzen, S. (2011). Peroxisome-generated hydrogen peroxide as important mediator of lipotoxicity in insulin-producing cells. *Diabetes* *60*, 200-208.

Endele, S., Fuhry, M., Pak, S.J., Zabel, B.U., and Winterpacht, A. (1999). LETM1, a novel gene encoding a putative EF-hand Ca(2+)-binding protein, flanks the Wolf-

Hirschhorn syndrome (WHS) critical region and is deleted in most WHS patients. *Genomics* 60, 218-225.

Engelfried, K., Vorgerd, M., Hagedorn, M., Haas, G., Gilles, J., Epplen, J.T., and Meins, M. (2006). Charcot-Marie-Tooth neuropathy type 2A: novel mutations in the mitofusin 2 gene (MFN2). *BMC Med Genet* 7, 53.

Esposti, M.D., Cristea, I.M., Gaskell, S.J., Nakao, Y., and Dive, C. (2003). Proapoptotic Bid binds to monolysocardiolipin, a new molecular connection between mitochondrial membranes and cell death. *Cell Death Differ* 10, 1300-1309.

Fariss, M.W., Chan, C.B., Patel, M., Van Houten, B., and Orrenius, S. (2005). Role of mitochondria in toxic oxidative stress. *Mol Interv* 5, 94-111.

Feng, J., Park, J., Cron, P., Hess, D., and Hemmings, B.A. (2004). Identification of a PKB/Akt hydrophobic motif Ser-473 kinase as DNA-dependent protein kinase. *J Biol Chem* 279, 41189-41196.

Forwood, J.K., Thakur, A.S., Guncar, G., Marfori, M., Mouradov, D., Meng, W., Robinson, J., Huber, T., Kellie, S., Martin, J.L., Hume, D.A., and Kobe, B. (2007). Structural basis for recruitment of tandem hotdog domains in acyl-CoA thioesterase 7 and its role in inflammation. *Proc Natl Acad Sci U S A* 104, 10382-10387.

Gao, T., Furnari, F., and Newton, A.C. (2005). PHLPP: A Phosphatase that Directly Dephosphorylates Akt, Promotes Apoptosis, and Suppresses Tumor Growth. *Molecular Cell* 18, 13-24.

Gosalakkal, J.A., and Kamoji, V. (2008). Reye syndrome and reye-like syndrome. *Pediatr Neurol* 39, 198-200.

Green, D.R., and Reed, J.C. (1998). Mitochondria and apoptosis. *Science* 281, 1309-1312.

Hackenbrock, C.R., Chazotte, B., and Gupte, S.S. (1986). The random collision model and a critical assessment of diffusion and collision in mitochondrial electron transport. *J Bioenerg Biomembr* 18, 331-368.

Herrero, L., Rubi, B., Sebastian, D., Serra, D., Asins, G., Maechler, P., Prentki, M., and Hegardt, F.G. (2005). Alteration of the malonyl-CoA/carnitine palmitoyltransferase I interaction in the beta-cell impairs glucose-induced insulin secretion. *Diabetes* 54, 462-471.

Hoffmann, B., Stockl, A., Schlame, M., Beyer, K., and Klingenberg, M. (1994). The reconstituted ADP/ATP carrier activity has an absolute requirement for cardiolipin as shown in cysteine mutants. *J Biol Chem* 269, 1940-1944.

Horie, Y., Suzuki, A., Kataoka, E., Sasaki, T., Hamada, K., Sasaki, J., Mizuno, K., Hasegawa, G., Kishimoto, H., Iizuka, M., Naito, M., Enomoto, K., Watanabe, S., Mak, T.W., and Nakano, T. (2004). Hepatocyte-specific Pten deficiency results in steatohepatitis and hepatocellular carcinomas. *J Clin Invest* 113, 1774-1783.

- Hu, T.H., Wang, C.C., Huang, C.C., Chen, C.L., Hung, C.H., Chen, C.H., Wang, J.H., Lu, S.N., Lee, C.M., Changchien, C.S., and Tai, M.H. (2007). Down-regulation of tumor suppressor gene PTEN, overexpression of p53, plus high proliferating cell nuclear antigen index predict poor patient outcome of hepatocellular carcinoma after resection. *Oncol Rep* 18, 1417-1426.
- Hunt, M.C., and Alexson, S.E. (2002). The role Acyl-CoA thioesterases play in mediating intracellular lipid metabolism. *Prog Lipid Res* 41, 99-130.
- Imai, J., Katagiri, H., Yamada, T., Ishigaki, Y., Suzuki, T., Kudo, H., Uno, K., Hasegawa, Y., Gao, J., Kaneko, K., Ishihara, H., Nijima, A., Nakazato, M., Asano, T., Minokoshi, Y., and Oka, Y. (2008). Regulation of pancreatic beta cell mass by neuronal signals from the liver. *Science* 322, 1250-1254.
- Iverson, S.L., Enoksson, M., Gogvadze, V., Ott, M., and Orrenius, S. (2004). Cardiolipin is not required for Bax-mediated cytochrome c release from yeast mitochondria. *J Biol Chem* 279, 1100-1107.
- Jiang, D., Zhao, L., and Clapham, D.E. (2009). Genome-wide RNAi screen identifies Letm1 as a mitochondrial Ca²⁺/H⁺ antiporter. *Science* 326, 144-147.
- Joseph, J.W., Koshkin, V., Saleh, M.C., Sivitz, W.I., Zhang, C.Y., Lowell, B.B., Chan, C.B., and Wheeler, M.B. (2004). Free fatty acid-induced beta-cell defects are dependent on uncoupling protein 2 expression. *J Biol Chem* 279, 51049-51056.
- Kanno, K., Wu, M.K., Agate, D.S., Fanelli, B.J., Wagle, N., Scapa, E.F., Ukomadu, C., and Cohen, D.E. (2007). Interacting proteins dictate function of the minimal START domain phosphatidylcholine transfer protein/StarD2. *J Biol Chem* 282, 30728-30736.
- Kiebish, M.A., Han, X., Cheng, H., Chuang, J.H., and Seyfried, T.N. (2008). Cardiolipin and electron transport chain abnormalities in mouse brain tumor mitochondria: lipidomic evidence supporting the Warburg theory of cancer. *J Lipid Res* 49, 2545-2556.
- Knobbe, C.B., Reifenberger, J., Blaschke, B., and Reifenberger, G. (2004). Hypermethylation and transcriptional downregulation of the carboxyl-terminal modulator protein gene in glioblastomas. *J Natl Cancer Inst* 96, 483-486.
- Krauss, S., Zhang, C.Y., Scorrano, L., Dalgaard, L.T., St-Pierre, J., Grey, S.T., and Lowell, B.B. (2003). Superoxide-mediated activation of uncoupling protein 2 causes pancreatic beta cell dysfunction. *J Clin Invest* 112, 1831-1842.
- Kuwana, T., Mackey, M.R., Perkins, G., Ellisman, M.H., Latterich, M., Schneiter, R., Green, D.R., and Newmeyer, D.D. (2002). Bid, Bax, and lipids cooperate to form supramolecular openings in the outer mitochondrial membrane. *Cell* 111, 331-342.
- Kwon, J., Lee, S.R., Yang, K.S., Ahn, Y., Kim, Y.J., Stadtman, E.R., and Rhee, S.G. (2004). Reversible oxidation and inactivation of the tumor suppressor PTEN in cells stimulated with peptide growth factors. *Proc Natl Acad Sci U S A* 101, 16419-16424.

- Leclercq, I.A., Da Silva Morais, A., Schroyen, B., Van Hul, N., and Geerts, A. (2007). Insulin resistance in hepatocytes and sinusoidal liver cells: mechanisms and consequences. *J Hepatol* *47*, 142-156.
- Lee, S.R., Yang, K.S., Kwon, J., Lee, C., Jeong, W., and Rhee, S.G. (2002). Reversible inactivation of the tumor suppressor PTEN by H₂O₂. *J Biol Chem* *277*, 20336-20342.
- Li, J., Romestaing, C., Han, X., Li, Y., Hao, X., Wu, Y., Sun, C., Liu, X., Jefferson, L.S., Xiong, J., Lanoue, K.F., Chang, Z., Lynch, C.J., Wang, H., and Shi, Y. (2010). Cardiolipin remodeling by ALCAT1 links oxidative stress and mitochondrial dysfunction to obesity. *Cell Metab* *12*, 154-165.
- Li, N., Frigerio, F., and Maechler, P. (2008a). The sensitivity of pancreatic beta-cells to mitochondrial injuries triggered by lipotoxicity and oxidative stress. *Biochem Soc Trans* *36*, 930-934.
- Li, Z., Berk, M., McIntyre, T.M., Gores, G.J., and Feldstein, A.E. (2008b). The lysosomal-mitochondrial axis in free fatty acid-induced hepatic lipotoxicity. *Hepatology* *47*, 1495-1503.
- Loh, K., Deng, H., Fukushima, A., Cai, X., Boivin, B., Galic, S., Bruce, C., Shields, B.J., Skiba, B., Ooms, L.M., Stepto, N., Wu, B., Mitchell, C.A., Tonks, N.K., Watt, M.J., Febbraio, M.A., Crack, P.J., Andrikopoulos, S., and Tiganis, T. (2009). Reactive oxygen species enhance insulin sensitivity. *Cell Metab* *10*, 260-272.
- Lucas, B., Grigo, K., Erdmann, S., Lausen, J., Klein-Hitpass, L., and Ryffel, G.U. (2005). HNF4 α reduces proliferation of kidney cells and affects genes deregulated in renal cell carcinoma. *Oncogene* *24*, 6418-6431.
- Lupi, R., Del Guerra, S., Fierabracci, V., Marselli, L., Novelli, M., Patane, G., Boggi, U., Mosca, F., Piro, S., Del Prato, S., and Marchetti, P. (2002). Lipotoxicity in human pancreatic islets and the protective effect of metformin. *Diabetes* *51 Suppl 1*, S134-137.
- Ma, B.J., Taylor, W.A., Dolinsky, V.W., and Hatch, G.M. (1999). Acylation of monolysocardiolipin in rat heart. *J Lipid Res* *40*, 1837-1845.
- Maira, S.M., Galetic, I., Brazil, D.P., Kaech, S., Ingley, E., Thelen, M., and Hemmings, B.A. (2001). Carboxyl-terminal modulator protein (CTMP), a negative regulator of PKB/Akt and v-Akt at the plasma membrane. *Science* *294*, 374-380.
- McClung, J.P., Roneker, C.A., Mu, W., Lisk, D.J., Langlais, P., Liu, F., and Lei, X.G. (2004). Development of insulin resistance and obesity in mice overexpressing cellular glutathione peroxidase. *Proc Natl Acad Sci U S A* *101*, 8852-8857.
- McKenzie, M., Lazarou, M., Thorburn, D.R., and Ryan, M.T. (2006). Mitochondrial respiratory chain supercomplexes are destabilized in Barth Syndrome patients. *J Mol Biol* *361*, 462-469.

Mendez-Sanchez, N., Arrese, M., Zamora-Valdes, D., and Uribe, M. (2007). Current concepts in the pathogenesis of nonalcoholic fatty liver disease. *Liver Int* 27, 423-433.

Miyawaki, T., Ofengeim, D., Noh, K.M., Latuszek-Barrantes, A., Hemmings, B.A., Follenzi, A., and Zukin, R.S. (2009). The endogenous inhibitor of Akt, CTMP, is critical to ischemia-induced neuronal death. *Nat Neurosci* 12, 618-626.

Nawa, M., Kanekura, K., Hashimoto, Y., Aiso, S., and Matsuoka, M. (2008). A novel Akt/PKB-interacting protein promotes cell adhesion and inhibits familial amyotrophic lateral sclerosis-linked mutant SOD1-induced neuronal death via inhibition of PP2A-mediated dephosphorylation of Akt/PKB. *Cell Signal* 20, 493-505.

Naylor, K., Ingeman, E., Okreglak, V., Marino, M., Hinshaw, J.E., and Nunnari, J. (2006). Mdv1 interacts with assembled dnm1 to promote mitochondrial division. *J Biol Chem* 281, 2177-2183.

Nowikovsky, K., Froschauer, E.M., Zsurka, G., Samaj, J., Reipert, S., Kolisek, M., Wiesenberger, G., and Schweyen, R.J. (2004). The LETM1/YOL027 gene family encodes a factor of the mitochondrial K⁺ homeostasis with a potential role in the Wolf-Hirschhorn syndrome. *J Biol Chem* 279, 30307-30315.

Ohtsuka, T., Nishijima, M., and Akamatsu, Y. (1993). A somatic cell mutant defective in phosphatidylglycerophosphate synthase, with impaired phosphatidylglycerol and cardiolipin biosynthesis. *J Biol Chem* 268, 22908-22913.

Osman, C., Voelker, D.R., and Langer, T. (2011). Making heads or tails of phospholipids in mitochondria. *J Cell Biol* 192, 7-16.

Ostrander, D.B., Sparagna, G.C., Amoscato, A.A., McMillin, J.B., and Dowhan, W. (2001). Decreased cardiolipin synthesis corresponds with cytochrome c release in palmitate-induced cardiomyocyte apoptosis. *J Biol Chem* 276, 38061-38067.

Ott, M., Robertson, J.D., Gogvadze, V., Zhivotovsky, B., and Orrenius, S. (2002). Cytochrome c release from mitochondria proceeds by a two-step process. *Proc Natl Acad Sci U S A* 99, 1259-1263.

Paradies, G., Petrosillo, G., Pistolese, M., and Ruggiero, F.M. (2001). Reactive oxygen species generated by the mitochondrial respiratory chain affect the complex III activity via cardiolipin peroxidation in beef-heart submitochondrial particles. *Mitochondrion* 1, 151-159.

Paradies, G., Petrosillo, G., Pistolese, M., and Ruggiero, F.M. (2002). Reactive oxygen species affect mitochondrial electron transport complex I activity through oxidative cardiolipin damage. *Gene* 286, 135-141.

Parcellier, A., Tintignac, L.A., Zhuravleva, E., Cron, P., Schenk, S., Bozusic, L., and Hemmings, B.A. (2009a). Carboxy-Terminal Modulator Protein (CTMP) is a mitochondrial protein that sensitizes cells to apoptosis. *Cell Signal* 21, 639-650.

Parcellier, A., Tintignac, L.A., Zhuravleva, E., Dummler, B., Brazil, D.P., Hynx, D., Cron, P., Schenk, S., Olivieri, V., and Hemmings, B.A. (2009b). The Carboxy-

Terminal Modulator Protein (CTMP) regulates mitochondrial dynamics. *PLoS One* 4, e5471.

Parone, P.A., Da Cruz, S., Tondera, D., Mattenberger, Y., James, D.I., Maechler, P., Barja, F., and Martinou, J.C. (2008). Preventing mitochondrial fission impairs mitochondrial function and leads to loss of mitochondrial DNA. *PLoS One* 3, e3257.

Perier, C., Tieu, K., Guegan, C., Caspersen, C., Jackson-Lewis, V., Carelli, V., Martinuzzi, A., Hirano, M., Przedborski, S., and Vila, M. (2005). Complex I deficiency primes Bax-dependent neuronal apoptosis through mitochondrial oxidative damage. *Proc Natl Acad Sci U S A* 102, 19126-19131.

Perreault, L., Ma, Y., Dagogo-Jack, S., Horton, E., Marrero, D., Crandall, J., and Barrett-Connor, E. (2008). Sex differences in diabetes risk and the effect of intensive lifestyle modification in the Diabetes Prevention Program. *Diabetes Care* 31, 1416-1421.

Piao, L., Li, Y., Kim, S.J., Sohn, K.C., Yang, K.J., Park, K.A., Byun, H.S., Won, M., Hong, J., Hur, G.M., Seok, J.H., Shong, M., Sack, R., Brazil, D.P., Hemmings, B.A., and Park, J. (2009). Regulation of OPA1-mediated mitochondrial fusion by leucine zipper/EF-hand-containing transmembrane protein-1 plays a role in apoptosis. *Cell Signal* 21, 767-777.

Pidugu, L.S., Maity, K., Ramaswamy, K., Surolia, N., and Suguna, K. (2009). Analysis of proteins with the 'hot dog' fold: prediction of function and identification of catalytic residues of hypothetical proteins. *BMC Struct Biol* 9, 37.

Ping, C., Lin, Z., Jiming, D., Jin, Z., Ying, L., Shigang, D., Hongtao, Y., Yongwei, H., and Jiahong, D. (2006). The phosphoinositide 3-kinase/Akt-signal pathway mediates proliferation and secretory function of hepatic sinusoidal endothelial cells in rats after partial hepatectomy. *Biochem Biophys Res Commun* 342, 887-893.

Piro, S., Spadaro, L., Russello, M., Spampinato, D., Oliveri, C.E., Vasquez, E., Benigno, R., Brancato, F., Purrello, F., and Rabuazzo, A.M. (2008). Molecular determinants of insulin resistance, cell apoptosis and lipid accumulation in non-alcoholic steatohepatitis. *Nutrition, Metabolism and Cardiovascular Diseases* 18, 545-552.

Rector, R.S., Thyfault, J.P., Wei, Y., and Ibdah, J.A. (2008). Non-alcoholic fatty liver disease and the metabolic syndrome: an update. *World J Gastroenterol* 14, 185-192.

Rhee, S.G. (1999). Redox signaling: hydrogen peroxide as intracellular messenger. *Exp Mol Med* 31, 53-59.

Rhee, S.G. (2006). Cell signaling. H₂O₂, a necessary evil for cell signaling. *Science* 312, 1882-1883.

Ricchi, M., Odoardi, M.R., Carulli, L., Anzivino, C., Ballestri, S., Pinetti, A., Fantoni, L.I., Marra, F., Bertolotti, M., Banni, S., Lonardo, A., Carulli, N., and Loria, P. (2009). Differential effect of oleic and palmitic acid on lipid accumulation and apoptosis in cultured hepatocytes. *J Gastroenterol Hepatol* 24, 830-840.

- Rijken, P.J., Houtkooper, R.H., Akbari, H., Brouwers, J.F., Koorengel, M.C., de Kruijff, B., Frentzen, M., Vaz, F.M., and de Kroon, A.I. (2009). Cardiolipin molecular species with shorter acyl chains accumulate in *Saccharomyces cerevisiae* mutants lacking the acyl coenzyme A-binding protein Acb1p: new insights into acyl chain remodeling of cardiolipin. *J Biol Chem* **284**, 27609-27619.
- Roe, C.R., Ding J. (2001). Mitochondrial fatty acid oxidation disorders. In *The Metabolic and Molecular Basis of Inherited Disease*. C.R.e.a. Scriver, ed. (New York: McGraw-Hill), pp. 2297-2326.
- Rujviphat, J., Meglei, G., Rubinstein, J.L., and McQuibban, G.A. (2009). Phospholipid association is essential for dynamin-related protein Mgm1 to function in mitochondrial membrane fusion. *J Biol Chem* **284**, 28682-28686.
- Salmena, L., Carracedo, A., and Pandolfi, P.P. (2008). Tenets of PTEN Tumor Suppression. *Cell* **133**, 403-414.
- Samuel, V.T., Liu, Z.-X., Qu, X., Elder, B.D., Bilz, S., Befroy, D., Romanelli, A.J., and Shulman, G.I. (2004). Mechanism of Hepatic Insulin Resistance in Non-alcoholic Fatty Liver Disease. *J. Biol. Chem.* **279**, 32345-32353.
- Samuels, Y., Diaz, L.A., Jr., Schmidt-Kittler, O., Cummins, J.M., DeLong, L., Cheong, I., Rago, C., Huso, D.L., Lengauer, C., Kinzler, K.W., Vogelstein, B., and Velculescu, V.E. (2005). Mutant PIK3CA promotes cell growth and invasion of human cancer cells. *Cancer Cell* **7**, 561-573.
- Sarbassov, D.D., Guertin, D.A., Ali, S.M., and Sabatini, D.M. (2005). Phosphorylation and regulation of Akt/PKB by the rictor-mTOR complex. *Science* **307**, 1098-1101.
- Sato, S., Fujita, N., and Tsuruo, T. (2000). Modulation of Akt kinase activity by binding to Hsp90. *Proc Natl Acad Sci U S A* **97**, 10832-10837.
- Sauvanet, C., Duvezin-Caubet, S., di Rago, J.P., and Rojo, M. (2010). Energetic requirements and bioenergetic modulation of mitochondrial morphology and dynamics. *Semin Cell Dev Biol* **21**, 558-565.
- Schlame, M. (2008). Cardiolipin synthesis for the assembly of bacterial and mitochondrial membranes. *J Lipid Res* **49**, 1607-1620.
- Serek, R., Forwood, J.K., Hume, D.A., Martin, J.L., and Kobe, B. (2006). Crystallization of the C-terminal domain of the mouse brain cytosolic long-chain acyl-CoA thioesterase. *Acta Crystallogr Sect F Struct Biol Cryst Commun* **62**, 133-135.
- Spiekerkoetter, U., and Wood, P.A. (2010). Mitochondrial fatty acid oxidation disorders: pathophysiological studies in mouse models. *J Inherit Metab Dis* **33**, 539-546.
- Spinazzi, M., Cazzola, S., Bortolozzi, M., Baracca, A., Loro, E., Casarin, A., Solaini, G., Sgarbi, G., Casalena, G., Cenacchi, G., Malena, A., Frezza, C., Carrara, F., Angelini, C., Scorrano, L., Salviati, L., and Vergani, L. (2008). A novel deletion in the GTPase domain of OPA1 causes defects in mitochondrial morphology and distribution, but not in function. *Hum Mol Genet* **17**, 3291-3302.

Stiles, B., Wang, Y., Stahl, A., Bassilian, S., Lee, W.P., Kim, Y.J., Sherwin, R., Devaskar, S., Lesche, R., Magnuson, M.A., and Wu, H. (2004). Liver-specific deletion of negative regulator Pten results in fatty liver and insulin hypersensitivity [corrected]. *Proc Natl Acad Sci U S A* 101, 2082-2087.

Taylor, W.A., and Hatch, G.M. (2003). Purification and characterization of monolysocardiolipin acyltransferase from pig liver mitochondria. *J Biol Chem* 278, 12716-12721.

Taylor, W.A., and Hatch, G.M. (2009). Identification of the human mitochondrial linoleoyl-coenzyme A monolysocardiolipin acyltransferase (MLCL AT-1). *J Biol Chem* 284, 30360-30371.

Tonks, N.K. (2006). Protein tyrosine phosphatases: from genes, to function, to disease. *Nat Rev Mol Cell Biol* 7, 833-846.

Twig, G., Elorza, A., Molina, A.J., Mohamed, H., Wikstrom, J.D., Walzer, G., Stiles, L., Haigh, S.E., Katz, S., Las, G., Alroy, J., Wu, M., Py, B.F., Yuan, J., Deeney, J.T., Corkey, B.E., and Shirihai, O.S. (2008). Fission and selective fusion govern mitochondrial segregation and elimination by autophagy. *EMBO J* 27, 433-446.

Ugi, S., Imamura, T., Maegawa, H., Egawa, K., Yoshizaki, T., Shi, K., Obata, T., Ebina, Y., Kashiwagi, A., and Olefsky, J.M. (2004). Protein phosphatase 2A negatively regulates insulin's metabolic signaling pathway by inhibiting Akt (protein kinase B) activity in 3T3-L1 adipocytes. *Mol Cell Biol* 24, 8778-8789.

van Gestel, R.A., Rijken, P.J., Surinova, S., O'Flaherty, M., Heck, A.J., Killian, J.A., de Kroon, A.I., and Slijper, M. (2010). The influence of the acyl chain composition of cardiolipin on the stability of mitochondrial complexes; an unexpected effect of cardiolipin in alpha-ketoglutarate dehydrogenase and prohibitin complexes. *J Proteomics* 73, 806-814.

Verhoeven, K., Claeys, K.G., Zuchner, S., Schroder, J.M., Weis, J., Ceuterick, C., Jordanova, A., Nelis, E., De Vriendt, E., Van Hul, M., Seeman, P., Mazanec, R., Saifi, G.M., Szigeti, K., Mancias, P., Butler, I.J., Kochanski, A., Ryniewicz, B., De Bleecker, J., Van den Bergh, P., Verellen, C., Van Coster, R., Goemans, N., Auer-Grumbach, M., Robberecht, W., Milic Rasic, V., Nevo, Y., Tournev, I., Guergueltcheva, V., Roelens, F., Vieregge, P., Vinci, P., Moreno, M.T., Christen, H.J., Shy, M.E., Lupski, J.R., Vance, J.M., De Jonghe, P., and Timmerman, V. (2006). MFN2 mutation distribution and genotype/phenotype correlation in Charcot-Marie-Tooth type 2. *Brain* 129, 2093-2102.

Vreken, P., Valianpour, F., Nijtmans, L.G., Grivell, L.A., Plecko, B., Wanders, R.J., and Barth, P.G. (2000). Defective remodeling of cardiolipin and phosphatidylglycerol in Barth syndrome. *Biochem Biophys Res Commun* 279, 378-382.

Waliany, S., Das, A.K., Gaben, A., Wisniewski, K.E., and Hofmann, S.L. (2000). Identification of three novel mutations of the palmitoyl-protein thioesterase-1 (PPT1) gene in children with neuronal ceroid-lipofuscinosis. *Hum Mutat* 15, 206-207.

- Wang, L., Wang, W.L., Zhang, Y., Guo, S.P., Zhang, J., and Li, Q.L. (2007). Epigenetic and genetic alterations of PTEN in hepatocellular carcinoma. *Hepatol Res* 37, 389-396.
- Wang, Y., Mohsen, A.W., Mihalik, S.J., Goetzman, E.S., and Vockley, J. (2010). Evidence for physical association of mitochondrial fatty acid oxidation and oxidative phosphorylation complexes. *J Biol Chem* 285, 29834-29841.
- Wei, H., Kim, S.J., Zhang, Z., Tsai, P.C., Wisniewski, K.E., and Mukherjee, A.B. (2008). ER and oxidative stresses are common mediators of apoptosis in both neurodegenerative and non-neurodegenerative lysosomal storage disorders and are alleviated by chemical chaperones. *Hum Mol Genet* 17, 469-477.
- Wei, J., Kang, H.W., and Cohen, D.E. (2009). Thioesterase superfamily member 2 (Them2)/acyl-CoA thioesterase 13 (Acot13): a homotetrameric hotdog fold thioesterase with selectivity for long-chain fatty acyl-CoAs. *Biochem J* 421, 311-322.
- Westin, M.A., Alexson, S.E., and Hunt, M.C. (2004). Molecular cloning and characterization of two mouse peroxisome proliferator-activated receptor alpha (PPARalpha)-regulated peroxisomal acyl-CoA thioesterases. *J Biol Chem* 279, 21841-21848.
- Xu, Y., Condell, M., Plesken, H., Edelman-Novemsky, I., Ma, J., Ren, M., and Schlame, M. (2006). A *Drosophila* model of Barth syndrome. *Proc Natl Acad Sci U S A* 103, 11584-11588.
- Xue, B., Kim, Y.B., Lee, A., Toschi, E., Bonner-Weir, S., Kahn, C.R., Neel, B.G., and Kahn, B.B. (2007). Protein-tyrosine phosphatase 1B deficiency reduces insulin resistance and the diabetic phenotype in mice with polygenic insulin resistance. *J Biol Chem* 282, 23829-23840.
- Yang, J., Cron, P., Thompson, V., Good, V.M., Hess, D., Hemmings, B.A., and Barford, D. (2002). Molecular mechanism for the regulation of protein kinase B/Akt by hydrophobic motif phosphorylation. *Mol Cell* 9, 1227-1240.
- Yoon, Y., Krueger, E.W., Oswald, B.J., and McNiven, M.A. (2003). The mitochondrial protein hFis1 regulates mitochondrial fission in mammalian cells through an interaction with the dynamin-like protein DLP1. *Mol Cell Biol* 23, 5409-5420.
- Zhang, M., Mileykovskaya, E., and Dowhan, W. (2002). Gluing the respiratory chain together. Cardiolipin is required for supercomplex formation in the inner mitochondrial membrane. *J Biol Chem* 277, 43553-43556.
- Zhang, M., Mileykovskaya, E., and Dowhan, W. (2005). Cardiolipin is essential for organization of complexes III and IV into a supercomplex in intact yeast mitochondria. *J Biol Chem* 280, 29403-29408.
- Zhang, M., Su, X., Mileykovskaya, E., Amoscato, A.A., and Dowhan, W. (2003). Cardiolipin is not required to maintain mitochondrial DNA stability or cell viability for *Saccharomyces cerevisiae* grown at elevated temperatures. *J Biol Chem* 278, 35204-35210.

Zhang, Z., Lee, Y.C., Kim, S.J., Choi, M.S., Tsai, P.C., Xu, Y., Xiao, Y.J., Zhang, P., Heffer, A., and Mukherjee, A.B. (2006). Palmitoyl-protein thioesterase-1 deficiency mediates the activation of the unfolded protein response and neuronal apoptosis in INCL. *Hum Mol Genet* 15, 337-346.

Zhao, H., Martin, B.M., Bisoffi, M., and Dunaway-Mariano, D. (2009). The Akt C-terminal modulator protein is an acyl-CoA thioesterase of the Hotdog-Fold family. *Biochemistry* 48, 5507-5509.

7. APPENDIX

7.1 Role of PKB/Akt in liver diseases

Zhuravleva E., Tschopp O., Hemmings B.A. (2010) Role of PKB/Akt in liver diseases. In "Signaling Pathways in Liver Diseases", 2nd edition. Ed. Dufour J.F. and Clavien P.A. Springer-Verlag

Introduction

PKB/Akt is a ubiquitous and evolutionarily conserved serine/threonine kinase that is recognized as a major coordinator of various intracellular signals. It controls cell responses to extrinsic stimuli and regulates cell metabolism, proliferation, and survival. Proper tuning of PKB activity via direct or indirect mechanisms is of utmost importance for stringent regulation of PKB-dependent cellular activities. Many diseases, such as cancer or metabolic disorders, are the result of, or are associated with, aberrant activity of the PI3K/PTEN/PKB pathway. In many tumors, the PI3K/PTEN/PKB pathway is activated by upstream mutations in PI3K or PTEN or by the amplification/overexpression/mutation of PKB isoforms themselves. Liver tumors are not the only pathological condition associated with disorders of this pathway. PKB has also been implicated in the development of hepatic insulin resistance, type 2 diabetes mellitus and, as has become evident over the past few years, in ischemia/reperfusion processes. In this chapter, the role of PKB in major physiological processes of cells is summarized and different liver disease conditions are considered by analyzing their pathophysiology from the perspective of PKB involvement.

Description of the PKB Family

The first publication identifying PKB as a serine/threonine kinase came from Jones et al. in 1991 [1]. The authors initially termed the kinase Rac, for *r*elated to the *A* and *C* kinases, but was then renamed PKB/Akt [2, 3]. Since the publication of these landmark studies more than 17 years ago, it became clear that PKB/Akt is one of the major targets of phosphatidylinositol 3-kinase (PI3K)-generated signals and is involved in the regulation of cell growth, proliferation, apoptosis, glucose metabolism, angiogenesis, and migration. Readers are referred to other excellent reviews covering the history of PKB discovery and in-depth analysis of its involvement in all these diverse cellular processes [4–7].

The mammalian genome encodes three isoforms of Akt/PKB: Akt1/PKB α , Akt2/PKB β , and Akt3/PKB γ , which are highly conserved despite being the products of three different genes located on different chromosomes. Interestingly, worms and flies have a single Akt/PKB protein. PKB family members share a similar domain structure containing an N-terminal pleckstrin homology (PH) domain [8], a catalytic domain and a C-terminal regulatory domain with a regulatory phosphorylation hydrophobic motif (HM) [4]. PKB that fully activated and exerts its biological functions is phosphorylated at two sites, one located within the activation loop of the kinase domain (Thr308 in PKB α) and the other within the HM (Ser473).

Although PKB isoforms are highly conserved (approximately 80% amino acid identity), they apparently perform distinct biological functions, which could reflect tissue specific expression. For instance, PKB α mRNA is present in the majority of organs with low levels in pancreas and skeletal muscle [9–11]; PKB β mRNA is highly abundant in insulin-responsive tissues such as skeletal

B. A. Hemmings (✉)
Friedrich Miescher Institute for Biomedical Research,
Maulbeerstrasse 66, 4058 Basel,
Switzerland
e-mail: brian.hemmings@fmi.ch

muscle, liver, and adipose tissue, and PKB γ mRNA levels are high in brain, testis, lung, mammary gland, and adipose. Interestingly, in tissues and organs with the highest levels of PKB β , PKB γ levels are the lowest [11].

Taking into account the complex cellular composition of the liver, it should be noted that hepatocytes are not the only cell types expressing PKB. Kupffer cells, hepatic stellate cells (HSC), and sinusoidal endothelial cells (SEC) also express this kinase and PKB is involved in their functions in normal physiological conditions as well as in pathological states. For example, Kupffer cells stimulated by lipoteichoic acid and lipopolysaccharide reduce the inflammatory response via activation of the PI3K/PKB

pathway [12]. It has also been suggested that PKB plays a key role in early liver regeneration and in the induction of cytokines secretion and the proliferation of SECs [13, 14].

Activation and Regulation of PKB/Akt

Activating Stimuli and Upstream Kinases

Growth factor (Table 16.1) binding promotes the recruitment and activation of class I PI3K after autophosphorylation of the receptor on tyrosine residues. At the

Table 16.1 List of selected PKB activators (top row) and PKB substrates assigned to two major groups: growth/survival/cell cycle-related and metabolism-related (middle and bottom rows)

	Growth factors and cytokines	Interactors and other molecules	Chemical compounds and other stimuli
Activators	Insulin Insulin like growth factor (IGF) Epidermal growth factor (EGF) Hepatic growth factor (HGF) Basic fibroblast growth factor (FGFb) Nerve growth factor (NGF) Platelet derived growth factor (PDGF) Vascular endothelial growth factor (VEGF) Leukemia inhibitory factor (LIF) Interleukins 2,3,4,5,8 (IL2,3,4,5,8) RANTES Stem cell factor Tumor necrosis factor alpha (TNF α)	Heat shock protein 90 kDa (Hsp90) BTB (POZ) domain containing 10 (BTBD10) Fused toes protein 1 Ft1 T-cell leukemia antigen 1 (Tcl1) Adaptor protein containing PH domain, PTB domain, and Leucine zipper motif (APPL) Akt phosphorylation enhancer (APE)	Orthovanadate (phosphatase inhibitor) Okadaic acid (phosphatase inhibitor) DNA damage Hydrogen peroxide/reactive oxygen species Hypoxia Heat shock Zinc, cadmium Exercise
	Growth, survival, and cell cycle related		
Substrates	BAD Caspase 9 FoxOs YAP Mdm2 IKK α p21 p27 TSC2 PRAS40 Hexokinases GSK3 α/β	Becomes a target for 14-3-3-proteins, is released from anti-apoptotic Bcl-2 proteins Inactivation, prevents formation of apoptosome Nuclear exclusion, prevents transcription of pro-apoptotic genes Inactivation, translocates to the cytosol from the nucleus Stabilization, leads to increase of p53 levels Inhibition, induces NF- κ B transcriptional activity Cytoplasmic retention, blocks cell-cycle progression Cytoplasmic retention, attenuates cell-cycle inhibition Inhibition, is released from Rheb, which leads to mTOR phosphorylation/activation Inhibition (when non-phosphorylated, binds to mTORC1 and inhibits its activity) Activation, promotes association of HK with mitochondrial membrane Inhibition, leads to stabilization of proteins involved in G1/S phase transition	
	Metabolism related		
	AS160 ACL PGC-1 α GSK3 α/β FoxOs Hexokinases PFK2	Inhibition, leads to release of GLUT4 and increase of glucose transport Activation, increases fatty acid synthesis Inactivation of co-activating transcriptional activity for FoxOs, HNF4 α , and other genes Inactivation, increase in glycogen synthesis Inactivation (when active, decreases glycolysis and fatty acids synthesis, increases gluconeogenesis) Activation, important for glucose utilization Activation, catalyzes production of fructose 2,6-bisphosphate, leads to increased glycolysis	

membrane the PI3K phosphorylates PtdIns(4,5)P₂ to form PtdIns(3,4,5)P₃, which then serves as docking site for a subgroup of proteins with PH domains. The PI3K family comprises of three classes, I, II, and III. Class I PI3Ks are heterodimers of distinct regulatory (p50-55/p85) and catalytic (p110 α , p110 β or p110 δ) subunits; their activity is directed mainly to the phosphorylation of PIP₂ to PIP₃. Class II and class III differ from class I in structure and function (for more comprehensive reviews see [15, 16]). PI3K is involved in the regulation of a wide range of cellular processes, such as cell growth, proliferation, differentiation, motility, survival, and intra-cellular trafficking; many of these PI3K effects are mediated by downstream PKB. The constitutive activation of PI3K class I due to a gain-of-function mutation (in the p110 α subunit, for example) or the downregulation of its

negative regulator PTEN (lipid phosphatase and tensin homolog deleted on chromosome ten) are striking features of many human cancers [17].

Thus, inactive PKB/Akt that is translocated to the plasma membrane (PM), undergoes a conformational change, attaches to phospholipid through a PH domain and becomes phosphorylated (schematic representation of PKB activation is shown on the Fig. 16.1). Once recruited to the PM, PKB is activated in a two-step process that requires phosphorylation on both Thr308 in the activation loop of the kinase domain and Ser473 within the HM of the regulatory domain. Thr308 is subjected to phosphorylation by PDK1 kinase, which is recruited to the PM through its PH domain; precomplexed PDK1 in cytoplasm [18, 19]. Notably, mutation of the PH domain of PDK1 in mice diminishes PKB

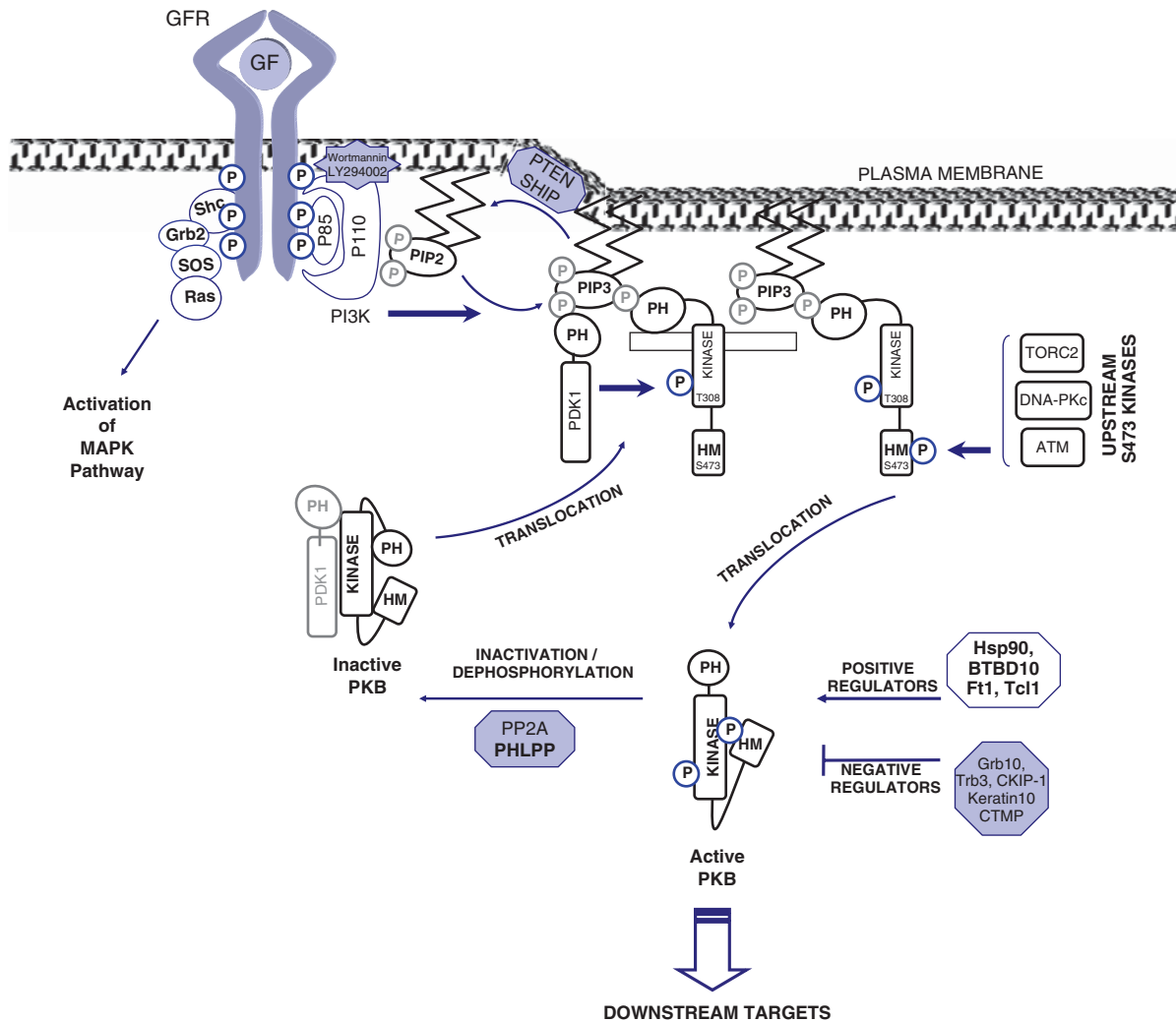


Fig. 16.1 Schematic representation of PKB activation and regulation (adapted from [6])

activation, leading to small size and insulin resistance [20].

PKB, monophosphorylated on Thr308 has ca. 10% of the activity of the fully phosphorylated enzyme. Additional Ser473 phosphorylation stabilizes the active conformation, allowing most PKB molecules to adopt a fully active state [21]. The identity of the kinase phosphorylating PKB on Ser473 remained controversial for many years; today it is accepted that the PI3K-related protein kinase family the TORC2 complex, DNA-PK, and ATM are responsible for this phosphorylation. The fact that mTORC2 is a Ser473 kinase for PKB is widely recognized [22, 23]. Work done on knock-out mice and *Drosophila* cells has provided genetic evidence favoring the hypothesis that components of the rapamycin-insensitive Rictor-mTOR complex have a shared positive role in the phosphorylation of the HM site of PKB [22]. DNA-PK has also been identified as an upstream Ser473 kinase of PKB [24, 25]. However, DNA-PK does not play a role in insulin-promoted activation of PKB in serum-sufficient cells. It has been shown that DNA-PKcs specifically phosphorylates PKB on Ser473 after DNA damage, thus promoting survival in response to genotoxic stress in vivo [25].

Activation of growth factor receptors (GFR) by a ligand (insulin, growth factors (GF)) induces their autophosphorylation and recruits the p85 regulatory subunit of phosphatidylinositol 3-kinase (PI3K). Subsequent activation of the p110 catalytic subunit leads to phosphorylation of phosphoinositol-(4,5)-bis phosphate (PIP2) and formation of the phosphoinositol-(3,4,5)-tris phosphate (PIP3). PIP3 is a substrate for lipid phosphatase, the tensin homolog PTEN, and the SH2-domain-containing inositol polyphosphate 5-phosphatase SHIP, which act as endogenous inhibitors of the PI3K-dependent pathway, indirectly inhibiting PKB activity. Wortmannin and LY294002 also inhibit PI3K. Once formed, PIP3 serve as docking sites for the PH domains of PDK1 and PKB, which translocate to the plasma membrane from the cytoplasm. As a result of this translocation, inactive PKB is phosphorylated by PDK1 on Thr308 in a regulatory kinase domain. The second phosphorylation event on Ser473 in the HM by upstream kinases such as TORC2, DNA-PKc, and ATM are cell-type and stimuli specific. It leads to conformational changes in the PKB molecule and full activation of the kinase. Activated PKB then translocates to different subcellular compartments, such as the nucleus, ER, Golgi, and

mitochondria, where it exerts its biological activity. Protein phosphatase 2A (PP2A) and a PH domain leucine-rich repeat protein phosphatase (PHLPP) dephosphorylate and inactivate PKB. Other negative regulators of PKB are Grb10, carboxyl-terminal modulator protein (CTMP), tribbles homolog 3 (Trb3), casein kinase 2-interacting protein-1 (CKIP-1), and keratin 10. Positive regulation of PKB activity may be achieved through interaction with BTBD10 and the heat shock proteins Hsp90 and Hsp27, which protect the PKB molecule from dephosphorylation. T-cell leukemia antigen-1 (Tcl-1) and fused toes protein-1 (Ft1) may also function as positive regulators of PKB. For more details on the activation and regulation of PKB please refer to the corresponding section of this chapter.

Positive Regulation of PKB via Interaction with Other Proteins

Positive regulation of PKB activity may be mediated through interaction with Hsp90, Tcl1, and Ft1 (see Table 16.1). Protein chaperone Hsp90, a prominent target for anticancer therapy, protects many kinases bearing activated mutations [26, 27]. It is known that activated PKB requires Hsp90 to maintain the phosphorylation state, which allows cancer cells to proliferate and circumvent apoptosis [28, 29]. T-cell leukemia antigen (Tcl1) interacts with PKB and enhances its kinase activity [30, 31]. It is highly activated in multiple neoplastic conditions, mainly T- and B-cell malignancies. Fused toes protein 1 (Ft1) was identified as a direct PKB interactor, leading to the enhanced phosphorylation of both Thr308 and Ser473 by promoting its interaction with the PDK1 [32].

Negative Regulation of PKB by Phosphatases

Certain cellular mechanisms counteract the activation of PKB. Negative regulation of PKB could be mediated either by a direct mechanism, such as intramolecular interactions, or indirectly by modulation of factors important for PKB activation.

The best-studied negative regulator of the PI3K/PKB pathway is PTEN, a tumor suppressor protein that is often inactivated in many disorders characterized by PKB hyperactivation, such as cancers and some metabolic diseases (described in detail below). This molecule acts as a lipid phosphatase by dephosphorylating PIP3 at the D3 position converting it to PIP2. This leads to inhibition of the PI3K pathway and reduces recruitment of PDK1 and PKB to the PM and thus, subsequently decreases PKB activity. At the transcription level, PTEN is positively regulated by p53, Myc, Egr-1, and PPAR γ , whereas Ras, JNK, Notch, and miR-21 are negative regulators of PTEN transcription (reviewed in [33]). Downregulation due to the loss of promoter activity or loss-of-function mutations of PTEN are distinct characteristics of many neoplastic diseases, including hepatocellular carcinoma (HCC) [34, 35].

Given that PKB activation is achieved by increased phosphorylation, protein phosphatases are direct negative regulators acting on phosphorylated PKB. Protein phosphatase 2A (PP2A) acts as a negative regulator by dephosphorylation of PKB at both sites [36, 37], but particularly at Thr308 [38]. Heat shock protein 90 (Hsp90), a general chaperone to numerous targets may inhibit PP2A-mediated dephosphorylation, offering PKB protection from inactivation. BTB (POZ) domain containing 10 (BTBD10) has also been reported to interact with PKB and protect it from PP2A-mediated dephosphorylation [39]. There is no structural similarity between BTBD10 and Hsp90 and, unlike Hsp90, BTBD10 does not affect PDK1 activity [40]. BTBD10 probably acts by binding to PP2A and its target. It remains to be established whether BTBD10 is a PKB-specific activator or whether it protects other PP2A targets.

A further phosphatase directly dephosphorylating Ser473 is the PHLPP, which has a PP2C-like catalytic core, is not sensitive to okadaic acid, and binds directly to PKB via a C-terminal PDZ motif [38]. This phosphatase is markedly reduced in several colon cancer and glioblastoma cell lines with elevated PKB phosphorylation. Recently, a second PHLPP isoform, PHLPP2, has been cloned [41]. In parallel to the different tissue expression patterns and substrate specificities of the different PKB isoforms, the PHLPP isoforms have been reported to show specificity for distinct PKB isoforms. PHLPP1 was shown to affect PKB β/γ while PHLPP2 influences the activity of PKB α/γ , with marked differences in the affected PKB substrates. These data led to the speculation that PHLPP1 may regulate PKB β and affect glucose

metabolism, while PHLPP2 is involved mostly in the regulation of PKB α and cell survival [41].

Further PKB/Akt Interactors

Molecules other than phosphatases also negatively regulate PKB activity. Grb10, a growth factor receptor-bound protein 10, interacts with numerous receptor tyrosine kinases and has been implicated in the regulation of the PI3K pathway downstream of the insulin receptor. Whether Grb10 has positive or negative effects on insulin- or IGF-receptor signaling remains controversial [42–44]. In 2005, it was shown that Grb10 and PKB form a constitutive complex that promotes kinase translocation to the PM; thus, it has been proposed that Grb10 functions as a PKB coactivator [45]. However, these studies were performed mainly *in vitro* and the *in vivo* role of Grb10 was unknown until recently. First, it was shown that overexpression of Grb10 in mice leads to insulin resistance [46] and the Liu group reported later that disruption of this gene enhances insulin signaling and sensitivity [43]. CTMP, shown to interact with PKB, delays Ser473 phosphorylation and thus inhibits kinase activation [47]. Keratin K10 is also a negative regulator of PKB, to which it binds and inhibits its intracellular translocation, leads to downregulation of PKB activity [48]. Casein kinase 2-interacting protein-1 (CKIP-1) has been shown recently to interact with the PH domain of PKB and inhibit kinase activity, thus suppressing tumor growth [49]. Tribbles homolog 3 (Trb3) is a pseudokinase that binds preferentially to nonphosphorylated PKB, thereby blocking Thr308 phosphorylation induced by insulin and other GF [50]. Trb3, the abundance of which increases during fasting, may be especially relevant for liver tissue. It was suggested that Trb3 activation is beneficial under fasting conditions, but that pathological overexpression after food intake may contribute to insulin resistance and hyperglycemia. However, genetic deletion of Trb3 in mice had a minimal effect on insulin-induced PKB activation in hepatic tissues, arguing that Trb3 has a minor effect on glucose and energy homeostasis [51]. Further studies are clearly needed to evaluate the importance of Trb3 in other contexts such as hypoxia and other stresses, and after tissue-specific deletions of Trb3. Overall, it may be concluded that fine tuning of PKB signaling occurs at different levels, beginning

with activation by a variety of exogenous signals, which is then contra-regulated via either direct dephosphorylation or interaction of numerous proteins with different domains of the kinase.

PKB Substrates and Their Functions

Regulation of PKB has been studied extensively ever since its discovery and all the results obtained have made clear that PKB, being so stringently regulated, is one of the most versatile proteins in the cell. The long list of PKB substrates can be divided into several subgroups corresponding to the processes in which PKB is involved. These include regulation of cell size, transcription, survival, antiapoptotic activity, and metabolism (for a recent review see [7]).

Regulation of Cell Size and Survival

Once activated following GF/insulin treatment (Table 16.1), PKB translocates from the cell membrane to its targets and phosphorylates them at the consensus site RXRXXS/T. Constitutive activation of PKB contributes greatly to aberrant cell cycle regulation, resulting in uncontrolled cell proliferation and suppressed apoptotic pathways. This prosurvival and antiapoptotic activity is exerted through phosphorylation of target proteins, leading to either activation or inhibition of their activities. The predominant mechanism by which PKB regulates cell size (cell mass) is activation of the mTOR complex 1 (mTORC1). This is exerted via phosphorylation of TSC2 within the complex TSC1/2 and abrogation of TSC2 activity. When nonphosphorylated, TSC2 prevents formation of Rheb-GTP. Upon TSC2 phosphorylation, Rheb-GTP accumulates and activates mTORC1, which in turn activates S6K1 and 4E-BP1, stimulating translation initiation and ribosome biogenesis [52–56]. Like TSC2, PKB also phosphorylates PRAS40 (proline-rich Akt substrate of 40 kDa) [57–59]. Overexpression of a mutant, which cannot be phosphorylated by PKB, blocks PKB-mediated activation of S6K1. Recently, PRAS40 has been found to associate with and be phosphorylated by mTORC1 and is thought to negatively regulate its signaling [59–62].

DNA double strand breaks and promotes PKB activation. Recently published work by Bozulic et al. has

implemented the role of PKB α isoform in promotion of cell survival and antiapoptotic processes upon genotoxic stress [25]. DNA-PK recruitment to double-stranded, damaged DNA results in activation of PKB α ; DNA-PK serves as an upstream kinase for PKB α and Ser473 PKB α phosphorylation occurs in the nucleus, presumably leading to the activation of transcription factors with prosurvival activity.

The importance of PKB for cell proliferation and survival is further illustrated by overexpression experiments in which myristoylated or constitutively active variants of PKB were introduced into either cells or mice in a tissue/organ-specific manner. For example, overactive PKB alone contributes to tumorigenesis; the overexpression of PKB in the prostate gives rise to neoplasia. Increase in PKB activity enhances the number and size of thymocytes, cardiomyocytes [63], pancreatic β -cells [64, 65] prostate epithelial cells [66], and hepatocytes [67]. In contrast, PKB α knock-out mice are small, suffer increased neonatal lethality and increased spontaneous apoptosis in the thymus [11, 68, 69]. This isoform was shown to be important for trophoblast differentiation and it was concluded that PKB α regulates placental development and differentiation. These multiple *in vivo* studies emphasize a role for PKB at different stages of development and point to an indispensable role of the PKB α isoform in guiding cell size and survival processes.

Regulation of Apoptosis

The first identified PKB target involved in apoptosis was the BH3-only protein Bad, which is a negative regulator of prosurvival Bcl-2 family members [70]. Phosphorylated on Ser136 by PKB, Bad becomes a target for 14-3-3 proteins, which triggers release of Bad from Bcl-2 proteins. Caspase 9, which is another PKB substrate with proapoptotic activity, participates in the formation of the apoptosome. Phosphorylation on Ser 196 inhibits protein activity and blocks caspase 9 induced cell death [71]. PKB substrates from the FoxO family (FoxO1-4) are inactivated upon phosphorylation via their exclusion from the nucleus, where they normally act as transcription factors. FoxOs target genes promote apoptosis, cell-cycle arrest, and various metabolic processes (see below); among these are Bim, Bad, and the proapoptotic protein FasL [72, 73]. Similar

to FoxO proteins, the proapoptotic protein YAP translocates to the cytosol after being phosphorylated, whereas when active in the nucleus, it activates transcription of proapoptotic genes such as p73 [73]. Overall, activation of the PKB pathway provides cells with survival signals that allow them to withstand apoptotic stimuli.

Cell Cycle Control

PKB-mediated control of cell-cycle progression has been shown to be crucial for the G1/S transition. This activity is mediated mainly by regulation of FoxO localization and p53 intracellular concentration (via Mdm2 stabilization). PKB also phosphorylates p21, which act as cell-cycle inhibitor. When phosphorylated it accumulates in the cytoplasm and cannot bind and inhibit CDK2, which allows cell-cycle transition. p21 can be regulated also at the transcriptional level by FoxO proteins, promoting antiproliferative effect. The Mdm2/p53 signaling pathway plays an extremely important role in the regulation of cell cycle progression [74]. Mdm2, which is an E3 ubiquitin-ligase targeting p53 to its degradation, is phosphorylated and consequently stabilized by active PKB [75]. Mdm2 stabilization consequently leads to p53 ubiquitination and degradation. Notably, the p53 pathway is the most mutated in cancer cells, including HCC. Its deregulation, i.e., loss-of-function, promotes cell cycle transition and blocks apoptosis, leading in many cases to cancer progression. Cell cycle transition, mediated by PKB, is closely associated with proliferation and apoptosis, greatly contributing to the events of transformation and regeneration.

Metabolism

The role of PKB in the regulation of metabolic pathways is tightly interconnected with its positive effects on cell growth and proliferation. The main PKB isoform important for executing these effects in insulin-sensitive tissues is PKB β (and to some extent PKB α). As already discussed, the principal sites of expression of the β isoform are liver, muscle, and adipose tissue. Analysis of PKB β KO mice revealed the importance of this particular isoform in mediating metabolic effects of PKB. Notably, PKB β KO mice exhibit impaired

insulin-mediated glucose uptake in muscle and in adipocytes and an inability to lower hepatic glucose production [76–78]. As a result, these mice are insulin resistant and glucose intolerant and exhibit subsequent β cell failure. All these phenomena are typical of type 2 diabetes mellitus (T2D), which is characterized by an increased insulin requirement compounded by decreased insulin secretion.

Role of PKB in Glucose Metabolism

PKB exerts its biological activity by actively stimulating glucose uptake. Here, the important substrate is AS160 (Akt substrate of 160 kDa, or TBC1D4), a molecule with Rab-GAP activity that has up to nine potential PKB phosphorylation sites. Upon phosphorylation, AS160 loses its GAP activity, which leads to the accumulation of Rab-GTP and, consequently, to the translocation of the glucose transporter molecule Glut4 to the PM and glucose uptake. In line with this, insulin-stimulated AS160 phosphorylation is substantially reduced in muscles of T2D patients. Thus, after uptake, glucose is exploited either in the pentose-phosphate pathway (PPP), is oxidized via glycolysis, or is stored in the form of glycogen. PKB can be viewed as an important signaling node that coordinates signals of metabolic and antiapoptotic pathways. This effect is mediated by hexokinases (HKs), which phosphorylate glucose to glucose-6-phosphate; it is used later in PPP or glycolysis. HKs are bound to the outer membrane of mitochondria and PKB activation maintains or enhances this association. This leads, in turn, to antiapoptotic effects of PKB/HKs on the cell via mitochondrial membrane stabilization [79]. Such effects require glucose and may be considered as a system linking cell survival and metabolism.

To a large extent PKB signaling affects both glycolysis and glycogenesis. Glycogen synthase, the enzyme catalyzing the last step in glycogen synthesis, is phosphorylated by glycogen synthase kinase 3 (GSK3) [80]; this phosphorylation leads to inactivation of glycogen synthase. Both the α and β isoforms of glycogen synthase kinase are PKB substrates. Phosphorylation on Ser21 and Ser9 of GSK3 α and β , respectively, leads to inactivation of the kinase, which in turn stimulates glycogenesis. The subsequent activity is of utmost importance in liver and muscle. Most of the research has been focused on the GSK3 β isoform, implicating it in

muscle glucose metabolism [81]; Woodgett's group has reported recently that the GSK3 α isoform is a major regulator of glucose turnover in the liver [82]. PKB activation also increases rates of glycolysis, which has been shown in numerous cancer lines [83]. Its overexpression correlates with increased glucose consumption and the accumulation of NADH and lactate without increase in oxygen usage, which suggests that it does not affect mitochondrial respiration. The fact that many tumors are characterized by increased PKB α activity raises the interesting possibility that PKB α regulates Glut1 membrane localization. Tumors often display overexpression of Glut1 on the cell surface as well as elevated glucose transport, which would identify PKB α as a cause of increased Glut1 expression and glycolysis.

Regulation of Lipid Metabolism

Insulin is a potent anabolic hormone and, in addition to glucose metabolism, it also regulates lipid homeostasis by increasing lipogenesis in the case of nutrient excess. PKB was shown to mediate insulin/PI3K effects through GSK3 inactivation, which when actively promotes degradation of sterol regulatory element binding proteins (SREBPs). It should be mentioned that a further PI3K-dependent kinase, atypical PKC, mediates the insulin effect on increased lipogenesis via increasing SREBP expression [84]. Three isoforms of SREBPs, -1a, -1c, and -1b, trigger expression of more than 30 genes involved in cholesterol metabolism, fatty acid, triglyceride, and phospholipid biosynthesis. In liver, as well as in adipose tissue, the predominant isoform is SREBP-1c, which upregulates transcription and expression of lipogenic enzymes such as fatty acid synthase (FAS) and ATP citrate lyase (ACL).

ACL is also a PKB substrate important for fatty acid synthesis. ACL links glucose metabolism to lipid synthesis by cleaving citrate to acetyl-CoA and oxaloacetate in the cytosol, thus supporting the synthesis of fatty acids, cholesterol, etc. [85]. ACL has been proposed as a target for anticancer therapy, since it is positively regulated in PKB-overexpressing tumors it mediates metabolic switches characteristic of cancer cells [86]. HCC, a neoplastic disease of liver, is associated with a marked increase in lipogenic enzymes and it was suggested that SREBP-1c is involved in this process [87].

FoxOs at the Crossroads of Metabolism and Survival: The Role of PGC-1 α

FoxO is a further target of PKB, belonging to a family of proteins associated with cell cycle regulation by PKB. FoxO also contributes to glucose homeostasis and is an important target of insulin action. FoxO1 promotes hepatic glucose production and regulates the differentiation of cells involved in metabolic control (reviewed in [88]). In the liver, FoxOs have been shown to increase gluconeogenesis and triglycerides (TG) metabolism via transcriptional upregulation of phosphoenolpyruvate carboxykinase (PEPCK) and glucose-6-phosphatase (G6Pase), and PPAR- γ coactivator 1 α (PGC-1 α). FoxOs decrease glycolysis and fatty acid/TG synthesis [89]. The results of liver-specific KO of FoxO1 illustrate the pivotal role of this transcription factor in promoting hepatic glucose production and provide details of the interconnection of the cAMP and insulin pathways in the regulation of glucose production [90].

Coactivator PGC-1 α is a well-recognized global regulator of liver metabolism in the fasting state that interacts with and recruits transcription factors to gene promoter regions [91]. It is involved in the control of gluconeogenic gene expression by coactivating FoxO1 and HNF-4 and was also shown to be associated with the promoter of the glucose G6Pase gene. It was found recently that PKB β directly phosphorylates and inhibits PGC-1 α activity, which suggests a further role for insulin and PKB in controlling lipid catabolism in the liver [92].

FoxOs also protect cells from oxidative stress via upregulation of MnSOD2, catalase, and other enzymes involved in detoxifying reactive oxygen species (ROS). This activity is highly conserved among mammals, in worms, and flies. Overexpression of constitutively active PKB results in increased susceptibility to oxidative stress [93]. In addition, it may also regulate amino acid uptake through the activity of the TSC2/mTORC2 pathway, but the complex network of the PKB/mTOR pathway is still not sufficiently defined.

Role of PKB in Liver Regeneration

The liver has an enormous capacity to regenerate after traumatic tissue loss or exposure to hepatotoxic

substances. It compensates efficiently for large tissue loss as experienced after surgical removal of intrahepatic tumors [94]. The mechanisms of this regeneration are still the subject of intense research and new players like serotonin have been discovered recently [95]. Liver regeneration in response to tissue damage is a complex and well-orchestrated process and many excellent studies cover this topic [96, 97]. After major tissue loss many cytokines and GF (e.g., HGF, EGF, VEGF, or PDGF) are released leading to proliferation of hepatocytes. Within 48 h, the majority of hepatocytes re-enter the cell cycle moving from G0 to S phase. After cessation of proliferation, hepatocytes regain cellular volume and the original liver volume is almost completely restored within 1 week in rodents. PKB is strongly activated by many GF shown to be crucial in hepatic regeneration, e.g., HGF, EGF, or PDGF [96]. During liver regeneration in a partial hepatectomy model, a robust and sustained activation of total PKB was observed [98]. Hepatic expression of constitutively active PKB α was associated with a three-fold increase in liver mass due to the increase in hepatocyte size without change in cell number [99]. Additionally, PKB-dependent hypertrophy of hepatocytes was sufficient for compensatory recovery of liver mass in liver-specific STAT3 mutant mice and in a thrombocytotic model of liver regeneration [100, 101]. In contrast, total PI3K inhibition with wortmannin, or selective inhibition with siRNA, resulted in a significant decrease in hepatocyte proliferation, especially at the earliest time points [102]. Liver regeneration appears to be dependent on the presence of PKB. However, the expected reduction in regenerative capacity in PKB α or PKB β mutant mice has not yet been demonstrated.

Involvement of the PI3K/PTEN/PKB Pathway in Liver Diseases

Liver diseases contribute significantly to human mortality and rising health-care expenditure. Although the liver can compensate for significant injury, there may be a significant decrease in function leading to organ failure. Proper functioning of the PKB network may be needed to maintain organ function and its deregulation is a significant factor in the development of certain hepatic diseases and liver-associated syndromes.

Insulin Resistance, Nonalcoholic Fatty Liver Disease, and Hepatosteatosis

Among liver diseases, nonalcoholic fatty liver disease (NAFLD) is becoming increasingly common; every third adult and tenth child/adolescent in the USA is affected by this condition [103]. NAFLD is considered to be a hepatic manifestation of a metabolic syndrome. The prerequisite feature of NAFLD is increased accumulation of lipids in hepatocytes, which can originate either from increased levels of nonesterified fatty acids (NEFA) circulating in the blood or from enhanced de novo synthesis of lipids in the cells. Whereas, simple steatosis seems to have a relatively benign clinical course, a subgroup of patients develops inflammatory changes, known as nonalcoholic steatohepatitis (NASH) and potentially liver cirrhosis with increased risk for HCC [104]. Increase in intracellular lipid metabolites may lead to activation of the PI3K/PKB pathway. Initial overactivation of the signaling cascade then results in inhibition of IRS-1, which mediates a negative feedback effect on PI3K activation, leading finally to the inhibition of insulin signaling. Patients with NAFLD display lower levels of phosphorylated PKB and an increase in Bax/Bcl-2 ratio [105]. A similar situation has been described for activated PKC ϵ , which led to the decrease in insulin-stimulated IRS-2 phosphorylation and hepatic insulin resistance [106]. Later, insulin resistance involves other peripheral organs, such as skeletal muscle and adipose tissue, eventually becoming systemic. Under physiological conditions, insulin released from the pancreas decreases glucose output from the liver but stimulates glucose uptake by muscle and adipose tissue. In patients with insulin resistance, a syndrome associated with impaired metabolic clearance of glucose, the concentration of NEFA in the bloodstream increases due to the high lipogenic effect of insulin. NEFA act by reducing adipocyte and muscle glucose uptake and promoting hepatic glucose output, which leads to increased blood glucose concentration. Obesity worsens the situation and leads to increased levels of NEFA released directly into the portal vein from visceral adipose. This adds to the vicious cycle leading to even higher insulin resistance.

Hepatocellular lipid accumulation concerns about 40% of the population and renders the liver particularly susceptible to inflammatory cytokines, endotoxins, iron accumulation, and oxidative stress [107].

The latter is caused to a large extent by increased intracellular lipids. Most studied are the effects of lipotoxicity on beta cells [108, 109] and cardiomyocytes [110], but hepatocytes are also affected significantly, via a direct or an indirect mechanism, often displaying mitochondrial dysfunction [111]. Key characteristics of mitochondrial dysfunction are respiratory chain defects that lead to an increase in ROS production. In addition to damaging mtDNA and respiratory chain enzymes, increase in ROS leads to the oxidation of many cytoplasmic enzymes, including PTEN. Thus, it is now clear that ROS are not only deleterious for the cell but are very important with respect to signaling molecules [112]. Their presence at low concentrations helps maintain certain basal levels of kinase activity, namely PI3K/PKB in cells not supplemented with GF. However, when cells are overloaded with ROS, this may lead to hyperactivation of the PI3K/PTEN/PKB pathway, to inhibition of FoxO1 and PGC-1 α and the transcription of adipogenic- and lipogenic- as well as beta-oxidation-related genes. This leads to liver steatosis and potentially to hepatic tumorigenesis.

The role of cell types other than hepatocytes in insulin resistance should not be neglected. Sinusoidal liver cells are often ignored but they are an important factor in the maintenance of the pathological situation of insulin resistance, exacerbating the oxidative damage of hepatocytes, as well as secreting the proinflammatory cytokines, TNF- α and IL6 [113]. It has been suggested that the degree of insulin sensitivity depends on the state of activation of stellate cells, which have phosphorylated IR and IRS1 when activated and do not respond further to insulin, thus failing in glucose uptake. Their activation brings hepatic tissue one step closer to the development of fibrosis and, ultimately, cirrhosis [113, 114].

Involvement of Phosphatases in Insulin Sensitivity

Beneficial for the restoration of insulin sensitivity may be the target of the PI3K/PKB pathway via a decrease in phosphatase activity and the negative regulation of PKB activity. This is indeed the case is shown by the protein tyrosine phosphatase 1 B (PTP1B), which negatively regulates insulin receptor and IRS-1 signaling knock-out mice. Disruption of the PTP1B gene in mice

leads to enhanced insulin sensitivity and decrease in adipose mass. In mice with polygenic insulin resistance, deficiency in PTP1B results in improved glucose tolerance and a decrease in the occurrence of diabetes [115]. Similarly, muscle-specific KO of PTP1B also has a beneficial effect on insulin sensitivity [114].

Another example of increased insulin sensitivity due to loss of lipid phosphatase activity are PTEN knock-out mice. Quite unexpectedly, in addition to the insulin hypersensitive phenotype, liver-specific PTEN knock-outs suffer from hepatomegaly and fatty liver, being at the same time overall leaner than their wild type littermates [116]. These mice have low levels of NEFA in the plasma and relative hypoinsulinemia concomitant with the higher PKB activity. They display an increased liver glycogen content and enhanced FA synthesis and secretion. PTEN null mice are in principle a further model of NAFLD that does not involve overnutrition and is not polygenic in nature. These mice are valuable for the absence of obesity/T2D, which is speculated not to be mandatory for insulin resistance but be only an associated complication. PTEN null mice provide a new insight into the *in vivo* role of PTEN, underlying the importance of negative regulators of PKB in insulin-signaling pathway in liver. HCC, recognized as a complication of NAFLD, is often accompanied by downregulation of PTEN, leading to the poor prognosis in HCC patients [29]. Deregulation of PTEN activity may be due to hypermethylation of its promoter [14], microRNA-21 induced degradation of PTEN mRNA [117], or loss-of-function mutations [118]. Alternatively, PTEN may be the target of increased ROS in cells, leading to its oxidation and blockage of the catalytic cystein residues, important for proper function [119]. In this context, PTEN heterozygous and liver-specific KOs are invaluable models for studying the pathogenesis of NAFLD, that later develops into steatohepatitis and progresses to liver carcinoma without any additional exogenous treatment.

The PI3K/PTEN/PKB Pathway in the Development of HCC

Alterations in PI3K/PKB signaling components are generally frequent in many tumors and HCC is not an exception. Various pathway components that provide a balance between cell survival and apoptosis are often

deregulated. A mutation in the PIK3CA gene, which encodes a p110 α subunit of PI3K class IA, is found in 35% of HCC cases, although it may depend on the population [120–122]. This is a gain-of-function mutation that results in enhanced oncogenic activity of PI3K. Other recent data have shown that the phosphorylation status of PKB may serve as a prognostic factor for early disease recurrence and poor prognosis [123]. In addition to altered metabolic regulation upon hyperactivation of PKB, many pro-survival and antiapoptotic activities start to prevail over cell death/apoptosis processes. Among the proapoptotic molecules downregulated in HCC are many PKB targets, including Bid, Bax, and p53. Proapoptotic molecule Bad was recently shown to be activated upon knock-down of hepatoma-derived growth factor (HDGF) in human HCC cell line HepG2. Tsang et al. reported that downregulation of HDGF leads to inactivation of PKB and ERK and induces Bad expression, leading to activation of the apoptotic pathway followed by the release of cytochrome c and the caspase 3 and 9 cleavage [124].

mTORC1, a further downstream target of PKB that is extremely important in HCC for growth and proliferation, angiogenesis, and resistance to apoptosis, is also affected as a result of PI3K/PKB hyperactivation [125]. Phosphorylation of the mTOR target p70S6 is associated with elevated cyclinD1 levels and decreased overall survival of patients with HCC, indicating the aggressive nature of HCC (p53, apoptosis, and mTOR are described more extensively in corresponding chapters of this book) [125, 126]. Several studies have shown that downregulation of PKB signaling promotes apoptosis and enhances susceptibility of HCC patients to anticancer drugs [127].

Another aspect of PKB involvement in liver carcinoma development and progression is an impact on tumor metabolism. It is known that PKB stimulates the biosynthesis of fatty acids via activation of SREBP, which leads to an increase in the concentrations of cellular fatty acids and PM components [128]. In addition to SREBP activation, PKB also has an impact on FAS expression. FAS has been shown to be significantly upregulated in various types of cancers whereas, except for liver and adipose tissues, FAS levels are usually quite low in normal tissues [129–131]. Many tumors switch their metabolism and start de novo synthesis of fatty acids as an energy component; FAS as one of the major enzymes of lipogenesis is consequently upregulated. FAS overexpression is often accompanied by the

induction of antiapoptotic mechanisms, leading to a selective advantage for tumor cells in survival and cell cycle progression. Indeed, this is the case in HCC, where key lipogenic enzymes such as FAS and ACL are markedly induced [69]. Until recently, the mechanism responsible for this upregulation was unclear. In 2008, the group of Watabe reported that upregulation of the FAS gene occurs under hypoxia conditions via PKB and SREBP-1 activation, and that inhibition of FAS overcomes hypoxia-induced chemoresistance, which is a major clinical problem in many cancer patients [132]. It is worth noting that changes in the metabolism of cancer cells, known as the Warburg effect, or glycolysis under normoxic conditions, lead to changes in redox balance. This, in turn, causes PTEN inactivation and subsequently PKB hyperactivation, all of which later contribute to the induction of FAS and enhancement of lipogenesis.

Viruses, PKB, and Liver Diseases

What makes patients with chronic liver diseases more prone to develop HCC? One important feature defining the outcome is PTEN status, which may serve as an independent prognostic marker of HCC associated with HCV patient survival and the presence of viral infections, such as combined hepatitis B and C (HBV/HCV) (for further details, see the corresponding chapters about HBV/HCV in this volume) [118, 133]. Hepatitis viruses are known to cause PKB activation. Thus, HCV protein NS5A may either activate PI3K via binding to its regulatory subunit or inhibit apoptosis by acting on the Bax protein [134, 135]. Furthermore, approximately 50% of patients with a chronic HCV infection develop liver steatosis and insulin resistance, mediated by increased oxidative stress, the activation of PI3K/PKB and the transactivation of PPAR γ and SREBP-1/2 [136–138]. On the other hand, insulin resistance may be linked to inhibition of PKB signaling, either through impairment of upstream IRS-1 and PI3K [139], or, as shown recently, through overexpression of protein phosphatase PP2A [140]. Recent analysis of HCC samples revealed that activation and overexpression of PKB and phosphorylation of its target GSK3 β are among the most consistent features in HBV-associated HCC [141]. Activation of the PKB pathway as a consequence of viral infection leads to antiapoptotic effects on infected cells. This is

the case with HBV protein HBx, which activates the PI3K/PKB/Bad prosurvival pathway. HBx was shown to affect PTEN expression by inhibiting the function of p53, an established transcriptional regulator of PTEN [142], and overexpression of PTEN in these cells may reverse signaling modulated by HBx and have a positive effect on apoptosis [143].

Conclusions

The serine/threonine protein kinase PKB is major downstream mediator of PI3K.

PKB coordinates a constellation of intracellular signals and controls cellular responses to a variety of extrinsic stimuli.

PKB regulates cell proliferation, survival, growth, glucose and lipid metabolism, and malignant transformation.

Insulin and other GF are potent PKB activators.

In many pathological conditions such as NAFLD or HCC the PI3K/PKB pathway is often overactivated due to aberration in the upstream regulation of the kinase.

PKB isoforms were shown to be amplified, overexpressed, or mutated in various types of cancer.

The importance of fine tuning of PKB activity can be displayed in one frame that incorporates PI3K/PKB signaling to pathophysiology of insulin resistance associated with other factors like viral infections and subsequent transition to NAFLD/NASH and later to the development and progression of fibrosis, cirrhosis, and finally HCC.

Targeting the PI3K/PTEN/PKB/mTOR pathway in order to alleviate burden of associated diseases seems to be an attractive, and, in some cases, successful approach, that could be exploited in targeted therapy.

Multiple Choice Questions

- Protein kinase B/Akt phosphorylates its substrates, which leads to
 - Activation of their function only
 - Inhibition of their function only
 - Activation/inhibition of their function and translocation to a different cellular compartment
- Protein kinase B/Akt has three isoforms, PKB α , β , γ , which
 - Are found in all species, from worms to humans
 - Have low conservation of amino acid sequence, but similar domain organization
 - Have distinct tissue distribution patterns
- Full activation of PKB requires
 - Phosphorylation on Ser473 within the hydrophobic motif
 - Phosphorylation on Thr308 in the kinase domain, which changes the conformation of kinase, and is followed by Ser473 phosphorylation
 - Dual phosphorylation on Thr308 and Ser473; it is still arguable whether it happens in parallel or consequently
- Which of the following statements is wrong?
 - PTEN is a lipid phosphatase that regulates the PI3K/PKB pathway. It is overexpressed in many cancer cell lines and its gain-of-function mutations are the hallmark of different cancers
 - PTP1B and PTEN are negative regulators of the PI3K/PKB pathway; mouse models show that decrease in the levels of PTP1B and PTEN may restore insulin sensitivity
 - PKB activity might be regulated via direct dephosphorylation, via interaction with protein other than phosphatases, via upstream modulation of PI3K activity
- The PKB β isoform is
 - The major isoform that regulates cell growth and proliferation; PKB β KO mice are smaller and have increased neonatal lethality
 - Expressed ubiquitously at similar levels in all tissues
 - Expressed at the highest levels in insulin-responsive tissues, and its ablation leads to development of insulin resistance and T2D in mice

Acknowledgements We thank Arnaud Parcellier, Lana Bozulic, Alexander Hergovich, and Patrick King for their critical reading of this manuscript. EZ is the recipient of a Swiss Bridge fellowship. OT is supported by the Gebert R uf Foundation (GRS 027/06) and Am elie Waring Foundation. The Friedrich Miescher Institute is part of the Novartis Research Foundation.

References

- Jones PF, Jakubowicz T, Pitossi FJ et al (1991) Molecular cloning and identification of a serine/threonine protein kinase of the second-messenger subfamily. *Proc Natl Acad Sci U S A* 88(10):4171–4175
- Bellacosa A, Testa JR, Staal SP et al (1991) A retroviral oncogene, akt, encoding a serine-threonine kinase containing an SH2-like region. *Science* 254(5029):274–277
- Coffer PJ, Woodgett JR (1991) Molecular cloning and characterisation of a novel putative protein-serine kinase related to the cAMP-dependent and protein kinase C families. *J Biochem* 201(2):475–481
- Brazil DP, Hemmings BA (2001) Ten years of protein kinase B signalling: a hard Akt to follow. *Trends Biochem Sci* 26(11):657–664
- Brazil DP, Yangand ZZ, Hemmings BA (2004) Advances in protein kinase B signalling: AKTion on multiple fronts. *Trends Biochem Sci* 29(5):233–242
- Fayard E, Tintignac LA, Baudry A et al (2005) Protein kinase B/Akt at a glance. *J Cell Sci* 118(Pt 24):5675–5678
- Manning BD, Cantley LC (2007) AKT/PKB signaling: navigating downstream. *Cell* 129(7):1261–1274
- Haslam RJ, Koideand HB, Hemmings BA (1993) Pleckstrin domain homology. *Nature* 363(6427):309–310
- Bellacosa A, Franke TF, Gonzalez-Portal ME et al (1993) Structure, expression and chromosomal mapping of c-akt: relationship to v-akt and its implications. *Oncogene* 8(3):745–754
- Altomare DA, Lyons GE, Mitsuuchi Y et al (1998) Akt2 mRNA is highly expressed in embryonic brown fat and the AKT2 kinase is activated by insulin. *Oncogene* 16(18):2407–2411
- Yang ZZ, Tschopp O, Hemmings-Mieszczak M et al (2003) Protein kinase B alpha/Akt1 regulates placental development and fetal growth. *J Biol Chem* 278(34):32124–32131
- Dahle MK, Overland G, Myhre AE et al (2004) The phosphatidylinositol 3-kinase/protein kinase B signaling pathway is activated by lipoteichoic acid and plays a role in Kupffer cell production of interleukin-6 (IL-6) and IL-10. *Infect Immun* 72(10):5704–5711
- Ping C, Xiaoling D, Jin Z et al (2006) Hepatic sinusoidal endothelial cells promote hepatocyte proliferation early after partial hepatectomy in rats. *Arch Med Res* 37(5):576–583
- Ping C, Lin Z, Jiming D et al (2006) The phosphoinositide 3-kinase/Akt-signal pathway mediates proliferation and secretory function of hepatic sinusoidal endothelial cells in rats after partial hepatectomy. *Biochem Biophys Res Commun* 342(3):887–893
- Wymann MP, Marone R (2005) Phosphoinositide 3-kinase in disease: timing, location, and scaffolding. *Curr Opin Cell Biol* 17(2):141–149
- Engelman JA, Luoand J, Cantley LC (2006) The evolution of phosphatidylinositol 3-kinases as regulators of growth and metabolism. *Nat Rev Genet* 7(8):606–619
- Samuels Y, Diaz LA Jr, Schmidt-Kittler O et al (2005) Mutant PIK3CA promotes cell growth and invasion of human cancer cells. *Cancer Cell* 7(6):561–573
- Alessi DR, James SR, Downes CP et al (1997) Characterization of a 3-phosphoinositide-dependent protein kinase which phosphorylates and activates protein kinase Balpha. *Curr Biol* 7(4):261–269
- Calleja V, Alcor D, Laguerre M et al (2007) Intramolecular and intermolecular interactions of protein kinase B define its activation in vivo. *PLoS Biol* 5(4):e95
- Bayascas JR, Wullschlegler S, Sakamoto K et al (2008) Mutation of the PDK1 PH domain inhibits protein kinase B/Akt, leading to small size and insulin resistance. *Mol Cell Biol* 28(10):3258–3272
- Yang J, Cron P, Thompson V et al (2002) Molecular mechanism for the regulation of protein kinase B/Akt by hydrophobic motif phosphorylation. *Mol Cell* 9(6):1227–1240
- Sarbassov DD, Guertin DA, Ali SM et al (2005) Phosphorylation and regulation of Akt/PKB by the rictor-mTOR complex. *Science* 307(5712):1098–1101
- Bhaskar PT, Hay N (2007) The two TORCs and Akt. *Dev Cell* 12(4):487–502
- Feng J, Park J, Cron P et al (2004) Identification of a PKB/Akt hydrophobic motif Ser-473 kinase as DNA-dependent protein kinase. *J Biol Chem* 279(39):41189–41196
- Bozulic L, Surucu B, Hynx D et al (2008) PKBalpha/Akt1 acts downstream of DNA-PK in the DNA double-strand break response and promotes survival. *Mol Cell* 30(2):203–213
- Jensen MR, Schoepfer J, Radimerski T et al (2008) NVP-AUY922: a small molecule HSP90 inhibitor with potent antitumor activity in preclinical breast cancer models. *Breast Cancer Res* 10(2):R33
- Stuhmer T, Zollinger A, Siegmund D et al (2008) Signalling profile and antitumour activity of the novel Hsp90 inhibitor NVP-AUY922 in multiple myeloma. *Leukemia* 22(8):1604–12
- Hostein I, Robertson D, DiStefano F et al (2001) Inhibition of signal transduction by the Hsp90 inhibitor 17-allylamino-17-demethoxygeldanamycin results in cytostasis and apoptosis. *Cancer Res* 61(10):4003–9
- Sato S, Fujitaand N, Tsuruo T (2000) Modulation of Akt kinase activity by binding to Hsp90. *Proc Natl Acad Sci U S A* 97(20):10832–7
- Laine J, Kunstle G, Obata T et al (2000) The protooncogene TCL1 is an Akt kinase coactivator. *Mol Cell* 6(2):395–407
- Pekarsky Y, Koval A, Hallas C et al (2000) Tcl1 enhances Akt kinase activity and mediates its nuclear translocation. *Proc Natl Acad Sci U S A* 97(7):3028–33
- Remy I, Michnick SW (2004) Regulation of apoptosis by the Ft1 protein, a new modulator of protein kinase B/Akt. *Mol Cell Biol* 24(4):1493–504
- Salmena L, Carracedoand A, Pandolfi PP (2008) Tenets of PTEN tumor suppression. *Cell* 133(3):403–414
- Horie Y, Suzuki A, Kataoka E et al (2004) Hepatocyte-specific Pten deficiency results in steatohepatitis and hepatocellular carcinomas. *J Clin Invest* 113(12):1774–83
- Hu TH, Wang CC, Huang CC et al (2007) Down-regulation of tumor suppressor gene PTEN, overexpression of p53, plus high proliferating cell nuclear antigen index predict poor patient outcome of hepatocellular carcinoma after resection. *Oncol Rep* 18(6):1417–26
- Andjelkovic M, Jakubowicz T, Cron P et al (1996) Activation and phosphorylation of a pleckstrin homology domain containing protein kinase (RAC-PK/PKB) promoted by serum

- and protein phosphatase inhibitors. *Proc Natl Acad Sci U S A* 93(12):5699–704
37. Ugi S, Imamura T, Maegawa H et al (2004) Protein phosphatase 2A negatively regulates insulin's metabolic signaling pathway by inhibiting Akt (protein kinase B) activity in 3T3-L1 adipocytes. *Mol Cell Biol* 24(19):8778–89
 38. Gao T, Furnariand F, Newton AC (2005) PHLPP: a phosphatase that directly dephosphorylates Akt, promotes apoptosis, and suppresses tumor growth. *Mol Cell* 18(1):13–24
 39. Nawa M, Kanekura K, Hashimoto Y et al (2008) A novel Akt/PKB-interacting protein promotes cell adhesion and inhibits familial amyotrophic lateral sclerosis-linked mutant SOD1-induced neuronal death via inhibition of PP2A-mediated dephosphorylation of Akt/PKB. *Cell Signal* 20(3):493–505
 40. Basso AD, Solit DB, Chiosis G et al (2002) Akt forms an intracellular complex with heat shock protein 90 (Hsp90) and Cdc37 and is destabilized by inhibitors of Hsp90 function. *J Biol Chem* 277(42):39858–39866
 41. Brognard J, Sierrecki E, Gao T et al (2007) PHLPP and a second isoform, PHLPP2, differentially attenuate the amplitude of Akt signaling by regulating distinct Akt isoforms. *Mol Cell* 25(6):917–31
 42. Liu F, Roth RA (1995) Grb-IR: a SH2-domain-containing protein that binds to the insulin receptor and inhibits its function. *Proc Natl Acad Sci U S A* 92(22):10287–10291
 43. Wang L, Balas B, Christ-Roberts CY et al (2007) Peripheral disruption of the Grb10 gene enhances insulin signaling and sensitivity in vivo. *Mol Cell Biol* 27(18):6497–505
 44. Wick KR, Werner ED, Langlais P et al (2003) Grb10 inhibits insulin-stimulated insulin receptor substrate (IRS)-phosphatidylinositol 3-kinase/Akt signaling pathway by disrupting the association of IRS-1/IRS-2 with the insulin receptor. *J Biol Chem* 278(10):8460–7
 45. Jahn T, Seipel P, Urschel S et al (2002) Role for the adaptor protein Grb10 in the activation of Akt. *Mol Cell Biol* 22(4):979–91
 46. Shiura H, Miyoshi N, Konishi A et al (2005) Meg1/Grb10 overexpression causes postnatal growth retardation and insulin resistance via negative modulation of the IGF1R and IR cascades. *Biochem Biophys Res Commun* 329(3):909–16
 47. Maira SM, Galetic I, Brazil DP et al (2001) Carboxyl-terminal modulator protein (CTMP), a negative regulator of PKB/Akt and v-Akt at the plasma membrane. *Science* 294(5541):374–80
 48. Paramio JM, Segrelles C, Ruiz S et al (2001) Inhibition of protein kinase B (PKB) and PKC{zeta} mediates keratin K10-induced cell cycle arrest. *Mol Cell Biol* 21(21):7449–7459
 49. Tokuda E, Fujita N, Oh-hara T et al (2007) Casein kinase 2-interacting protein-1, a novel Akt pleckstrin homology domain-interacting protein, down-regulates PI3K/Akt signaling and suppresses tumor growth in vivo. *Cancer Res* 67(20):9666–76
 50. Du K, Herzig S, Kulkarni RN et al (2003) TRB3: a tribbles homolog that inhibits Akt/PKB activation by insulin in liver. *Science* 300(5625):1574–7
 51. Okamoto H, Latres E, Liu R et al (2007) Genetic deletion of Trb3, the mammalian *Drosophila* tribbles homolog, displays normal hepatic insulin signaling and glucose homeostasis. *Diabetes* 56(5):1350–1356
 52. Gulati P, Thomas G (2007) Nutrient sensing in the mTOR/S6K1 signalling pathway. *Biochem Soc Trans* 35(Pt 2):236–8
 53. Pende M, Kozma SC, Jaquet M et al (2000) Hypoinsulinaemia, glucose intolerance and diminished beta-cell size in S6K1-deficient mice. *Nature* 408(6815):994–7
 54. Constantinou C, Clemens MJ (2005) Regulation of the phosphorylation and integrity of protein synthesis initiation factor eIF4GI and the translational repressor 4E-BP1 by p53. *Oncogene* 24(30):4839–50
 55. Fingar DC, Richardson CJ, Tee AR et al (2004) mTOR controls cell cycle progression through its cell growth effectors S6K1 and 4E-BP1/eukaryotic translation initiation factor 4E. *Mol Cell Biol* 24(1):200–16
 56. Hara K, Yonezawa K, Kozlowski MT et al (1997) Regulation of eIF-4E BP1 phosphorylation by mTOR. *J Biol Chem* 272(42):26457–63
 57. Wang L, Harrisand TE, Lawrence JC Jr (2008) Regulation of proline-rich Akt substrate of 40 kDa (PRAS40) function by mammalian target of rapamycin complex 1 (mTORC1)-mediated phosphorylation. *J Biol Chem* 283(23):15619–27
 58. Thedieck K, Polak P, Kim ML et al (2007) PRAS40 and PRR5-like protein are new mTOR interactors that regulate apoptosis. *PLoS ONE* 2(11):e1217
 59. Sancak Y, Thoreen CC, Peterson TR et al (2007) PRAS40 is an insulin-regulated inhibitor of the mTORC1 protein kinase. *Mol Cell* 25(6):903–15
 60. Fonseca BD, Smith EM, Lee VH et al (2007) PRAS40 is a target for mammalian target of rapamycin complex 1 and is required for signaling downstream of this complex. *J Biol Chem* 282(34):24514–24
 61. Oshiro N, Takahashi R, Yoshino K et al (2007) The proline-rich Akt substrate of 40 kDa (PRAS40) is a physiological substrate of mammalian target of rapamycin complex 1. *J Biol Chem* 282(28):20329–39
 62. Vander Haar E, Lee SI, Bandhakavi S et al (2007) Insulin signalling to mTOR mediated by the Akt/PKB substrate PRAS40. *Nat Cell Biol* 9(3):316–23
 63. Condorelli G, Drusco A, Stassi G et al (2002) Akt induces enhanced myocardial contractility and cell size in vivo in transgenic mice. *Proc Natl Acad Sci U S A* 99(19):12333–8
 64. Bernal-Mizrachi E, Wen W, Stahlhut S et al (2001) Islet beta cell expression of constitutively active Akt1/PKB alpha induces striking hypertrophy, hyperplasia, and hyperinsulinemia. *J Clin Invest* 108(11):1631–8
 65. Trumper K, Trumper A, Trusheim H et al (2000) Integrative mitogenic role of protein kinase B/Akt in beta-cells. *Ann N Y Acad Sci* 921:242–50
 66. Graff JR, Konicek BW, McNulty AM et al (2000) Increased AKT activity contributes to prostate cancer progression by dramatically accelerating prostate tumor growth and diminishing p27Kip1 expression. *J Biol Chem* 275(32):24500–24505
 67. Ono H, Shimano H, Katagiri H et al (2003) Hepatic Akt activation induces marked hypoglycemia, hepatomegaly, and hypertriglyceridemia with sterol regulatory element binding protein involvement. *Diabetes* 52(12):2905–2913
 68. Yang ZZ, Tschopp O, Di-Poi N et al (2005) Dosage-dependent effects of Akt1/protein kinase Balpha (PKBalpha) and Akt3/PKBgamma on thymus, skin, and cardiovascular and nervous system development in mice. *Mol Cell Biol* 25(23):10407–18

69. Cho H, Thorvaldsen JL, Chu Q et al (2001) Akt1/PKBalpha is required for normal growth but dispensable for maintenance of glucose homeostasis in mice. *J Biol Chem* 276(42):38349–52
70. Datta SR, Dudek H, Tao X et al (1997) Akt phosphorylation of BAD couples survival signals to the cell-intrinsic death machinery. *Cell* 91(2):231–41
71. Cardone MH, Roy N, Stennicke HR et al (1998) Regulation of cell death protease caspase-9 by phosphorylation. *Science* 282(5392):1318–21
72. Brunet A, Bonni A, Zigmond MJ et al (1999) Akt promotes cell survival by phosphorylating and inhibiting a Forkhead transcription factor. *Cell* 96(6):857–68
73. Basu S, Totty NF, Irwin MS et al (2003) Akt phosphorylates the Yes-associated protein, YAP, to induce interaction with 14–3–3 and attenuation of p73-mediated apoptosis. *Mol Cell* 11(1):11–23
74. Horvath MM, Wang X, Resnick MA et al (2007) Divergent evolution of human p53 binding sites: cell cycle versus apoptosis. *PLoS Genet* 3(7):e127
75. Feng J, Tamaskovic R, Yang Z et al (2004) Stabilization of Mdm2 via decreased ubiquitination is mediated by protein kinase B/Akt-dependent phosphorylation. *J Biol Chem* 279(34):35510–7
76. Dummmler B, Tschopp O, Hynx D et al (2006) Life with a single isoform of Akt: mice lacking Akt2 and Akt3 are viable but display impaired glucose homeostasis and growth deficiencies. *Mol Cell Biol* 26(21):8042–51
77. Cho H, Mu J, Kim JK et al (2001) Insulin resistance and a diabetes mellitus-like syndrome in mice lacking the protein kinase Akt2 (PKB beta). *Science* 292(5522):1728–31
78. Garofalo RS, Orena SJ, Rafidi K et al (2003) Severe diabetes, age-dependent loss of adipose tissue, and mild growth deficiency in mice lacking Akt2/PKB beta. *J Clin Invest* 112(2):197–208
79. Majewski N, Nogueira V, Bhaskar P et al (2004) Hexokinase-mitochondria interaction mediated by Akt is required to inhibit apoptosis in the presence or absence of Bax and Bak. *Mol Cell* 16(5):819–30
80. Cross DAE, Alessi DR, Cohen P et al (1995) Inhibition of glycogen synthase kinase-3 by insulin mediated by protein kinase B. *Nature* 378(6559):785–789
81. McManus EJ, Sakamoto K, Armit LJ et al (2005) Role that phosphorylation of GSK3 plays in insulin and Wnt signaling defined by knockin analysis. *Embo J* 24(8):1571–83
82. MacAulay K, Doble BW, Patel S et al (2007) Glycogen synthase kinase 3[alpha]-specific regulation of murine hepatic glycogen metabolism. *Cell Metab* 6(4):329–337
83. Elstrom RL, Bauer DE, Buzzai M et al (2004) Akt stimulates aerobic glycolysis in cancer cells. *Cancer Res* 64(11):3892–9
84. Taniguchi CM, Kondo T, Sajan M et al (2006) Divergent regulation of hepatic glucose and lipid metabolism by phosphoinositide 3-kinase via Akt and PKC[lambda]/[zeta]. *Cell Metab* 3(5):343–353
85. Berwick DC, Hers I, Heesom KJ et al (2002) The Identification of ATP-citrate lyase as a protein kinase B (Akt) substrate in primary adipocytes. *J Biol Chem* 277(37):33895–33900
86. Bauer DE, Hatzivassiliou G, Zhao F et al (2005) ATP citrate lyase is an important component of cell growth and transformation. *Oncogene* 24(41):6314–22
87. Yahagi N, Shimano H, Hasegawa K et al (2005) Co-ordinate activation of lipogenic enzymes in hepatocellular carcinoma. *Eur J Cancer* 41(9):1316–1322
88. Gross DN, van den Heuveland AP, Birnbaum MJ (2008) The role of FoxO in the regulation of metabolism. *Oncogene* 27(16):2320–2336
89. Zhang W, Patil S, Chauhan B et al (2006) FoxO1 regulates multiple metabolic pathways in the liver: effects on gluconeogenic, glycolytic, and lipogenic gene expression. *J Biol Chem* 281(15):10105–17
90. Matsumoto M, Pocai A, Rossetti L et al (2007) Impaired regulation of hepatic glucose production in mice lacking the forkhead transcription factor Foxo1 in liver. *Cell Metab* 6(3):208–16
91. Handschin C, Spiegelman BM (2006) Peroxisome proliferator-activated receptor gamma coactivator 1 coactivators, energy homeostasis, and metabolism. *Endocr Rev* 27(7):728–35
92. Li X, Monks B, Ge Q et al (2007) Akt/PKB regulates hepatic metabolism by directly inhibiting PGC-1alpha transcription coactivator. *Nature* 447(7147):1012–6
93. Zheng X, Yang Z, Yue Z et al (2007) FOXO and insulin signaling regulate sensitivity of the circadian clock to oxidative stress. *Proc Natl Acad Sci U S A* 104(40):15899–904
94. Clavien PA, Petrowsky H, DeOliveira ML et al (2007) Strategies for safer liver surgery and partial liver transplantation. *N Engl J Med* 356(15):1545–59
95. Lesurtel M, Graf R, Aleil B et al (2006) Platelet-derived serotonin mediates liver regeneration. *Science* 312(5770):104–7
96. Michalopoulos GK (2007) Liver regeneration. *J Cell Physiol* 213(2):286–300
97. Taub R (2004) Liver regeneration: from myth to mechanism. *Nat Rev Mol Cell Biol* 5(10):836–47
98. Hong F, Nguyen VA, Shen X et al (2000) Rapid activation of protein kinase B/Akt has a key role in antiapoptotic signaling during liver regeneration. *Biochem Biophys Res Commun* 279(3):974–9
99. Mullany LK, Nelsen CJ, Hanse EA et al (2007) Akt-mediated liver growth promotes induction of cyclin E through a novel translational mechanism and a p21-mediated cell cycle arrest. *J Biol Chem* 282(29):21244–52
100. Haga S, Ogawa W, Inoue H et al (2005) Compensatory recovery of liver mass by Akt-mediated hepatocellular hypertrophy in liver-specific STAT3-deficient mice. *J Hepatol* 43(5):799–807
101. Murata S, Matsuo R, Ikeda O et al (2008) Platelets promote liver regeneration under conditions of Kupffer cell depletion after hepatectomy in mice. *World J Surg* 32(6):1088–96
102. Jackson LN, Larson SD, Silva SR et al (2008) PI3K/Akt activation is critical for early hepatic regeneration after partial hepatectomy. *Am J Physiol Gastrointest Liver Physiol* 294(6):G1401–10
103. Angulo P (2007) GI epidemiology: nonalcoholic fatty liver disease. *Aliment Pharmacol Therap* 25(8):883–889
104. Rector RS, Thyfault JP, Wei Y et al (2008) Non-alcoholic fatty liver disease and the metabolic syndrome: an update. *World J Gastroenterol* 14(2):185–92

105. Piro S, Spadaro L, Russello M et al (2008) Molecular determinants of insulin resistance, cell apoptosis and lipid accumulation in non-alcoholic steatohepatitis. *Nutr Metab Cardiovasc Dis* 18(8):545–552
106. Samuel VT, Liu Z-X, Qu X et al (2004) Mechanism of Hepatic Insulin Resistance in Non-alcoholic Fatty Liver Disease. *J Biol Chem* 279(31):32345–32353
107. Mendez-Sanchez N, Arrese M, Zamora-Valdes D et al (2007) Current concepts in the pathogenesis of nonalcoholic fatty liver disease. *Liver Int* 27(4):423–33
108. Lupi R, Del Guerra S, Fierabracci V et al (2002) Lipotoxicity in human pancreatic islets and the protective effect of metformin. *Diabetes* 51(Suppl 1):S134–7
109. Joseph JW, Koshkin V, Saleh MC et al (2004) Free fatty acid-induced beta-cell defects are dependent on uncoupling protein 2 expression. *J Biol Chem* 279(49):51049–56
110. Dyntar D, Eppenberger-Eberhardt M, Maedler K et al (2001) Glucose and palmitic acid induce degeneration of myofibrils and modulate apoptosis in rat adult cardiomyocytes. *Diabetes* 50(9):2105–2113
111. Li Z, Berk M, McIntyre TM et al (2008) The lysosomal-mitochondrial axis in free fatty acid-induced hepatic lipotoxicity. *Hepatology* 47(5):1495–503
112. Rhee SG (1999) Redox signaling: hydrogen peroxide as intracellular messenger. *Exp Mol Med* 31(2):53–9
113. Leclercq IA, Da Silva Morais A, Schroyen B et al (2007) Insulin resistance in hepatocytes and sinusoidal liver cells: mechanisms and consequences. *J Hepatol* 47(1):142–56
114. Delibegovic M, Bence KK, Mody N et al (2007) Improved glucose homeostasis in mice with muscle-specific deletion of protein-tyrosine phosphatase 1B. *Mol Cell Biol* 27(21):7727–34
115. Xue B, Kim YB, Lee A et al (2007) Protein-tyrosine phosphatase 1B deficiency reduces insulin resistance and the diabetic phenotype in mice with polygenic insulin resistance. *J Biol Chem* 282(33):23829–40
116. Stiles B, Wang Y, Stahl A et al (2004) Liver-specific deletion of negative regulator Pten results in fatty liver and insulin hypersensitivity [corrected]. *Proc Natl Acad Sci U S A* 101(7):2082–7
117. Vinciguerra M, Sgroi A, Veyrat-Durebex C et al (2009) Unsaturated fatty acids inhibit the expression of tumor suppressor phosphatase and tensin homolog (PTEN) via microRNA-21 up-regulation in hepatocytes. *Hepatology* 49:1176–1184
118. Wang L, Wang WL, Zhang Y et al (2007) Epigenetic and genetic alterations of PTEN in hepatocellular carcinoma. *Hepatol Res* 37(5):389–396
119. Lee SR, Yang KS, Kwon J et al (2002) Reversible inactivation of the tumor suppressor PTEN by H₂O₂. *J Biol Chem* 277(23):20336–42
120. Lee JW, Soung YH, Kim SY et al (2004) PIK3CA gene is frequently mutated in breast carcinomas and hepatocellular carcinomas. *Oncogene* 24(8):1477–1480
121. Tanaka Y, Kanai F, Tada M et al (2006) Absence of PIK3CA hotspot mutations in hepatocellular carcinoma in Japanese patients. *Oncogene* 25(20):2950–2
122. Villanueva A, Chiang DY, Newell P et al (2008) Pivotal role of mTOR signaling in hepatocellular carcinoma. *Gastroenterology* 135(6): 1972–1983, 1983 e1–e11
123. Nakanishi K, Sakamoto M, Yamasaki S et al (2005) Akt phosphorylation is a risk factor for early disease recurrence and poor prognosis in hepatocellular carcinoma. *Cancer* 103(2):307–12
124. Tsang TY, Tang WY, Tsang WP et al (2008) Downregulation of hepatoma-derived growth factor activates the Bad-mediated apoptotic pathway in human cancer cells. *Apoptosis* 13(9):1135–47
125. Cotler S, Hay N, Xie H et al (2008) Immunohistochemical expression of components of the Akt-mTORC1 pathway is associated with hepatocellular carcinoma in patients with chronic liver disease. *Dig Dis Sci* 53(3):844–849
126. Baba HA, Wohlschlaeger J, Cicinnati VR et al (2009) Phosphorylation of p70S6 kinase predicts overall survival in patients with clear margin-resected hepatocellular carcinoma. *Liver Int* 29:399–405
127. Choudhari SR, Khan MA, Harris G et al (2007) Deactivation of Akt and STAT3 signaling promotes apoptosis, inhibits proliferation, and enhances the sensitivity of hepatocellular carcinoma cells to an anticancer agent Atiprimod. *Mol Cancer Ther* 6(1):112–121
128. Porstmann T, Griffiths B, Chung YL et al (2005) PKB/Akt induces transcription of enzymes involved in cholesterol and fatty acid biosynthesis via activation of SREBP. *Oncogene* 24(43):6465–81
129. Yang YA, Morin PJ, Han WF et al (2003) Regulation of fatty acid synthase expression in breast cancer by sterol regulatory element binding protein-1c. *Exp Cell Res* 282(2):132–137
130. Pflug BR, Pecher SM, Brink AW et al (2003) Increased fatty acid synthase expression and activity during progression of prostate cancer in the TRAMP model. *Prostate* 57(3):245–54
131. Kuhajda FP (2000) Fatty-acid synthase and human cancer: new perspectives on its role in tumor biology. *Nutrition* 16(3):202–208
132. Furuta E, Pai SK, Zhan R et al (2008) Fatty acid synthase gene is up-regulated by hypoxia via activation of Akt and sterol regulatory element binding protein-1. *Cancer Res* 68(4):1003–11
133. Rahman MA, Kyriazanos ID, Ono T et al (2002) Impact of PTEN expression on the outcome of hepatitis C virus-positive cirrhotic hepatocellular carcinoma patients: possible relationship with COX II and inducible nitric oxide synthase. *Int J Cancer* 100(2):152–7
134. Street A, Macdonald A, Crowder K et al (2004) The hepatitis C virus NS5A protein activates a phosphoinositide 3-kinase-dependent survival signaling cascade. *J Biol Chem* 279(13):12232–12241
135. Chung YL, Sheuand ML, Yen SH (2003) Hepatitis C virus NS5A as a potential viral Bcl-2 homologue interacts with Bax and inhibits apoptosis in hepatocellular carcinoma. *Int J Cancer* 107(1):65–73
136. Kim KH, Shin H-J, Kim K et al (2007) Hepatitis B virus X protein induces hepatic steatosis via transcriptional activation of SREBP1 and PPAR[γ]. *Gastroenterology* 132(5):1955–1967
137. Choi YH, Kim HI, Seong J et al (2004) Hepatitis B virus X protein modulates peroxisome proliferator-activated receptor [γ] through protein-protein interaction. *FEBS Lett* 557(1–3):73–80

138. Waris G, Felmlee DJ, Negro F et al (2007) Hepatitis C virus induces proteolytic cleavage of sterol regulatory element binding proteins and stimulates their phosphorylation via oxidative stress. *J Virol* 81(15):8122–30
139. Aytug S, Reich D, Sapiro LE et al (2003) Impaired IRS-1/PI3-kinase signaling in patients with HCV: a mechanism for increased prevalence of type 2 diabetes. *Hepatology* 38(6):1384–92
140. Bernsmeier C, Duong FH, Christen V et al (2008) Virus-induced over-expression of protein phosphatase 2A inhibits insulin signalling in chronic hepatitis C. *J Hepatol* 49(3):429–40
141. Boyault S, Rickman DS, de Reynies A et al (2007) Transcriptome classification of HCC is related to gene alterations and to new therapeutic targets. *Hepatology* 45(1):42–52
142. Chung T-W, Lee Y-C, Ko J-H et al (2003) Hepatitis B virus X protein modulates the expression of PTEN by inhibiting the function of p53, a transcriptional activator in liver cells. *Cancer Res* 63(13):3453–3458
143. Kang-Park S, Im JH, Lee JH et al (2006) PTEN modulates hepatitis B virus-X protein induced survival signaling in Chang liver cells. *Virus Res* 122(1–2):53–60

7.2 The Carboxyl Terminal Modulator Protein (CTMP) regulates mitochondrial dynamics

Parcellier A., Tintignac L.A., Zhuravleva E., Dummler B., Brazil D.P., Hynx D., Cron P., Schenk S., Olivieri V., Hemmings B.A. The Carboxyl Terminal Modulator Protein (CTMP) regulates mitochondrial dynamics. PLoS ONE, 2009; 4(5):e5471

The Carboxy-Terminal Modulator Protein (CTMP) Regulates Mitochondrial Dynamics

Arnaud Parcellier¹*, Lionel A. Tintignac¹*, Elena Zhuravleva¹, Bettina Dummler¹, Derek P. Brazil¹*, Debby Hynx¹, Peter Cron¹, Susanne Schenk¹, Vesna Olivieri², Brian A. Hemmings¹*

1 Friedrich Miescher Institute for Biomedical Research, Basel, Switzerland, **2** Interdisciplinary Center of Microscopy, Biozentrum, University of Basel, Basel, Switzerland

Abstract

Background: Mitochondria are central to the metabolism of cells and participate in many regulatory and signaling events. They are looked upon as dynamic tubular networks. We showed recently that the Carboxy-Terminal Modulator Protein (CTMP) is a mitochondrial protein that may be released into the cytosol under apoptotic conditions.

Methodology/Principal Findings: Here we report an unexpected function of CTMP in mitochondrial homeostasis. In this study, both full length CTMP, and a CTMP mutant refractory to N-terminal cleavage and leading to an immature protein promote clustering of spherical mitochondria, suggesting a role for CTMP in the fission process. Indeed, cellular depletion of CTMP led to accumulation of swollen and interconnected mitochondria, without affecting the mitochondrial fusion process. Importantly, *in vivo* results support the relevance of these findings, as mitochondria from livers of adult CTMP knockout mice had a similar phenotype to cells depleted of CTMP.

Conclusions/Significance: Together, these results lead us to propose that CTMP has a major function in mitochondrial dynamics and could be involved in the regulation of mitochondrial functions.

Citation: Parcellier A, Tintignac LA, Zhuravleva E, Dummler B, Brazil DP, et al. (2009) The Carboxy-Terminal Modulator Protein (CTMP) Regulates Mitochondrial Dynamics. PLoS ONE 4(5): e5471. doi:10.1371/journal.pone.0005471

Editor: Rafael Linden, Universidade Federal do Rio de Janeiro (UFRJ), Instituto de Biofísica da UFRJ, Brazil

Received: February 10, 2009; **Accepted:** April 10, 2009; **Published:** May 7, 2009

Copyright: © 2009 Parcellier et al. This is an open-access article distributed under the terms of the Creative Commons Attribution License, which permits unrestricted use, distribution, and reproduction in any medium, provided the original author and source are credited.

Funding: DPB, BD and AP were supported by grants from the Swiss Cancer League. LAT was a long-term EMBO fellowship recipient (#ALTF460). EZ is the recipient of a Swiss Bridge fellowship. The FMI is part of the Novartis Research Foundation. The funders had no role in study design, data collection and analysis, decision to publish, or preparation of the manuscript.

Competing Interests: The authors have declared that no competing interests exist.

* E-mail: brian.hemmings@fmi.ch

† Current address: UCD Diabetes Research Centre, UCD Conway Institute, University College Dublin, Belfield, Dublin, Ireland

‡ These authors contributed equally to this work.

Introduction

Mitochondria are the site of metabolic and survival functions important in organism development, immunity, aging and pathogenesis [1–3]. It is becoming clear that these crucial functions within the cell rely on the integrity of the complex double-membrane mitochondria structure that compartmentalizes vastly different enzymatic activities, mainly involved in oxidative phosphorylation [4], the TCA cycle, gluconeogenesis [5], death signal integration [6,7] and the amplification and transmission of mitochondrial DNA (mtDNA) [8]. Mitochondria within healthy cells are often organized into a dynamic tubular and branched network that undergoes intensive remodeling in response to various stimuli related to cell death [9–11] as well as metabolic and developmental processes [12]. The anti-apoptotic Bcl-2 family member Bcl-xL and the antagonist BH3 only proteins Bak/Bax were shown to regulate mitochondrial shape in healthy cells as well as in cells undergoing apoptosis [13,14]. Thus, the increasing reports of the involvement of signaling proteins in the modulation of mitochondria expose a link between mitochondrial function and dynamics in the regulation of metabolism, cell death, neurotransmission, cell cycle control and development [15].

Studies with yeast led to the identification of the conserved mammalian “mitochondria-shaping” proteins. Profusion proteins, such as the dynamin-related protein mitofusins 1 and 2 (Mfn1 and Mfn2), are integral components of the outer mitochondrial membrane (OMM), essential to mitochondria tethering and fusion [16,17]. These proteins act together with the optic atrophy protein 1 (OPA1), and an inner mitochondrial membrane (IMM) located dynamin-like GTPase mutated in heritable optical atrophy [18]. Conversely, the dynamin-related protein 1 (Drp1/DNM1) is a cytosolic protein, recruitment of which to the OMM by the anchored fission 1 protein (Fis1p/FIS1) adaptor initiates and controls the fission and distribution of mitochondria in cells [19].

Previously, we identified the Carboxy-Terminal Modulator Protein (CTMP) in a two-hybrid search for PKB/Akt binding partners [20]. CTMP has been shown to inhibit PKB/Akt activation at the plasma membrane in response to various stimuli and also to have tumor suppressor-like functions. This notion was strengthened by the observation that primary glioblastomas exhibit downregulation of CTMP mRNA levels due to promoter hypermethylation [21]. We recently reported the mitochondrial localization of endogenous and exogenous CTMP [22]. CTMP exhibits a dual sub-mitochondrial localization as a membrane-

bound pool and a free pool of mature CTMP in the intermembrane space; it was released from the mitochondria into the cytosol early during apoptosis. CTMP overexpression was associated with an increase in mitochondrial membrane depolarization, caspase-3 and polyADP-ribose polymerase (PARP) cleavage. In contrast, CTMP knockdown resulted in a marked reduction in the loss of mitochondrial membrane potential as well as a decrease in caspase-3 and PARP activation. Mutant CTMP retained in the mitochondria lost its capacity to sensitize cells to apoptosis. Thus, proper maturation of CTMP appears essential for its pro-apoptotic function. Finally, we demonstrated that CTMP delayed PKB/Akt phosphorylation following cell death induction, suggesting that CTMP regulates apoptosis via inhibition of PKB/Akt.

Here we show that compromising Carboxy-Terminal Modulator Protein (CTMP) integrity by preventing its N-terminal cleavage by point mutation or by a knockdown approach affected mitochondrial network organization in cells. CTMP depletion did not affect mitochondria intercomplementation but enhanced the interconnected network, suggesting that CTMP positively influences the mitochondrial fission process, arguing for a potential role of CTMP in regulating mitochondrial functions.

Results

A defect in N terminal cleavage of CTMP expression leads to swollen mitochondria

HeLa cells transfected with full-length CTMP GFP-tagged expressed CTMP in the mitochondria (Fig. 1A). Cells expressing high levels of CTMP induced a change in mitochondrial phenotype in some cells, with more rounded shaped mitochondria evident in these cells (Fig. 1A, lower panels). CTMP contains a conserved N-terminal cleavable mitochondrial localization signal (MLS) and is located almost exclusively in mammalian cell mitochondria. CTMP has been found to be strongly associated with the inner mitochondrial membrane or free in the intermembrane space [22]. Most MLS are cleaved by a mitochondrial processing peptidase (MPP) that recognizes a special sequence comprising a positive arginine residue at position -2 and/or -10 from the cleavage site [23,24]. The CTMP sequence displays a highly probable R-2 site at serine 35, surrounded by a hydrophobic residue at $+1$ and a serine at $+2$. A CTMP mutant (m5) in which R34, F36 and S37/38 have been mutated to alanine (Fig. 1B) leads to the expression of a non-mature CTMP that still bears the MLS and that cannot be released to the cytosol after apoptosis induction [22]. Similar to full-length CTMP, we observed that over-expression of a CTMP mutant m5 refractory to N-terminal cleavage promoted the formation of rounded, ball-shaped mitochondria, compared with the tubular structures observed in cells transfected with the wild-type protein (Fig. 1C), or untransfected cells (Fig. S1). It should be noted that CTMP subcellular distribution was not affected by its over-expression. These data led us to hypothesize that CTMP may regulate mitochondrial biogenesis.

Loss of CTMP affects mitochondria morphology

Mitochondrial dynamics is regulated by continuous fusion and fission events. Previous reports indicate that cellular depletion of pro-fission proteins, such as Drp1 or the pro-fusion proteins Mfn-1 and -2, leads to the formation of an interconnected or a fragmented mitochondrial network, respectively [16,17,25]. In contrast, overexpression of Mfn-1 or Mfn-2 produces an imbalance in mitochondrial dynamics in a dose-dependent manner and subsequently the perinuclear clustering of the entire mitochondrial network. The putative involvement of CTMP in

mitochondrial network rearrangement was further investigated by siRNA-mediated depletion of CTMP in HeLa cells. Efficient and reproducible knockdown of CTMP protein was achieved in cells transfected with two independent CTMP siRNAs (Si#1 and Si#2) compared with the mock siRNA (Si-cont) (Fig. 2A).

Cells expressing RFP-labeled mitochondria (mt-RFP) were used to monitor the impact of CTMP depletion on mitochondrial network organization. In these cells, loss of CTMP protein led to a twofold decrease in tubular mitochondrial subpopulation (type II) compared with control cells (Fig. 2B). Although most CTMP-negative cells displayed filamentous mitochondria, detailed confocal examination showed the accumulation of a mixed network of interconnected swollen and thick mitochondria (Fig. 2C; type I Si-CTMP#1 and #2) compared with the Si-cont transfected cells (Fig. 2C; type I Si-cont). To further explore the correlation between CTMP protein depletion and mitochondria remodeling at the single-cell level, tetracycline repressor-expressing HeLa cells were stably transfected with sh-RNA specifically targeting CTMP (CTMP-Sh; targeting a sequence distinct from the previously described Si#1 and Si#2) or control sh-RNA (Fig. 3A). We confirmed that organization of the mitochondrial network in CTMP-depleted cells was similar to the previously observed network (Fig. 3B). The population of cells exhibiting a swollen interconnected mitochondrial network was evident 3 days after tetracycline treatment (Fig. 3C). Combined, these results strongly suggest that the modulation of CTMP protein levels and maturation affect mitochondrial shape.

CTMP depletion does not impair mitochondrial fusion

To determine whether loss of CTMP function affected mitochondrial fusion or fission, an intermitochondrial complementation assay was carried out using CTMP-depleted cells [26,27]. Forty-eight hours after transfection with CTMP siRNA (Si#1, Si#2) or the siRNA control (Si-cont), HeLa cells carrying labeled mitochondria (mt-GFP and mt-RFP) were mixed in equal proportions and fused by addition of PEG 1500. Heterokaryons were fixed at the indicated times and mitochondrial fusion kinetics assessed by examination using confocal microscopy of the yellow fluorescence resulting from the mixing of matrix-targeted GFP and RFP mitochondria (Fig. 4A). CTMP-depleted cells completed mitochondria fusion with kinetics comparable to those of control cells (Fig. 4B). These data suggested that CTMP is not critical for the mitochondrial fusion process and further supports the conclusion that the effects of CTMP depletion result from an altered fission process.

CTMP deletion reveals an extensively interconnected mitochondrial network in mouse liver

We next examined the effect of CTMP deletion on mitochondrial shape at the whole organism level. CTMP knockout mice generated in our lab were viable and fertile and showed no obvious phenotype. A summary of the knockout strategy is given in Fig. 5A, B. We further validated the mitochondrial localization of CTMP in mouse tissue. Immunodetection of CTMP protein in wild-type (WT), heterozygous and homozygous knockout mice showed a correlation between loss of CTMP protein and CTMP allele disruption (data not shown). Mitochondria from WT and CTMP knockout ($-/-$) mouse livers were purified by differential and density gradient centrifugation (Fig. 5C, left panel). Immunoblot analysis of the collected fractions demonstrated the purity of the mitochondria (cytochrome c and mHsp70) and the absence of cytosolic contaminants (actin). As expected, CTMP immunodetection showed that mouse CTMP protein co-purified with the mitochondrial fraction, as confirmed by the loss of a signal in

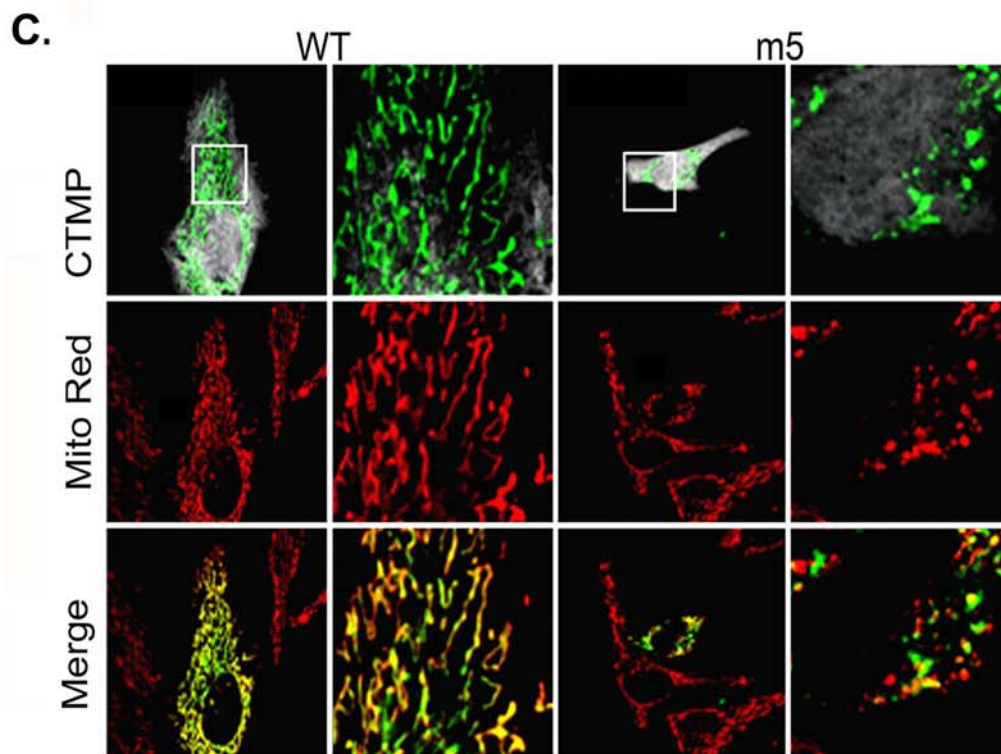
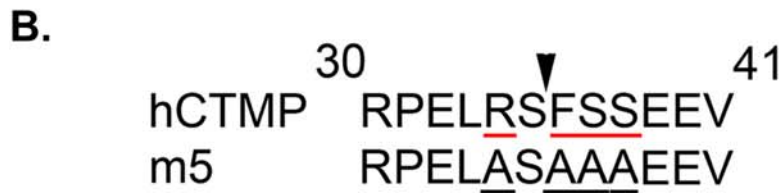
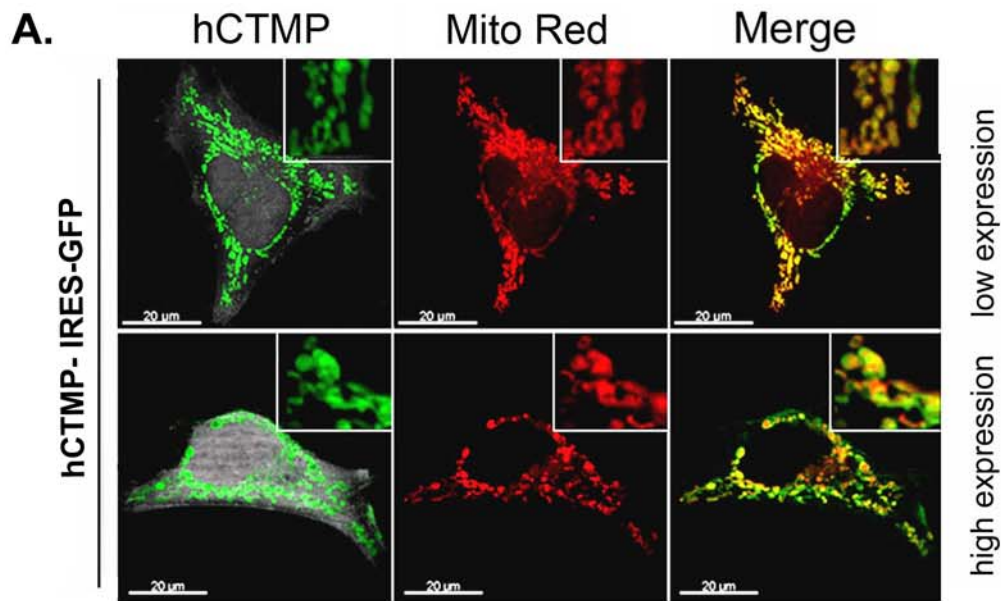


Figure 1. Interfering with CTMP maturation leads to swollen mitochondria. (A) Full length human CTMP tagged with GFP was transfected into HeLa cells at low (upper panels) or high (lower panels) levels of expression. Mitochondria were visualized with Mitotracker Red. Merged fluorescence indicates CTMP-GFP expression in mitochondria. The round appearance of mitochondria is visible in cells with high levels of CTMP

expression (lower panels). (B) Amino acid sequence of the R-2 predicted MPP cleavage site (indicated by the arrow) in human CTMP and a CTMP mutant (m5) in which R34, F36 and S37/38 have been mutated to alanine. (C) Twenty-four hours after transfection with CTMP-IRES-GFP or the m5 point mutant, HeLa cells were fixed and stained for CTMP and mitochondria as indicated. A detail of the squared area is shown in the right panel. Representative confocal pictures of three independent experiments are shown.
doi:10.1371/journal.pone.0005471.g001

samples from CTMP knockout mice (Fig. 5C). Electron microscopy of thin liver sections from WT and CTMP knockout mice revealed a correlation between the ablation of CTMP and the appearance of elongated mitochondria (Fig. 5D lower panels), compared with the round and compact mitochondria in the liver of wild-type animals (Fig. 5D upper panels). Accordingly, mitochondria were found to be elongated in hepatocytes isolated from CTMP knockout mice ($-/-$), compared with round and compact mitochondria observed in hepatocytes of wild-type animals (Fig. S2). Interestingly, loss of CTMP did not interfere with mitochondria biogenesis, since the number of mitochondrial DNA copies measured by real time PCR was the same in brown adipose tissue (Fig. S3A) and in hepatocytes (Fig. S3B) from both WT and knockout animals ($-/-$). Taken together, these results demonstrate that depletion of CTMP protein impairs mitochondria shape and structure both *in vitro* and *in vivo*.

Discussion

We provide here the first evidence that CTMP, previously reported to be an inhibitor of PKB/Akt [20], is involved in the modulation of mitochondria homeostasis. We have shown that interference with CTMP expression and/or protein maturation

critically affected mitochondria morphology. Loss of cellular CTMP expression led to the establishment of an interconnected mitochondrial network in 40% of cells without affecting cell viability (data not shown). Furthermore, CTMP knockdown appeared to have a second long-term effect leading to the accumulation of swollen mitochondria, either interconnected or tubular. Importantly, such a phenotype has been reported previously in cells depleted for proteins involved in the regulation of the mitochondrial fission process, such as Drp1 or the recently identified Drp1-binding protein MARCH-5 [14,28]. Mitochondria from CTMP knockdown cells efficiently fuse *in vitro*, suggesting that the observed phenotype, presumably caused by imbalanced fusion/fission, does not result from a dysfunction in mitochondrial fusion. Indeed, we provide evidence that CTMP function in mitochondria is tightly linked to its submitochondrial distribution, where it is found in both soluble and membrane-bound mitochondrial fractions [22]. Expression of a non-cleavable mutant of CTMP (refractory to mitochondrial membrane peptidase cleavage) in HeLa cells promoted dissociation of the mitochondrial network into individual round-shaped, dilated mitochondria.

We recently reported that CTMP is released early from mitochondria into the cytosol upon apoptosis and we demonstrat-

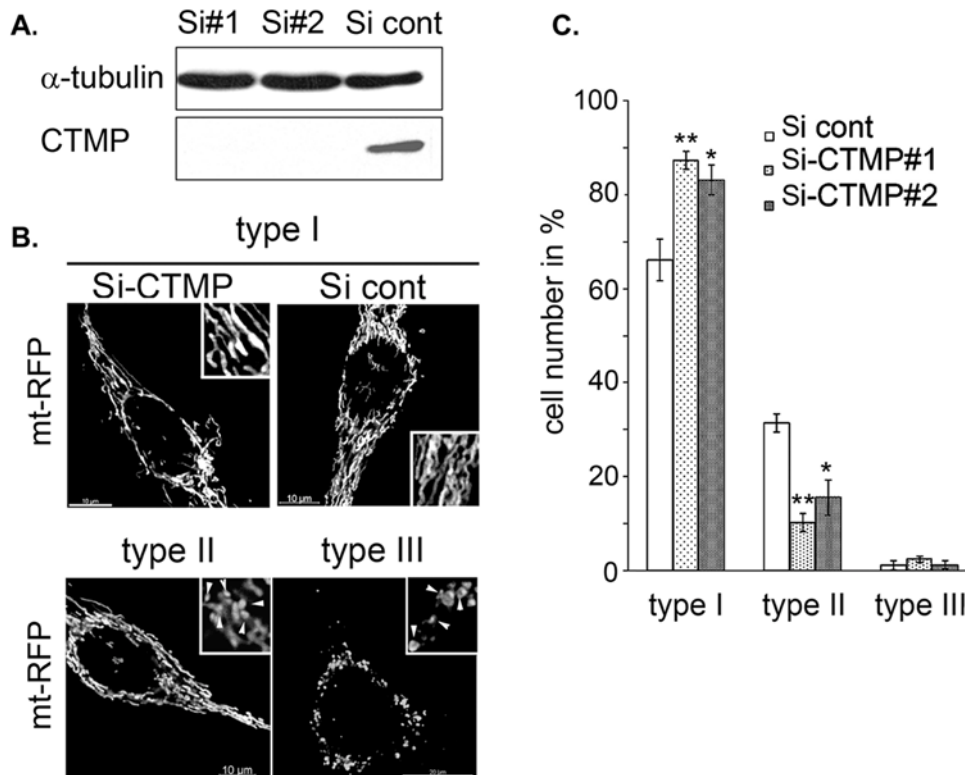


Figure 2. Loss of CTMP affects mitochondria morphology. (A) Immunoblot detection of CTMP using 75 μ g of protein lysates extracted from HeLa cells 48 h after transfection with control SiRNA (cont) or CTMP SiRNA#1 or #2. (B) Representative confocal picture of mitochondria shape in HeLa cells expressing mt-RFP and treated as in (A). (C) Morphological analysis of mitochondria shape in HeLa cells treated as in (A). For each experiment, at least 200 cells were counted in three distinct fields. Data are means \pm SEM, n=2. The differences in mean values are statistically significant (Si cont compared to Si-CTMP#1 and Si-CTMP#2) as determined by 1-way ANOVA; * P \leq 0.05, ** P \leq 0.001.
doi:10.1371/journal.pone.0005471.g002

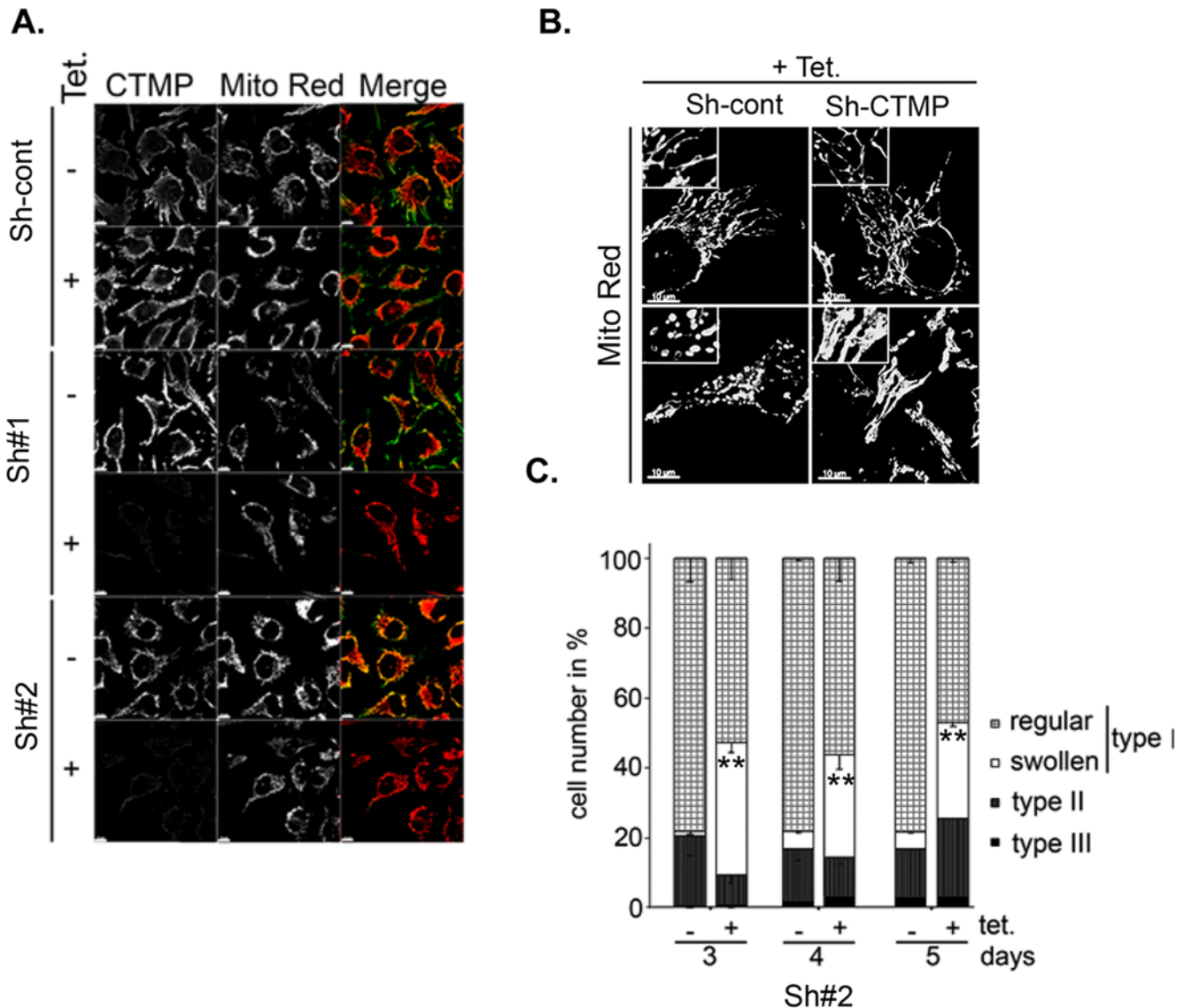


Figure 3. CTMP expression affects mitochondrial network organization. (A) Confocal microscopy of CTMP expression in tetracycline inducible HeLa clones stably expressing pTer plasmid coding for a control short hairpin (Sh-cont) or a short hairpin directed against CTMP (Sh#1 and Sh#2). Cells were visualized by immunofluorescence after 5 days culture in the presence or absence of tetracycline (2 μ g/mL), together with the MitoTracker Red. (B) Representative confocal pictures of mitochondrial shape in tetracycline-inducible HeLa clones cultured 5 days in the presence of tetracycline. Mitochondria were visualized with MitoTracker Red. (C) Morphological analysis of mitochondria shape in HeLa Tet-on clones treated as in (A) for 3, 4 or 5 days. For each experiment, at least 200 cells were counted in three distinct fields. Data are means \pm SEM, $n = 2$. The differences in mean values are statistically significant (Sh#2 minus tetracycline compared to Sh#2 plus tetracycline) as determined by 1-way ANOVA; ** $P \leq 0.001$. doi:10.1371/journal.pone.0005471.g003

ed that CTMP overexpression is associated with an increase in mitochondrial membrane depolarization and the activation of apoptotic markers such as caspase-3 and PARP. Furthermore, we observed that CTMP depletion or a defect in CTMP maturation leads to inhibition of apoptosis. We suggested that CTMP regulates apoptosis via PKB/Akt inhibition since we detected a delay in PKB/Akt phosphorylation in cells overexpressing CTMP in which apoptosis was induced [22]. Similarly, other recent reports suggest that the regulation of OPA1 relies on the activity of a presenilin-associated rhomboid-like protein (PARL), a protease that regulates OPA1 release into the inner mitochondrial space [29]. Furthermore, Cipolat et al. [30] suggested that the loss of this soluble OPA1 species in PARL $^{-/-}$ cells is responsible for their

extreme sensitivity to apoptotic stimuli. They further proposed a complex mechanism by which both soluble and inner mitochondrial membrane-anchored OPA1 regulates the tight closure of the mitochondria cristae, preventing massive release of cytochrome c into the inter-mitochondrial space.

Taken together, these observations lead us to hypothesize that accumulation of a premature form of CTMP in the inner mitochondrial membrane (due to inhibition of mitochondrial membrane peptidase cleavage) may be responsible for the observed mitochondrial phenotype. Moreover, *in vitro* characterization of the molecular mechanisms regulating inner mitochondrial membrane dynamics are as yet poorly understood. Surprisingly, a subtle abnormal mitochondrial phenotype in the

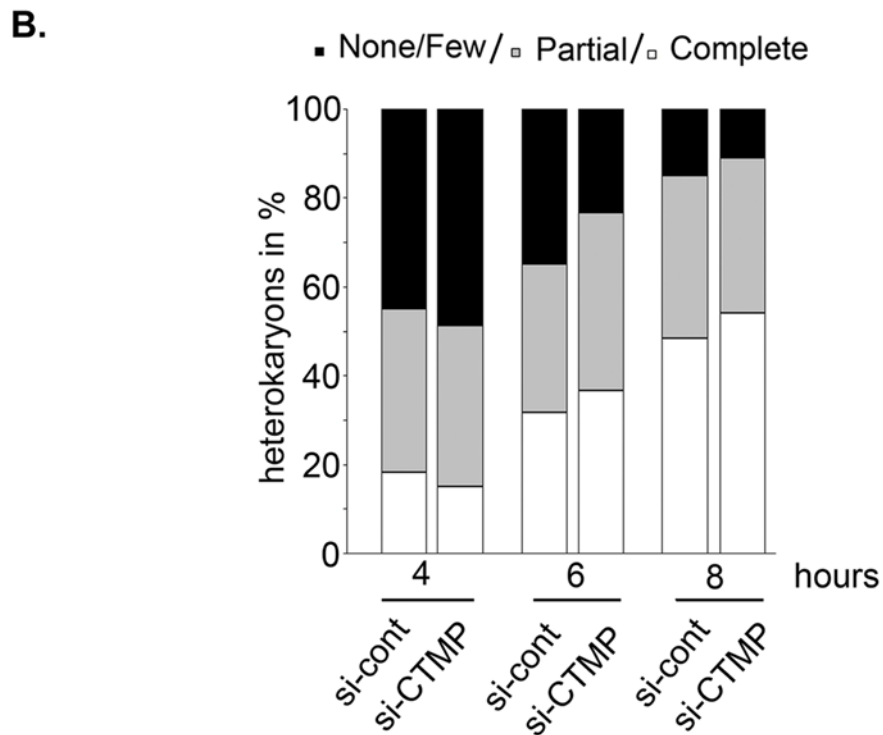
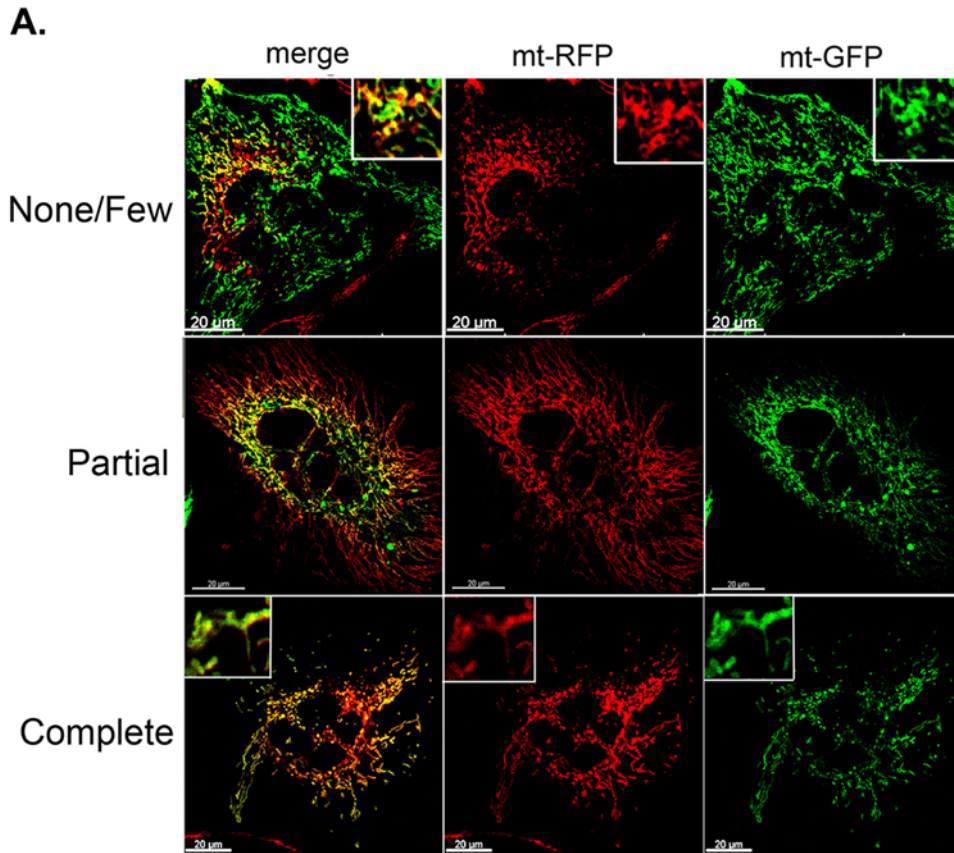


Figure 4. CTMP is not required for mitochondrial fusion. (A) HeLa cells expressing mt-RFP and mt-GFP transfected with either siRNA#1 and #2 against CTMP or the siRNA control were fused in 50% PEG1500 for 60 s, washed and fixed at different times (4, 6 and 8 h). (B) Time-course of mitochondrial fusion in HeLa cells treated as in (A). Mitochondrial fusion was measured from 30 randomly selected polykaryons and classified as described in (A), $n=2$.

doi:10.1371/journal.pone.0005471.g004

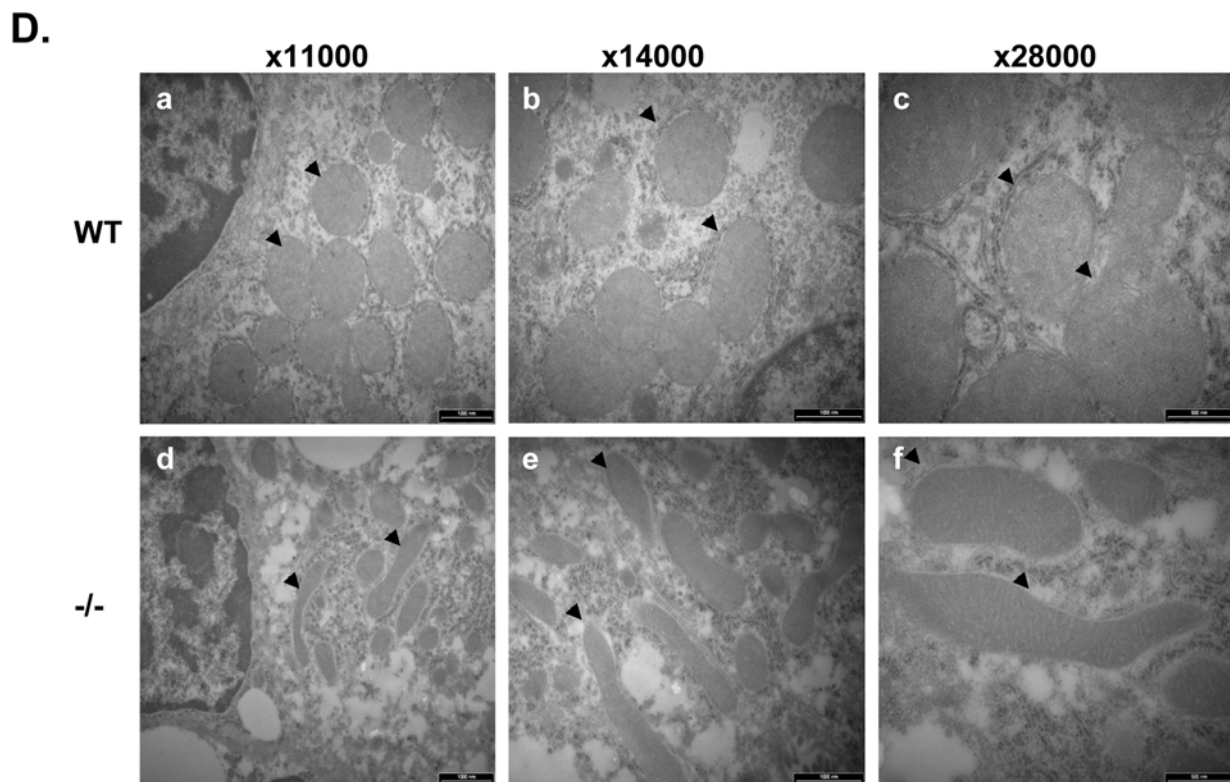
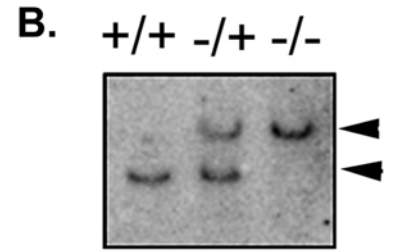
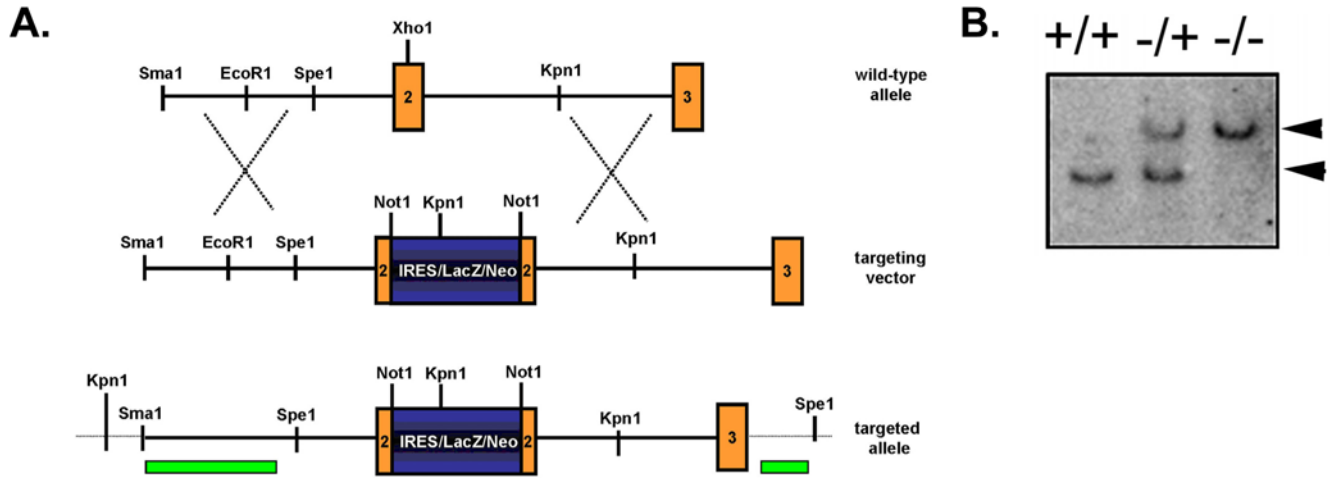


Figure 5. The mitochondrial network is extensively interconnected in CTMP knockout mice liver. (A) Summary of the knockout strategy used to generate CTMP knockout mice. (B) Genotyping of CTMP $+/+$ (wild-type), $+/-$ (heterozygous) and $-/-$ (knockout) mice. Genomic DNA was digested using Spe1 and probed using a CTMP cDNA fragment. A wild-type band (9 kb, lower band) and a CTMP knockout band (14 kb, upper band) are indicated. (C) Summary of the mitochondria purification strategy outlined in Materials and Methods (left panel). Percoll gradient-isolated liver mitochondria from wild-type (WT) or CTMP knockout ($-/-$) mice were separated by SDS-PAGE and immunoblotted for α -actin, mHsp70, cytochrome c and CTMP (right panel). (D) Representative electron micrographs of liver mitochondria ultrastructure in (top) wild-type and (bottom) CTMP knockout mice. Arrows indicate normal liver mitochondria (top) and elongated mitochondria (bottom). Representative images of mitochondria shape from different experiments (blind) are shown at different magnifications ($\times 11,000$, $\times 14,000$, $\times 28,000$). doi:10.1371/journal.pone.0005471.g005

brain tissue of PKB/Akt knockout mice has been reported recently [31]. These animals display fewer and larger mitochondrial structures, and the authors suggest that PKB/Akt plays a significant role in mitochondrial biogenesis. In addition, PKB/Akt has been shown to translocate to the outer mitochondrial membrane, following plasma membrane activation [32–34]. Although the biological significance of the translocation of active PKB/Akt to the mitochondria is not yet clear, it has been reported to be cell-type and stimulus-specific [35,36]. Thus, CTMP may modulate PKB/Akt activity in a specific subcellular compartment, e.g. the mitochondria or the cytosol, depending on the nature of the stimulus (survival or apoptosis). Further investigation is needed to integrate the direct and/or indirect modulation of PKB/Akt activity in this model and more experiments will be required to address the biological activity of CTMP.

Striking similarities exist between the mitochondria network rearrangement observed in CTMP knockdown cells and those already reported in cells knocked down for the Drp1 fission protein or cells missing a functional OPA1 protein [14,29]. Nonetheless, the loss of electron absorbance observed in CTMP knockout mice liver mitochondria further supports the involvement of CTMP in the maintenance of inner mitochondrial membrane integrity. Thus, the phenotype observed following CTMP depletion with respect to mitochondrial network rearrangements is less penetrant than those already reported for the key mitochondria-shaping proteins. Moreover, CTMP protein depletion did not affect HeLa cell growth or mitochondrial transmembrane potential measured *in vitro* (data not shown). Most interestingly, it has been shown that CTMP interacts with LETM1, another mitochondrial protein involved in mitochondrial morphology [37]. LETM1 is located in the inner membrane of mitochondria and oligomerized in higher molecular weight complexes [38]. LETM1 has been found to be deleted in Wolf-Hirschhorn syndrome (WHS), a complex congenital syndrome characterized by microcephaly, growth and mental retardation, seizures, epilepsy and other associated symptoms [39,40]. LETM1 is considered as playing a major role in the pathogenesis of seizures. The function of LETM1 in apoptosis, mitochondrial homeostasis and mitochondrial dynamics is well documented, although the different reports drew different conclusions [37,38,41]. Thus, it will be very exciting to further investigate the interplay between CTMP and LETM1 in regulating mitochondrial dynamics and functions in future studies. In particular, it would be of interest to explore the phenotype of CTMP knockout mice in the context of Wolf-Hirschhorn syndrome.

It is plausible that CTMP mediates its effect by modulating the activity of the key regulators of mitochondrial dynamics and further experiments should address the biological mechanism by which CTMP regulates mitochondrial functions. We have demonstrated already that CTMP exhibits a dual submitochondrial localization. Therefore, the tight association between CTMP protein integrity and maintenance of mitochondria shape observed in this study provides a novel opportunity to investigate the mitochondrial function of CTMP in metabolic regulation.

Materials and Methods

Cloning and plasmids construction

All CTMP untagged plasmids used in this study were constructed following PCR amplification of hCTMP cDNA [20] and inserted into the *Bam*HI and *Eco*RI sites of the pcDNA4-IRES-GFP plasmid [42]. CTMP point mutant (m5) was generated by site-directed mutagenesis. To C-terminally tag the CTMP protein, the pcDNA3.1-Myc-RFP plasmid was constructed by subcloning the mRFP1 (monomeric Red Fluorescent Protein 1) cDNA [43] into the *Kpn*I and *Eco*RV sites of the hygromycin resistant vector pcDNA3.1-Myc. The following sequences encoded the CTMP-SiRNA#1 5'-UCGUCAUGACUGCCAAUCU-3' 5'-AGAUUGGCAGUCAUGACGA-3' and CTMP Si-RNA#2 5'-CCCAUUUCUUGA-CCCAAA-3', 5'-UUUGGGUCAAG AAAAUGGG-3' used in this study. The control SiRNAs were directed against the fluorescein protein 5'-UUCUCCGAACGUGUCACGU-3' and 5'-ACGUGA-CACGU UCGGAGAA-3' (Quiagen). To stably induce expression of short hairpins in cells, the CTMP-specific tandem sequences 5'-GATCCCAAGACCCTATACTCAGA GGCGTTCAAGAGAC-GCCTCTGAGTAGGGTCTTTTTGGAAA-3' and 5'-AGCT-TTT CCAAAAAGACCCTACTCAGAGGCGTCTCTTGAAC-GCCTCTGAGT ATGGG TCGG-3' were cloned in the *Bgl*II/*Hind*III sites of pTer vector [44]. The pTer control construct (cont-Sh) used was directed against luciferase as previously described [45] or a scramble sequence 5'-GATCCCA GAGACAGCTACCAAGACTTCAAGAGAGTCCCTGGTAGCTGTCTCTTTTTTTGGAAA 3' and 5'-AGCTTTTTCCAAAAAAGAGACAGCTAC-CAAGGACTCTCTTGAAGTCCTTGGTAG CTG TCT CTGG3'. All construct sequences were confirmed using an ABI PRISM 3700 DNA Analyzer (Applied Biosystems).

Antibodies

CTMP monoclonal antibodies were generated by repeated immunization of BALB/c mice with 50–100 μ g of purified full-length His-CTMP protein (produced in *E. coli*), using Stimune (Prionics AG, Schlieren Switzerland) as an adjuvant. Two months after the priming injection, splenic lymphocytes cells were fused with P3AG8.653 myeloma cell line (ATCC) and cultured according to standard procedures. After ELISA screening of hybridomas clone supernatants, epitope mapping was carried out for the clone used in this study (52F11) using the GST-CTMP deletion mutant and synthetic polypeptides. The monoclonal anti-CTMP antibody characterized is IgG1. Anti- α -tubulin (YL 1/2) antibody was used as hybridoma supernatants. The commercial mouse anti-mHsp70 (JG1) was from Affinity BioReagents, mouse anti-cytochrome c was from R&D System and rat α -actin was from Santa Cruz Biotechnology.

Transient and stable transfections

HeLa cells were grown in Dulbecco's Medium (Gibco) supplemented with 10% fetal calf serum. HeLa cell lines stably expressing the tetracycline repressor (HeLa Tet-on) and/or mitochondria-labeled cells (mt-GFP, mt-RFP) were cultured in

medium supplemented with 100 ng/mL and 0.4 mg/mL G418 (Sigma), respectively. For transfection, cells were plated in 6-well plates or 10-cm dishes and transfected the following day at 60% confluence using Lipofectamine 2000 following the manufacturer's instruction (Invitrogen). Small inhibitory RNA delivery was achieved with Oligofectamine (Invitrogen). Stable clones expressing CTMP short hairpins or negative controls were selected 48 h after transfection by addition of 0.8 mg/mL Zeocin and positive clones were further maintained in 0.4 mg/mL Zeocin.

Protein extraction and mitochondria isolation

For whole cell extracts, cells were washed in 1× PBS and resuspended in lysis buffer (50 mM Tris [pH 7.4], 150 mM NaCl, 10% glycerol, 0.5% NP40, 0.5 mM Na-orthovanadate, 50 mM NaF, 80 mM β-glycerophosphate, 10 mM Na-pyrophosphate, 1 mM dithiothreitol, 1 mM EGTA, 10 μg leupeptin/ml and 10 μg aprotinin/ml). Mitochondria isolation was carried out as previously described [41]. Briefly, cells were washed twice in 100 mM sucrose, 1 mM ethylene glycol-bis(β-aminoethyl ether)-tetraacetic acid (EGTA), 20 mM 3-(N-morpholino) propanesulfonic acid (MOPS), pH 7.4 and 1 mg/mL BSA. The pellet was resuspended in the same buffer solution supplemented with 10 mM triethanolamine, 5% (v/v) Percoll, 0.1 mg/mL digitonin for 3 min at 4°C and homogenized with a Potter homogenizer (10 strokes, 1'000 rpm) before being diluted 1/5 in 300 mM sucrose, 1 mM EGTA, 20 mM MOPS, pH 7.4 and 1 mg/mL BSA, and centrifuged at 2'500 *g* for 5 min at 4°C. The supernatant containing mitochondria was collected and centrifuged at 10'000 *g* for 10 min at 4°C to collect mitochondria as a pellet. Isolated mitochondria were washed twice in the same conditions before being resuspended and further processed.

Western-blotting

For Western blot analysis, protein lysates were prepared by homogenization of various organs in lysis buffer (50 mM Tris-HCl, pH 8.0, 120 mM NaCl, 1% NP-40, 40 mM β-glycerophosphate, 10% glycerol, 4 μM leupeptin, 0.05 mM phenylmethylsulfonyl fluoride, 1 mM benzamidine, 50 mM NaF, 1 mM Na₃VO₄, 5 mM EDTA, 1 μM Microcystin LR). Homogenates were centrifuged twice (13'000 rpm for 10 min at 4°C) to remove cell debris. Protein concentrations were determined using the Bradford assay. Proteins were separated by 12% or 10% sodium dodecyl sulfate-polyacrylamide gel electrophoresis and then transferred to Immobilon-P polyvinylidene difluoride membranes (Millipore).

Immunostaining

For immunostaining, cells were grown on coverslips for 24 h following transfection with different plasmids or siRNAs. Where mitochondria were visualized by MitoTracker Red, cells were treated with 300 nM MitoTracker Red CMXRos for 15 min before being washed in PBS and fixed in 3% paraformaldehyde/2% sucrose. Cells were further permeabilized using 0.2% Triton ×100 (3 min at room temperature) before being washed in PBS and incubated together with an appropriate dilution of the primary antibody for 1 h at room temperature in 1% BSA/1% goat serum. This was followed by incubation with secondary antibodies at 1:100 for 45 min at room temperature. After a final washing, coverslips were mounted in Vectashield medium (Vector lab) and visualized on a laser scanning microscope (Olympus FV500). Confocal images were processed using the Imaris program (Bitplane AG, Zürich, Switzerland) and Photoshop 6.0 (Adobe System Inc).

Mitochondria intercomplementation

HeLa cells carrying different fluorescent mitochondria (mt-RFP or mt-GFP) were mixed 1/1 and plated on coverslips 24 h after transfection. Mt-GFP HeLa cells were pre-treated for 20 h with 1 mM trichostatin to increase GFP expression levels. After washes in FCS-free DMEM, droplets of 50% PEG 1500 were added directly to cells and aspirated after 45–60 s. After several washes, cells were collected and fixed at the indicated times and processed for immunofluorescence. Heterokaryons were visualized by DNA staining of the nucleus (To-Pro-3 iodide) and/or α-tubulin staining.

Generation of CTMP knockout mice

For the generation of CTMP mutant mice, a mouse genomic DNA fragment containing exons 2 and 3 was cloned into the pBluescript vector and a *NotI* site was generated in exon 2. A ~5-kb IRES-lacZ-Neo cassette was inserted into the *NotI* site, which introduced a translational frame shift. The targeting vector was linearized and electroporated into 129/Ola ES cells. ES cell clones were screened by Southern blotting. DNA was digested with *SpeI* and probed with an external probe. An internal probe was then used on *KpnI*-digested DNA for further characterization of ES cell clones that were positive for homologous recombination. Correctly targeted ES cells were used to generate chimeras. Male chimeras were mated with wild-type C57BL/6 females to obtain CTMP+/- mice, which were intercrossed to produce CTMP homozygous mutants. Progeny were genotyped for the presence of a targeted allele by multiplex PCR.

Liver mitochondria isolation

All steps were carried out at 4°C. Mice were housed and terminated according to Swiss legislation. Following termination, freshly dissected liver tissues were immersed and extracted in MSH buffer (pH 7.3) (5 mM HEPES, 70 mM sucrose, 210 mM mannitol, supplemented with 1 mM EDTA), before homogenization in a glass homogenizer (at 500 rpm) in MSH Buffer (supplemented with anti-proteases inhibitors) and centrifugation for 10 min at 800 *g*. The fat coat was removed after centrifugation (10,000 *g* for 10 min at 4°C) and the pellet was manually resuspended in 80 ml of mitochondrial isolation buffer (MSH buffer: 36 μl/ml aprotinin, 5 μl/ml PMSF, 1 μl/ml leupeptin). A crude mitochondrial pellet was isolated by differential centrifugation (3,000 *g*, 10,000 *g* and 9,000 *g*) before being layered on top of a 20-mL Percoll solution (39.3 ml of Percoll, 73.5 ml of 10 mM HEPES, and 13.2 ml of 2.5 M sucrose) and centrifuged at 26,000 rpm for 45 min at 4°C. A pure mitochondria layer was collected below the peroxisome layer and washed twice in mitochondrial isolation buffer before being submitted to protein quantification.

Transmission electron microscopy

Samples were collected from the same regions of liver (left lobe and median lobe neighboring the gallbladder) for both wild-type [2 females (27,5 and 42 weeks old) and 1 male (42 weeks old)] and CTMP knockout mice [2 females (27,5 and 42 weeks old) and 1 male (42 weeks old)] and immediately fixed for 1 h in 3% paraformaldehyde and 0.5% glutaraldehyde in PBS buffer (pH 7.4), washed twice in PBS and post-fixed for 1 h in 1% osmium tetroxide (OSO₄). After dehydration with a graded ethanol series (50–100%) and infiltration in 100% acetone, samples were embedded using an Epoxy-Embedding kit (Epon, FLUKA) for 24 h at 60°C. Thin sections (60–70nm) were obtained on Ultracut (Reichert-Jung) and analyzed on a TEM Moragni 268D (Philips) at 80 kV.

Supporting Information

Figure S1

Found at: doi:10.1371/journal.pone.0005471.s001 (2.26 MB TIF)

Figure S2

Found at: doi:10.1371/journal.pone.0005471.s002 (3.10 MB TIF)

Figure S3

Found at: doi:10.1371/journal.pone.0005471.s003 (1.17 MB TIF)

Supplementary Text S1

Found at: doi:10.1371/journal.pone.0005471.s004 (0.03 MB DOC)

References

- Balaban RS, Nemoto S, Finkel T (2005) Mitochondria, oxidants, and aging. *Cell* 120: 483–495.
- Green DR, Kroemer G (2004) The pathophysiology of mitochondrial cell death. *Science* 305: 626–629.
- McWhirter SM, Tenover BR, Maniatis T (2005) Connecting mitochondria and innate immunity. *Cell* 122: 645–647.
- Smeitink JA, Zeviani M, Turnbull DM, Jacobs HT (2006) Mitochondrial medicine: a metabolic perspective on the pathology of oxidative phosphorylation disorders. *Cell Metab* 3: 9–13.
- McBride HM, Neuspil M, Wasiak S (2006) Mitochondria: more than just a powerhouse. *Curr Biol* 16: R551–560.
- Green DR (2005) Apoptotic pathways: ten minutes to dead. *Cell* 121: 671–674.
- Parcellier A, Tintignac LA, Zhuravleva E, Hemmings BA (2008) PKB and the mitochondria: AKTing on apoptosis. *Cell Signal* 20: 21–30.
- Brandon M, Baldi P, Wallace DC (2006) Mitochondrial mutations in cancer. *Oncogene* 25: 4647–4662.
- Cereghetti GM, Scorrano L (2006) The many shapes of mitochondrial death. *Oncogene* 25: 4717–4724.
- Youle RJ (2005) Morphology of mitochondria during apoptosis: worms-to-beetles in worms. *Dev Cell* 8: 298–299.
- Youle RJ, Karbowski M (2005) Mitochondrial fission in apoptosis. *Nat Rev Mol Cell Biol* 6: 657–663.
- Detmer SA, Chan DC (2007) Functions and dysfunctions of mitochondrial dynamics. *Nat Rev Mol Cell Biol* 8: 870–879.
- Delivani P, Adrain C, Taylor RC, Duriez PJ, Martin SJ (2006) Role for CED-9 and Egl-1 as regulators of mitochondrial fission and fusion dynamics. *Mol Cell* 21: 761–773.
- Jagasia R, Grote P, Westermann B, Conradt B (2005) DRP-1-mediated mitochondrial fragmentation during EGL-1-induced cell death in *C. elegans*. *Nature* 433: 754–760.
- Chan DC (2006) Mitochondria: dynamic organelles in disease, aging, and development. *Cell* 125: 1241–1252.
- Chen H, Detmer SA, Ewald AJ, Griffin EE, Fraser SE, et al. (2003) Mitofusins Mfn1 and Mfn2 coordinately regulate mitochondrial fusion and are essential for embryonic development. *J Cell Biol* 160: 189–200.
- Rojo M, Legros F, Chateau D, Lombes A (2002) Membrane topology and mitochondrial targeting of mitofusins, ubiquitous mammalian homologs of the transmembrane GTPase Fzo. *J Cell Sci* 115: 1663–1674.
- Delettre C, Lenaers G, Griffioen JM, Gigarel N, Lorenzo C, et al. (2000) Nuclear gene OPA1, encoding a mitochondrial dynamin-related protein, is mutated in dominant optic atrophy. *Nat Genet* 26: 207–210.
- Smirnova E, Shurland DL, Ryazantsev SN, van der Bliek AM (1998) A human dynamin-related protein controls the distribution of mitochondria. *J Cell Biol* 143: 351–358.
- Maira SM, Galetic I, Brazil DP, Kaech S, Ingley E, et al. (2001) Carboxyl-terminal modulator protein (CTMP), a negative regulator of PKB/Akt and v-Akt at the plasma membrane. *Science* 294: 374–380.
- Knobbe CB, Reifemberger J, Blaschke B, Reifemberger G (2004) Hypermethylation and transcriptional downregulation of the carboxyl-terminal modulator protein gene in glioblastomas. *J Natl Cancer Inst* 96: 483–486.
- Parcellier A, Tintignac LA, Zhuravleva E, Cron P, Schenk S, et al. (2009) Carboxy-Terminal Modulator Protein (CTMP) is a mitochondrial protein that sensitizes cells to apoptosis. *Cell Signal*.
- Gakh O, Cavadini P, Isaya G (2002) Mitochondrial processing peptidases. *Biochim Biophys Acta* 1592: 63–77.
- Taylor AB, Smith BS, Kitada S, Kojima K, Miyaura H, et al. (2001) Crystal structures of mitochondrial processing peptidase reveal the mode for specific cleavage of import signal sequences. *Structure* 9: 615–625.
- Ishihara N, Jofuku A, Eura Y, Mihara K (2003) Regulation of mitochondrial morphology by membrane potential, and DRP1-dependent division and FZO1-dependent fusion reaction in mammalian cells. *Biochem Biophys Res Commun* 301: 891–898.
- Legros F, Lombes A, Frachon P, Rojo M (2002) Mitochondrial fusion in human cells is efficient, requires the inner membrane potential, and is mediated by mitofusins. *Mol Biol Cell* 13: 4343–4354.
- Mattenberger Y, James DI, Martinou JC (2003) Fusion of mitochondria in mammalian cells is dependent on the mitochondrial inner membrane potential and independent of microtubules or actin. *FEBS Lett* 538: 53–59.
- Nakamura N, Kimura Y, Tokuda M, Honda S, Hirose S (2006) MARCH-V is a novel mitofusin 2- and Drp1-binding protein able to change mitochondrial morphology. *EMBO Rep* 7: 1019–1022.
- Frezza C, Cipolat S, Martins de Brito O, Micaroni M, Beznoussenko GV, et al. (2006) OPA1 controls apoptotic cristae remodeling independently from mitochondrial fusion. *Cell* 126: 177–189.
- Cipolat S, Rudka T, Hartmann D, Costa V, Sernec L, et al. (2006) Mitochondrial rhomboid PARL regulates cytochrome c release during apoptosis via OPA1-dependent cristae remodeling. *Cell* 126: 163–175.
- Wright GL, Maroulakou IG, Eldridge J, Liby TL, Sridharan V, et al. (2008) VEGF stimulation of mitochondrial biogenesis: requirement of AKT3 kinase. *Faseb J* 22: 3264–3275.
- Andjelkovic M, Alessi DR, Meier R, Fernandez A, Lamb NJ, et al. (1997) Role of translocation in the activation and function of protein kinase B. *J Biol Chem* 272: 31515–31524.
- Kunkel MT, Ni Q, Tsien RY, Zhang J, Newton AC (2005) Spatio-temporal dynamics of protein kinase B/Akt signaling revealed by a genetically encoded fluorescent reporter. *J Biol Chem* 280: 5581–5587.
- Sasaki K, Sato M, Umezawa Y (2003) Fluorescent indicators for Akt/protein kinase B and dynamics of Akt activity visualized in living cells. *J Biol Chem* 278: 30945–30951.
- Ahmad N, Wang Y, Haider KH, Wang B, Pasha Z, et al. (2006) Cardiac protection by mitoKATP channels is dependent on Akt translocation from cytosol to mitochondria during late preconditioning. *Am J Physiol Heart Circ Physiol* 290: H2402–2408.
- Bijur GN, Jope RS (2003) Rapid accumulation of Akt in mitochondria following phosphatidylinositol 3-kinase activation. *J Neurochem* 87: 1427–1435.
- Piao L, Li Y, Kim SJ, Sohn KC, Yang KJ, et al. (2009) Regulation of OPA1-mediated mitochondrial fusion by leucine zipper/EF-hand-containing transmembrane protein-1 plays a role in apoptosis. *Cell Signal*.
- Dimmer KS, Navoni F, Casarin A, Trevisson E, Ende S, et al. (2008) LETM1, deleted in Wolf-Hirschhorn syndrome is required for normal mitochondrial morphology and cellular viability. *Hum Mol Genet* 17: 201–214.
- Bergemann AD, Cole F, Hirschhorn K (2005) The etiology of Wolf-Hirschhorn syndrome. *Trends Genet* 21: 188–195.
- Zollino M, Lecce R, Fischetto R, Murolo M, Faravelli F, et al. (2003) Mapping the Wolf-Hirschhorn syndrome phenotype outside the currently accepted WHS critical region and defining a new critical region, WHSCR-2. *Am J Hum Genet* 72: 590–597.
- Tamai S, Iida H, Yokota S, Sayano T, Kiguchiya S, et al. (2008) Characterization of the mitochondrial protein LETM1, which maintains the mitochondrial tubular shapes and interacts with the AAA-ATPase BCS1L. *J Cell Sci* 121: 2588–2600.
- Tintignac LA, Sirri V, Leibovitch MP, Lecluse Y, Castedo M, et al. (2004) Mutant MyoD lacking Cdc2 phosphorylation sites delays M-phase entry. *Mol Cell Biol* 24: 1809–1821.
- Shaner NC, Campbell RE, Steinbach PA, Giepmans BN, Palmer AE, et al. (2004) Improved monomeric red, orange and yellow fluorescent proteins derived from *Discosoma* sp. red fluorescent protein. *Nat Biotechnol* 22: 1567–1572.
- van de Wetering M, Oving I, Muncan V, Pon Fong MT, Brantjes H, et al. (2003) Specific inhibition of gene expression using a stably integrated, inducible small-interfering-RNA vector. *EMBO Rep* 4: 609–615.
- Hergovich A, Lamla S, Nigg EA, Hemmings BA (2007) Centrosome-associated NDR kinase regulates centrosome duplication. *Mol Cell* 25: 625–634.

Acknowledgments

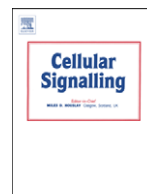
We acknowledge our FMI colleagues and core facilities for contributions to this study. We thank Dr. M. Rojo (INSERM, Université Pierre et Marie Curie, Paris, France) and Dr. DR. Green (St. Jude Children's Research Hospital, Memphis, USA) for plasmids. We also acknowledge Dr. P. King, Dr. L. Bozulic and R. Kohler for editing the manuscript.

Author Contributions

Conceived and designed the experiments: AP LAT. Performed the experiments: AP LAT EZ DH VO. Analyzed the data: AP LAT EZ BAH. Contributed reagents/materials/analysis tools: LAT EZ BD DPB PC SS. Wrote the paper: AP LAT.

7.3 Carboxy-Terminal Modulator Protein (CTMP) is a mitochondrial protein that sensitizes cells to apoptosis

Parcellier A., Tintignac L.A., Zhuravleva E., Cron P., Schenk S., Bozulic L., Hemmings B.A. Cell Signal, 2009; 21(4):639-50



Carboxy-Terminal Modulator Protein (CTMP) is a mitochondrial protein that sensitizes cells to apoptosis

Arnaud Parcellier¹, Lionel A. Tintignac¹, Elena Zhuravleva, Peter Cron, Susanne Schenk, Lana Bozulic, Brian A. Hemmings^{*}

Friedrich Miescher Institute for Biomedical Research, Maulbeerstrasse 66, 4058 Basel, Switzerland

ARTICLE INFO

Article history:

Received 27 October 2008
Received in revised form 15 December 2008
Accepted 2 January 2009
Available online 8 January 2009

Keywords:

CTMP
PKB
Mitochondria
Apoptosis

ABSTRACT

The Carboxy-Terminal Modulator Protein (CTMP) protein was identified as a PKB inhibitor that binds to its hydrophobic motif. Here, we report mitochondrial localization of endogenous and exogenous CTMP. CTMP exhibits a dual sub-mitochondrial localization as a membrane-bound pool and a free pool of mature CTMP in the inter-membrane space. CTMP is released from the mitochondria into the cytosol early upon apoptosis. CTMP overexpression is associated with an increase in mitochondrial membrane depolarization and caspase-3 and polyADP-ribose polymerase (PARP) cleavage. In contrast, CTMP knock-down results in a marked reduction in the loss of mitochondrial membrane potential as well as a decrease in caspase-3 and PARP activation. Mutant CTMP retained in the mitochondria loses its capacity to sensitize cells to apoptosis. Thus, proper maturation of CTMP is essential for its pro-apoptotic function. Finally, we demonstrate that CTMP delays PKB phosphorylation following cell death induction, suggesting that CTMP regulates apoptosis via inhibition of PKB.

© 2009 Elsevier Inc. All rights reserved.

1. Introduction

The mitochondria are one of the major sites in the regulation of cellular metabolism and survival that are crucial for organism development, immunity, aging and pathogenesis [1–3]. These complex cellular functions rely on both the proteomic and the structural integrity of mitochondria, which together contribute to facilitate specific enzymatic activities involved in a variety of functions including oxidative phosphorylation [4], the TCA cycle, gluconeogenesis [5], death signal integration [6] and the amplification and transmission of mitochondrial DNA (mtDNA) [7].

Recently almost 1100 genes encoding mitochondrial proteins in the mouse was reported [8]. Whilst a small number of these mitochondrial proteins are encoded by mtDNA, the vast majority are encoded in the nucleus. Studies into the mechanism by which nuclear transcribed genes that are then translated and located in the cytosol are transported into the mitochondria, have shown that many of these proteins possess a Mitochondrial Localization Signal (MLS) which targets the protein into the mitochondria. Once correctly located in the mitochondria this signal is often cleaved, resulting in a functional protein that can act inside the mitochondria, or via retrograde movement be released back to cytosol to perform cytoplasmic functions [9].

The serine/threonine kinase PKB/Akt is a key effector of the evolutionary conserved PI3 K signaling module that transduces crucial extracellular cues,

such as growth factors and death signals [10–12]. Chronic activation of the PI3 K-PKB pathway, results in tumorigenesis and metastasis [13–18], and can protect tumor cells from apoptosis via inhibition of many proapoptotic proteins, such as Bax, Bid, YAP, mdm2/p53 and others.

CTMP was initially identified as a cytosolic interactor of PKB, which prevents its activation at the plasma membrane in response to various stimuli [19,20], and exhibit tumor suppressor-like functions [19]. This notion was strengthened by the observation that primary glioblastomas exhibit downregulation of CTMP mRNA levels due to promoter hypermethylation [21]. Despite this the physiological localization and function of CTMP is still poorly understood [22].

Here we identify CTMP as a mitochondrial protein, capable of sensitizing cells to apoptosis. Once CTMP is synthesized, it translocates to the mitochondria via a MLS and undergoes maturation through cleavage of this MLS by mitochondrial peptidases. Upon apoptotic stimuli, CTMP is then released into the cytosol and promotes apoptosis with a concomitant delay/inhibition of PKB activation. Our overexpression and loss-of-function studies reported herein, reveal CTMP as a regulator of the apoptotic process, which must be processed in the mitochondrion and then released into the cytosol in order to fulfil these functions.

2. Materials and methods

2.1. Cloning and plasmids construction

All untagged CTMP plasmids used in this study were constructed following PCR amplification of hCTMP cDNA [19] and inserted into the *Bam*HI and *Eco*RI sites of the pcDNA4-IRES-GFP plasmid [23]. CTMP

^{*} Corresponding author. Tel.: +41 61 6974872, +41 61 6974046; fax: +41 61 6973976.
E-mail address: brian.hemmings@fmi.ch (B.A. Hemmings).

¹ Authors contributed equally to the work.

point mutants (m1–3) were generated by site-directed mutagenesis. To C-terminally tag the CTMP protein, the pcDNA3.1-Myc-RFP plasmid was constructed by subcloning the *mRFP1* (monomeric Red Fluorescent Protein 1) cDNA [24] into the *KpnI* and *EcoRV* sites of the hygromycin resistant vector pcDNA3.1-Myc. Wild-type CTMP and deletion mutants were further generated by subcloning of CTMP PCR fragments in the *NheI* and *KpnI* sites upstream of the Myc-RFP tag. pcDNA3-Flag-hBcl2 was a gift from Dr. Christoph Borner.

2.2. Short hairpins targeting CTMP

To stably induce expression of short hairpins in cells, the CTMP-specific tandem sequences 5'-GATCCCAAGACCTATACTCAGAGGCGTTCAGAGACGCTCTGAGTAGGGTCTTTTGGAAA-3' and 5'-AGCTTTTC-CAAAAAGACCTACTCA GAGGCGTCTCTTGAACGCTCTGAG-TATGGTCCGG-3' were cloned in the *BglII*/*HindIII* sites of pTer vector [25]. The pTER control construct (cont-Sh) used was directed against luciferase as previously described [26] or a scramble sequence 5'-GAGTCCTT GGTAGCTGTCTCTTTTGGAAA3' and 5'-AGCTTTTC-CAAAAAGAGACAGCTACCAAGGACTCTCTTGAAGTCCTTGG-TAGCTGTCTCTGG3'. All construct sequences were confirmed using an ABI PRISM 3700 DNA Analyzer (Applied Biosystems).

2.3. Cell lines, transient and stable transfection, reagents

HEK293, HeLa, and LN229 cells were grown in Dulbecco's Medium (Gibco) supplemented with 10% foetal calf serum. HeLa cell lines stably expressing the tetracycline repressor (HeLa Tet-on) were cultured in medium supplemented with 100 ng/mL G418 (Sigma). For transfection, cell lines (HeLa, HeLa Tet-on cells) were plated in 6-well plates or 10-cm dishes and transfected the following day at 60% confluence using Lipofectamine 2000 following the manufacturer's instruction (Invitrogen). Stable clones expressing CTMP, short hairpins or negative controls were selected 48 h after transfection by addition of 0.8 mg/mL Zeocin and positive clones were further maintained in 0.4 mg/mL Zeocin. Actinomycin D and etoposide were from Sigma; zVAD-fmk was from R&D System.

2.4. Antibodies

CTMP monoclonal antibodies were generated by repeated immunization of BALB/c mice with 50–100 µg of purified full-length His-CTMP protein (produced in *E coli*), using Stimune (Prionics AG, Schlieren, Switzerland) as an adjuvant. Two months after the priming injection, splenic lymphocytes cells were fused with P3AG8.653 myeloma cell line (ATCC) and cultured according to standard procedures. After ELISA screening of hybridoma clone supernatants, epitope mapping was carried out for the four clones used in this study (52F11, 4B13 and 41G21) using the GST-CTMP deletion mutant and synthetic polypeptides. All monoclonal anti-CTMP antibodies characterized are IgG1.

The antibodies anti-Myc (9E10), anti-HA (12CA5), anti- α -tubulin (YL 1/2), anti-PKB (AB10) were used as hybridoma supernatants and rabbit anti-hLetm1 (epitope amino acids 349 to 740) [27] was kindly provided by Dr. R. J. O'Brien (Caritas St. Elizabeth's Medical Center, Boston, USA). The commercial mouse anti-mHsp70 (JG1) was from Affinity BioReagents, mouse anti-cytochrome c and rabbit anti-Htr2a/Omi were from R&D System, anti-cleaved PARP and rabbit monoclonal anti-caspase-3 from Cell Signaling Technology. The commercial anti-phospho Ser473 PKB/AKT antibody was from Alexis and anti-Bcl2 from Santa Cruz Biotechnology.

2.5. Protein extraction and mitochondria fractionation

For whole cell extracts, cells were washed in PBS 1X and resuspended in lysis buffer (50 mM Tris pH 7.4, 150 mM NaCl, 10% glycerol, 0.5% NP40,

0.5 mM Na-orthovanadate, 50 mM NaF, 80 mM β -glycerophosphate, 10 mM Na-pyrophosphate, 1 mM dithiothreitol, 1 mM EGTA, 10 µg leupeptin/ml and 10 µg aprotinin/ml).

Mitochondria isolation was carried out as described [28]. Briefly, cells were washed twice in 100 mM sucrose, 1 mM ethylene glycol-bis (β -aminoethyl ether)-tetraacetic acid (EGTA), 20 mM 3-(*N*-morpholino)propanesulfonic acid (MOPS) pH 7.4 and 1 mg/mL BSA. The pellet was resuspended in the same buffer solution supplemented with 10 mM triethanolamine, 5% (v/v) Percoll, 0.1 mg/mL digitonin for 3 min at 4 °C and homogenized in a Potter homogenizer (10 strokes, 1000 rpm) before being diluted 1/5 in 300 mM sucrose, 1 mM EGTA, 20 mM MOPS pH 7.4 and 1 mg/mL BSA, and centrifuged at 2500 g for 5 min at 4 °C. The supernatant containing mitochondria was collected and centrifuged at 10,000 g for 10 min at 4 °C to collect mitochondria as a pellet. Isolated mitochondria were washed twice in the same conditions before being resuspended and further processed.

2.6. Western blotting

For Western blot analysis, protein lysates were prepared by using lysis buffer (50 mM Tris-HCl pH 8.0, 120 mM NaCl, 1% NP-40, 40 mM β -glycerophosphate, 10% glycerol, 4 µM leupeptin, 0.05 mM phenylmethylsulfonyl fluoride, 1 mM benzamide, 50 mM NaF, 1 mM Na₃VO₄, 5 mM EDTA, 1 µM Microcystin LR). Homogenates were centrifuged twice (13,000 rpm for 10 min at 4 °C) to remove cell debris. Protein concentrations were determined using the Bradford assay and proteins separated by 12% or 10% sodium dodecyl sulfate-polyacrylamide gel electrophoresis and before transfer to Immobilon-P polyvinylidene difluoride membranes (Millipore).

2.7. Immunostaining

For immunostaining, cells were grown on coverslips for 24 h following treatment. To visualize mitochondria, cells were treated with 300 nM Mito Tracker Red CMXRos for 15 min before being washed in PBS and fixed in 3% paraformaldehyde/2% sucrose. Cells were further permeabilized using 0.2% Triton X100 (3 min at room temperature) before being washed in PBS and incubated together with the appropriate dilution of the primary antibody for 1 h at room temperature in 1% BSA/1% goat serum. This was followed by incubation with secondary antibodies including donkey anti-mouse-fluorescein isothiocyanate (FITC) (Jackson Immunoresearch Inc.) at 1:100 together with 1 µM To-Pro-3 iodide (DNA, Molecular Probes Inc) for 45 min at room temperature. After final washing, coverslips were mounted in Vectashield medium (Vector lab) and visualized with a laser scanning microscope (Olympus FV500). Confocal images were processed using the Imaris program (Bitplane AG, Zurich, Switzerland) and Photoshop 6.0 (Adobe System Inc).

2.8. Measurement of mitochondrial membrane potential

Mitochondrial membrane potential ($\Delta\psi_m$) was measured with the MitoProbe™ 1,1',3,3,3',3'-hexamethylindodicarbocyanine iodide (DiIC₁(5)) assay kit (Molecular Probes) as instructed by the manufacturer. Briefly, cells (including floating cells) grown in 6-well plates were collected following mild trypsinization. Trypsinized cells were washed once with PBS, and the cells were resuspended in 500 µl PBS. Resuspended cells were labelled with 50 nM DiIC₁(5) (excitation/emission, 638/658 nm) at 37 °C in the dark for 30 min. Labelled cells were washed once in PBS and analysed by fluorescence-activated cell sorting using a FACSCalibur (Becton Dickinson) flow cytometer.

2.9. Hoechst staining

Cells (including floating cells) were collected following mild trypsinization. Trypsinized cells were washed once with PBS and the

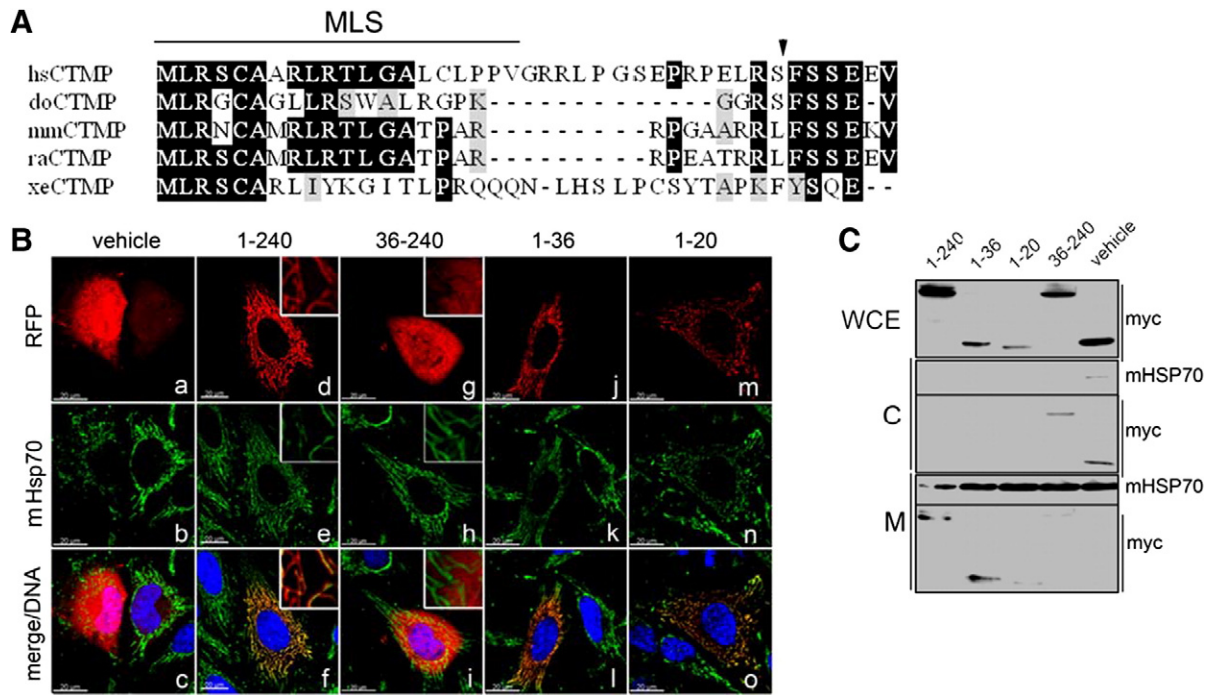


Fig. 1. CTMP contains a functional N-terminal mitochondrial localization signal (MLS). (A) Alignment of CTMP proteins from human (hsCTMP, Uniprot: Q5T1C6), dog (doCTMP, Refseq: XP_851465), mouse (mmCTMP, Uniprot: Q3UUI3), rat (raCTMP, Uniprot: Q566R0) and Xenopus (xeCTMP, Uniprot: Q6GLK2). The sequences were collected using PSI-BLAST against the Uniprot and Refseq sequence collections at the myHits server of the SIB (myhits.isb-sib.ch). The alignment is based on ClustalW at the same server, with some manual refinement. The arrow between positions 36 and 37 of the human protein shows the candidate cleavage site for the N-terminal mitochondrial targeting sequence predicted by TargetP (www.cbs.dtu.dk/services/TargetP/) in the human and mouse sequences. (B) HeLa cells were transfected with a C-terminus Myc-RFP tagged CTMP, CTMP deletion mutant, or empty vector. Cells were visualized by immunofluorescence 24 h after transfection; mitochondria were immunostained with anti-mHsp70 (mitochondrial Hsp70) mAbs visualized by a FITC coupled anti-mouse Abs. Yellow in the third panel depicts co-localization. (C) Whole cell extract (WCE) (20 µg) of transfected HeLa cells (treated as in B), differential centrifugation-purified mitochondria and the cytosolic compartment were analysed by SDS-PAGE and immunoblotted for myc (RFP fusion proteins) and mHsp70 (mitochondria). (For interpretation of the references to colour in this figure legend, the reader is referred to the web version of this article.)

cells resuspended in PBS. The nuclear chromatin was stained with Hoechst 33342 for 30 min at 37 °C. After staining, nuclear morphology was studied under UV light by fluorescence microscopy (Nikon E800). Apoptotic cells were characterized by condensed and/or fragmented nuclei. For each sample, 300 cells were examined.

3. Results

3.1. CTMP is a mitochondrial protein targeted by an N-terminal signal sequence

Bioinformatics analysis of the CTMP amino acid sequence with subcellular localization prediction tools [TargetP (www.cbs.dtu.dk/services/TargetP/), iPSORT, MitoProt] identified an N-terminal mitochondrial localization signal (MLS) conserved in CTMP orthologues (Fig. 1A) [29,30]. To assess the function of the human CTMP mitochondria targeting sequence, full-length protein and deletion mutants were C-terminally fused to the monomeric red fluorescent protein 1 (mRFP1) and the subcellular localization of the chimeric protein was assessed by immunocytochemistry. The staining pattern of the full-length fusion protein overlapped with the mitochondrial marker anti-mHsp70 (mitochondrial Hsp70) (Fig. 1B, a–f). In contrast, a CTMP deletion mutant lacking the first 36 amino acids (36–240) was excluded from the mitochondria and accumulated in the cytosol and to a lower extent in the nucleus (Fig. 1B, g–i), supporting the concept that the CTMP N-terminus is responsible for mitochondrial targeting. Conclusive evidence was obtained by assessing the ability of C-terminal deletion mutants of CTMP to efficiently relocate the cytoplasmic/nuclear mRFP1 protein to the mitochondria. Both immunocytochemistry and biochemical fractionation experiments demonstrated that the first 20 amino acids of CTMP are sufficient to relocate mRFP1 to the mitochondria, as measured by co-localization

with mHsp70 staining (Fig. 1B, l–o). Moreover, Western blotting of mitochondrial and cytosolic extracts of HeLa cells confirmed that CTMP is a mitochondrial protein bearing a conserved and functional MLS in the 20 first amino acids (Fig. 1C). To test whether the subcellular localization was an artefact due to CTMP overexpression, the presence of endogenous human CTMP in mitochondria was assessed by immunocytochemistry and subcellular fractionation. To this end, anti-CTMP monoclonal antibodies were generated against the recombinant human CTMP protein. Anti-CTMP antibody 52F11 specificity was tested on different cell lines transfected with CTMP, the deletion mutant or an empty vector (Fig. 2A) in the presence or absence of peptide epitope (Fig. 2B). Immunocytochemistry performed with the mouse monoclonal antibody 52F11 showed mitochondrial staining in both HeLa cells and LN229 (a glioblastoma cell line known to express a high level of CTMP [19]) (Fig. 2C). Specificity of the signal was confirmed by peptide competition with the 52F11 antigenic epitope peptide containing amino acids 100–118 of hCTMP (Fig. 2C). Mitochondria from HeLa and LN229 were isolated biochemically and immunoblot analysis confirmed the integrity (cytochrome c and mHsp70 positive) and the purity (α -tubulin negative) of the mitochondrial fractions. Anti-CTMP immunoblotting showed that endogenous CTMP essentially co-purified with the mitochondrial protein marker (Fig. 2D).

Altogether, these results demonstrate that the nuclear CTMP gene encodes a conserved mitochondrial protein targeted to the mitochondria via an N-terminal signal peptide.

3.2. Mitochondria contain both membrane-bound and soluble CTMP species

To determine the exact sub-mitochondrial localization of CTMP, mitochondrial membranes were selectively permeabilized by

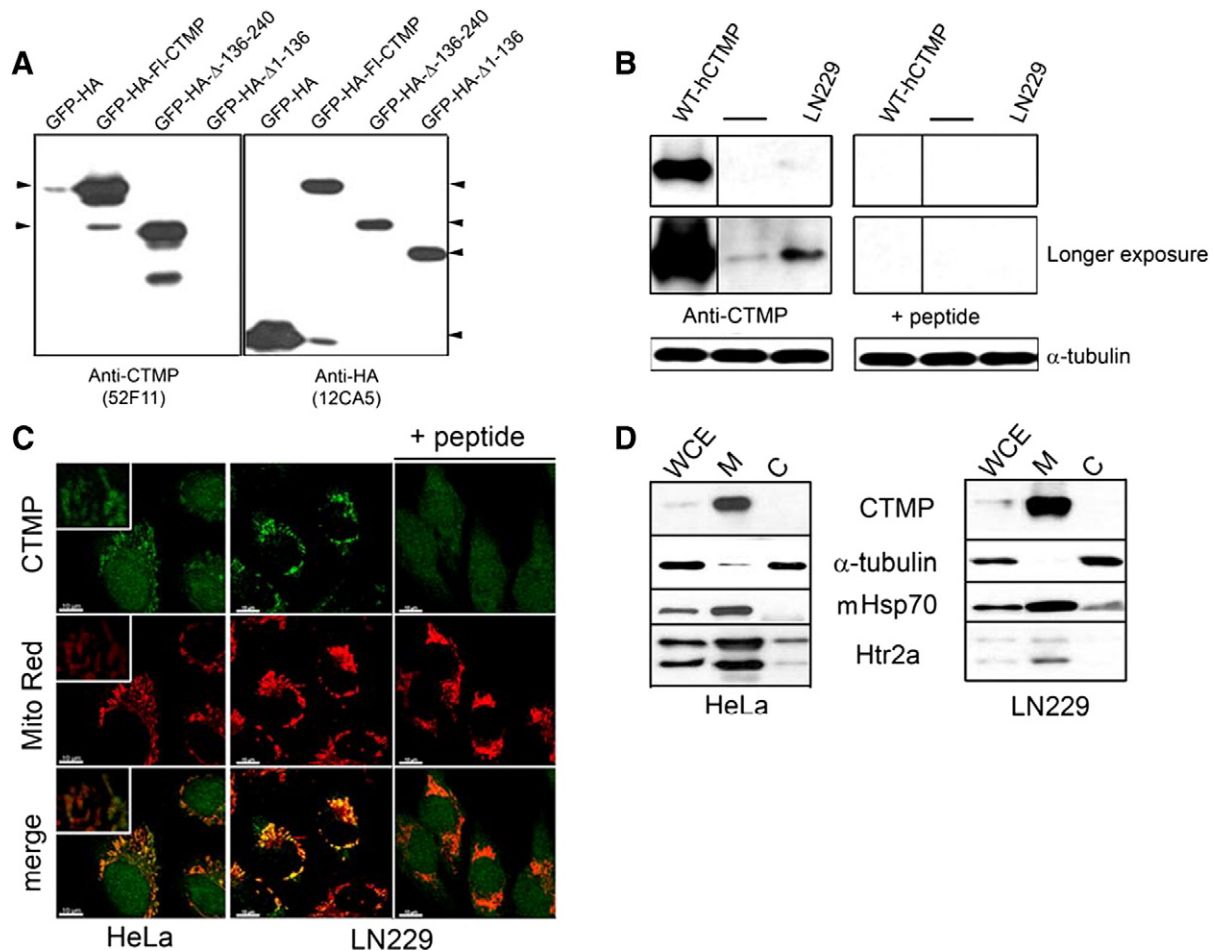


Fig. 2. CTMP is a mitochondrial protein. (A) Whole cell extracts of HEK293 cells transfected with N-terminus GFP-HA tagged hCTMP, CTMP deletion mutant, or empty vector (40 μ g) were analysed by SDS/PAGE gel and immunoblotted with monoclonal 52F11 anti-CTMP antibody or anti-HA. (B) Proteins extracted from HeLa cells transfected with untagged hCTMP or empty vector, and LN229 cells (50 μ g) were analysed by SDS/PAGE gel and immunoblotted with monoclonal 52F11 anti-CTMP antibody in the presence or absence of peptide epitope (0.5 mg/mL). (C) HeLa and LN229 cells were immunostained with anti-CTMP 52F11 antibody in the presence or absence of peptide epitope (0.5 mg/mL) and visualized by a FITC-coupled secondary antibody. Mitochondria were stained with the MitoTracker Red. Yellow in the third panel depicts co-localization. (D) HeLa and LN229 whole cell extract (WCE) (20 μ g), differential centrifugation-purified mitochondria and cytosolic fractions were analysed by SDS-PAGE and immunoblotted for CTMP, Htr2A and mHsp70 (mitochondria) and α -tubulin (cytosol). (For interpretation of the references to colour in this figure legend, the reader is referred to the web version of this article.)

incubating cells with increasing concentrations of digitonin [31,32]. Mitochondrial outer membrane disruption was achieved by incubation of cells in digitonin at 0.1 mg/mL, as assessed by immunodetection of cytochrome-c protein (Fig. S1). Digitonin at 0.9 mg/mL disrupted the inner membrane (mHsp70 staining) (Fig. 3A). Myc immunodetection of C-terminal-tagged CTMP-myc-RFP protein fusion showed positive staining that overlapped with RFP fluorescence at a low digitonin concentration (0.3 mg/mL), suggesting that the C-terminal of CTMP is accessible from the inner mitochondrial space. To gain further insights into CTMP sub-mitochondrial localization, mitochondria isolated from HeLa cells were fractionated by carbonate treatment into a membrane pellet (P) and a soluble fraction (S). Immunoblotting for CTMP showed that the endogenous protein co-purified with both membrane-associated protein Letm1 [33] and soluble proteins of the supernatant fraction (cytochrome c and mHsp70) (Fig. 3B). Moreover, exogenous untagged CTMP showed the same co-purification pattern from HeLa cells (Fig. 3C). The combined results from these experiments suggest that CTMP is strongly associated with the mitochondrial inner membrane. Thus, we propose the existence of two sub-mitochondrial CTMP populations: an inner mitochondrial membrane-associated pool and a free soluble form in the inner mitochondrial space. Interestingly, immunodetection of the overexpressed untagged CTMP revealed a dual electrophoresis mobility pattern characterized by a slow-

(27 kDa) and a fast-migrating form (25 kDa) (Fig. 3C). Only the smaller species was detected in the mitochondrial soluble fraction, suggesting that posttranslational modification regulates CTMP sub-mitochondrial sorting.

3.3. Mitochondrial processing of the CTMP N-terminus

The vast majority of N-terminal MLS are matrix-targeting signals cleaved by the mitochondrial processing peptidase [34,35]. Despite the fact that the MPP amino acid cleavage sequence is highly degenerate, the requirement for a positive arginine residue at positions -2 and/or -10 from the cleavage site has been established by several authors [36,37]. CTMP sequence analysis showed a highly probable R-2 site at serine 35, surrounded by a hydrophobic residue at +1 and a serine at +2 (Fig. 4A). The functionality of this putative cleavage site was assessed by the generation of various CTMP point mutants and determination of their electrophoretic mobilities (Fig. 4A). Immunodetection of the CTMP m1, -m2 and -m3 mutants showed accumulation of a single larger form (premature, 27 kDa). In contrast, WT-CTMP and the m1 mutant were mostly detectable as fast-migrating bands (mature, 25 kDa) (Fig. 4B). A monoclonal antibody specific for the first 25 amino acids of the human CTMP protein was used to further test this hypothesis. Only the m3 mutant was detected by the 4B13 antibody, whereas the 52F11 antibody

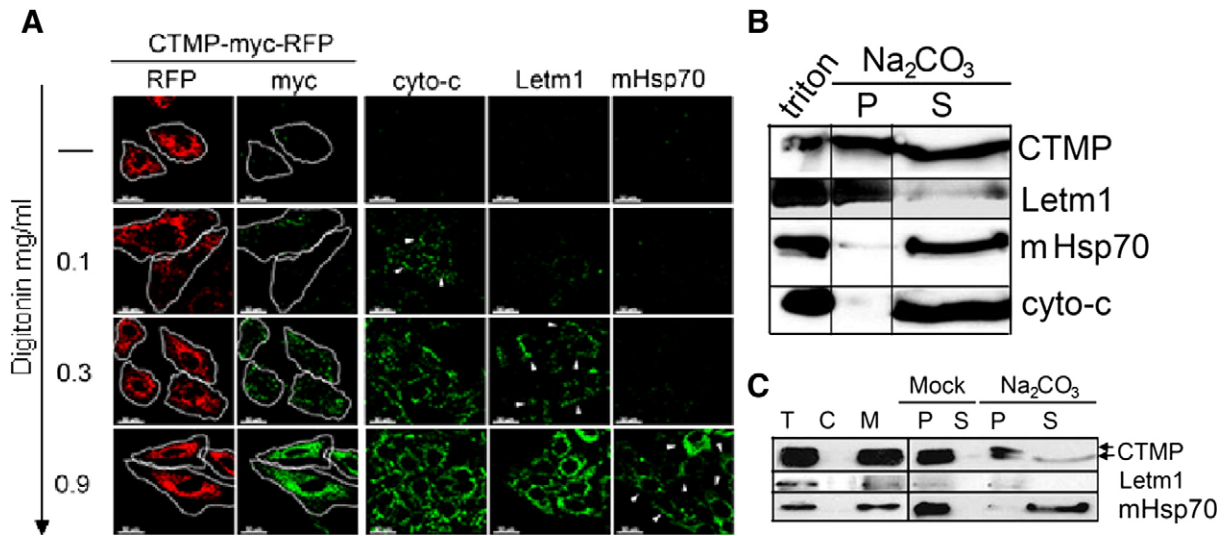


Fig. 3. Soluble and membrane-bound CTMP species reside in the mitochondria. (A) HeLa cells transfected or not with wild-type CTMP-myc harbouring a C-Terminal RFP tag were fixed and treated with the indicated concentrations of digitonin (0, 0.1, 0.3, 0.9 mg/mL). The overexpressed protein was detected by RFP fluorescence (red) and anti-myc antibody (green) by confocal microscopy. The digitonin-dependent mitochondrial permeabilization was estimated by sequential immunodetection of the mitochondrial protein cytochrome-c (inner mitochondrial space and cristae), Letm1 (inner membrane) and mHsp70 (matrix). (B) Mitochondria were extracted from HeLa cells and 20 µg of protein was separated by SDS/PAGE after Triton X-100 extraction or carbonate-dependent isolation of membrane-bound protein (P) and soluble/weakly bound protein (S) and immunoblotted with the correspondent antibodies. (C) Mitochondria extracted from HeLa cells transiently transfected with the full-length untagged CTMP were treated as in (B). (For interpretation of the references to colour in this figure legend, the reader is referred to the web version of this article.)

directed against the central region of CTMP detected both the 25-kDa and 27-kDa forms (Fig. 4C). These results suggest that most CTMP is processed in cells by cleavage of its N-terminal region. To test whether mutation of the CTMP cleavage site affects sorting to the mitochondria, CTMP mutants were transfected into HeLa cells and their subcellular localizations assessed. The m3 mutant co-purified with the mitochondrial marker and co-localized with mitochondria in cells (Fig. 4D, E). Together, these data demonstrate that the N terminal portion of CTMP is cleaved in the mitochondria by the

mitochondrial protein peptidase to generate a mature CTMP protein (amino acids 36–240).

3.4. CTMP is released from mitochondria into the cytosol upon apoptosis

As described above, CTMP is a mitochondrial protein localized both at the inner membrane and in the inter-membrane space of the mitochondria (IMS). Many pro-apoptotic proteins, e.g. cytochrome c, AIF, and Smac/Diablo, reside within the IMS and can be released into

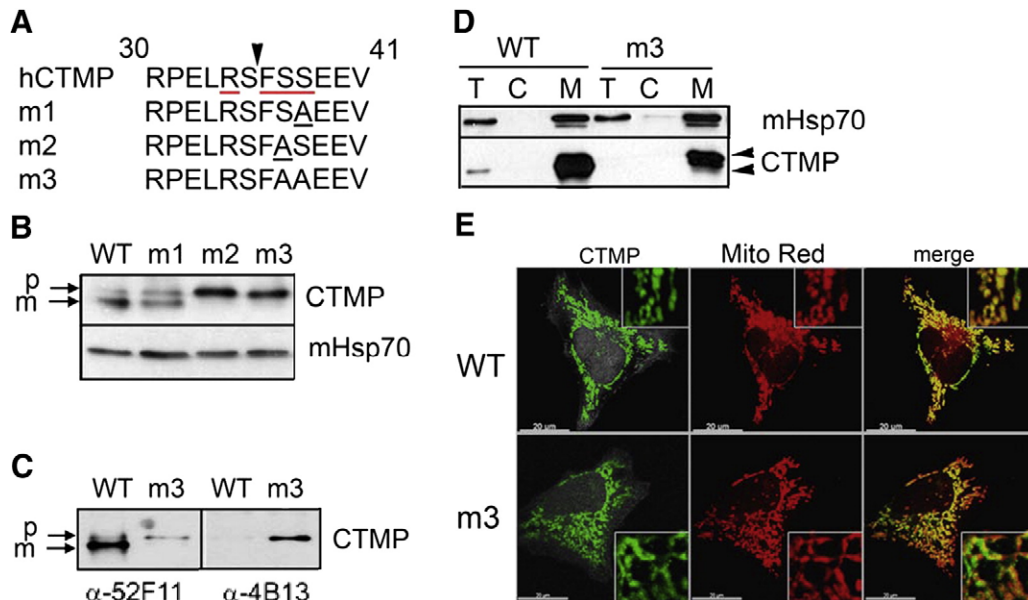


Fig. 4. CTMP is N-terminally processed in the mitochondria. (A) Amino acid sequence of the R-2 predicted MPP cleavage site (indicated by an arrow) in human CTMP, and a point-mutation series. (B) HeLa cells were transfected with empty vector, untagged wild-type CTMP, or CTMP point mutants described in (A). WCE (20 µg) was separated on SDS/PAGE and immunoblotted for CTMP protein together with mHsp70 as a loading control; (p) and (m) arrows correspond to pre- and mature CTMP protein, respectively. (C) The extracts as in (B) were separated by SDS/PAGE and the immunoblotted using 52F11 anti-CTMP antibody (epitope amino acids 100–118) or 4B13 anti-CTMP antibody (amino acids 1–25). (D) Whole cell lysate, detergent-purified mitochondria (10 µg) and cytosolic compartment of HeLa cells transfected with untagged CTMP, or CTMP point mutant m3 were analysed by SDS-PAGE and immunoblotted for CTMP and the CTMP m3 mutant. (E) HeLa cells were fixed and stained for CTMP (green) and mitochondria (red) as indicated. Representative confocal pictures from three different experiments are shown. Yellow in the third panel depicts co-localization. (For interpretation of the references to colour in this figure legend, the reader is referred to the web version of this article.)

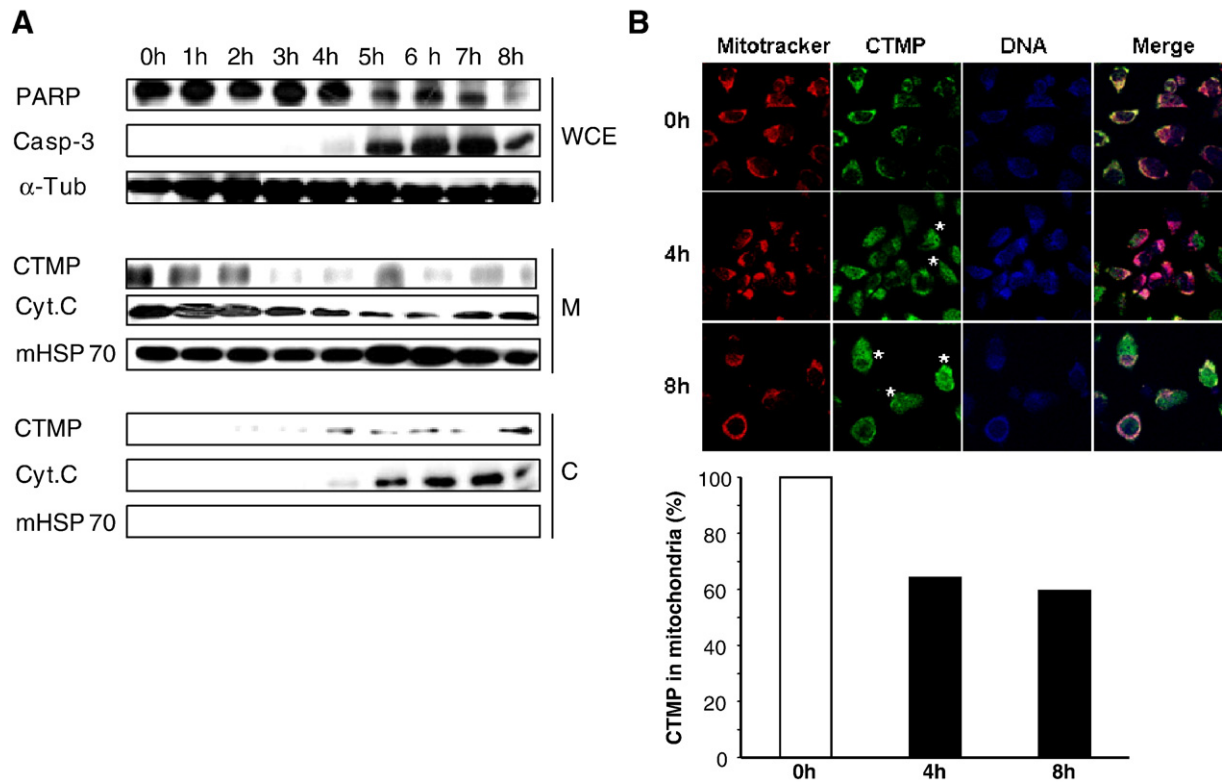


Fig. 5. CTMP is released into the cytosol upon apoptosis. (A) HeLa cells were treated with 2 μ M actinomycin D for the indicated times and then fractionated into cytosolic (C) and mitochondrial (M) fractions. Apoptosis was monitored by measuring PARP cleavage and decrease in pro-caspase-3. Mitochondrial HSP70 was used as a control for mitochondria purification. (B) HeLa cells were treated with 2 μ M actinomycin D for 4 and 8 h then immunostained with anti-CTMP 41G21 antibody and a FITC-coupled secondary antibody. Mitochondria were stained with Mitotracker and cytosolic CTMP was monitored by counting at least 200 cells per time point.

the cytosol upon permeabilization of the mitochondrial outer membrane [38–40]. Therefore, we investigated whether CTMP is present in the cytoplasm after induction of apoptosis. HeLa cells were treated with actinomycin D for 8 h and fractionated into mitochondrial and cytosolic samples. As assessed by PARP and caspase-3 cleavage, apoptosis occurred 4 h into the treatment. At the same time, CTMP appeared in the cytosolic fraction and the amount of CTMP in the mitochondrial fraction declined (Fig. 5A, B). A similar result was obtained using etoposide as the apoptosis inducer and treatment for 24 and 48 h (Fig. S2). CTMP and cytochrome c were released with the same kinetics, which suggests that cytosolic CTMP after cell death induction corresponds to the free pool of CTMP from the IMS. Moreover, after 8 h treatment with actinomycin D, approximately 50% of CTMP remained in the mitochondria (Fig. 5B).

3.5. CTMP overexpression sensitizes cells to apoptosis

To determine whether CTMP has an effect on cell death, we first transfected HeLa cells with a construct allowing CTMP overexpression and induced apoptosis using actinomycin D (0.25 μ M for 12 h). As monitored by counting cells positive for Hoechst staining, CTMP overexpression significantly increased the degree of cell death occurring after actinomycin D treatment (Fig. 6A). Similar results were obtained in HEK293 cells (Fig. S3A). In a stable HeLa cell line with a high and constant expression of CTMP (Fig. S3B), chemical-induced cell death was assessed by monitoring mitochondrial membrane depolarization. Apoptosis induced by actinomycin D or etoposide was significantly higher in cells overexpressing CTMP than in control cells transfected with the empty vector (Fig. 6B, D, E and S3C). Caspase-3 and PARP cleavage were much more efficient in cells with a high level of CTMP when apoptosis was induced by actinomycin D (Fig. 6C). Thus,

CTMP protein sensitizes cells to apoptosis mediated by cytotoxic agents such as actinomycin D and etoposide.

3.6. CTMP depletion and a defect in CTMP maturation lead to apoptosis resistance

To validate the apparent function of CTMP in apoptosis sensitization, we generated a cell line in which CTMP was stably down-regulated and measured apoptosis following actinomycin D treatment. Tetracycline repressor-expressing HeLa cells were stably transfected with shRNA specifically targeting CTMP (CTMP Sh) or control shRNA (Scramble) and knock-down efficiency determined by immunoblotting (Fig. 7B). Neither CTMP depletion nor CTMP overexpression had any effect on cell proliferation (Fig. S4A). CTMP depletion not only decreased actinomycin D-mediated apoptosis twofold after 15 h treatment but also delayed apoptosis. This was initiated after 7 h treatment in CTMP Sh cells and after 4 h in the control cells (Fig. 7A). Moreover, non-cleaved caspase-3 was still detectable 7 h after apoptosis induction in cells lacking CTMP but was depleted after only 4 h in cells transfected with scramble RNA (Fig. 7B). This was also true for a second clone of CTMP Sh (data not shown).

The IMS localization of CTMP could be regulated by posttranslational modification and the N terminus of CTMP is cleaved in the mitochondria by the mitochondrial protein peptidase to generate a mature CTMP protein (amino acids 36–240) (Fig. 4). Therefore, we investigated whether a mutant immature CTMP protein (CTMP m3) also sensitizes cells to apoptosis. Whereas maximum release of CTMP occurred after 12 h actinomycin-D treatment, the mutant protein refractory to N-terminal cleavage was only found in the mitochondrial fraction; in contrast, cytochrome c was efficiently relocated to the

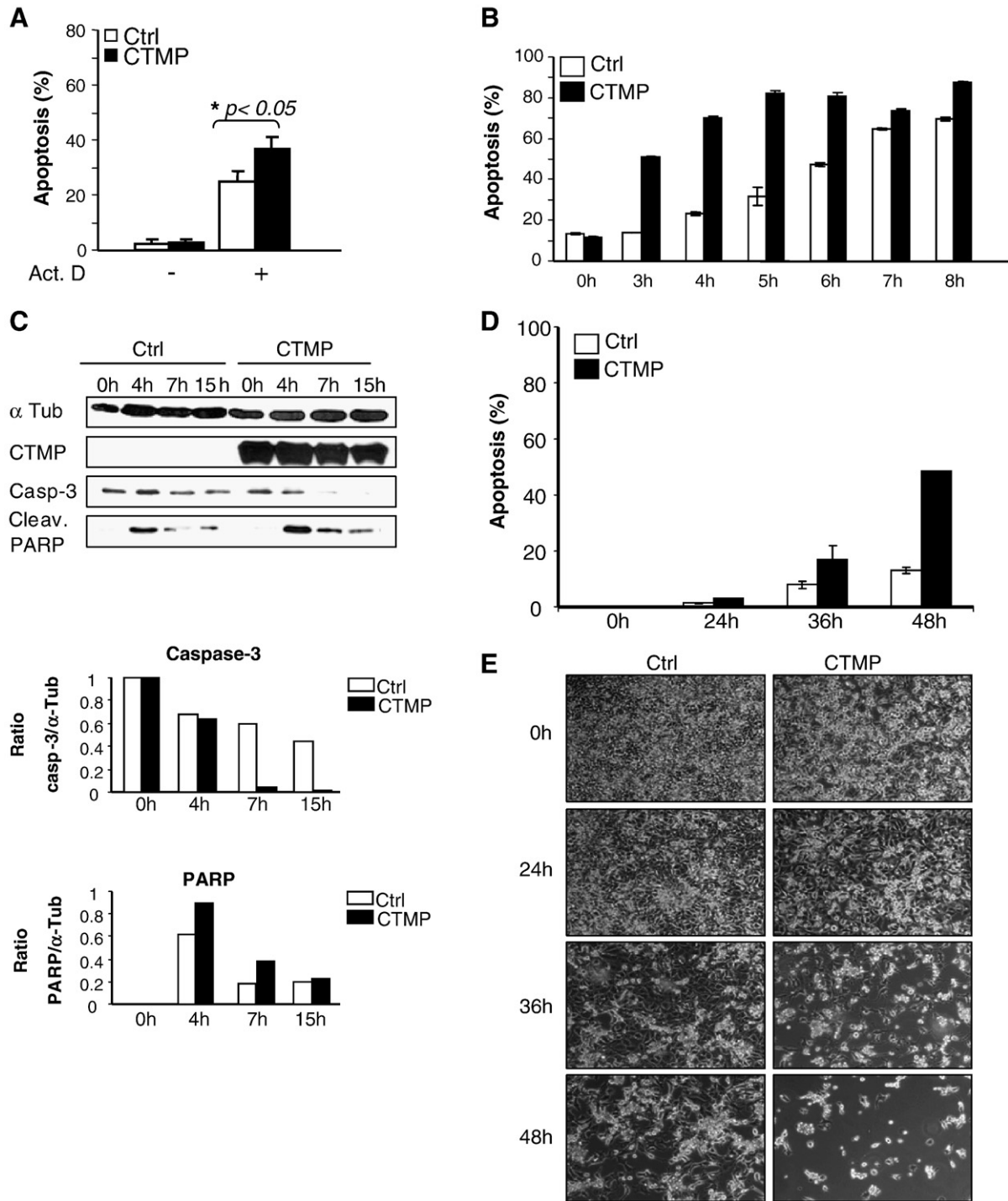


Fig. 6. CTMP sensitizes cells to apoptosis. (A) HeLa cells were transiently transfected with pcDNA3-IRES-GFP (Ctrl) or pcDNA3-IRES-CTMP (CTMP) and treated 24 h later with 0.25 μ M actinomycin D for 12 h. Apoptosis was measured by Hoechst staining (3×100 cells were counted). HeLa inducible cell lines expressing CTMP (CTMP) or not (Ctrl) were induced by tetracycline (2 μ g/mL) for 5 days and then treated with 2 μ M actinomycin D (B) or 100 μ M etoposide (D) for the indicated times. Apoptosis was determined by measuring the loss of mitochondrial membrane potential ($\Delta\psi_m$) using MitoProbe™ DiIC₁(5). Data are the means and standard deviations from three independent experiments. (C) α -Tubulin, CTMP, caspase-3 and PARP cleavage were detected by immunoblotting. Caspase-3 and PARP cleavage were quantified using ImageQuant software™ (GE Healthcare). One representative experiment of three is shown. (E) Etoposide-induced apoptosis (100 μ M) was examined by phase contrast microscopy in control (Ctrl) and CTMP-overexpressing cells (CTMP) for the indicated times.

cytoplasm (Fig. 7C). Induction of apoptosis in cells stably overexpressing CTMP m3 was delayed compared with control cells. After 4 h actinomycin D treatment, apoptosis was twofold lower in cells overexpressing the CTMP mutant (Fig. 7D). Caspase-3 was still present in cells expressing the mutant CTMP but was completely lacking in the control cells (Fig. 7E). However, the decrease in cell death mediated by CTMP m3 was not maintained over time. Surprisingly, apoptosis

increased in these cells after 15 h (Fig. 7D) and after 24 h treatment (data not shown). It is possible that prolonged induction of cell death results in the complete dismantling of the mitochondria, leading to release of the CTMP mutant protein into the cytosol, where it sensitizes cells to apoptosis. Altogether, these results confirm that CTMP behaves as a pro-apoptotic protein and strongly suggest that CTMP maturation and release into the cytosol is required for its effect on cell death.

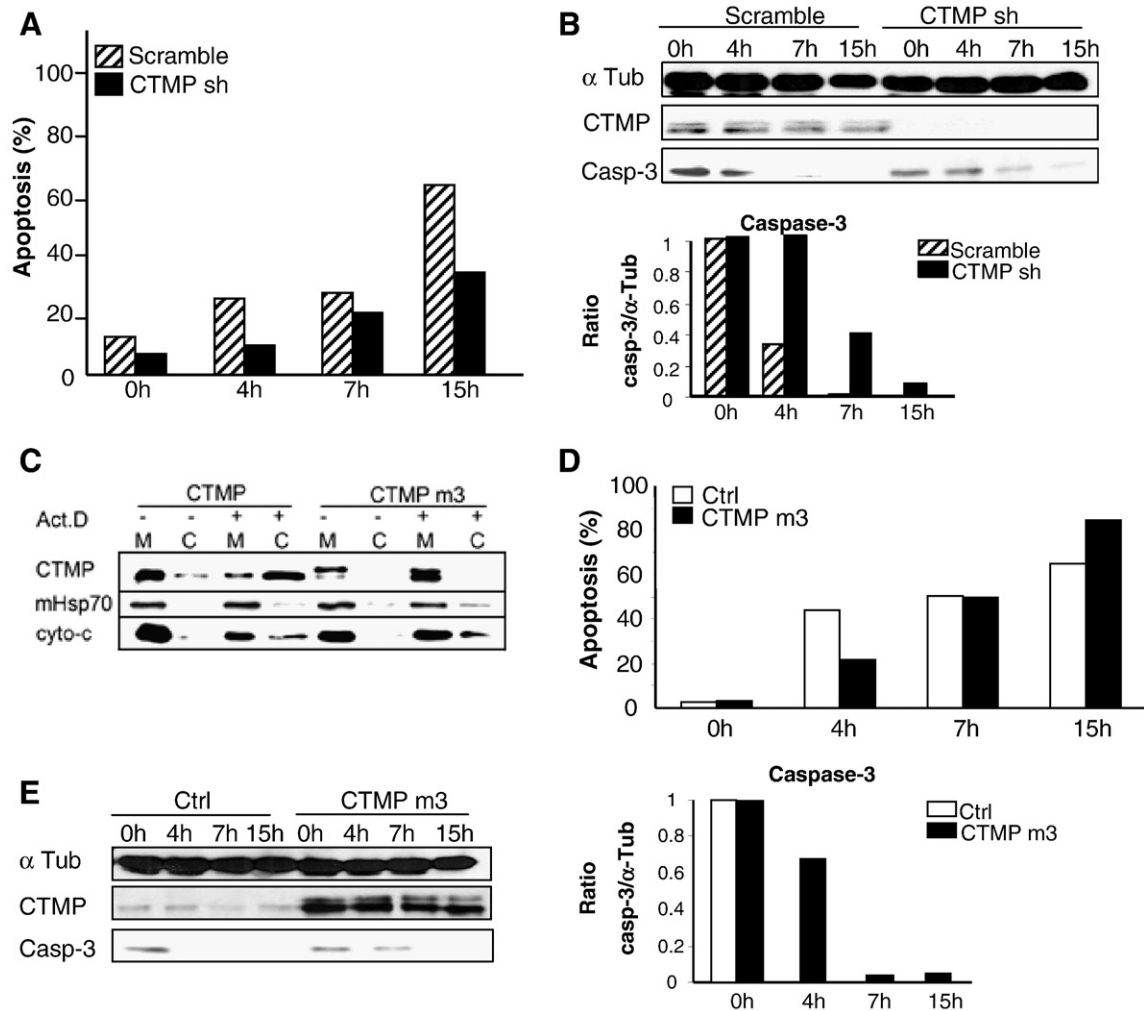


Fig. 7. CTMP depletion and a defect in CTMP maturation lead to apoptosis resistance. (A) HeLa inducible cell lines expressing scramble RNA or short-hairpin RNA targeting CTMP (CTMP Sh) were induced by tetracycline (2 $\mu\text{g}/\text{mL}$) for 5 days and then treated with 2 μM actinomycin D for the indicated times. Apoptosis was determined by measuring loss of mitochondrial membrane potential ($\Delta\psi_m$) using MitoProbe™ DiI_{C1}(5). (C) HeLa cells were transfected with untagged wild-type CTMP or CTMP m3. Cells were treated with DMSO or 2 μM actinomycin D for 12 h and then fractionated into mitochondrial (M) and cytosolic fractions (C). CTMP, mHSP70 and cytochrome c were detected by immunoblotting. (D) HeLa inducible cell lines expressing CTMP m3 or not (Ctrl) were induced by tetracycline (2 $\mu\text{g}/\text{mL}$) for 5 days and then treated with 2 μM actinomycin D for the indicated times. Apoptosis was measured as described previously. (B and E) α -Tubulin, CTMP and caspase-3 cleavage were detected by immunoblotting. Caspase-3 cleavage was quantified using ImageQuant software™ (GE Healthcare). One representative experiment of three is shown.

3.7. Bcl-2 but not caspase inhibition blocks apoptosis sensitization mediated by CTMP

To investigate whether the pro-apoptotic effect of CTMP is inhibited by blocking caspases, the main effectors of apoptosis in cells, we treated control cells or cells overexpressing CTMP with actinomycin D in the presence or not of the broad-spectrum caspase-inhibitor zVAD-fmk. Control cells treated with zVAD-fmk showed negligible apoptosis compared with cells overexpressing CTMP. In the latter, there was no significant decrease in cell death (Fig. 8A). Moreover, caspase inhibition did not prevent CTMP release into the cytosol after actinomycin D-mediated apoptosis in HeLa cells (Fig. 8B, S5A). CTMP was released with kinetics very similar to that of cytochrome c, as observed previously (Fig. 5A). The caspase inhibitor zVAD-fmk does not affect cytochrome c release [41–44]. Thus, caspase activation appears not to be required for CTMP release from the mitochondria. CTMP-mediated sensitization of apoptosis is apparently caspase independent, although we showed that CTMP overexpression results in a marked decrease in pro-caspase-3 in actinomycin D- or etoposide-treated cells. We, therefore, propose a feedback mechanism in which cytosolic CTMP activates further pro-apoptotic molecules that finally induce caspase cleavage. Bcl-2 is an anti-apoptotic protein localized at the mitochon-

drial membrane and able to interfere with programmed cell death by inhibiting the release of many pro-apoptotic proteins into the cytosol [40,45–47]. We expressed Bcl-2 transiently in control cells and in cells overexpressing CTMP and monitored apoptosis following actinomycin D treatment. The Bcl-2 transfection efficiency was assessed by immunoblotting (Fig. S5B). The level of cell death in control cultures was higher than in our previous experiments (Fig. 8C, left panel), most probably because of a deleterious effect of the transfection, which conditioned cells to death mediated by actinomycin D. With this in mind, we measured apoptosis up to 8 h instead of 15 h. Whilst CTMP sensitized cells to apoptosis, Bcl-2 expression almost completely inhibited actinomycin D-induced cell death in control and CTMP-overexpressing cultures (Fig. 8C, right panel). Most important, Bcl-2 transfection blocked CTMP release into the cytosol to the same extent as cytochrome c (Fig. 8D). This finding supports the conclusion that cell death sensitization mediated by CTMP results from its release into the cytosol.

3.8. CTMP delays PKB phosphorylation on Ser473 occurring upon apoptosis

CTMP was described previously as a negative regulator of PKB [19]. However, these results were obtained using a CTMP construct flag-

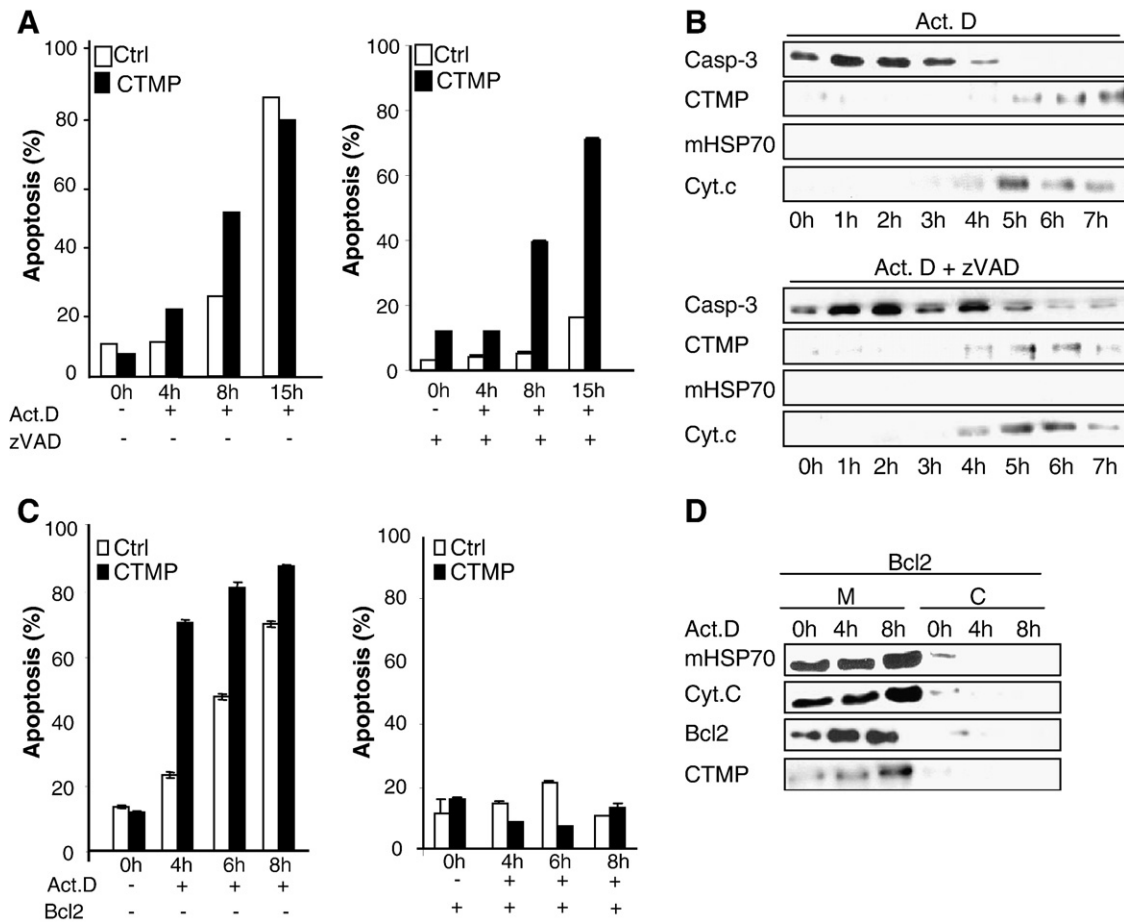


Fig. 8. CTMP release and CTMP-mediated apoptosis are blocked by Bcl-2 but not by the inhibition of caspases. (A) HeLa inducible cell lines expressing CTMP (CTMP) or not (Ctrl) were induced by tetracycline (2 $\mu\text{g}/\text{mL}$) for 5 days and then treated with 2 μM actinomycin D with or without zVAD-fmk (100 μM) for the indicated times. Apoptosis was measured using MitoProbe™ DiIC₁(5). (B) HeLa cells were treated with 2 μM actinomycin D with and without zVAD-fmk (100 μM) for the indicated times. Cytosolic extracts were analyzed by SDS-PAGE and caspase-3, CTMP, mHSP70 and cytochrome c detected by immunoblotting. (C) HeLa inducible cell lines expressing CTMP (CTMP) or not (Ctrl) were induced by tetracycline (2 $\mu\text{g}/\text{mL}$) for 4 days and then transfected with an empty vector or a flag-hBcl2 for 24 h in a tetracycline medium (2 $\mu\text{g}/\text{mL}$). Cells were treated with 2 μM actinomycin D for the indicated times and apoptosis monitored as described in (A). (D) HeLa cells were transiently transfected with Flag-hBcl2 for 24 h and then treated with 2 μM actinomycin D for the indicated times. CTMP release from mitochondria (M) into the cytosol (C) was monitored by immunoblotting. mHSP70, cytochrome c and Bcl-2 were used as controls. Data are the means and standard deviations from three independent experiments.

tagged at the N terminus, which apparently interfered with its proper localization. The presence of such positively charged amino acids in the N terminal region apparently facilitates protein insertion at the plasma membrane and, therefore, its interaction with PKB. We proposed that mitochondria-localized CTMP is released into the cytosol, where it negatively regulates PKB activation. To test this, we investigated whether CTMP interferes with PKB signalling during apoptosis. PKB is considered to be an anti-apoptotic protein [48,49], and has been reported recently to be phosphorylated and activated in response to genotoxic stress [50]. We demonstrated that PKB is phosphorylated transiently on Ser473 following actinomycin D (Fig. 9) or etoposide-treatment (Fig. S7) of cells transfected with an empty vector. Maximal phosphorylation was observed after 4 h of Actinomycin D treatment, with a slight decrease at 7 h. In contrast, Ser473 phosphorylation was delayed in cells overexpressing CTMP, being barely detectable after 4 h of treatment and only strongly visible after 7 h of apoptosis induction (Fig. 9A). We also observed that PKB Thr308 was phosphorylated after actinomycin D-treatment. Overexpression of CTMP could delay PKB Thr308 phosphorylation (Fig. S6). Importantly, there was no delay of phosphorylation in cells treated with actinomycin-D after CTMP knock-down (Fig. 9B). In these conditions, Ser473 phosphorylation occurred 4 h after apoptosis induction and was slightly higher after 7 h. Thus, CTMP is able to counteract PKB phosphorylation, as already described [19]. In cells overexpressing the

CTMP mutant CTMP m3, which cannot be released into the cytosol, Ser473 was also phosphorylated without delay after 4 h and 7 h actinomycin D treatment (Fig. 9C), suggesting that CTMP sequestered in the mitochondria cannot affect PKB phosphorylation on Ser473. However, the general level of PKB phosphorylation in CTMP m3 cells was lower than in control cells. For a reason not yet determined, cells overexpressing the mutant CTMP did not respond to the apoptotic stimulus with the intensity observed in the control cells. Taken together, these results show that CTMP delays PKB phosphorylation occurring at the onset of apoptosis. Thus, CTMP apparently sensitizes cells to apoptosis at least in part by inhibiting PKB activity.

4. Discussion

Approximately 10–15% of nuclear-encoded genes are mitochondrial pre-proteins synthesized on cytosolic ribosomes and directed to the surface of the mitochondria via their mitochondrial localization sequences. We report here that CTMP, a previously reported inhibitor of PKB/Akt [19], possesses the main characteristics of nuclear-encoded mitochondrial proteins, and we provide the first evidence that CTMP is able to modulate apoptosis. We have shown in different cell lines that both exogenous and endogenous CTMP reside in the mitochondria. *In silico* and *in vitro* approaches both revealed a critical requirement for the conserved N-terminal extension of CTMP in the proper sorting and

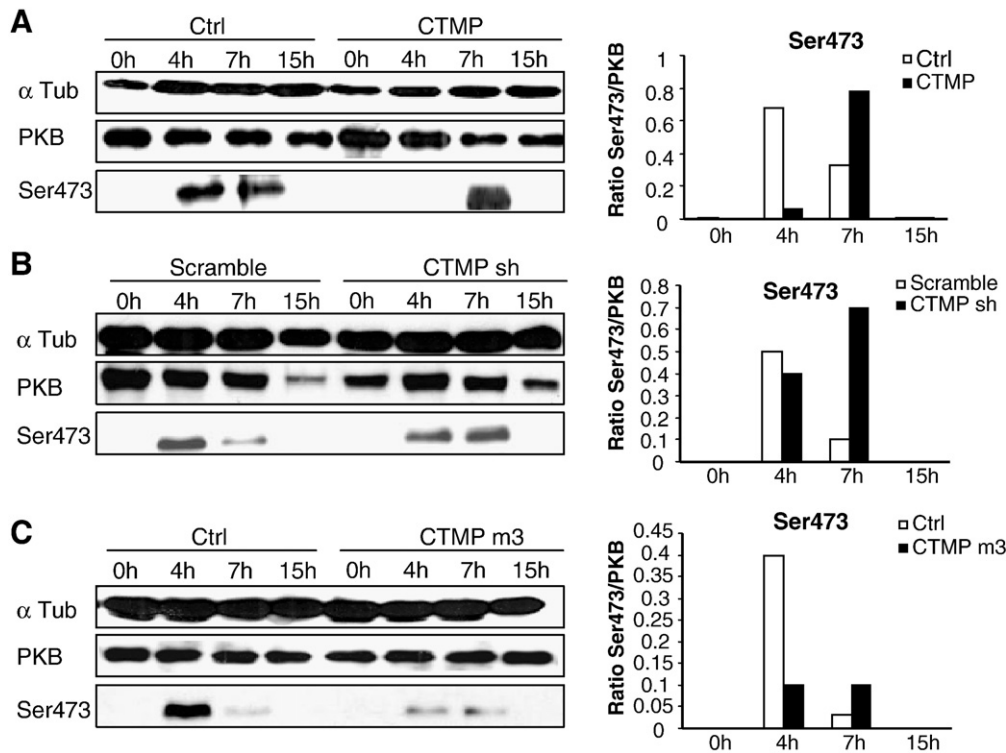


Fig. 9. CTMP delays PKB phosphorylation on Ser473 occurring upon induction of apoptosis. HeLa inducible cell lines expressing (A) CTMP, (B) shCTMP or (C) CTMP m3 were induced by tetracycline (2 $\mu\text{g}/\text{mL}$) for 5 days and then treated with 2 μM actinomycin D for the indicated times. Ctrl in (A) and (C) represents cells transfected with an empty vector whereas scramble RNA was transfected in (B). α -Tub, PKB, and Ser473 were detected by immunoblotting. Phospho-Ser473 was quantified using ImageQuant software™ (GE Healthcare).

localization of the mature protein into mitochondria. Moreover, a CTMP mutant refractory to mitochondrial membrane peptidase cleavage appeared to be sequestered in the mitochondrial inner membrane, suggesting that CTMP processing is similar to that previously described for mitochondrial class 1 proteins [34]. In the present study, we also found that CTMP is released from the mitochondria into the cytosol following cytotoxic stimulation.

CTMP overexpression sensitizes cells to apoptosis, whereas CTMP depletion or a defect in the CTMP maturation process lead to reduced or delayed cell death. Cells overexpressing CTMP, when not treated with a cytotoxic agent, do not suffer more apoptosis than control cells (Figs. 6B, D, and 8A), i.e. CTMP has no pro-apoptotic effects *per se*, but rather potentiates cell death occurring after apoptosis stimulation. Indeed, we observed that expression of a CTMP mutant lacking the first 36 amino acids that only resides in the cytosol does not induce apoptosis (data not shown). Thus the CTMP effect on apoptosis is dependent on the death stimulus applied to cells and is not only related to CTMP subcellular localization. Therefore, CTMP is not to be considered an inducer of apoptosis but rather as a protein able to sensitize cells to the process. CTMP knock-out mice recently generated in our laboratory are viable, fertile and, so far, exhibit only very subtle changes in phenotype. Preliminary data have shown that preputial glands from knock-out animals are significantly larger than in the wild type (unpublished data). Furthermore, caspase-3 was cleaved less in CTMP knock-out preputial glands. These observations confirm our results showing that lack of CTMP decreases apoptosis and may explain the increased size of preputial glands in knock-out animals. These mice will be characterized in detail and CTMP apoptotic functions studied *in vivo*.

The delay in PKB phosphorylation on Ser473 brought about by CTMP after induction of apoptosis suggests that pro-apoptotic effects of CTMP are mediated partially by PKB inhibition. CTMP was previously reported to be a negative regulator of PKB. These data were obtained using the Flag-CTMP construct, in which the tag was

attached to the N terminus of CTMP [19]. The epitope tag apparently interfered with CTMP localization and prevented CTMP import into the mitochondria. Instead, due to the presence of positively charged amino acids in the N terminal region, the protein apparently inserted into the plasma membrane and facilitated an interaction of CTMP with PKB. We now propose that CTMP localized in mitochondria under certain circumstances participates in the regulation of PKB signalling. Upon apoptosis, CTMP is released into the cytosol, where it appears to regulate PKB activation negatively. Further, PKB has been shown to translocate to different subcellular compartments, including the mitochondrial outer membrane, following plasma membrane activation [51–53]. Although the biological significance of the translocation of active PKB to the mitochondria is not yet clear, it has been reported to be cell type and stimulus specific [54,55]. These observations, combined with our results, lead us to propose a dynamic model by which CTMP modulates PKB activity in a specific subcellular compartment, the mitochondria or the cytosol, depending on the nature of the stimulus (survival or apoptosis). So far, we have not recorded any interaction between PKB and CTMP under apoptotic conditions (data not shown), which argues for an indirect mechanism by which CTMP delays PKB phosphorylation and, thus, its activation. PKB is at the crossroads of several mitochondria-mediated cell death pathways and is considered to be a strong anti-apoptotic protein [40,56,57]. Thus, plotting the apoptotic pathway in which PKB is involved, and that may be modulated by CTMP, is worthy of future study. Three PKB isoforms (PKB α , PKB β and PKB γ) have been identified in mammals that share a high degree of structural similarity and sequence homology. It is well established that each isoform plays a unique as well as a common role in cells [58]. Indeed, PKB proteins have crucial functions preventing cells entering apoptosis and there is evidence that the pro-survival effect of the isoforms is redundant [59–61]. Whether the effect of CTMP on apoptosis is specific or not for particular PKB isoforms needs to be investigated further.

Recently, a study showed unexpected data about enhancing PKB signalling by CTMP. The authors claim that CTMP overexpression induces PKB phosphorylation, leading to increased phosphorylation of downstream substrates, promoting survival and glucose metabolism [62]. Why they are not able to reproduce the inhibitory effect of CTMP on PKB activation is not yet clear. However, similarly to what Maira and colleagues did, they used a Flag-CTMP construct, in which the tag was attached to the N terminus of CTMP. As already described above, the epitope tag interferes with CTMP localization and does not allow CTMP to be imported into the mitochondria. Thus, CTMP function as a positive regulator of PKB signaling has to be considered as an artifact and cannot reflect the physiological role of CTMP in cells. In addition, another recent article favoring our observations that CTMP is a negative regulator of PKB showed that lentivirus-based CTMP delivery inhibits PKB activity through selective suppression of Ser473 phosphorylation, and preventing activation of PKB substrates involved in cell cycle [63].

PKB phosphorylation on the Thr308 residue of the activation loop and on the Ser473 residue of the hydrophobic motif are necessary for its full activation. Phosphoinositide-dependent kinase 1 (PDK1) phosphorylates Thr308 in the catalytic domain of PKB [64]. Recently, PKB and PDK1 were found in a preactivation complex, which is maintained in an inactive state through a PKB intramolecular interaction [65]. Regulation of Ser473 phosphorylation appears to be more complex. Several candidates were proposed to be the kinase responsible for phosphorylation of PKB Ser473 residue including PKB itself [66], PDK1 [67], integrin-linked kinase-1 (ILK1) [68], mitogen activated protein kinase activated protein kinase 2 (MAPKAP-K2) [69], protein kinase C β II (PKC β II) [70], and the members of the PI3 K-related protein kinase family including DNA dependent protein kinase (DNA-PK) [71,72], Ataxia telangiectasia mutated (ATM) [73], and mTOR complex 2 (mTORC2) [74]. Recently, interesting studies indicate that Ser473 phosphorylation is regulated in a stimulus specific manner. Thus, Ser473 is phosphorylated by mTORC2 under conditions of growth and mitogen stimulation [75] and in a situation of stress, as following DNA damage or presence of CpG DNA, we and others have established DNA-PK as the major PKB Ser473 kinase [50,76]. Our findings place PKB downstream of DNA-PK in the DNA damage response signaling cascade, where it provides a pro-survival signal, in particular by affecting transcriptional p21 regulation. Furthermore, this function is apparently restricted to the PKB α isoform. Moreover, in a recent study using genetically mouse models we reported that DNA-PK phosphorylated PKB on Ser473 upon DNA damage induced by gamma irradiation *in vivo*. In contrast, DNA-PK was dispensable for insulin and growth factor-induced PKB activation. [77]. Whether the PKB phosphorylation observed in apoptotic cells is dependent or not on DNA-PK will be further investigated. DNA-PK distribution will be also examined in our system since it has recently been shown that it can shuttle from the nucleus to the cytosol upon specific treatment [78]. As well, delineating the interplay between CTMP and Ser473 kinases would be of interest.

We have seen that Bcl2 was able to block CTMP release to the cytosol occurring upon induction of apoptosis (Fig. 8C and D). Bcl2 is known to be a potent anti-apoptotic protein, localized at the mitochondrial membrane. It is the founding member of the Bcl2 family of more than 30 proteins, including both pro- and anti-apoptotic molecules, and it has been well described that it can block apoptosis induced by various stimuli [79]. Interestingly, PKB has been reported to directly modulate Bcl2 pro-apoptotic members and therefore, PKB has been considered to be at the intersection of mitochondria-mediated cell death pathways [80–84]. The mechanism by which Bcl2 prevents CTMP to be release to the cytosol has not been yet investigated. It might be similar to the one inhibiting cytochrome c to get out of the mitochondria. Cytochrome c is retained in the cristae of the mitochondrial matrix and is considered to be a key molecule in programmed cell death [85]. Its release into the cytosol has been shown to be controlled by the pro-fusion protein OPA1 (optic atrophy

protein 1), which ensures that cytochrome c is sequestered into the mitochondria by maintaining the integrity of the cristae junctions [86,87]. We have observed that cytochrome c release into the cytosol occurs slightly earlier in cells overexpressing CTMP and treated with actinomycin D (unpublished data).

Since CTMP and cytochrome c release are almost concomitant, a positive feedback loop in which CTMP would indirectly target the mitochondria to liberate cytochrome c in the cytosol is very unlikely. However, we can speculate a role of CTMP in regulating mitochondrial dynamics. It has been shown that initiation of cell death triggered by cytochrome c release could be coordinated by “mitochondrial-shaping” proteins [88–90]. Among them, both pro-fission dynamin-related protein 1 (Drp1) and OPA1 have been described frequently as proteins involved in apoptosis [86,87]. Indeed, upon the induction of cell death the tubular and branched mitochondrial network undergoes remodelling, leading to its complete fragmentation [91,92]. Drp1 overexpression modulates mitochondrial dynamics and increases susceptibility to various apoptotic stimuli, whereas its cellular depletion shows protective effects [93]. Therefore, an imbalanced fusion/fission process is believed to disrupt the submitochondrial compartmentalization of many proteins needed to maintain mitochondria homeostasis, thus leading to apoptosis [40]. It is possible that CTMP mediates its effect by modulating the activity of some regulators of mitochondrial dynamics. Further experiments addressing the biological activity of CTMP are required [94].

To conclude, we have shown here for the first time that CTMP is a mitochondrial protein, localized both at the inner membrane and in the inner membrane space. CTMP is processed to get mature and released to the cytosol upon cell death stimulation. Cytosolic CTMP sensitizes cells to apoptosis, presumably by delaying PKB phosphorylation on Ser473 occurring in response to death signals. Delineating the mechanisms by which CTMP gets out of the mitochondria and positively modulates apoptosis needs further efforts, and these mechanisms are still under investigation.

Acknowledgements

We acknowledge our FMI colleagues and core facilities for contributions to this study, especially Dr. M. Rebhan for bioinformatic analysis and Dr. M. Hanada for CTMP mutant construction. We thank Dr. C. Borner (Albert Ludwigs University, Freiburg, Germany) and Dr. D.R. Green (St. Jude Children's Research Hospital, Memphis, USA) for plasmids. We also thank B. Surucu for help with experiments and Dr. P. King for editing the manuscript. LAT was the recipient of a long-term EMBO fellowship, AP was supported by grants from the Swiss Cancer League (OCS-01167-09-2001) and EZ is the recipient of a Swiss Bridge fellowship. The FMI is part of the Novartis Research Foundation.

Appendix A. Supplementary data

Supplementary data associated with this article can be found, in the online version, at [doi:10.1016/j.cellsig.2009.01.016](https://doi.org/10.1016/j.cellsig.2009.01.016).

References

- [1] R.S. Balaban, S. Nemoto, T. Finkel, *Cell* 120 (4) (2005) 483.
- [2] D.R. Green, G. Kroemer, *Science* 305 (5684) (2004) 626.
- [3] S.M. McWhirter, B.R. Tenover, T. Maniatis, *Cell* 122 (5) (2005) 645.
- [4] J.A. Smeitink, M. Zeviani, D.M. Turnbull, H.T. Jacobs, *Cell Metab.* 3 (1) (2006) 9.
- [5] H.M. McBride, M. Neuspiel, S. Wasiak, *Curr. Biol.* 16 (14) (2006) R551.
- [6] D.R. Green, *Cell* 121 (5) (2005) 671.
- [7] M. Brandon, P. Baldi, D.C. Wallace, *Oncogene* 25 (34) (2006) 4647.
- [8] D.J. Pagliarini, S.E. Calvo, B. Chang, S.A. Sheth, S.B. Vafai, S.E. Ong, G.A. Walford, C. Sugiana, A. Boneh, W.K. Chen, D.E. Hill, M. Vidal, J.G. Evans, D.R. Thorburn, S.A. Carr, V.K. Mootha, *Cell* 134 (1) (2008) 112.
- [9] N. Regev-Rudzki, O. Yogev, O. Pines, *J. Cell Sci.* 121 (Pt 14) (2008) 2423.
- [10] B. Dummler, B.A. Hemmings, *Biochem. Soc. Trans.* 35 (Pt 2) (2007) 231.
- [11] E. Fayard, L.A. Tintignac, A. Baudry, B.A. Hemmings, *J. Cell Sci.* 118 (Pt 24) (2005) 5675.
- [12] B.D. Manning, L.C. Cantley, *Cell* 129 (7) (2007) 1261.

- [13] D.A. Altomare, H.Q. Wang, K.L. Skele, A. De Rienzo, A.J. Klein-Szanto, A.K. Godwin, J.R. Testa, *Oncogene* 23 (34) (2004) 5853.
- [14] N. Hay, *Cancer Cell* 8 (3) (2005) 179.
- [15] J. Hutchinson, J. Jin, R.D. Cardiff, J.R. Woodgett, W.J. Muller, *Mol. Cell. Biol.* 21 (6) (2001) 2203.
- [16] A.J. Philp, I.G. Campbell, C. Leet, E. Vincan, S.P. Rockman, R.H. Whitehead, R.J. Thomas, W.A. Phillips, *Cancer Res.* 61 (20) (2001) 7426.
- [17] L.H. Saal, K. Holm, M. Maurer, L. Memeo, T. Su, X. Wang, J.S. Yu, P.O. Malmstrom, M. Mansukhani, J. Enoksson, H. Hibshoosh, A. Borg, R. Parsons, *Cancer Res.* 65 (7) (2005) 2554.
- [18] J.J. Zhao, O.V. Gjoerup, R.R. Subramanian, Y. Cheng, W. Chen, T.M. Roberts, W.C. Hahn, *Cancer Cell* 3 (5) (2003) 483.
- [19] S.M. Maira, I. Galetic, D.P. Brazil, S. Kaech, E. Ingley, M. Thelen, B.A. Hemmings, *Science* 294 (5541) (2001) 374.
- [20] K.S. Chae, M. Martin-Caraballo, M. Anderson, S.E. Dryer, *J. Neurophysiol.* 93 (3) (2005) 1174.
- [21] C.B. Knobbe, J. Reifenberger, B. Blaschke, G. Reifenberger, *J. Natl. Cancer Inst.* 96 (6) (2004) 483.
- [22] N. Maeda, W. Fu, A. Ortin, M. de las Heras, H. Fan, *J. Virol.* 79 (7) (2005) 4440.
- [23] L.A. Tintignac, V. Sirri, M.P. Leibovitch, Y. Lecluse, M. Castedo, D. Metivier, G. Kroemer, S.A. Leibovitch, *Mol. Cell. Biol.* 24 (4) (2004) 1809.
- [24] N.C. Shaner, R.E. Campbell, P.A. Steinbach, B.N. Giepmans, A.E. Palmer, R.Y. Tsien, *Nat. Biotechnol.* 22 (12) (2004) 1567.
- [25] M. van de Wetering, I. Oving, V. Muncan, M.T. Pon Fong, H. Brantjes, D. van Leenen, F.C. Holstege, T.R. Brummelkamp, R. Agami, H. Clevers, *EMBO Rep.* 4 (6) (2003) 609.
- [26] A. Hergovich, S. Lamla, E.A. Nigg, B.A. Hemmings, *Mol. Cell* 25 (4) (2007) 625.
- [27] S. Schlickum, A. Moghekar, J.C. Simpson, C. Steglich, R.J. O'Brien, A. Winterpacht, S.U. Ende, *Genomics* 83 (2) (2004) 254.
- [28] F. Grandjean, L. Bremaud, J. Robert, M.H. Ratinaud, *Biochem. Pharmacol.* 63 (5) (2002) 823.
- [29] K. Nakai, P. Horton, *Trends Biochem. Sci.* 24 (1) (1999) 34.
- [30] O. Emanuelsson, H. Nielsen, S. Brunak, G. von Heijne, *J. Mol. Biol.* 300 (4) (2000) 1005.
- [31] D.E. Knight, M.C. Scrutton, *Biochem. J.* 234 (3) (1986) 497.
- [32] H. Otera, S. Ohsakaya, Z. Nagaura, N. Ishihara, K. Mihara, *Embo J.* 24 (7) (2005) 1375.
- [33] K.S. Dimmer, F. Navoni, A. Casarin, E. Trevisson, S. Ende, A. Winterpacht, L. Salvati, L. Scorrano, *Hum. Mol. Genet.* 17 (2) (2008) 201.
- [34] J.M. Herrmann, K. Hell, *Trends Biochem. Sci.* 30 (4) (2005) 205.
- [35] W. Neupert, M. Brunner, *Nat. Rev. Mol. Cell Biol.* 3 (8) (2002) 555.
- [36] A.B. Taylor, B.S. Smith, S. Kitada, K. Kojima, H. Miyaura, Z. Otwinowski, A. Ito, J. Deisenhofer, *Structure* 9 (7) (2001) 615.
- [37] O. Gakh, P. Cavadini, G. Isaya, *Biochim. Biophys. Acta* 1592 (1) (2002) 63.
- [38] L. Galluzzi, M.C. Maiuri, I. Vitale, H. Zischka, M. Castedo, L. Zitvogel, G. Kroemer, *Cell Death Differ.* 14 (7) (2007) 1237.
- [39] G. Kroemer, L. Galluzzi, C. Brenner, *Physiol. Rev.* 87 (1) (2007) 99.
- [40] A. Parcellier, L.A. Tintignac, E. Zhuravleva, B.A. Hemmings, *Cell. Signal.* 20 (1) (2008) 21.
- [41] T. Glaser, M. Weller, *Biochem. Biophys. Res. Commun.* 281 (2) (2001) 322.
- [42] J.A. Heibin, M. Barry, B. Motyka, R.C. Bleackley, *J. Immunol.* 163 (9) (1999) 4683.
- [43] R.M. Kluck, E. Bossy-Wetzel, D.R. Green, D.D. Newmeyer, *Science* 275 (5303) (1997) 1132.
- [44] M. Schuler, E. Bossy-Wetzel, J.C. Goldstein, P. Fitzgerald, D.R. Green, *J. Biol. Chem.* 275 (10) (2000) 7337.
- [45] D.R. Green, J.C. Reed, *Science* 281 (5381) (1998) 1309.
- [46] J.C. Reed, *Blood* 111 (7) (2008) 3322.
- [47] R.J. Youle, A. Strasser, *Nat. Rev. Mol. Cell Biol.* 9 (1) (2008) 47.
- [48] T.F. Franke, D.R. Kaplan, L.C. Cantley, *Cell* 88 (4) (1997) 435.
- [49] B.A. Hemmings, *Science* 275 (5300) (1997) 628.
- [50] L. Bozulich, B. Surucu, D. Hynx, B.A. Hemmings, *Mol. Cell* 30 (2) (2008) 203.
- [51] M. Andjelkovic, D.R. Alessi, R. Meier, A. Fernandez, N.J. Lamb, M. Frech, P. Cron, P. Cohen, J.M. Lucocq, B.A. Hemmings, *J. Biol. Chem.* 272 (50) (1997) 31515.
- [52] M.T. Kunkel, Q. Ni, R.Y. Tsien, J. Zhang, A.C. Newton, *J. Biol. Chem.* 280 (7) (2005) 5581.
- [53] K. Sasaki, M. Sato, Y. Umezawa, *J. Biol. Chem.* 278 (33) (2003) 30945.
- [54] N. Ahmad, Y. Wang, K.H. Haider, B. Wang, Z. Pasha, O. Uzun, M. Ashraf, *Am. J. Physiol. Heart Circ. Physiol.* 290 (6) (2006) H2402.
- [55] G.N. Bijur, R.S. Jope, *J. Neurochem.* 87 (6) (2003) 1427.
- [56] S. Jin, R.S. DiPaola, R. Mathew, E. White, *J. Cell Sci.* 120 (Pt 3) (2007) 379.
- [57] D.W. Parsons, T.L. Wang, Y. Samuels, A. Bardelli, J.M. Cummins, L. DeLong, N. Silliman, J. Ptak, S. Szabo, J.K. Willson, S. Markowitz, K.W. Kinzler, B. Vogelstein, C. Lengauer, V.E. Velculescu, *Nature* 436 (7052) (2005) 792.
- [58] R.M. Biondi, A. Kieloch, R.A. Currie, M. Deak, D.R. Alessi, *Embo J.* 20 (16) (2001) 4380.
- [59] X. Liu, Y. Shi, M.J. Birnbaum, K. Ye, R. De Jong, T. Oltersdorf, V.L. Giranda, Y. Luo, *J. Biol. Chem.* 281 (42) (2006) 31380.
- [60] C. Quevedo, D.R. Kaplan, W.B. Derry, *Curr. Biol.* 17 (3) (2007) 286.
- [61] L. Yang, M. Sun, X.M. Sun, G.Z. Cheng, S.V. Nicosia, J.Q. Cheng, *J. Biol. Chem.* 282 (15) (2007) 10981.
- [62] H. Ono, H. Sakoda, M. Fujishiro, M. Anai, A. Kushiya, Y. Fukushima, H. Katagiri, T. Ogihara, Y. Oka, H. Kamata, N. Horike, Y. Uchijima, H. Kurihara, T. Asano, *Am. J. Physiol. Cell Physiol.* 293 (5) (2007) C1576.
- [63] S.K. Hwang, J.T. Kwon, S.J. Park, S.H. Chang, E.S. Lee, Y.S. Chung, G.R. Beck Jr., K.H. Lee, L. Piao, J. Park, M.H. Cho, *Gene Ther.* 14 (24) (2007) 1721.
- [64] D.R. Alessi, S.R. James, C.P. Downes, A.B. Holmes, P.R. Gaffney, C.B. Reese, P. Cohen, *Curr. Biol.* 7 (4) (1997) 261.
- [65] V. Calleja, D. Alcor, M. Laguerre, J. Park, B. Vojnovic, B.A. Hemmings, J. Downward, P.J. Parker, B. Larjani, *PLoS Biol.* 5 (4) (2007) e95.
- [66] A. Toker, A.C. Newton, *J. Biol. Chem.* 275 (12) (2000) 8271.
- [67] A. Balendran, R. Currie, C.G. Armstrong, J. Avruch, D.R. Alessi, *J. Biol. Chem.* 274 (52) (1999) 37400.
- [68] S. Persad, S. Attwell, V. Gray, N. Mawji, J.T. Deng, D. Leung, J. Yan, J. Sanghera, M.P. Walsh, S. Dedhar, *J. Biol. Chem.* 276 (29) (2001) 27462.
- [69] D.R. Alessi, M. Andjelkovic, B. Caudwell, P. Cron, N. Morrice, P. Cohen, B.A. Hemmings, *Embo J.* 15 (23) (1996) 6541.
- [70] Y. Kawakami, H. Nishimoto, J. Kitaura, M. Maeda-Yamamoto, R.M. Kato, D.R. Littman, M. Leitges, D.J. Rawlings, T. Kawakami, *J. Biol. Chem.* 279 (46) (2004) 47720.
- [71] A.M. Dragoi, X. Fu, S. Ivanov, P. Zhang, L. Sheng, D. Wu, G.C. Li, W.M. Chu, *Embo J.* 24 (4) (2005) 779.
- [72] J. Feng, J. Park, P. Cron, D. Hess, B.A. Hemmings, *J. Biol. Chem.* 279 (39) (2004) 41189.
- [73] J.G. Viniestra, N. Martinez, P. Modirassari, J.H. Losa, C. Parada Cobo, V.J. Lobo, C.I. Luquero, L. Alvarez-Vallina, S. Ramon y Cajal, J.M. Rojas, R. Sanchez-Prieto, *J. Biol. Chem.* 280 (6) (2005) 4029.
- [74] D.D. Sarbassov, D.A. Guertin, S.M. Ali, D.M. Sabatini, *Science* 307 (5712) (2005) 1098.
- [75] C. Shiota, J.T. Woo, J. Lindner, K.D. Shelton, M.A. Magnuson, *Dev. Cell* 11 (4) (2006) 583.
- [76] K.A. Boehme, R. Kulikov, C. Blattner, *Proc. Natl. Acad. Sci. U. S. A.* 105 (22) (2008) 7785.
- [77] B. Surucu, L. Bozulich, D. Hynx, A. Parcellier, B.A. Hemmings, *J. Biol. Chem.* 283 (44) (2008) 30025.
- [78] E. Huston, M.J. Lynch, A. Mohamed, D.M. Collins, E.V. Hill, R. MacLeod, E. Krause, G.S. Baillie, M.D. Houslay, *Proc. Natl. Acad. Sci. U. S. A.* 105 (35) (2008) 12791.
- [79] D.L. Vaux, S. Cory, J.M. Adams, *Nature* 335 (6189) (1988) 440.
- [80] S.R. Datta, A. Brunet, M.E. Greenberg, *Genes Dev.* 13 (22) (1999) 2905.
- [81] S.J. Gardai, D.A. Hildeman, S.K. Frankel, B.B. Whitlock, S.C. Frasch, N. Borregaard, P. Marrack, D.L. Bratton, P.M. Henson, *J. Biol. Chem.* 279 (20) (2004) 21085.
- [82] N. Majewski, V. Nogueira, R.B. Robey, N. Hay, *Mol. Cell. Biol.* 24 (2) (2004) 730.
- [83] A. Nechushtan, C.L. Smith, Y.T. Hsu, R.J. Youle, *Embo J.* 18 (9) (1999) 2330.
- [84] H. Yamaguchi, H.G. Wang, *Oncogene* 20 (53) (2001) 7779.
- [85] B. Zhivotovsky, S. Orrenius, O.T. Brustugun, S.O. Doskeland, *Nature* 391 (6666) (1998) 449.
- [86] S. Cipolat, T. Rudka, D. Hartmann, V. Costa, L. Serneels, K. Craessaerts, K. Metzger, C. Frezza, W. Annaert, L. D'Adamio, C. Derks, T. Dejaegere, L. Pellegrini, R. D'Hooge, L. Scorrano, B. De Strooper, *Cell* 126 (1) (2006) 163.
- [87] C. Frezza, S. Cipolat, O. Martins de Brito, M. Micaroni, G.V. Beznoussenko, T. Rudka, D. Bartoli, R.S. Polishuck, N.N. Danial, B. De Strooper, L. Scorrano, *Cell* 126 (1) (2006) 177.
- [88] G.M. Cereghetti, L. Scorrano, *Oncogene* 25 (34) (2006) 4717.
- [89] E. Gottlieb, *Cell* 126 (1) (2006) 27.
- [90] L. Pellegrini, L. Scorrano, *Cell Death Differ.* 14 (7) (2007) 1275.
- [91] S. Frank, B. Gaume, E.S. Bergmann-Leitner, W.W. Leitner, E.G. Robert, F. Catez, C.L. Smith, R.J. Youle, *Dev. Cell* 1 (4) (2001) 515.
- [92] R. Jagasia, P. Grote, B. Westermann, B. Conradt, *Nature* 433 (7027) (2005) 754.
- [93] Y.J. Lee, S.Y. Jeong, M. Karbowski, C.L. Smith, R.J. Youle, *Mol. Biol. Cell* 15 (11) (2004) 5001.
- [94] J.R. Cross, A. Postigo, K. Blight, J. Downward, *Cell Death Differ.* 115 (6) (2008) 997.

7.4 PKB and the mitochondria: AKTing on apoptosis

Parcellier A., Tintignac L.A., Zhuravleva E., Hemmings B.A. Cell Signal, 2008;
20(1):21-30

Review

PKB and the mitochondria: AKTing on apoptosis

Arnaud Parcellier, Lionel A. Tintignac, Elena Zhuravleva, Brian A. Hemmings*

Friedrich Miescher Institute for Biomedical Research, Maulbeerstrasse 66, 4058 Basel, Switzerland

Received 6 July 2007; accepted 18 July 2007

Available online 25 July 2007

Abstract

Cellular homeostasis depends upon the strict regulation of responses to external stimuli, such as signalling cascades triggered by nutrients and growth factors, and upon cellular metabolism. One of the major molecules coordinating complex signalling pathways is protein kinase B (PKB), a serine/threonine kinase also known as Akt. The number of substrates known to be phosphorylated by PKB and its interacting partners, as well as our broad understanding of how PKB is implicated in responses to growth factors, metabolic pathways, proliferation, and cell death via apoptosis is constantly increasing. Activated by the insulin/growth factor-phosphatidylinositol 3-kinase (PI3K) cascade, PKB triggers events that promote cell survival and prevent apoptosis. It is also now widely accepted that mitochondria are not just suppliers of ATP, but that they participate in regulatory and signalling events, responding to multiple physiological inputs and genetic stresses, and regulate both cell proliferation and death. Thus, mitochondria are recognized as important players in apoptotic events and it is logical to predict some form of interplay with PKB. In this review, we will summarize mechanisms by which PKB mediates its anti-apoptotic activities in cells and survey recent developments in understanding mitochondrial dynamics and their role during apoptosis.

© 2007 Elsevier Inc. All rights reserved.

Keywords: AKT/PKB; Mitochondria; Apoptosis; Mitochondrial fission/fusion

Contents

1.	Introduction	22
2.	PKB and mitochondria: inter-connection in cell survival	22
2.1.	Direct modulation of apoptosis mediated by PKB	24
2.1.1.	Bcl-2 pro-apoptotic members	24
2.1.2.	AIF	24
2.1.3.	Htra2/Omi	24
2.1.4.	Caspase-9	25
2.1.5.	DNA fragmentation factor (DFF40/CAD).	25
2.1.6.	Acinus	25
2.1.7.	The SAPK pathway	25
2.1.8.	Heat-shock proteins	25
2.1.9.	GSK-3.	25
2.1.10.	Hexokinases.	25
2.2.	Indirect modulation of apoptosis mediated by PKB	26
2.2.1.	Forkhead family members	26
2.2.2.	Murine double minute 2 (Mdm2)	26
2.2.3.	NF- κ B	26
2.2.4.	Cyclic AMP-response element-binding protein (CREB)	26

* Corresponding author. Tel.: +41 61 6974872; fax: +41 61 6973976.

E-mail address: brian.hemmings@fmi.ch (B.A. Hemmings).

2.2.5. Yes-associated protein (YAP)	27
2.3. PKB isoform redundancy during apoptosis	27
3. New insight into apoptosis: initiation and further directions	27
4. Conclusions	28
Acknowledgements	28
References	28

1. Introduction

After the p53 pathway, the PI3K–PTEN–PKB/Akt signalling pathway is one of the most mutated pathways associated with cancer [1,2]. Together they may be seen as a network regulating cell responses to external stimuli and metabolic processes. Once activated, PI3K mediates conversion of PIP2 (phosphatidylinositol (4,5)-bisphosphate) into PIP3 (phosphatidylinositol (3,4,5)-trisphosphate), leading to the recruitment of downstream targets to the cell membrane and their subsequent activation [3]. PKB, a serine/threonine kinase also known as Akt, is recognized to be a primary mediator of the downstream effects of PI3K, coordinating a variety of intracellular signals and, thus, controlling cell responses to extrinsic stimuli and regulating cell proliferation and survival [4,5]. Under normal physiological conditions, PKB is activated by growth factors, insulin, and DNA damage, and is translocated from the cell membrane to its target genes, supporting the complex regulatory network [6,7].

Activated PKB is localized to various subcellular compartments, including the Golgi, endoplasmic reticulum, mitochondria and nucleus [8], where it phosphorylates substrates or interacts with other molecules. PKB effects on the regulation of cell proliferation are mediated by multiple effectors. For example, anti-apoptotic activity is resolved through the inactivation of many pro-apoptotic factors. In contrast to the p53 pathway, which is silenced in cancer cells, the PI3K–PTEN–PKB/Akt pathway is activated in many tumours as a result of upstream mutations in PI3K [9–12] or PTEN (phosphatase and tensin homologue mutated in multiple advanced cancer) [1,13], or of the amplification/overexpression/mutation of PKB isoforms themselves [10,14–19]. Consequently, the constitutive activation of PKB contributes greatly to aberrant cell cycle regulation, a hallmark of many cancers, resulting in uncontrolled cell proliferation and suppressed apoptotic pathways [20–24].

Mitochondria are now recognized as important players in apoptotic events. About two billion years ago, after the incorporation of purple eubacteria and the formation of a symbiotic relationship, cells acquired the ability to survive in a new environment, utilizing aerobic metabolism [25,26]. As a key node in oxidative metabolism in eukaryotes, mitochondria supply the majority of cellular energy, sustaining viability and normal cell functions. It is now widely accepted that mitochondria are not solely ATP suppliers but participate in regulatory and signalling events, responding to multiple physiological inputs and genetic stresses and regulating cell proliferation and death. They sense and integrate signals from

translocated proteins and Ca^{2+} fluxes, and transmit them to oxidative stress and other metabolic pathways [27]. Mitochondria have been shown to be dynamic tubular networks that constantly undergo fusion and fission in response to local environmental changes, with associated changes in morphology. Following pro-apoptotic stimulation leading to permeabilization of the outer mitochondrial membrane (OMM), numerous proteins are released from the mitochondria to the cytosol, where they act either by activating caspases in the cytosol or by stimulating endonuclease activity in the nucleus. In addition to OMM permeabilization, it has also been reported that the remodelling of cristae occurs early in the apoptotic process, favouring the release of cytochrome *c*. It was suggested recently that proteins known to regulate mitochondrial fusion in yeast [28] are regulators of cristae remodelling [29,30]. This connection between mitochondrial morphology, cristae remodelling and apoptotic events still remains to be clarified, but a place for mitochondria in the constellation of intracellular pathways cannot be excluded.

Several excellent reviews have discussed the role of PKB in the development of a variety of metabolic diseases and cancer [11,31] or the substrate specificity of PKB [32]. Many reviews have also described the role of mitochondria in metabolic disorders and apoptotic processes. Here we focus on the role of PKB in apoptosis, accentuating its networking with the mitochondria in the regulation and inter-connection of metabolic pathways and cell survival.

2. PKB and mitochondria: inter-connection in cell survival

Of its various cellular functions, there is extensive evidence that PKB plays a central role in regulating growth factor-mediated cell survival and blocking cell death [22]. For example, transgenic mice that constitutively express active PKB α in mammary glands show a delay in mammary gland involution due to the inhibition of cell death [33]. PKB has also been shown to exert a neuroprotective effect against brain damage in genetically modified mice expressing an active form of PKB in neuronal cells [34]. Cell death is critical for the organization of cells and tissues in the body. In animals, the physiological mechanism of cell death is an active and gene-regulated process [35]. Apoptosis deregulation is involved in the pathogenesis of various diseases and, thus, strict control of the apoptotic machinery is required [36]. Moreover, apoptosis is one of the principal cell death mechanisms triggered by cytotoxic drugs in tumour cells [37] and novel apoptosis-targeted therapies are now advancing from pre-clinical and clinical trials to clinical application [38,39].

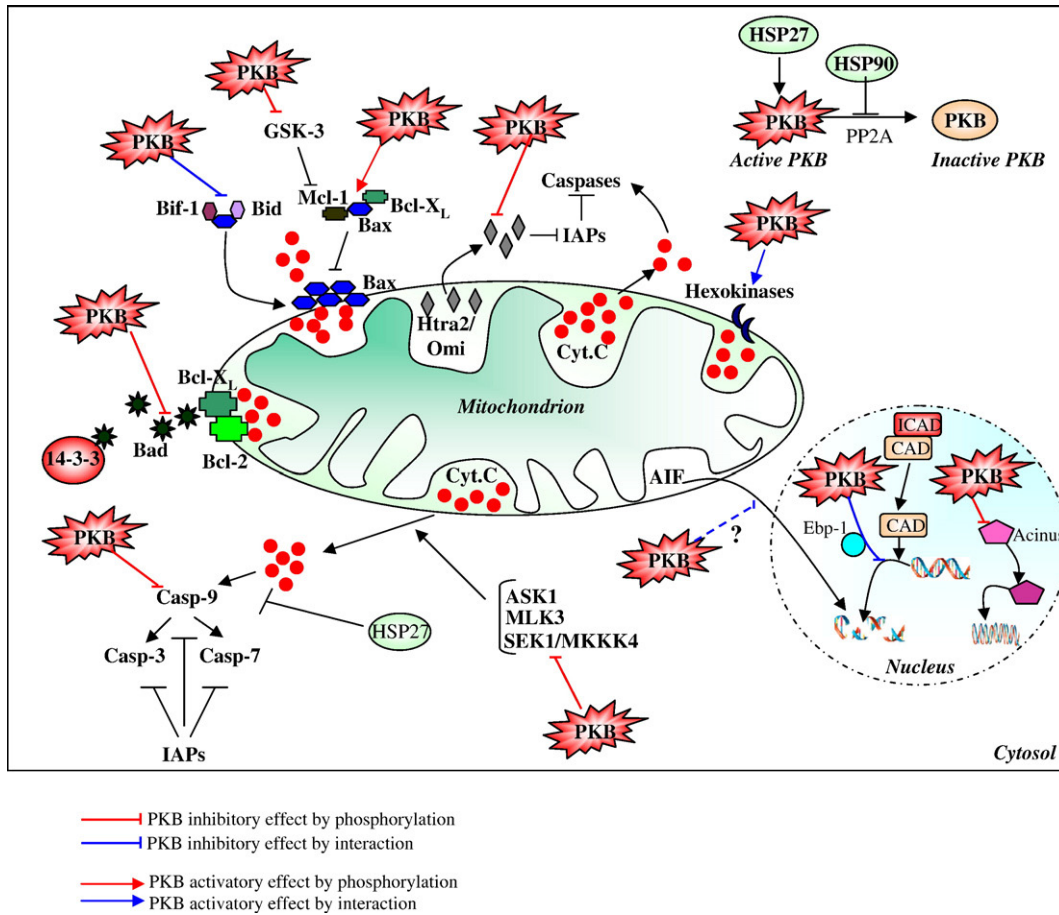


Fig. 1. Direct modulation of apoptosis by PKB. Mitochondria play a pivotal role in apoptosis regulation, acting as a central cell executioner by releasing various pro-apoptotic molecules (cytochrome *c*, Htra2/Omi, AIF) from their intermembrane space into the cytosol. At the pre-mitochondrial level, the anti-apoptotic HSP27 and HSP90 proteins stimulate and protect PKB activation, reinforcing PKB effects on cell death, for example by inhibiting the SAPK pathway. The Bcl-2 family of proteins may represent a critical checkpoint in the mitochondrial intrinsic pathway of apoptosis and its members control cytochrome *c* release to the cytosol. By phosphorylating the pro-apoptotic molecule Bad, PKB induces its association with 14-3-3 proteins in the cytosol and thus contributes to the inhibition of Bad cell death functions. PKB also phosphorylates another pro-apoptotic member of the Bcl-2 family, Bax. Phosphorylated Bax promotes heterodimerization with Mcl-1 and Bcl-X_L, leading to abrogation of Bax activity. Moreover, PKB has been found to phosphorylate and negatively regulate the Mcl-1 inhibitor, GSK-3. PKB is also inhibits Bax functions by directly interfering with the interaction of Bax with Bid or Bif-1. Cytochrome *c* release can also be blocked by binding of PKB to hexokinases, thus inhibiting apoptosis-associated hexokinase detachment from mitochondria. Htra2/Omi and AIF, two further mitochondrial proteins released into the cytosol upon apoptosis, can be inhibited by PKB phosphorylation or PKB interaction, respectively. At the post-mitochondrial level, PKB may phosphorylate and inactivate caspase-9, resulting in the abolition of the caspase cascade. PKB can also move to the nucleus, where it inhibits DNA fragmentation and condensation by effects on CAD and acinus, respectively.

The two main pathways of apoptosis described for mammals are the extrinsic and the intrinsic pathways. The extrinsic or death receptor-mediated pathway plays a major role in, for example, the immune system (for more information, see reviews [40,41]). The intrinsic pathway, also called the mitochondrial-dependent pathway, is activated in response to extracellular or intracellular insults such as DNA damage. The first evidence for the involvement of mitochondria in apoptosis was obtained 15 years ago, when Stanley Korsmeyer’s lab showed that the Bcl-2 protein, which was already known to be an anti-apoptotic protein, was localized at the mitochondrial membrane and was able to interfere with programmed cell death. It is now widely accepted that mitochondria play a pivotal role in the regulation of apoptosis. These organelles are not only required for ATP production, but also act as a central cell “executioner” by releasing various pro-apoptotic molecules from their intermembrane space into the cytosol [42]. Pioneering biochemical fractionation and reconstitution studies by

Wang and collaborators have shed light on this pathway [43,44]. Cytochrome *c*, a well-known component of the mitochondrial respiratory chain, appears to be the key protein of the programmed cell death process [45]. The mechanism of cytochrome *c* release has been the subject of intense investigations and different models have been proposed. Recent studies propose a two-step release in which the cytochrome *c* is first detached from the mitochondrial inner membrane, and then extruded upon permeabilization of the outer membrane [46]. Once in the cytosol, cytochrome *c* interacts with its adaptor molecule Apaf-1 (apoptotic protease activation factor-1), thereby triggering the ATP/dATP-dependent oligomerization of Apaf-1 [43,47]. Oligomerized Apaf-1 binds to procaspase-9, leading to the formation of the caspase-9 activation complex, the so-called apoptosome [48]. In turn, activated caspase-9 triggers proteolytic maturation of pro-caspase-3 and -7 responsible for the cleavage of several proteins, and this finally leads to the biological and morphological features characteristic of

apoptotic cell death [49]. Other pro-apoptotic molecules like AIF (apoptosis inducing factor), Smac/Diablo (second mitochondria-derived activator of caspases/direct inhibitor of apoptosis-binding protein with a low isoelectric point), HtrA2/Omi (high temperature requirement protein), and the endonuclease G are also released from the mitochondrial intermembrane space into the cytosol, and trigger apoptosis. However, the modes of action of these proteins are completely different to that of cytochrome *c*. For example, the flavoprotein AIF and the endonuclease G operate through a caspase-independent pathway. They participate in chromatin condensation and DNA fragmentation in mammalian cells, respectively [50–53]. On the other hand, Smac/Diablo and HtrA2/Omi both activate apoptosis by neutralizing the inhibitory activity of the IAPs (inhibitory apoptotic proteins) that associate with and inhibit caspases [54]. Thus, the permeabilization of the mitochondrial outer membrane, allowing the release of intermembrane space proteins, appears to be the key step in the apoptotic process. Current models explaining mitochondrial outer membrane permeabilization include: (1) the induction of mitochondrial permeability transition [55,56], (2) the modulation of ions fluxes and hypotonicity [57], (3) a caspases feed-back loop [58] and specific caspase-2 engagement to the mitochondria [59,60], and (4) the involvement of Bcl-2 family proteins [61,62]. Presumably, these mechanisms are dependent on cell type and the nature of the stimulus.

Like PKB, the Bcl-2 protein has also been shown to play a role in cancer progression. Bcl-2 was originally cloned from the *t*(14;18) translocation breakpoint found in follicular B-cell lymphomas [63]. However, in contrast to PKB, Bcl-2 does not promote cell proliferation but rather blocks cell death induced by various stimuli [64]. Bcl-2 is the founding member of the Bcl-2 family of more than 30 proteins, including both pro- and anti-apoptotic molecules. Three main subgroups of these proteins have been defined, in part by structural homologies: (1) Bcl-2-like survival factors (e.g. Bcl-2, Bcl-X_L, Mcl-1), (2) Bax-like death factors (e.g. Bax, Bak), (3) BH3-only death factors (e.g. Bid, Bad) [57]. Members of this family are critical checkpoints in the intrinsic pathway of apoptosis. It has been proposed that Bcl-2-related proteins act as a “rheostat” regulating sensitivity of cells to apoptosis. In this scenario, the mitochondrion appears to be a central, important integrator of Bcl-2 protein activities. Thus, cell fate depends on the balance between anti- and pro-apoptotic members of the Bcl-2 family [65,66].

PKB is able to directly or indirectly modulate apoptosis [21,67]. The direct effects are connected to phosphorylation events or interactions with cell death actors (Fig. 1), whereas the indirect regulation of apoptosis is mediated rather through the transcriptional responses to apoptotic stimuli (Fig. 2). In both cases, PKB is at the crossroads of several mitochondria-mediated cell death pathways and is, thus, an important target for cancer therapy [68,69].

2.1. Direct modulation of apoptosis mediated by PKB

2.1.1. Bcl-2 pro-apoptotic members

Bad, as the first PKB target involved in apoptosis to be identified (in 1997) [70,71] is a pro-apoptotic member of the

Bcl-2 family of proteins that binds Bcl-2 or Bcl-X_L. In this way, Bad blocks their anti-apoptotic properties. However, phosphorylation of Bad on Ser136 by PKB releases it from the complex with Bcl-2/Bcl-X_L that is localized on the mitochondrial membrane and subsequently promotes its association with 14-3-3 proteins in the cytosol. Thus, by phosphorylating Bad, PKB inhibits its cell death functions [72].

Bax is a further pro-apoptotic member of the Bcl-2 family that is regulated by the PKB signalling pathway. The Bax protein resides mainly in the cytosol of healthy cells, but apoptotic stimuli induce a conformational change that exposes its N- and C-termini. This new Bax folding appears to be required for its insertion into mitochondrial membranes [73], where it forms oligomers causing cytochrome *c* release and apoptotic cell death. Overexpression of active PKB suppresses the relocalization of Bax to mitochondria, and PKB also inhibits the Bax conformational change, preventing disruption of the mitochondrial membrane potential and caspase-3 activation [74]. The mechanism by which PKB suppresses Bax oligomerization was first reported in two papers published in 2004 and 2005 [75,76]. Both showed that PKB phosphorylates Bax on Ser184. The phosphorylated form of Bax is found predominantly in the cytosol where it promotes heterodimerization with Mcl-1 and Bcl-X_L. PKB is the physiological Bax kinase responsible for abrogation of its pro-apoptotic activities. An alternative explanation is that PKB directly interferes with the interaction of Bax with Bid or Bif-1, both of which contribute to Bax conformational changes [77].

2.1.2. AIF

The apoptosis inducing factor (AIF) is normally confined to the mitochondrial intermembrane space and is released into the cytosol upon induction of apoptosis, depending on the cell type and the nature of the stimulus [78]. Once in the cytosol, mature AIF translocates to the nucleus, where it induces chromatin condensation and high-molecular-weight (50-kb) DNA fragmentation [79]. Recently, it has been shown that an active form of PKB blocks ceramide-induced neuronal apoptosis through inhibition of AIF translocation to the nucleus [80]. However, ceramide treatment has also been reported to induce PKB dephosphorylation [81]. The mechanism by which PKB mediates the inhibition of AIF inhibition needs further investigation but AIF can now be considered to be a promising novel PKB target.

2.1.3. Htra2/Omi

Htra2/Omi is a serine protease synthesized as a precursor and localized in the mitochondria [82]. Following apoptotic stimuli, the N-terminal part of Htra2/Omi is cleaved and the protein is released to the cytosol, where it induces apoptosis by inhibiting IAPs (inhibitors of apoptosis) [83,84]. A recent report showed that PKB α and PKB β phosphorylate mitochondria-released Htra2/Omi on Ser212 *in vitro* and *in vivo* [85]. This results in attenuation of Htra2/Omi serine protease activity and decreases its pro-apoptotic functions. The phosphorylated form of Htra2/Omi still interferes with but fails to cleave XIAP. PKB may also inhibit Htra2/Omi release from mitochondria to the cytosol in response to cisplatin treatment.

2.1.4. Caspase-9

Caspase-9 acts as an initiator of the apoptotic process as part of the apoptosome complex. It has been reported that PKB directly phosphorylates human caspase-9 on Ser196, resulting in its inactivation [86]. However, the phosphorylation site found in human caspase-9 is not conserved and is not present in other mammalian species such as mouse, rat and monkey [87]. Thus, the role of PKB in caspase-9 regulation remains to be clarified.

2.1.5. DNA fragmentation factor (DFF40/CAD)

A caspase-activated DNase, DFF40/CAD, has been shown to have a major role in DNA fragmentation, which along with condensation is a further hallmark of apoptosis. DFF40/CAD resides in the nucleus as a complex with its specific inhibitor DFF45/ICAD. Apoptotic activation of caspase -3 and -7 results in DFF45/ICAD cleavage, leading to active DFF40/CAD nuclease release [88]. Ebp1, a ubiquitous protein of the cytosol and nucleus, has been identified recently as a factor contributing to the inhibition of DNA fragmentation by DFF40/CAD. PKC-dependent phosphorylation of Ebp1 has been reported to stimulate its binding to phosphorylated nuclear PKB in nerve growth factor-treated PC12 cells. The resulting complex interacted with DFF40/CAD, inhibiting its DNA fragmentation activity and enhancing Ebp1 anti-apoptotic activity. Thus, PKB contributes to the suppression of apoptosis through an interaction with Ebp1 [89]. However, this effect appears to be independent of PKB kinase activity.

2.1.6. Acinus

Acinus is a nuclear pro-apoptotic protein activated by caspase cleavage and involved in chromatin condensation [90]. Recently, it was shown that PKB phosphorylation of acinus on Ser422 and Ser573 leads to resistance of acinus to caspase cleavage and inhibition of chromatin condensation [91]. Moreover, abolishing phosphorylation of acinus by PKB through mutagenesis, accelerated its proteolytic degradation and also chromatin condensation. Thus, PKB may promote cell survival by blocking acinus nuclear apoptotic effects.

2.1.7. The SAPK pathway

Activation of the stress-activated protein kinase (SAPK) pathway is thought to trigger mitochondria-dependent apoptosis in response to many types of stress. SAPK is composed of two groups of kinases, JNK and p38 MAP kinase. PKB was reported to phosphorylate three kinases upstream of SAPK, namely ASK1, MLK3 and SEK1/MKKK4. PKB phosphorylates ASK1 on Ser83 [92], MLK3 on Ser674 [93] and SEK1/MKKK4 on Ser78 [94]. Phosphorylation results in the inactivation of these three proteins and promotes cell survival.

2.1.8. Heat-shock proteins

The ubiquitous and highly conserved stress- or heat-shock proteins (HSPs) are induced in response to a wide variety of physiological and environmental insults and allow the cells to survive otherwise lethal conditions [95]. Various mechanisms have been proposed to account for the cytoprotective functions of HSPs: (1) by assisting the correct folding of stress-accumulated misfolded proteins and preventing their aggregation, (2) by

interacting with components of the apoptotic machinery, and (3) by interfering with the proteasome-mediated degradation of selected proteins under stress conditions [96]. The HSP family of proteins comprises several members but only two have been convincingly reported to play a role in PKB-mediated cell survival [97,98]. HSP90 has been shown to form a complex with PKB *in vivo*. By binding to PKB, HSP90 inhibits the dephosphorylation of PKB mediated by protein phosphatase 2A and its sustained activation prevents cell death. HSP27, a small heat-shock protein found to inhibit apoptosis by binding cytochrome *c* released into the cytosol, has been described as a PKB activator during various forms of stress [99]. In cells subjected to oxidative stress, PKB is activated gradually and the association with HSP27 concomitantly increases. In a recent report, prevention of PKB/HSP27 interaction by anti-HSP27 antibody treatment resulted in inhibition of PKB phosphorylation on Ser473 and induction of apoptosis [100]. Moreover, it was shown that HSP27 contributes to the protection of L929 mouse cells from cisplatin-induced apoptosis by enhancing PKB activation [101].

2.1.9. GSK-3

The glycogen synthase kinase 3 (GSK-3) has two isoforms, GSK-3 α and GSK-3 β , that are inactivated upon phosphorylation by PKB on Ser21 and Ser9, respectively [102]. Inhibition of GSK-3 has been found to protect against apoptosis in many circumstances [103], although the molecular basis for this was not clearly understood until recently. In 2006, Green and co-workers showed that GSK-3 induces apoptosis upon interleukin-3 withdrawal by stimulating phosphorylation of the anti-apoptotic member of the Bcl-2 family, Mcl-1. As a consequence, ubiquitination of the phosphorylated Mcl-1 was increased, leading to its degradation by the proteasome and facilitating cytochrome *c* release and apoptosis [104]. This clearly demonstrates the crucial need for PKB regulation, since PKB negatively regulates GSK-3 activation and, therefore, Mcl-1 stability.

2.1.10. Hexokinases

Cell survival and energy metabolism are closely linked and PKB appears to be a common mediator of both metabolic and anti-apoptotic effects of growth factors. Similarly to Bcl-2, activated PKB is able to maintain mitochondrial integrity by inhibiting cytochrome *c* release in mammalian cells [105]. However, unlike Bcl-2, PKB requires the availability of glucose for these effects [106,107]. These observations led to investigations of the role of mitochondrial hexokinases as mediators of PKB anti-apoptotic properties. Hexokinases have a crucial function in the cellular uptake and utilization of glucose. They control the first step of glucose metabolism by catalysing ATP-dependent phosphorylation of glucose to glucose-6-phosphate [108]. Two hexokinase isoforms, HKI and HKII, have been shown to specifically bind to the outer mitochondrial membrane (OMM) at mitochondrial contact sites [109]. Several reports present mitochondrial hexokinases as downstream effectors of growth factor- and PKB-mediated cell survival. PKB is able to block apoptosis-associated hexokinase detachment from mitochondria [106] and, thus, PKB/hexokinase interaction

may in some way prevent cytochrome *c* release. This was confirmed by the finding that HKI and HKII can mimic the ability of PKB to inhibit apoptosis [110]. Moreover, like PKB, mitochondrial hexokinases require glucose for promoting cell survival and hexokinase association with mitochondria correlates with PKB ability to maintain OMM integrity [77,111]. Lastly, the disruption of hexokinase/mitochondria interaction impairs anti-apoptotic and mitochondrial integrity-promoting functions of PKB [110]. It would appear that the metabolic regulatory function of PKB has evolved into an adaptive sensing system involving mitochondrial hexokinases and a coupling metabolism to cell survival [112].

2.2. Indirect modulation of apoptosis mediated by PKB

The control of apoptosis execution mediated by PKB also involves changes in the transcription programme. By regulating transcriptional factors responsible for the expression of pro- or anti-apoptotic molecules, PKB also plays a crucial role in determining cell fate (Fig. 2).

2.2.1. Forkhead family members

It has been shown that PKB is able to directly phosphorylate Forkhead protein (FoxO) isoforms (FKHR/FoxO1, FoxO2, FKHL1/FoxO3 and AFX/FoxO4) and in this way it is responsible for their nuclear exclusion and inactivation [113,114]. FoxO target genes are important for inhibition of cell survival and the promotion of apoptosis. For example, FoxO proteins regulate expression of Bcl-2 family members such as Bim (Bcl-2 interacting mediator of cell death) or Bcl-6 [115].

2.2.2. Murine double minute 2 (*Mdm2*)

Mdm2 is an E3 ubiquitin ligase whose expression is induced by p53. As a feed-back loop, Mdm2 then controls intracellular

levels of the tumour suppressor p53. p53 is a major regulator of cell death and is commonly inhibited under conditions in which the PKB pathway is activated [116]. It has been reported that PKB binds to and phosphorylates Mdm2, allowing its nuclear import and increasing its ubiquitin ligase activity [117,118]. More recently, Feng et al. showed that PKB is able to inhibit Mdm2 self-ubiquitination via phosphorylation of Mdm2 on Ser166 and Ser188. Introduction of a constitutively active form of PKB into cells induces Mdm2 phosphorylation on these specific residues and leads to stabilization of the Mdm2 protein. This strongly suggests that PKB controls the Mdm2/p53 signalling pathway by decreasing Mdm2 proteasomal degradation [119].

2.2.3. *NF-κB*

It is well known that control of the inflammatory response and apoptosis are closely linked to NF-κB activation. Deregulation of NF-κB activity can lead to the development of diseases such as autoimmune diseases or cancer [120]. Most of the time, NF-κB is activated after degradation of its inhibitor, I-κBα. Firstly, I-κB kinase (IKK) is phosphorylated and activated and in turn mediates I-κBα phosphorylation, leading to its degradation by the ubiquitin/proteasome system. Thus, NF-κB is free and translocates to the nucleus where it activates pro-survival genes including Bcl-X_L, caspases inhibitors [121] and c-Myb [122]. PKB has been shown to regulate IKK activity by phosphorylating IKK at the Thr23 residue. This activates IKK, which then targets I-κBα for proteasomal degradation [61,123].

2.2.4. Cyclic AMP-response element-binding protein (*CREB*)

There are several reports that CREB transcription factors are required for the survival of certain cell types [124]. It has been shown that PKB phosphorylates CREB on Ser133, leading to CREB activation and the promotion of cell survival through

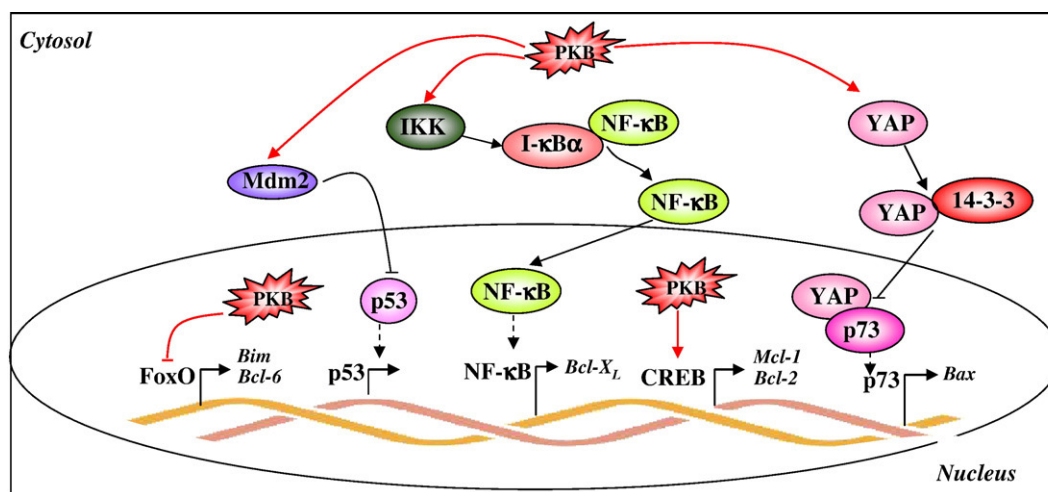


Fig. 2. Indirect modulation of apoptosis. The mediation of apoptosis execution by PKB also involves changes in the transcription program. By regulating transcription factors responsible for the expression of pro- or anti-apoptotic molecules, PKB also plays a crucial role in cell fate. PKB phosphorylates and inhibits FoxO and also activates CREB after its phosphorylation, resulting in the upregulation of anti-apoptotic Bcl-2 family members. Moreover, by phosphorylating and activating IKK, PKB induces I-κBα phosphorylation. Thus, NF-κB is activated and induces expression of Bcl-2 anti-apoptotic proteins. On the other hand, phosphorylation by PKB stabilizes Mdm2 and increases Mdm2 ubiquitin ligase activity, leading to a decrease in p53 transcriptional activity. Transcriptional activity of p73 is also indirectly inhibited by PKB; p73 co-activator YAP is phosphorylated by PKB, after which it interacts with 14-3-3 proteins in the cytosol and is then no longer able to bind p73. As a consequence, p73 cannot activate target genes like Bax.

stimulation of the expression of specific cellular genes [125]. It has been demonstrated also that PKB contributes to the activation of the anti-apoptotic Mcl-1 through a transcription factor complex containing CREB [126]. Moreover, enhanced CREB activity mediated by PKB has been reported to increase Bcl-2 promoter activity and, therefore, to inhibit apoptosis [127]. Finally, CREB phosphorylation and activation by PKB is also responsible for an increase in PKB expression, thus reinforcing PKB anti-apoptotic functions [128].

2.2.5. Yes-associated protein (YAP)

YAP protein has been identified recently as a new PKB substrate [129]. YAP is phosphorylated on Ser127 by PKB, after which it binds to 14-3-3 proteins within the cytoplasm. Consequently, YAP is no longer localized in the nucleus and cannot function as a co-activator of transcription factors, including p73. Thus, PKB suppresses YAP ability to promote p73-mediated transcription of pro-apoptotic genes like Bax.

2.3. PKB isoform redundancy during apoptosis

Three PKB isoforms (PKB α , PKB β and PKB γ) have been identified in mammals. They share a high degree of structural similarity and sequence homology. It is well established that each isoform plays a unique as well as a common role in cells [130]. PKB α knock-out mice are growth retarded, PKB β knock-out mice develop diabetes-like syndrome, and PKB γ knock-out mice show reduced brain size [131]. PKB proteins have crucial functions in preventing cells from apoptosis and there is evidence that the pro-survival effect of the PKB isoforms is redundant. For example, PKB α and PKB β seem to be dispensable for cell survival in isolated osteoclast precursors, probably because of the redundant function of PKB γ [132]. It has been shown also that PKB α and PKB β are both able to phosphorylate and inactivate the pro-apoptotic Htra2/Omi [85], suggesting that the two proteins share common functions regulating apoptosis. Moreover, in a recent study PKB α /PKB β double knock-out mouse embryonic fibroblasts (MEF PKB α /PKB β DKO) were viable until 80% of PKB γ was depleted using siRNA technology [133]. By reintroducing PKB α or PKB γ into MEF (PKB α /PKB β DKO), the authors were able to counteract the apoptotic effects observed in this cell line under normal or stressed conditions. This suggests that only a small proportion of active PKB is needed to block apoptosis, although cells under stress require more PKB to survive. Another example of PKB isoform redundancy has been described recently in *Caenorhabditis elegans* [134], when it was shown that both PKB α and PKB β negatively regulate DNA-damage-induced apoptosis.

3. New insight into apoptosis: initiation and further directions

Recent reports that the initiation of apoptosis triggered by cytochrome *c* release is coordinated by a class of signalling proteins initially identified as “mitochondrial-shaping” proteins strengthens the notion that the same set of signalling proteins

regulates antagonist functions within mitochondria [135–137]. This was originally illustrated in *C. elegans*, where the anti-apoptotic Bcl-2 family member CED-9 (Bcl-X_L in mammals) and its antagonist the BH3-only protein egl1 (Bak/Bax) were shown to regulate mitochondrial shape in cells targeted to die as well as in healthy cells [138,139]. Among the growing network of signalling molecules, including GTPases, E3 ligases, AAA proteases and phosphatases, involved in mitochondria biogenesis in mammals, both pro-fission dynamin-related protein 1 (Drp1/DNM1) and pro-fusion optic atrophy protein 1 (OPA1/mitochondrial genome maintenance 1Mgm1 in yeast) have been consistently shown to participate in apoptosis. Indeed, upon apoptosis induction, the tubular and branched mitochondrial network undergoes intensive remodelling, resulting in its complete fragmentation [139,140]. The two GTPases Drp1 and OPA1 are central regulators of fission/fusion-dependent mitochondrial dynamics. The dynamin-related protein member OPA1, located at the inner membrane and mutated in dominant optic atrophy, together with the integral outer membrane (OMM) mitofusins 1 and 2 [Mfn1/FZO1 (Fuzzy ognon 1), Mfn2/FZO2] independently coordinate fusion and tethering of the mitochondria, respectively. Conversely, the cytosolic dynamin-related protein 1 Drp1 functions in association with its recruiting partner of the OMM, the Fis1 protein (Fis1p/FIS1). Modulation of mitochondrial dynamics concomitantly with overexpression of pro-fission protein hFis1 or Drp1 is linked to increased susceptibility to various apoptotic stimuli. On the other hand, promotion of mitochondrial network fusion by Drp1 mutant Drp1K38A or cellular depletion of the pro-fission protein has been shown to have a protective effect [140,141]. Indeed, effects on mitochondrial structure by imbalanced fusion/fission may disrupt the sub-mitochondrial compartmentalization of the very different enzymatic activities needed to maintain mitochondria homeostasis and, thus, lead to apoptosis as a secondary indirect event. Indeed, extensive use of transmitted electron microscopy and tomography has shed some light on this issue by demonstrating the prime involvement of internal mitochondria remodelling in apoptosis initiation and regulation.

In fact, most of the mitochondrial pool of cytochrome *c* (80–85%) is retained in the cristae of the mitochondria matrix, where tight juxtaposition of the membrane prevents its release into the IMS, which is considered to be the upstream event preceding apoptotic-dependant release of cytochrome *c* (and other factors discussed above) from the mitochondria [142,143]. Sequestration of cytochrome *c* in the cristae is ensured by the ability of both IMM integral and IMS soluble OPA1 protein to oligomerize and maintain the integrity of the cristae junctions [30]. A recent major breakthrough was the demonstration by Cipolat and co-workers that the rhomboid protease PARL regulates cytochrome *c* release via OPA1-dependent processing [29]. Targeted inactivation of the PARL gene in mouse leads to severe growth retardation and cachexia, presumably caused by increased apoptosis, leading to animal death (8–12 weeks after birth) [30]. Moreover, PARL $^{-/-}$ cells show hypersensitivity to intrinsic apoptotic stimuli (as demonstrated by increased kinetics of cytochrome *c* release) correlated to the absence of OPA1 oligomers, despite exhibiting normal mitochondrial morphology and dynamics [29,30]. Thus,

the re-introduction of a PARL-processed form of OPA1 protein, which is restricted to the IMS, is sufficient to restore a normal apoptotic response in these cells.

In summary, the involvement of mitochondrial-shaping proteins in the regulation of apoptosis should be examined carefully as changes in the complex double-membrane ultra-structure of the mitochondria may have collateral effects that are not necessarily a part of the apoptotic process. As illustrated by the involvement of OPA1 and Drp1 protein in mitochondrial cristae remodelling, the integration and amplification of the cytosolic signals into a complex and multi-step intra-mitochondrial signalling pathway appears central to the initiation of apoptosis. In this context, research over the next few years should increase our mechanistic understanding of the spatial and temporal parameters influencing the dynamics of PKB anti-apoptotic properties. Work already initiated has demonstrated the ability of active PKB to translocate to the OMM or to be actively imported into the mitochondrial sub-compartment in various cell systems [8,144,145], suggesting its possible involvement in the direct regulation of intra-mitochondrial signalling.

4. Conclusions

In the last decade, our understanding of PKB activation and mechanisms for promoting cell survival has expanded rapidly. Several PKB substrates involved in apoptosis have been described and many processes inhibiting cell death have been identified. In this context, the mitochondrion appears to be the key organelle in which PKB drives its anti-apoptotic activities. More precisely, PKB acts at different mitochondrial levels to sustain cell life: pre-mitochondrial, mitochondrial and post-mitochondrial. By modulating transcription factor activity or inhibiting nucleus condensation/fragmentation, PKB interferes with upstream mitochondrial cell death signals, but it also maintains mitochondrial integrity by reinforcing the roles of key players acting on mitochondrial membranes (Bcl-2 family members). Moreover, caspase activity, which represents mitochondrial downstream events in the apoptotic process, can be prevented by PKB in different ways. Recently, several studies have shown that mitochondria can also be fragmented in cells that normally undergo programmed cell death, supporting the notion that mitochondrial remodelling plays an important role in the process. The function of PKB in this context is still not clear and further investigations of its possible role as a modulator of mitochondrial dynamics are required. This could lead to a major breakthrough in our understanding of PKB functions in cell survival. Altogether, the recent discoveries relating to PKB substrates involved in apoptosis, as well as progress on pharmaceutical compounds that specifically target PKB, could lead to the generation of powerful tools for cancer therapy.

Acknowledgements

We thank Lana Bozulic, Banu Surucu, Elisabeth Fayard and Debby Hynx for the help and critical reading of this manuscript. AP is a recipient of an Oncosuisse fellowship, LT is a recipient

of an EMBO long-term post-doctoral fellowship and EZ is a recipient of a Swiss Bridge fellowship. The Friedrich Miescher Institute is part of the Novartis Research Foundation.

References

- [1] M. Cully, H. You, A.J. Levine, T.W. Mak, *Nat. Rev., Cancer* 6 (3) (2006) 184.
- [2] J. Luo, B.D. Manning, L.C. Cantley, *Cancer Cells* 4 (4) (2003) 257.
- [3] L.C. Cantley, *Science* 296 (5573) (2002) 1655.
- [4] F.M. Foster, C.J. Traer, S.M. Abraham, M.J. Fry, *J. Cell Sci.* 116 (Pt 15) (2003) 3037.
- [5] M.P. Wymann, M. Zvelebil, M. Laffargue, *Trends Pharmacol. Sci.* 24 (7) (2003) 366.
- [6] D.P. Brazil, Z.Z. Yang, B.A. Hemmings, *Trends Biochem. Sci.* 29 (5) (2004) 233.
- [7] J. Tan, D.E. Hallahan, *Cancer Res.* 63 (22) (2003) 7663.
- [8] K. Sasaki, M. Sato, Y. Umezawa, *J. Biol. Chem.* 278 (33) (2003) 30945.
- [9] Z. Liu, T.M. Roberts, *Cell Cycle* 5 (7) (2006) 675.
- [10] L.H. Saal, K. Holm, M. Maurer, L. Memeo, T. Su, X. Wang, J.S. Yu, P.O. Malmstrom, M. Mansukhani, J. Enoksson, H. Hibshoosh, A. Borg, R. Parsons, *Cancer Res.* 65 (7) (2005) 2554.
- [11] Y. Samuels, K. Ericson, *Curr. Opin. Oncol.* 18 (1) (2006) 77.
- [12] Y. Samuels, Z. Wang, A. Bardelli, N. Silliman, J. Ptak, S. Szabo, H. Yan, A. Gazdar, S.M. Powell, G.J. Riggins, J.K. Willson, S. Markowitz, K.W. Kinzler, B. Vogelstein, V.E. Velculescu, *Science* 304 (5670) (2004) 554.
- [13] J.S. Kim, C. Lee, C.L. Bonifant, H. Ransom, T. Waldman, *Mol. Cell. Biol.* 27 (2) (2007) 662.
- [14] D.A. Altomare, S. Tanno, A. De Rienzo, A.J. Klein-Szanto, S. Tanno, K.L. Skele, J.P. Hoffman, J.R. Testa, *J. Cell. Biochem.* 88 (1) (2003) 470.
- [15] A. Bellacosa, D. de Feo, A.K. Godwin, D.W. Bell, J.Q. Cheng, D.A. Altomare, M. Wan, L. Dubeau, G. Scambia, V. Masciullo, G. Ferrandina, P. Benedetti Panici, S. Mancuso, G. Neri, J.R. Testa, *Int. J. Cancer* 64 (4) (1995) 280.
- [16] J.Q. Cheng, A.K. Godwin, A. Bellacosa, T. Taguchi, T.F. Franke, T.C. Hamilton, P.N. Tsichlis, J.R. Testa, *Proc. Natl. Acad. Sci. U. S. A.* 89 (19) (1992) 9267.
- [17] J.Q. Cheng, B. Ruggeri, W.M. Klein, G. Sonoda, D.A. Altomare, D.K. Watson, J.R. Testa, *Proc. Natl. Acad. Sci. U. S. A.* 93 (8) (1996) 3636.
- [18] Q. Meng, C. Xia, J. Fang, Y. Rojanasakul, B.H. Jiang, *Cell. Signal.* 18 (12) (2006) 2262.
- [19] B.A. Ruggeri, L. Huang, M. Wood, J.Q. Cheng, J.R. Testa, *Mol. Carcinog.* 21 (2) (1998) 81.
- [20] D.P. Brazil, J. Park, B.A. Hemmings, *Cell* 111 (3) (2002) 293.
- [21] T.F. Franke, D.R. Kaplan, L.C. Cantley, *Cell* 88 (4) (1997) 435.
- [22] M.M. Hill, B.A. Hemmings, *Pharmacol. Ther.* 93 (2-3) (2002) 243.
- [23] S.G. Kennedy, A.J. Wagner, S.D. Conzen, J. Jordan, A. Bellacosa, P.N. Tsichlis, N. Hay, *Genes Dev.* 11 (6) (1997) 701.
- [24] I. Vivanco, C.L. Sawyers, *Nat. Rev. Cancer* 2 (7) (2002) 489.
- [25] D.R. Green, J.C. Reed, *Science* 281 (5381) (1998) 1309.
- [26] L. Margulis, *Proc. Natl. Acad. Sci. U. S. A.* 93 (3) (1996) 1071.
- [27] M.J. Goldenthal, J. Marin-Garcia, *Mol. Cell. Biochem.* 262 (1-2) (2004) 1.
- [28] G.A. McQuibban, S. Saurya, M. Freeman, *Nature* 423 (6939) (2003) 537.
- [29] S. Cipolat, T. Rudka, D. Hartmann, V. Costa, L. Serneels, K. Craessaerts, K. Metzger, C. Frezza, W. Annaert, L. D'Adamio, C. Derks, T. Dejaegere, L. Pellegrini, R. D'Hooge, L. Scorrano, B. De Strooper, *Cell* 126 (1) (2006) 163.
- [30] C. Frezza, S. Cipolat, O. Martins de Brito, M. Micaroni, G.V. Beznoussenko, T. Rudka, D. Bartoli, R.S. Polishuck, N.N. Danel, B. De Strooper, L. Scorrano, *Cell* 126 (1) (2006) 177.
- [31] B. Vogelstein, K.W. Kinzler, *Nat. Med.* 10 (8) (2004) 789.
- [32] B.D. Manning, L.C. Cantley, *Cell* 129 (7) (2007) 1261.
- [33] K.L. Schwertfeger, M.M. Richert, S.M. Anderson, *Mol. Endocrinol.* 15 (6) (2001) 867.
- [34] N. Ohba, S. Kiryu-Seo, M. Maeda, M. Muraoka, M. Ishii, H. Kiyama, *Neurosci. Lett.* 359 (3) (2004) 159.
- [35] J.F. Kerr, A.H. Wyllie, A.R. Currie, *Br. J. Cancer* 26 (4) (1972) 239.

- [36] M.D. Jacobson, M. Weil, M.C. Raff, *Cell* 88 (3) (1997) 347.
- [37] E. Solary, N. Droin, A. Bettaieb, L. Corcos, M.T. Dimanche-Boitrel, C. Garrido, *Leukemia* 14 (10) (2000) 1833.
- [38] U. Fischer, K. Schulze-Osthoff, *Cell Death Differ.* 12 (Suppl 1) (2005) 942.
- [39] J.C. Reed, *Trends Mol. Med.* 7 (7) (2001) 314.
- [40] N.N. Danial, S.J. Korsmeyer, *Cell* 116 (2) (2004) 205.
- [41] B. Fadeel, S. Orrenius, *J. Intern. Med.* 258 (6) (2005) 479.
- [42] D. Spierings, G. McStay, M. Saleh, C. Bender, J. Chipuk, U. Maurer, D.R. Green, *Science* 310 (5745) (2005) 66.
- [43] P. Li, D. Nijhawan, I. Budihardjo, S.M. Srinivasula, M. Ahmad, E.S. Alnemri, X. Wang, *Cell* 91 (4) (1997) 479.
- [44] H. Zou, W.J. Henzel, X. Liu, A. Lutschg, X. Wang, *Cell* 90 (3) (1997) 405.
- [45] B. Zhivotovsky, S. Orrenius, O.T. Brustugun, S.O. Doskeland, *Nature* 391 (6666) (1998) 449.
- [46] M. Ott, J.D. Robertson, V. Gogvadze, B. Zhivotovsky, S. Orrenius, *Proc. Natl. Acad. Sci. U. S. A.* 99 (3) (2002) 1259.
- [47] Y. Hu, M.A. Benedict, L. Ding, G. Nunez, *EMBO J.* 18 (13) (1999) 3586.
- [48] H. Zou, Y. Li, X. Liu, X. Wang, *J. Biol. Chem.* 274 (17) (1999) 11549.
- [49] J.D. Robertson, S. Orrenius, B. Zhivotovsky, *J. Struct. Biol.* 129 (2-3) (2000) 346.
- [50] E. Dugas, S.A. Susin, N. Zamzami, K.F. Ferri, T. Irinopoulou, N. Larochette, M.C. Prevost, B. Leber, D. Andrews, J. Penninger, G. Kroemer, *FASEB J.* 14 (5) (2000) 729.
- [51] N. Joza, S.A. Susin, E. Dugas, W.L. Stanford, S.K. Cho, C.Y. Li, T. Sasaki, A.J. Elia, H.Y. Cheng, L. Ravagnan, K.F. Ferri, N. Zamzami, A. Wakeham, R. Hakem, H. Yoshida, Y.Y. Kong, T.W. Mak, J.C. Zuniga-Pflucker, G. Kroemer, J.M. Penninger, *Nature* 410 (6828) (2001) 549.
- [52] L.Y. Li, X. Luo, X. Wang, *Nature* 412 (6842) (2001) 95.
- [53] S.A. Susin, H.K. Lorenzo, N. Zamzami, I. Marzo, B.E. Snow, G.M. Brothers, J. Mangion, E. Jacotot, P. Costantini, M. Loeffler, N. Larochette, D.R. Goodlett, R. Aebersold, D.P. Siderovski, J.M. Penninger, G. Kroemer, *Nature* 397 (6718) (1999) 441.
- [54] C. Du, M. Fang, Y. Li, L. Li, X. Wang, *Cell* 102 (1) (2000) 33.
- [55] C.P. Baines, R.A. Kaiser, N.H. Purcell, N.S. Blair, H. Osinska, M.A. Hambleton, E.W. Brunskill, M.R. Sayen, R.A. Gottlieb, G.W. Dorn, J. Robbins, J.D. Molkentin, *Nature* 434 (7033) (2005) 658.
- [56] P.X. Petit, M. Gubern, P. Dioletz, S.A. Susin, N. Zamzami, G. Kroemer, *FEBS Lett.* 426 (1) (1998) 111.
- [57] V. Gogvadze, S. Orrenius, B. Zhivotovsky, *Biochim. Biophys. Acta* 1757 (5-6) (2006) 639.
- [58] J.E. Ricci, R.A. Gottlieb, D.R. Green, *J. Cell Biol.* 160 (1) (2003) 65.
- [59] P. Lassus, X. Opitz-Araya, Y. Lazebnik, *Science* 297 (5585) (2002) 1352.
- [60] J.D. Robertson, V. Gogvadze, A. Kropotov, H. Vakifahmetoglu, B. Zhivotovsky, S. Orrenius, *EMBO Rep.* 5 (6) (2004) 643.
- [61] L.P. Kane, V.S. Shapiro, D. Stokoe, A. Weiss, *Curr. Biol.* 9 (11) (1999) 601.
- [62] R.M. Kluck, E. Bossy-Wetzell, D.R. Green, D.D. Newmeyer, *Science* 275 (5303) (1997) 1132.
- [63] Y. Tsujimoto, L.R. Finger, J. Yunis, P.C. Nowell, C.M. Croce, *Science* 226 (4678) (1984) 1097.
- [64] D.L. Vaux, S. Cory, J.M. Adams, *Nature* 335 (6189) (1988) 440.
- [65] B. Fadeel, B. Zhivotovsky, S. Orrenius, *FASEB J.* 13 (13) (1999) 1647.
- [66] E. Yang, S.J. Korsmeyer, *Blood* 88 (2) (1996) 386.
- [67] B.A. Hemmings, *Science* 275 (5300) (1997) 628.
- [68] S. Jin, R.S. DiPaola, R. Mathew, E. White, *J. Cell Sci.* 120 (Pt 3) (2007) 379.
- [69] D.W. Parsons, T.L. Wang, Y. Samuels, A. Bardelli, J.M. Cummins, L. DeLong, N. Silliman, J. Ptak, S. Szabo, J.K. Willson, S. Markowitz, K.W. Kinzler, B. Vogelstein, C. Lengauer, V.E. Velculescu, *Nature* 436 (7052) (2005) 792.
- [70] S.R. Datta, H. Dudek, X. Tao, S. Masters, H. Fu, Y. Gotoh, M.E. Greenberg, *Cell* 91 (2) (1997) 231.
- [71] L. del Peso, M. Gonzalez-Garcia, C. Page, R. Herrera, G. Nunez, *Science* 278 (5338) (1997) 687.
- [72] S.R. Datta, A. Brunet, M.E. Greenberg, *Genes Dev.* 13 (22) (1999) 2905.
- [73] A. Nechushtan, C.L. Smith, Y.T. Hsu, R.J. Youle, *EMBO J.* 18 (9) (1999) 2330.
- [74] H. Yamaguchi, H.G. Wang, *Oncogene* 20 (53) (2001) 7779.
- [75] S.J. Gardai, D.A. Hildeman, S.K. Frankel, B.B. Whitlock, S.C. Frasch, N. Borregaard, P. Marrack, D.L. Bratton, P.M. Henson, *J. Biol. Chem.* 279 (20) (2004) 21085.
- [76] M. Xin, X. Deng, *J. Biol. Chem.* 280 (11) (2005) 10781.
- [77] N. Majewski, V. Nogueira, R.B. Robey, N. Hay, *Mol. Cell. Biol.* 24 (2) (2004) 730.
- [78] C. Cande, F. Cecconi, P. Dessen, G. Kroemer, *J. Cell Sci.* 115 (Pt 24) (2002) 4727.
- [79] S.W. Yu, H. Wang, M.F. Poitras, C. Coombs, W.J. Bowers, H.J. Federoff, G.G. Poirier, T.M. Dawson, V.L. Dawson, *Science* 297 (5579) (2002) 259.
- [80] N.H. Kim, K. Kim, W.S. Park, H.S. Son, Y. Bae, *J. Cell. Biochem.* (in press), doi:10.1002/jcb.21344.
- [81] B.A. Stoica, V.A. Movsesyan, P.M.t. Lea, A.I. Faden, *Mol. Cell. Neurosci.* 22 (3) (2003) 365.
- [82] Y. Suzuki, Y. Imai, H. Nakayama, K. Takahashi, K. Takio, R. Takahashi, *Mol. Cell* 8 (3) (2001) 613.
- [83] W. Li, S.M. Srinivasula, J. Chai, P. Li, J.W. Wu, Z. Zhang, E.S. Alnemri, Y. Shi, *Nat. Struct. Biol.* 9 (6) (2002) 436.
- [84] Q.H. Yang, R. Church-Hajduk, J. Ren, M.L. Newton, C. Du, *Genes Dev.* 17 (12) (2003) 1487.
- [85] L. Yang, M. Sun, X.M. Sun, G.Z. Cheng, S.V. Nicosia, J.Q. Cheng, *J. Biol. Chem.* 282 (15) (2007) 10981.
- [86] M.H. Cardone, N. Roy, H.R. Stennicke, G.S. Salvesen, T.F. Franke, E. Stanbridge, S. Frisch, J.C. Reed, *Science* 282 (5392) (1998) 1318.
- [87] E. Fujita, A. Jinbo, H. Matuzaki, H. Konishi, U. Kikkawa, T. Momoi, *Biochem. Biophys. Res. Commun.* 264 (2) (1999) 550.
- [88] M. Enari, H. Sakahira, H. Yokoyama, K. Okawa, A. Iwamoto, S. Nagata, *Nature* 391 (6662) (1998) 43.
- [89] J.Y. Ahn, X. Liu, Z. Liu, L. Pereira, D. Cheng, J. Peng, P.A. Wade, A.W. Hamburger, K. Ye, *EMBO J.* 25 (10) (2006) 2083.
- [90] S. Sahara, M. Aoto, Y. Eguchi, N. Imamoto, Y. Yoneda, Y. Tsujimoto, *Nature* 401 (6749) (1999) 168.
- [91] Y. Hu, J. Yao, Z. Liu, X. Liu, H. Fu, K. Ye, *EMBO J.* 24 (20) (2005) 3543.
- [92] A.H. Kim, G. Khursigara, X. Sun, T.F. Franke, M.V. Chao, *Mol. Cell. Biol.* 21 (3) (2001) 893.
- [93] M.K. Barthwal, P. Sathyanarayana, C.N. Kundu, B. Rana, A. Pradeep, C. Sharma, J.R. Woodgett, A. Rana, *J. Biol. Chem.* 278 (6) (2003) 3897.
- [94] H.S. Park, M.S. Kim, S.H. Huh, J. Park, J. Chung, S.S. Kang, E.J. Choi, *J. Biol. Chem.* 277 (4) (2002) 2573.
- [95] E. Schmitt, M. Gehrman, M. Brunet, G. Multhoff, C. Garrido, *J. Leukoc. Biol.* 81 (1) (2007) 15.
- [96] A. Parcellier, S. Gurbuxani, E. Schmitt, E. Solary, C. Garrido, *Biochem. Biophys. Res. Commun.* 304 (3) (2003) 505.
- [97] M.J. Rane, Y. Pan, S. Singh, D.W. Powell, R. Wu, T. Cummins, Q. Chen, K.R. McLeish, J.B. Klein, *J. Biol. Chem.* 278 (30) (2003) 27828.
- [98] D.B. Solit, A.D. Basso, A.B. Olshen, H.I. Scher, N. Rosen, *Cancer Res.* 63 (9) (2003) 2139.
- [99] H. Konishi, H. Matsuzaki, M. Tanaka, Y. Takemura, S. Kuroda, Y. Ono, U. Kikkawa, *FEBS Lett.* 410 (2-3) (1997) 493.
- [100] R. Wu, H. Kausar, P. Johnson, D.E. Montoya-Durango, M. Merchant, M.J. Rane, *J. Biol. Chem.* 282 (30) (2007) 21598.
- [101] Y. Zhang, X. Shen, *Clin. Cancer Res.* 13 (10) (2007) 2855.
- [102] D.A. Cross, D.R. Alessi, P. Cohen, M. Andjelkovich, B.A. Hemmings, *Nature* 378 (6559) (1995) 785.
- [103] M. Pap, G.M. Cooper, *J. Biol. Chem.* 273 (32) (1998) 19929.
- [104] U. Maurer, C. Charvet, A.S. Wagman, E. DeJardin, D.R. Green, *Mol. Cell* 21 (6) (2006) 749.
- [105] S.G. Kennedy, E.S. Kandel, T.K. Cross, N. Hay, *Mol. Cell. Biol.* 19 (8) (1999) 5800.
- [106] K. Gottlob, N. Majewski, S. Kennedy, E. Kandel, R.B. Robey, N. Hay, *Genes Dev.* 15 (11) (2001) 1406.
- [107] J.C. Rathmell, C.J. Fox, D.R. Plas, P.S. Hammerman, R.M. Cinalli, C.B. Thompson, *Mol. Cell. Biol.* 23 (20) (2003) 7315.
- [108] R.B. Robey, N. Hay, *Oncogene* 25 (34) (2006) 4683.
- [109] J.E. Wilson, *Rev. Physiol., Biochem. Pharmacol.* 126 (1995) 65.

- [110] N. Majewski, V. Nogueira, P. Bhaskar, P.E. Coy, J.E. Skeen, K. Gottlob, N.S. Chandel, C.B. Thompson, R.B. Robey, N. Hay, *Mol. Cell* 16 (5) (2004) 819.
- [111] J.M. Bryson, P.E. Coy, K. Gottlob, N. Hay, R.B. Robey, *J. Biol. Chem.* 277 (13) (2002) 11392.
- [112] R.B. Robey, N. Hay, *Cell Cycle* 4 (5) (2005) 654.
- [113] A. Brunet, A. Bonni, M.J. Zigmond, M.Z. Lin, P. Juo, L.S. Hu, M.J. Anderson, K.C. Arden, J. Blenis, M.E. Greenberg, *Cell* 96 (6) (1999) 857.
- [114] G.J. Kops, N.D. de Ruiter, A.M. De Vries-Smits, D.R. Powell, J.L. Bos, B.M. Burgering, *Nature* 398 (6728) (1999) 630.
- [115] B.M. Burgering, R.H. Medema, *J. Leukoc. Biol.* 73 (6) (2003) 689.
- [116] M. Oren, *Cell Death Differ.* 10 (4) (2003) 431.
- [117] T.M. Gottlieb, J.F. Leal, R. Seger, Y. Taya, M. Oren, *Oncogene* 21 (8) (2002) 1299.
- [118] L.D. Mayo, D.B. Donner, *Proc. Natl. Acad. Sci. U. S. A.* 98 (20) (2001) 11598.
- [119] J. Feng, R. Tamaskovic, Z. Yang, D.P. Brazil, A. Merlo, D. Hess, B.A. Hemmings, *J. Biol. Chem.* 279 (34) (2004) 35510.
- [120] J. Dutta, Y. Fan, N. Gupta, G. Fan, C. Gelinias, *Oncogene* 25 (51) (2006) 6800.
- [121] M. Barkett, T.D. Gilmore, *Oncogene* 18 (49) (1999) 6910.
- [122] A. Lauder, A. Castellanos, K. Weston, *Mol. Cell. Biol.* 21 (17) (2001) 5797.
- [123] O.N. Ozes, L.D. Mayo, J.A. Gustin, S.R. Pfeffer, L.M. Pfeffer, D.B. Donner, *Nature* 401 (6748) (1999) 82.
- [124] A.S. Coutts, N. La Thangue, *Biochem. Soc. Symp.* (73) (2006) 181.
- [125] K. Du, M. Montminy, *J. Biol. Chem.* 273 (49) (1998) 32377.
- [126] J.M. Wang, J.R. Chao, W. Chen, M.L. Kuo, J.J. Yen, H.F. Yang-Yen, *Mol. Cell. Biol.* 19 (9) (1999) 6195.
- [127] S. Pugazhenti, A. Nesterova, C. Sable, K.A. Heidenreich, L.M. Boxer, L.E. Heasley, J.E. Reusch, *J. Biol. Chem.* 275 (15) (2000) 10761.
- [128] J.E. Reusch, D.J. Klemm, *J. Biol. Chem.* 277 (2) (2002) 1426.
- [129] S. Basu, N.F. Totty, M.S. Irwin, M. Sudol, J. Downward, *Mol. Cell* 11 (1) (2003) 11.
- [130] H. Cho, J.L. Thorvaldsen, Q. Chu, F. Feng, M.J. Birnbaum, *J. Biol. Chem.* 276 (42) (2001) 38349.
- [131] E. Fayard, L.A. Tintignac, A. Baudry, B.A. Hemmings, *J. Cell Sci.* 118 (Pt 24) (2005) 5675.
- [132] T. Sugatani, K.A. Hruska, *J. Biol. Chem.* 280 (5) (2005) 3583.
- [133] X. Liu, Y. Shi, M.J. Birnbaum, K. Ye, R. De Jong, T. Oltersdorf, V.L. Giranda, Y. Luo, *J. Biol. Chem.* 281 (42) (2006) 31380.
- [134] C. Quevedo, D.R. Kaplan, W.B. Derry, *Curr. Biol.* 17 (3) (2007) 286.
- [135] G.M. Cereghetti, L. Scorrano, *Oncogene* 25 (34) (2006) 4717.
- [136] E. Gottlieb, *Cell* 126 (1) (2006) 27.
- [137] L. Pellegrini, L. Scorrano, *Cell Death Differ.* 14 (7) (2007) 1275.
- [138] P. Delivani, C. Adrain, R.C. Taylor, P.J. Duriez, S.J. Martin, *Mol. Cell* 21 (6) (2006) 761.
- [139] R. Jagasia, P. Grote, B. Westermann, B. Conradt, *Nature* 433 (7027) (2005) 754.
- [140] S. Frank, B. Gaume, E.S. Bergmann-Leitner, W.W. Leitner, E.G. Robert, F. Catez, C.L. Smith, R.J. Youle, *Dev. Cell* 1 (4) (2001) 515.
- [141] Y.J. Lee, S.Y. Jeong, M. Karbowski, C.L. Smith, R.J. Youle, *Mol. Biol. Cell* 15 (11) (2004) 5001.
- [142] M. Germain, J.P. Mathai, H.M. McBride, G.C. Shore, *EMBO J.* 24 (8) (2005) 1546.
- [143] L. Scorrano, M. Ashiya, K. Buttle, S. Weiler, S.A. Oakes, C.A. Mannella, S.J. Korsmeyer, *Dev. Cell* 2 (1) (2002) 55.
- [144] N. Ahmad, Y. Wang, K.H. Haider, B. Wang, Z. Pasha, O. Uzun, M. Ashraf, *Am. J. Physiol. Heart. Circ. Physiol.* 290 (6) (2006) H2402.
- [145] G.N. Bijur, R.S. Jope, *J. Neurochem.* 87 (6) (2003) 1427.

8. ACKNOWLEDGEMENTS

I would like to thank my supervisor, Brian Arthur Hemmings, for giving me a chance to perform work on this exciting project. I appreciate research freedom given to me, the scientific challenges, and the constant support during my thesis preparation.

I would also like to say many thanks to my PhD committee members, Jean Pieters, Patrick Matthias, and Matthias Wymann, for their guidance and advice during the course of my work.

I would like to thank all the members of Dr Hemmings' lab for their scientific criticism and important contributions to this project. Special thanks goes to Debby Hynx for her fantastic support during the *in vivo* work, and Arnaud Parcellier for sharing with me CTMP work during its early developmental stages. I am also very grateful to Bettina Duemmler who generated Them5 knock-out mouse and from whom I inherited the project. And, of course, thanks to all the mice that helped me to conduct this research!

I would like to thank Oliver Tschopp for his important input to my research plans and for help with the experiments. Many thanks to Michael Rebhan for his help with the initial bioinformatics analysis that built the platform for our further work.

Thanks to all my friends who supported me so much! Thank you for encouraging me and sharing these years with me. I am extremely grateful to my family, always encouraging me to go further, follow my dream, and learn lessons from all my experience! Thank you for all your love and your presence in my life! And last but not least thanks to Ahmad, who always makes me look at things from different point of view. Thank you for your encouraging and understanding, and your presence next to me!

9. CURRICULUM VITAE

Personal information

Elena Zhuravleva
Nationality: Russian
Date of birth: 09 September 1982

Address:
Schuetzengraben 9
4051 Basel
Switzerland

Email elena.zhuravleva@fmi.ch
elena.zhuravleva@yahoo.com
Phone +41(0) 79 5306044 (mobile)

Education

07/2006-present

PhD student at Friedrich Miescher Institute, Brian A Hemmings' group

02/2005-05/2006

Research Scholar, Fox Chase Cancer Center, ICR (Philadelphia, PA, USA), Immunobiology working group.

09/1999-06/2006

Russian State Medical University (Moscow, Russia)
M.D. in Medical Biochemistry, MSc. in Biochemistry, Major in Molecular Biology/Immunology

Patents

Patent on "THEM5- MODIFIED MODELS OF NON-ALCOHOLIC FATTY LIVER DISEASE", WO2010/049494. Inventors: Hemmings, B.A., Duemmler B., Zhuravleva E.

Achievements

- I received an MSc diploma in Medical Biochemistry with honors from the Russian State Medical University in 2006
- I was awarded a Research Scholarship at the Fox Chase Cancer Center to perform my Masters project in 2005-2006

Practical training

2004 Practical laboratory course/training in the Oncology Institute (Moscow, Russia).

2003 Part-time Intern at the Central Clinical Hospital (Moscow, Russia).

2002-2003 Part-time Clinical Assistant in the Laboratory of Clinical Immunology, Center for obstetrics, gynecology and perinatology (Moscow, Russia).

2001-2003 Part-time Technician in the Department of Immunology, Russian State Medical University.

Conferences and meetings

- 2010 FEBS Workshop on “Therapeutic targets in Cancer Cell Metabolism & Death”, oral presentation (in place of invited speaker Brian A Hemmings)
- 2009 Energy Homeostasis Symposium, Stein am Rhein, Switzerland
- 2008 CIG Symposium “Cancer and Metabolism”, Lausanne, Switzerland
- 2006 4th Swiss apoptosis meeting
- 2006-2010 Internal FMI annual meetings
- 2003 Russian Scientific Pirogov Conference – oral presentation, 3rd place award

Publications

- Zhuravleva E., Tschopp O., Hemmings B.A. (2010). Role of PKB/Akt in liver diseases. In “Signaling Pathways in Liver Diseases”, 2nd edition ed. Dufour JF and Clavien PA, Springer Verlag
- Arnaud Parcellier, Lionel A. Tintignac, Elena Zhuravleva, Bettina Duemmler, Derek P. Brazil Vesna Olivieri, Susanne Schenk, Peter Cron, Debby Hynx and Brian A. Hemmings The Carboxyl Terminal Modulator Protein (CTMP) regulates mitochondrial dynamics. PLoS ONE, 2009; 4(5):e5471
- Parcellier, A., L.A. Tintignac, E. Zhuravleva, et al., Carboxy-Terminal Modulator Protein (CTMP) is a mitochondrial protein that sensitizes cells to apoptosis. Cell Signal, 2009; 21(4):639-50.
- Parcellier A, Tintignac LA, Zhuravleva E, Hemmings BA. PKB and the mitochondria: AKTing on apoptosis. Cell Signal, 2008; 20:21-30

Interests

- Sports (spinning, hiking, swimming, running)
- Photography
- Books (history, fiction)
- Travel